

AGH - University of Science and Technology  
Faculty of Geology, Geophysics and Environmental Protection  
Department of General Geology and Environment Protection  
Akademia Górniczo-Hutnicza im. Stanisława Staszica  
Wydział Geologii, Geofizyki i Ochrony Środowiska  
Katedra Geologii Ogólnej, Ochrony Środowiska i Geoturystyki

**Rozprawa Doktorska**  
**PhD Dissertation**

**THE COMPLEX TECTONIC EVENTS AND THEIR  
INFLUENCE ON FORMATION OF MINERAL DEPOSITS  
IN NORTHWEST VIETNAM  
(WYDARZENIA KSZTAŁTUJĄCE TEKTONIKĘ PÓŁNOCNO-  
ZACHODNIEGO WIETNAMU I ICH WPŁYW NA  
POWSTAWANIE SUROWCÓW MINERALNYCH)**

**Khuong The Hung**

Promotor (Advisor): **dr hab. inż. Jan Golonka, prof. nadzw. AGH**

**Kraków 2010**

THE RESEARCH WAS CARRIED OUT  
UNDER  
THE SCHOLARSHIP  
OF RECTOR OF AGH UNIVERSITY OF SCIENCE AND  
TECHNOLOGY PROF. DR HAB. ANTONI TAJDUŚ  
AND  
TEKTONIKA I ZŁOŻA SUROWCÓW MINERALNYCH  
PÓŁNOCNEGO WIETNAMU  
FACULTY OF GEOLOGY, GEOPHYSICS  
AND ENVIRONMENTAL PROTECTION,  
DEPARTMENT OF GENERAL GEOLOGY  
AND ENVIRONMENT PROTECTION  
“BADANIA WŁASNE” GRANT

## TABLE OF CONTENTS

<b>1. INTRODUCTION</b>	<b>3</b>
1.1. Purpose of dissertation	3
1.2. Location of the study area	3
1.3. Modern geomorphology and hydrographic features	5
1.4. History of Investigations	7
<b>2. OUTLINE OF GEOLOGY</b>	<b>10</b>
2.1. General geology	10
2.1.1. Sedimentary rocks	10
2.1.2. Magmatic units	11
2.2. Geological structures	13
2.2.1. Faults	13
2.2.2. Nappes	15
2.3. Plate tectonics	16
2.4. Tectonic subdivision of Northwestern Vietnam	17
<b>3. METHODOLOGY</b>	<b>19</b>
3.1. Division of magmatic rocks	20
3.2. The method of mineralization analysis	21
3.3. Digital elevation model and remote sensing image	22
3.4. Focal mechanism solution of earthquakes	24
<b>4. MAGMATICS</b>	<b>27</b>
4.1. The characteristics of magmatism in northwestern Vietnam	27
4.1.1. Petrography and geochronology	27
4.1.2. Geochemistry	39
4.2. Discussion	53
<b>5. GEOMORPHOTECTONIC MODELING</b>	<b>70</b>
5.1. Geomorphic introduction	71
5.2. Lineament models	71
5.2.1. Literature review	71
5.2.2. Digital elevation model and remote sensing image	72
5.2.3. Criteria adopted for determining the tectonic lineaments	77
5.2.4. Lineament extraction by drainage network analysis	79
5.2.5. Lineament extraction by terrain analysis	81
5.2.6. Lineament correlation between the drainage network and terrain analysis	83
5.3. Domain analysis of aligned morphological features and geological field data	85
5.3.1. Red River fault zone (RRFZ)	85
5.3.2. Dien Bien-Lai Chau fault zone (DBFZ)	88
5.4. Results and Discussions	95
<b>6. EARTHQUAKES</b>	<b>97</b>
6.1. Distribution of earthquake epicentres in the northern Vietnam	97
6.2. Focal mechanism of earthquakes in the northwestern Vietnam	101
6.3. Characteristics of fault based on their focal mechanisms	103

6.3.1. Son La Fault	103
6.3.2. Da River fault	103
6.3.3. Dien Bien – Lai Chau Fault	104
6.3.4. Chieng Khuong Fault	104
6.3.5. Red River fault zone (RRFZ)	105
<b>6.4. Discussion</b>	<b>107</b>
<b>7. MINERALIZATION</b>	<b>108</b>
<b>7.1. Mineral deposits</b>	<b>108</b>
7.1.1. Iron	109
7.1.2. Chromium	110
7.1.3. Copper	110
7.1.4. Lead-zinc	115
7.1.5. Gold	117
7.1.6. Allite - siallite	120
7.1.7. Molybdenum	121
7.1.8. Pyrite	122
7.1.9. Potassium-sodium	124
7.1.10. Graphite	124
7.1.11. Rare earth and radioactive ores	125
<b>7.2. Discussion</b>	<b>126</b>
7.2.1. Mineralization related to geological setting	126
7.2.2. Geochemical anomaly related mineralization	130
7.2.3. Hydrothermal alteration related to mineralization	132
<b>8. SUMMARY AND CONCLUSIONS</b>	<b>132</b>
<b>8.1. Geological evolution and tectonics in northwestern Vietnam</b>	<b>132</b>
<b>8.2. Metallogeny</b>	<b>137</b>
8.2.1. Metallogenic type related to metamorphic rocks during Proterozoic	137
8.2.2. Metallogeny in Early Palaeozoic –Devonian- Carboniferous	137
8.2.3. Metallogenic type related to Upper Permian Ophiolite belt	138
8.2.4. Metallogeny in Late Permian-Triassic Indosinian	138
8.2.5. Metallogeny in Yanshanian (Jurassic-Cretaceous)	139
8.2.6. Metallogeny in Himalayan (Palaeogene)	139
<b>8.3. Conclusion, tectonic processes conducive to the formation of the mineral deposits-</b>	<b>139</b>
<b>ACKNOWLEDGEMENTS</b>	<b>141</b>
<b>REFERENCES</b>	<b>142</b>
<b>APPENDIX</b>	<b>158</b>
<b>Appendix 1: Geochronological data and chemical compositions of ore deposits, size and content of orebodies, and their statistical distribution, list of ore deposits and occurrences in relation to host rocks of the NWVN.</b>	<b>158</b>
<b>Appendix 2 - NEIC: Earthquake Search Results (<a href="http://www.neic.cr.usgs.gov">http://www.neic.cr.usgs.gov</a>)</b>	<b>163</b>
<b>Appendix 3: Global CMT Catalog</b>	<b>165</b>

## **1. INTRODUCTION**

### **1.1. Purpose of dissertation**

This research aims gaining knowledge on tectonic evolution and its influence on formation of mineral deposits (mainly endogenic ores) within the northwestern Vietnam (NWVN). The dissertation will provide a synthetic elaboration of geological history of the northwestern Vietnam, presentation of major tectonic events based on magmatic processes and related to distribution of mineralization. In addition, it also attempts to quantify spatial associations between mineral deposits and geological features, especially the correlation between ore deposits and magmatism. The thesis consists of eight chapters. Chapter 1 provides introduction and purpose, describes modern geomorphology, hydrographic features and previous works on the thesis related subjects. The second chapter puts forward an outline of geological structure and plate tectonic setting of the study area. Chapter 3 is focused on the methodology, explanation of the applied methods. Chapter 4 discusses magmatic characteristics and attempts to explain mechanism responsible for magmatic processes. Chapter 5 carries out a geomorphotectonic modeling of the NWVN area based on DEM construction and remote sensing image analysis; recognized tectonic lineaments and typical structure. Chapter 6 studies and discusses earthquakes, their distribution and relationship to fault zones; it is considered as evidence proving tectonic activity in the present time. Chapter 7 talks about the mineralization, its distribution and some controlling factors. Finally, the last chapter discusses the tectonic evolution and metallogeny of the NWVN, summarizing documentation contained in chapters 1 to 7 and providing conclusions. The studies were conducted at the Department of General Geology and Environment Protection; Faculty of Geology, Geophysics and Environmental Protection; AGH - University of Science and Technology during the period from 2007 to 2010.

The important part of the study was also published in the Journal of the Geological Society of Poland (*Annales Societatis Geologorum Poloniae*) under the title: "Overview of magmatism in Northwestern Vietnam". The preliminary results were also presented in Slovakia during the international conference 6<sup>th</sup> Meeting of the Central European Tectonic Studies Group (CETeG) under the title: "Major plates and events shaping the complex tectonics of Northwest Vietnam" in April 2008.

### **1.2. Location of the study area**

The Vietnam country is located in the eastern part of the Indochinese peninsula; it is a strip of land shaped like the letter "S". China borders on it to the north, Laos and Cambodia to the west, the South China Sea (East Sea) to the east and south. The study area is located in the Northern Vietnam. It comprises an area of 23,100 square kilometers with different landforms from the north to the south due to climatic, tectonic and lithological factors. The geology of the area includes ophiolite complex, intrusion complexes, volcanic rocks, terrigenous and carbonates sedimentary rocks ranging in age from Proterozoic till the present. This research covers the study of on the Song Hong (Red river), Song Da (Da river), Tu Le, Song Ma and Sam Nua regions, corresponding to the northwestern Vietnam, bounded to the north by the

boundary between China and Vietnam, to the south by the boundary between Vietnam and Laos, to the east by the Song Hong fault and to the west by the Dien Bien-Sop Cop fault zone. The area's coordinates of interest are mentioned in the Table 1 (area indicated by a rectangle in the Figs 1.1B & 1.2).

Corner Coordinates	VN-2000		LONG-LAT	
	X (m)	Y (m)	LONG	LAT
<b>Bottom Left</b>	48,295,000	2,328,000	103°03'	21°02'
<b>Top Right</b>	48,445,000	2,482,000	104°18'	22°25'

Table 1.1 Coordinates of the study area

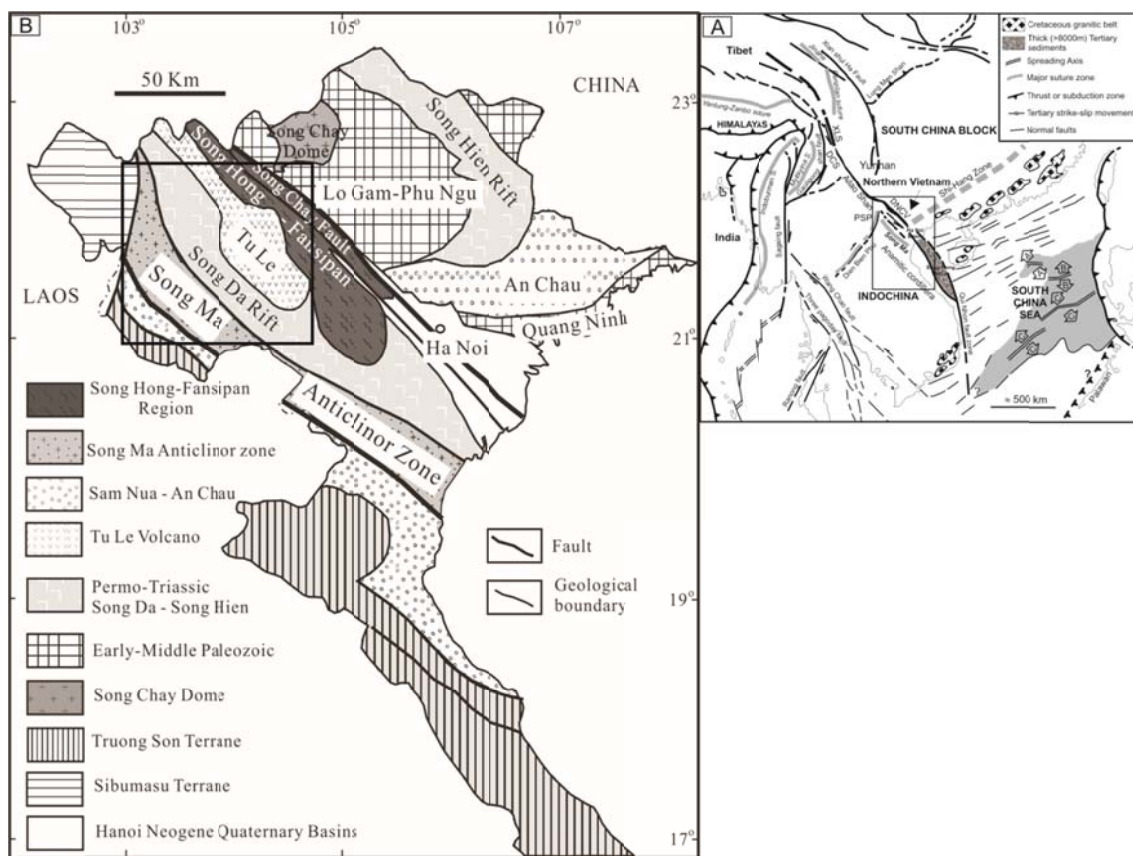


Fig. 1.1. A – Position of the Northern Vietnam within the SE Asia (after Leloup et al., 1995; 2001); B – Tectonic sketch map of the northern Vietnam and showing location of the study area (after Tran Van Tri et al., 1979).

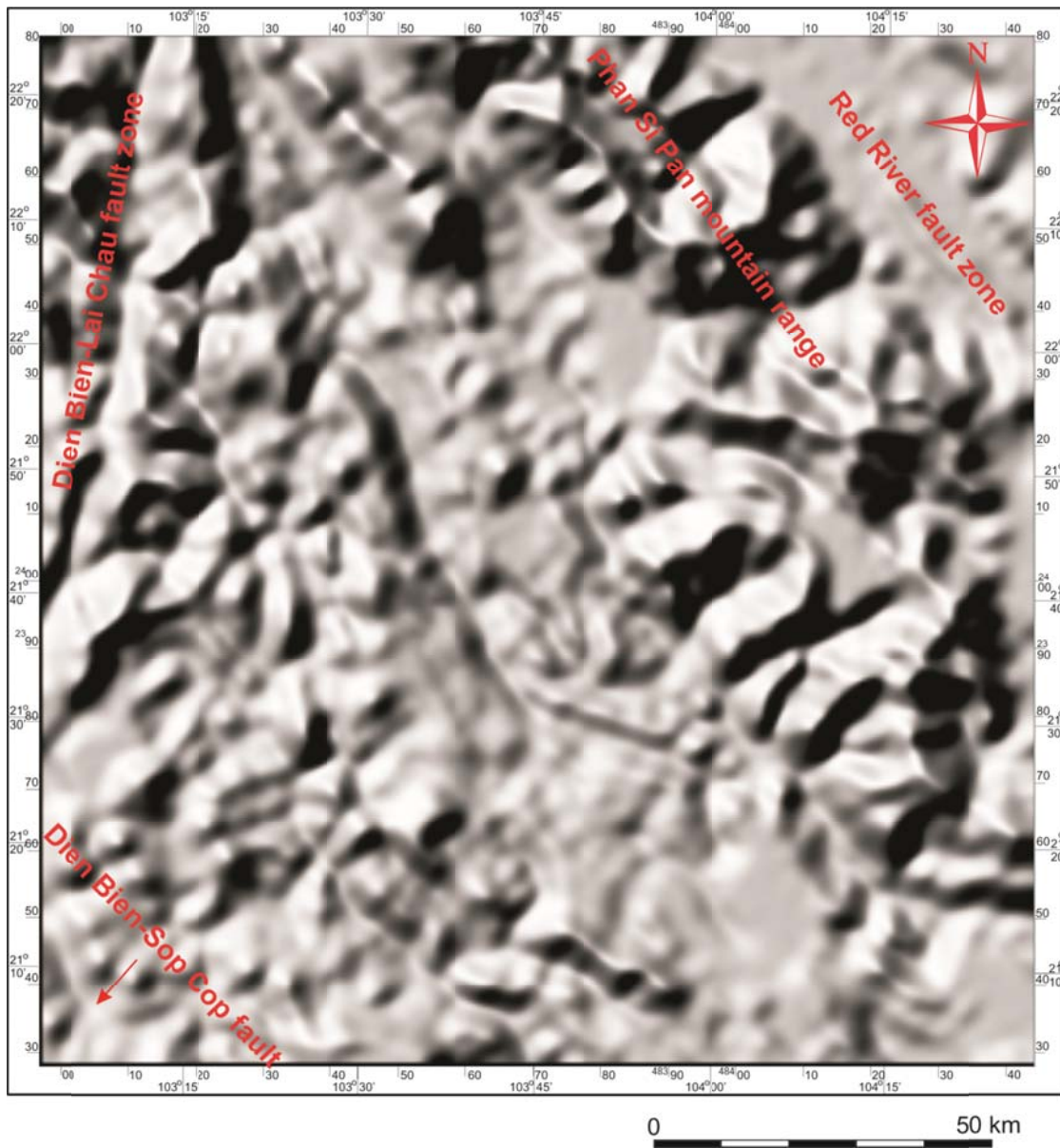


Fig. 1.2. Location of the Northwestern Vietnam marked on the digital elevation model showing the Red River fault zone, Dien Bien-Lai Chau fault zone, Dien Bien-Sop Cop fault and Phan Si Pan mountain range.

### 1.3. Modern geomorphology and hydrographic features

Morphologically the Vietnam area is a mountainous region, with over three quarters of the land area covered by hills and mountains. The mountain areas fall superficially into three distinct regions: (1) the mountains of northeastern Vietnam, which lie at the northeast of the Red River; (2) the Hoang Lien Son ridge area of northwestern Vietnam, northwest of the Red River, which represents a southern extension of the Himalayas; (3) the Truong Son (Annamite) range forms the backbone of Southeast Asia along the western border of Vietnam.

Other distinct geomorphologic areas of the country are coastal plains and the wide leveled alluvial valleys of the Me Kong and Song Hong (Red River) rivers.

The Northwestern Vietnam belongs to the southern extension of the Himalayas (Henduan mountains) extending from Yunnan into northern Vietnam. It contains number of high elevations range – Hoang Lien Son, Phi Si Lung and Phu Den Dinh. They form a large, clearly outlined montage region in the northwest of the country, with a relatively large area of uplands above 2000 m, and a number of peaks reaching 2500-3000 m a.s.l. The highest points of mainland Southeast Asia are situated here, they are the Phan Si Pan (3143 m), Ta Giang Pinh (3096 m), Phi Si Lung (3076 m), Luong (2985 m), Phoung Chang (2825 m), Lang Kung (2817 m) and many others. Most of them are formed by Upper Mesozoic granite intrusions or quartzites. To the south of main ridges lies at an area of complex, foldbelts known as the Song Da and Dien Bien Phu synclines and the Song Ma anticline (Fromaget, 1941).

Continuous limestone Sin Chai, Son La and Moc Chau plateaus reaching elevations up to 1500-1700 m a.s.l. spread along the Da River from the Chinese border to the South China Sea coast. Narrow canyons or very deep river valleys separate the plateaus and ridges. These Sin Chai, Son La, and Moc Chau plateaus are made up by Devonian and Triassic limestones. They contain spectacular areas of highly eroded karst topography such found within Lai Chau, Son La, Hoa Binh, Thanh Hoa, Nghe An and Quang Binh provinces (Dovjikov *et al.*, 1965).

Due to geomorphologic characteristics, most drainage networks of the NWVN flow in southeastward direction (Fig. 1.3). Different trends occur in the Lai Chau area. Da River changes few times its direction, finally flowing southeastward toward the Bat Bat (Son Tay) area. It is probably caused by the geodynamic regime during Cenozoic times, expressed by movement along the Song Da fault zone.

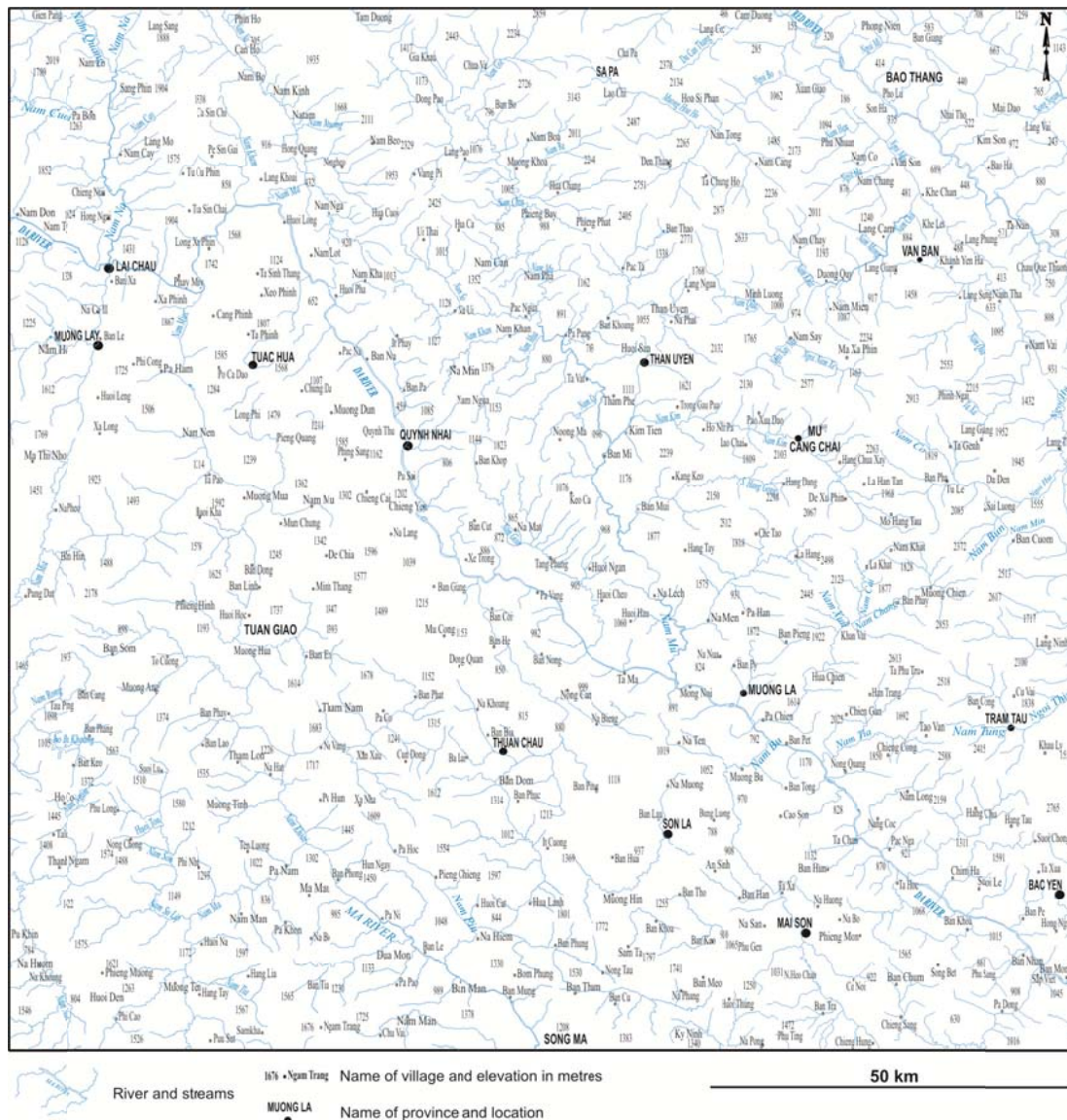


Fig. 1.3. Drainage network map of the NWN area (compiled from State Department for Cartography, and Geodesy and Cartographic Department of General Staff of the Vietnam published from 1990 to 1994).

#### 1.4. History of Investigations

Copper, zinc, tin and gold have been mined in Vietnam since the Bronze age and silver, iron and some non-metallics (especially kaolin) probably since the 1st century B.C. They were extracted mostly by Chinese miners, migrating to Vietnam especially under the Ming dynasty; "Chinese workings" are found on numerous mineral deposits. The exploitation of the country mineral resources was intensified after the French occupation of Indochina in 1884. Coal, gold, tin, chromite, zinc, antimony, apatite, talc and some other minerals were exploited from the beginning of this century, mainly for the export to France. Particularly, since the beginning of the 20th century the French has exploited lead, zinc and copper from Hoa Binh area and coal from Quang Ninh province. Dussault (1920) had done a preliminary survey of small area in the

northern part of the NWVN on a large scale (1:500,000) during the first stage of deposits' exploration in the Laos's territory and nearby area of Vietnam. One year later, in 1921, a general investigation on the regional geology of the NWVN was realized by Jacob (1921) in the framework of geological study on "Nord Annam et le Tonkin" in Central and Northern Vietnam. During this work, the first geological map of the Van Yen area (belongs to NWVN) was constructed, reflecting some nappe elements (thrust faults). Using Jacob's (1921) results, Fromaget (1928, 1937, and 1941) has compiled the Geological Map of Northwestern Tonkin and Northern Upper Laos in 1:500,000 scale, and mapped out the basic outlines of geological structures on the NWVN. The famous Fromaget' point of view well defined basic fold and thrust deformation in the SE Asia that took place in Triassic and was marked by the unconformity of Upper Triassic red beds, resting on underlying folded Middle Triassic strata. Fromaget (1928, 1937, and 1941) has originally introduced and established the name Indosinian orogeny as well as divided SE Asia according to the Indosinian structural framework. During this time, the French geologists have established petrological studies of the alkaline magmatism in Vietnam. The alkaline amphibole (arfvedsonite) and alkaline pyroxene (aegirine) minerals were described for the first time by Idding (1913) from magmatic rocks of the Phong Tho – Lai Chau area. Bourret (1922, 1925) has described some outlines of the metamorphic rocks and plutons in the North and North Central Vietnam, the nepheline syenite gneisses – hastingsite was described from the Pia Ma massif (northwestern Bac Kan area).

Since 1960, the Russian and Vietnamese geologists used the geosynclinal theory to analyze structure and tectonics of the SE Asia and NWVN, especially as the research works of Dovjikov (eds., 1965), Gatinskii *et al.* (1970), Ngo Thuong San (1965), Tran Duc Luong (1970), Tran Van Tri *et al.* (1977), etc. However, their ideas have provided answers concerning questions on unified tectonic boundaries, structural units and their distributions, geodynamic evolution, metallogenic potentials, and so on.

Based on mapping and geological surveys, the Geological Map of Northern Vietnam at 1:500,000 scale was compiled by Dovjikov (eds., 1965). In this map, NWVN area was investigated in details, and clarified many stratigraphic and magmatism problems. Since 1965, the Geological Mapping Divisions (GMD) at the geological survey of Northern Vietnam issued geological map sheets of the smaller scale of 1:200,000. Tran Van Tri (eds., 1977) modified the Geological map of northern Vietnam on the scale of 1:1,000,000.

Also from 1975, the theory of global plate tectonics was applied for the first time by Le Thac Xinh and Ta Hoang Tinh (1975). They attempt analyzing the structures and metallogenic epochs of Vietnam. Soon after their work, Le Nhu Lai (1980, 1983), Nguyen Xuan Tung (1982, 1992), and Le Thac Xinh & Nguyen Dang Dat (1984) presented tectonic evolution of the Vietnam follow the plate tectonic theory. They argued that in the NWVN area represented the rifted regime, perhaps related to the ophiolite belt, and in the Song Ma and Song Da zones, there was a post rifted regime that took place along cataclastic fault zones in Late Triassic. On a SE Asia scale, several publications, such as Hutchison (1975) or Huang (1977), applied the plate tectonics on structural and tectonic investigations. In addition, some authors also combined the geosynclinal and plate tectonic theories for interpretation and analysis of the

geological structure of Vietnam (Nguyen Nghiem Minh, 1978; Tran Van Tri, 1994). It was not until 2006 when several time interval maps (thirty two) have been presented, which depict the global plate tectonic configuration as well as paleogeography and lithofacies for SE Asia region from Cambrian to Neocene (Golonka *et al.*, 2006a). These authors recognized several blocks and events shaping the complex tectonics of Northwestern Vietnam.

From 1992 to 1996, the revision of the complete mapping set of North Central Vietnam sheet series including NWVN area was processed by GMD with the exposition of main data about mineral resources on the geological map. These revisions include in addition the supplementation of new materials received in recent years on geology, as well as on mineral resources. Based on these results, Tran Duc Luong and Nguyen Xuan Bao (1995) conducted detailed petrological studies and well defined series of the magmatic rocks in Vietnam. Moreover, Tran Trong Hoa *et al.* (1996, 1998) investigated granitoid rocks in the Northern Vietnam using geochemical and geochronological methods. They recognized tectonic settings of these rocks as well as metallogenic evolution of the Northern Vietnam. Recently, a review of the nature and distribution of the magmatism of the Truong Son belts led to distinguishing a southward oceanic subduction along Song Ma zone beneath Indochina block (Tran Trong Hoa *et al.*, 2008).

Together with geological mapping, mineral resource explorations and small scale metallogeny research in NWVN were conducted during the period from 1965 to 2000. It was not until 1991 when a Metallogenic map of Vietnam on 1:1,000,000 scale was assembled and published (Nguyen Nghiem Minh & Vu Ngoc Hai, 1991), in which NWVN was recognized as an area having Au, Ag, Pb-Zn, Sn, W-Mo (Be), and Cr potential. Furthermore, Nguyen Ngoc Lien (ed., 1990) reported details on the mineral deposits of the Song Ma, Song Da zones, and Tran Van Tri (ed., 2000) also reported on the mineral deposits of Vietnam.

From 1999 to 2009, the cooperation between the Polish Academy of Sciences and the Vietnamese Academy of Science and Technology was carried out. During this period, several field missions were organized in northern Vietnam, including the NWVN area. Research was focused on “Geodynamics of the Northern Vietnam”. Polish team included Professors Witold Zuchiewicz, Antoni K. Tokarski, Anna Świerczewska and Andrzej Żelaźniewicz among the others. The results of the investigation were published in several papers, one of the most important publications is special issue on the Cenozoic geodynamics of northern Vietnam by Nguyen Trong Yem, Tokarski, A. K., Tran Trong Hoa, Zuchiewicz, A. W., Tran Tuan Anh, Świerczewska, A., and Nguyen Quoc Cuong, eds. (2009).

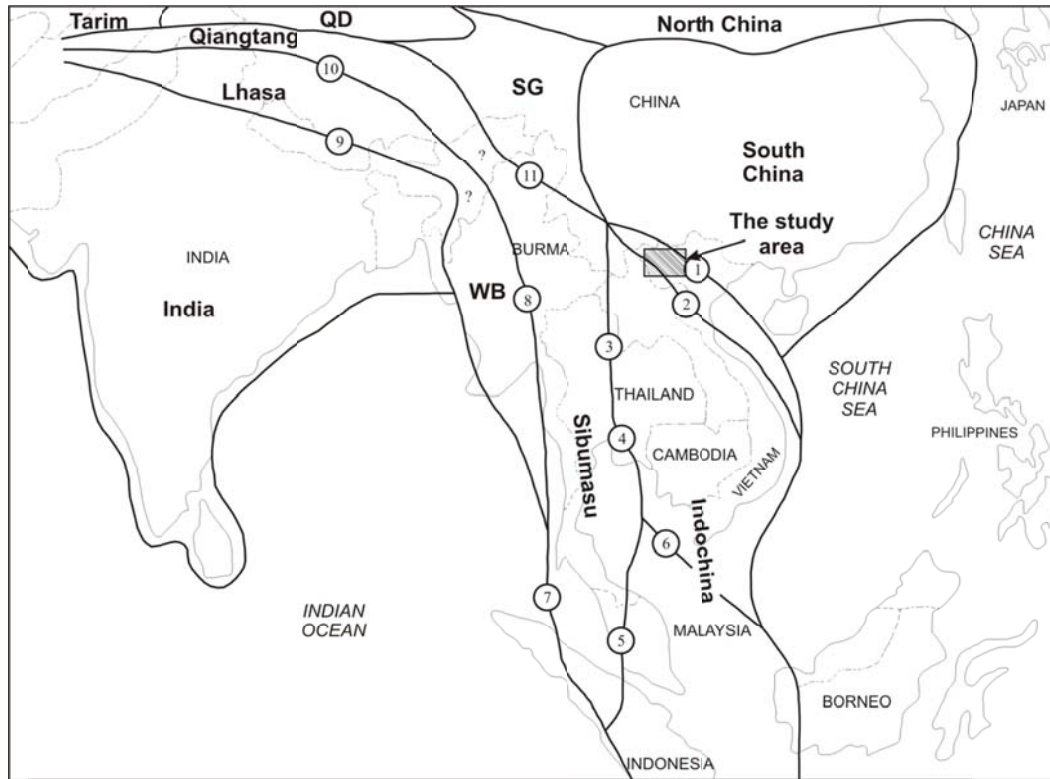


Fig. 1.4. Main plates and terranes of Southeast Asia. Partially from Metcalfe (1998), Golonka (2006a,c).

WB - West Burma

SG - Songpan Ganzi accretionary complex

QD - Quidam terrane.

Sutures and major strike-slip faults:

1 - Red River zone, 2 - Song Ma, 3 - Nan-Uttaradit

4 - Sra Kaeo, 5 - Raub Bentong, 6 - Three Pagodas,

7 - Woyla, 8 - Shan boundary

9 - Indus Yarlung Zangbo

10 - Banggong, 11 - Ailaoshan.

## 2. OUTLINE OF GEOLOGY

### 2.1. General geology

Most lithologies of the NWVN are Mesozoic sedimentary sequences including acidic volcanic rocks, and carbonates and terrigenous sedimentary rocks. Neoproterozoic, Proterozoic, Palaeozoic and Cenozoic rocks consisting of flysch, carbonates sedimentary rocks, schists, phyllites and basalts, and Quaternary sediments also occur therein. Generally, the Neoproterozoic, Proterozoic, Palaeozoic and Mesozoic lithologies were intruded by the Palaeozoic, Mesozoic and Cenozoic intrusive bodies (Fig. 2.1).

#### 2.1.1. Sedimentary rocks

More than forty lithostratigraphic formations have been identified in the NWVN. They are divided into 8 complexes.

1. Neoproterozoic complex includes Xuan Dai group, Nam Su Lu and Nam Co formations, Bo Xinh group and Sa Pa group.
2. Cambrian complex contains Cam Duong, Ben Khe, and Ham Rong formations.
3. Ordovician – Silurian complex contains Dong Son, Sinh Vinh and Bo Hieng formations.
4. Silurian – Devonian complex contains Ban Pap, Nam Pia, Tay Trang, Nam Cuoi, Ban Nguon, Nam Sap, and Ban Cai formations.
5. Carboniferous-Permian complex includes Da Nieng, Bac Son, Ban Diet, Yen Duyet, Si Phay, Na Vang formations.
6. Triassic complex includes Tan Lac, Hoang Mai, Dong Giao, Nam Tham, Muong Trai, Lai Chau, Nam Mu, Pac Ma, Suoi Bang formations.
7. Jurassic-Cretaceous complex contains Nam Thép, Nam Po, Nam Ma, Yen Chau formations.
8. Neogene - Quaternary sediments form the last complex.

Mesozoic terrigenous, terrigeno-effusive and acidic effusive formations occupy the large central part of the NWVN, while Proterozoic, Palaeozoic flyschoid and carbonaceous sedimentary formations cover smaller area in the northeast and the southwest parts of NWVN. The Cenozoic formations are distributed mainly along the river catchment's area. The Palaeozoic and Mesozoic sedimentary rocks have been intruded by Mesozoic granites and small Cenozoic intrusive bodies.

### ***2.1.2. Magmatic units***

Magmatic rocks consist of intrusive and extrusive rocks, occupying large part of the NWVN (Fig. 2.1) and forming bodies of various sizes (Tran Van Tri, ed., 1979; Tran Duc Luong & Nguyen Xuan Bao, eds., 1995). Main magmatic activities took place during Late Palaeozoic, Mesozoic and Cenozoic, resulting in various types of granites, gabbros and acidic volcanic rocks, namely: Nui Nua and Ban Xang ultramafics, gabbroic Bo Xinh, Chieng Khuong granitoid complexes, Huoi Hao basalt Formation; Cam Thuy, Vien Nam mafic effusive formations, Dien Bien Phu, Song Ma, Phia Bioc granitoid complexes; basalts of Suoi Be Formation, gabbroic Nam Chien, Tu Le-Ngoi Thia volcanic, Muong Hum, Phu Sa Phin, Ye Yen Sun granitoid complexes; Nam Xe-Tam Duong, Pu Sam Cap, Coc Pia subalkaline to alkaline syenite complexes, and Pu Tra volcanogenic Formation. The Proterozoic gabbroic Bao Ha and granite of Xom Giau complexes are distributed along Red River fault zone and in NE area, while Palaeozoic mafic-ultramafic Nui Nua, gabbroic Bo Xinh, granitoid Chieng Khuong, Song Chay complexes are distributed in both NE and SW parts of NWVN, along Song Ma and Song Hong fault zones. The Cenozoic igneous rocks, comprising Ye Yen Sun, Nam Xe-Tam Duong, Pu Sam Cap, Coc Pia granitoid complexes, are distributed in central part of the NWVN area.

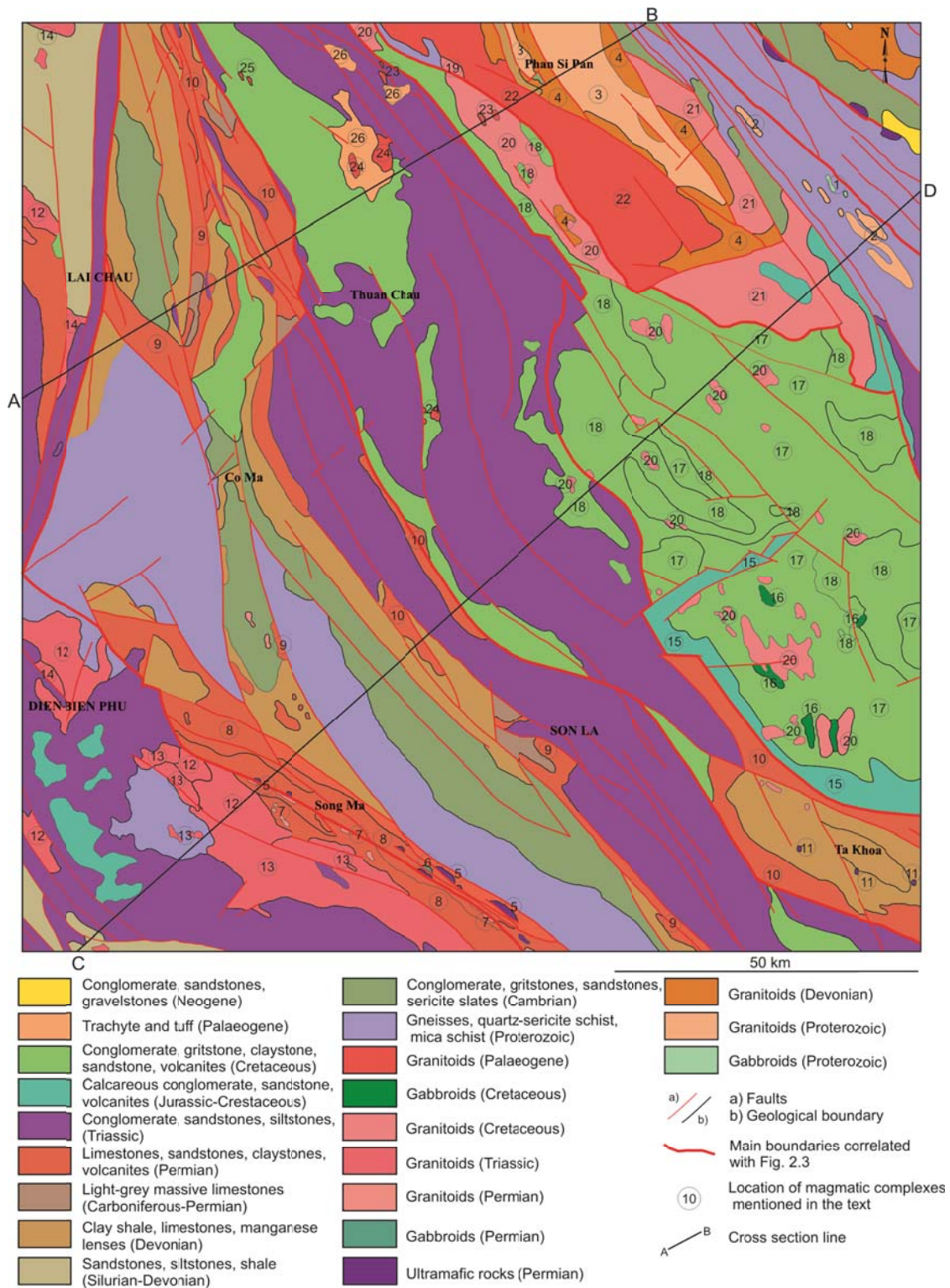


Fig. 2.1. Geological map of the NWNV area (compiled from geological maps of the northern Vietnam at 1:200,000 scale). 1 – Bao Ha complex, 2 – Xom Giau complex, 3 – Po Sen complex, 4 – Song Chay complex, 5 – Nui Nua complex, 6 – Bo Xinh complex, 7 – Chieng Khuong complex, 8 – Huoi Hao Formation, 9 – Cam Thuy Formation, 10 – Vien Nam Formation, 11 – Ban Xang complex, 12 – Dien Bien Phu complex, 13 – Song Ma complex, 14 – Phia Bioc complex, 15 – Suoi Be Formation, 16 – Nam Chien complex, 17 – Tu Le volcanic

subcomplex, 18 – Ngòi Thia volcanic subcomplex, 19 – Muong Hum complex, 20 – Phu Sa Phin complex, 21 – East Ye Yen Sun complex, 22 – West Ye Yen Sun complex, 23 – Nam Xe-Tam Duong complex, 24 – Pu Sam Cap complex, 25 – Coc Pia complex, 26 – Pu Tra Formation.

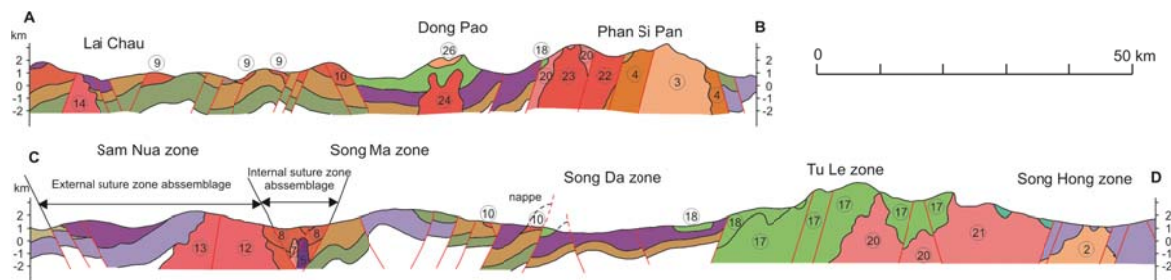


Fig. 2.2. Generalised cross-sections across the NWVN area. Cross-section locations on Fig. 2.1.

## 2.2. Geological structures

### 2.2.1. Faults

Faults of the NWVN play an important role in the present structural plan. Major fault systems represent the main dividing boundaries of tectonic regions, zones and structural complexes. Most faults trend NW-SE are of NW-SE, some faults display also sub-longitudinal and sub-meridian directions. In many cases they have a long development history showing also resuscitating during neotectonic stage. Generally, it is possible to divide the fault systems of NWVN into marginal deep seated, marginal, and intrazonal faults.

#### *Northwest-southeast fault system*

1. Song Ma (Ma River) fault. It is not only a single fault but to a complex set of major parallel fault systems, which extend along the Valley of Ma River, from the Chieng Khuong to Pac Nam and Bo Xinh. Depending on location, local name were also assigned in Vietnamese literature (Na Hiem-Phieng Na, Chieng Khuong faults etc.) to the segments of Song Ma fault. Small-size ultramafic bodies are arranged in strings along the fault zone, there is. The foliated mafic effusives of the Bo Xinh complex and metamorphosed rocks of the Nam Co Formation arranged along the edge of the fault belong to these bodies. The rocks of the Dien Bien Phu complex are crushed and mylonitized along the southwest contact of fault zone. The mylonitization zone is hundred meters wide. Hydrothermal alterations developed along the margin of Song Ma granite massif. Two deep-seated faults of the system define the boundary between the Sam Nua and Song Ma structural zones. These nearly vertical faults have displacement amplitude of 1.6-2 km and a depth of about 30km (Nguyen Nghiem Minh & Vu Ngoc Hai, 1991). The Song Ma fault shows a long development history which has been lasted from Pre-Cambrian to the present day. This history is evidenced by various phases of magmatic intrusions and extrusives of various ages and genesis along the fault strike. Morphodynamic features of the Song Ma fault zone are very complex, displaying changes associate with the fault evolution. Present tectonic activities of the fault zone can be recognized by earthquakes.

2. Son La fault. This is a dextral strike-slip fault with the slip surface dipping northeastward. It consists of several faults. The major Thuan Chau-Na Vien fault, regarded as a fault zone, display features of typical strike-slip, deep-seated fault. The other small faults control the linear structure of the Song Da structural zone. The overthrust faults play important role in this zone. From Huoi Long through Chieng Ve to Suoi Nhu, on the distance above 150km, the Son La fault separates the Late Palaeozoic-Early Mesozoic and Late Proterozoic plates. The rocks are laminated along the cataclastic zones in this zone. The mafic effusives of the Cam Thuy Formation are associated with this zone. In the Song Ma area, , the Son La fault plays a role of an intrazonal fault, which is formed along anticline fold axis of the Song Ma structural zone.

3. Song Da (Da River) fault. This fault is located along the left side of the Da river. It stretches northwestward, including some upthrow fault of southwestern dip. It plays the role as the boundary between the Song Ma and Song Da structural zones. Thus, it can be considers as a marginal fault. Along the fault, there is a destruction zone accompanied by Late Permian-Early Triassic mafic effusives of Vien Nam Formation. In some places, there is a small through filled up with Late Triassic coal-bearing beds of the Suoi Bang Formation. These features are perhaps associated with the opening of the Song Da ocean in Permo-Triassic and its closing during Late Triassic times. Geomorphologic observations allow to distinguished many narrow valleys (Nam Que, Pa Ha, etc.) along the fault. The occurrences of thermal water sources are also common along the fault zone. Therefore, the fault is still activating in the present time. Results of geophysical investigations indicate the Song Da fault plunge northeastward with a dip of 65°.

4. Van Yen-Nam Xe-Phong Tho fault. It is also known as the Muong La-Bac Yen or Phong Tho-Nam Pia fault (Phan Trong Trinh, 2004; Tran Van Thang & Van Duc Tung, 2006). It consists of several winding faults, some of them plunge southwestward. They extend long the Nam Mu stream and play the role of the boundary between the Tu Le and Song Da structural zones. In the study area, this fault stretch from Bac Yen through Phong Tho to the Vietnam-Chinese border. The fault zone often contains the mafic effusives attributed at present to the Vien Nam Formation accompanied by felsic and alkaline intrusives of Cretaceous to Palaeogene age. Geomorphologic studies indicate the existence of depressions along the faults. These lowlands form several narrow valleys. According to gravitational data, the Van Yen-Nam Xe-Phong Tho fault plunge southwestward with a dip of 60°. It stretches on hundreds kilometers.

5. Song Hong (Red River) fault includes some faults trending in NW-SE direction. This is a system of normal faults. According to the geological and geophysical data, most of them plunge northeastward with the dip of 72°. The deformations within the Song Hong fault zone reach depth of ~30km and width of 22km. Many pull-apart basins are associated with the fault zone, they form grabens filled up with Neogene sediments of great thickness. Ultramafic intrusions of unknown age and thermal water occurrences are also associated with the Song Hong fault zone.

6. Phong Tho fault. This fault is situated in the margin of Hoang Lien Son along boundary between the Phan Si Pan and Tu Le zones and displays features, we can consider of a marginal

fault. The Phong Tho and Van Yen-Nam Xe-Phong Tho faults form a “handle” of the Tu Le structural zone as a “the Tu Le ladle” (Tran Van Tri *et al.*, 1977). Cenozoic mafic intrusion of the Muong Hum complex, alkaline rhyolites of the Tu Le subcomplex and granite, granosyenite of the Phu Sa Phin complex occur along the fault zone.

7. Dien Bien-Sop Cop fault. It is located in the southwestern part of the investigated area and clearly visible on a surface. Dien Bien-Sop Cop fault extend from the Dien Bien, Tay Trang through Muong Xoi to Sop Cop, trending in NW-SE direction and forming crushed zones from 10m to over 100m wide. The Tay Trang Formation, upper Palaeozoic limestone of the Bac Son Formation and coal-bearing bed of the Suoi Bang Formation occur along the fault zone. Thermal and mineral springs are common along the fault. According to the results of gravitational studies, this intrazonal fault, plunges at 85-90° angle, with the displacement amplitude of 1.5km. Moreover, many small faults of the NW-SE direction play a role in deformation of intrazonal structures.

#### *Northeast-southwest fault system*

This fault system is weakly developed in the study area; there are only some small faults in the southwest of Dien Bien town and distributed in the Phan Si Pan structural zone, in upper course of the Nhap, Chum, Suoi Be, and Ti Ang streams. In the northeastern area, they are mainly distributed in the Tu Le middle-late Mesozoic intracontinental volcanic depression zone generally of 2.5-10 km long.

#### *Sublongitudinal fault system*

The Dien Bien-Lai Chau fault zone is composed of two nearly parallel main faults stretching in longitudinal direction from the Lai Chau town to Dien Bien town. Generally, the Dien Bien-Lai Chau regional fault is rather steep, plunging ~85° northeastward, forming the boundary between the Song Ma and Muong Te structural zones. A long graben filled up with Middle-Late Triassic terrigenous beds of the Lai Chau Formation developed in the fault zone. The fault strike-slip movement during Cenozoic times is responsible for the origin of the Dien Bien Phu valley. Present tectonic activities of the fault are expressed by earthquakes.

#### **2.2.2. Nappes**

Ductile thrust nappes, with associated recumbent folds exist in the NWVN area. The involved material is affected only by low-grade metamorphic conditions. The nappes system is equivalent to the “nappe néotriasique” defined in Tonkin (presently northern Central Vietnam) by Fromaget (1937, 1941), thus confirming the validity of his descriptions and interpretations.

The A-B and C-D geological cross sections for NWVN extend from southwest to northeast and represent general structure and fault characters of the study area. The first section (Fig. 2.2), from the Dong Bao area to near Phan Si Pan mountain range, shows coarse sandstone, calcareous siltstone, and black clay shale, mapped as Triassic. Towards to NE, the Cretaceous conglomerates and sandstones, and subvolcanic rocks dominate. The section depict the older Triassic rocks thrust over younger Cretaceous strata, indicating some existence of thrust faults (nappes) in this area.

The second section (Fig. 2.2), from the Sam Nua to margin of Song Ma zones, shows the relationship of the suture assemblage with other structural features. On the basis of the spatial occurrence, relationship between tectonostratigraphic assemblages as well as the deformational styles, the suture zone can be subdivided into two distinctive parts, the internal and external zones. The internal zone incorporates reworked and highly strained rocks, represented by exotic, mélangé-style tectonic blocks of variable size, composition, and origin. These blocks include abundant ophiolitic-style ultramafic and mafic boudins, which are possibly derived from ancient oceanic complex, mylonitized plagiogranitic gneisses or marbly limestone blocks, and other paragneissic and/or orthogneissic remnants. The exotic blocks are bounded by highly-strained mylonitic zones that extend tens to hundreds of km, within which all rocks were flattened, strongly sheared, isoclinal folded and heavily metamorphosed up to amphibolite facies. The external zone is flanked by dismembered, variably strained early Palaeozoic heterogeneous sedimentary packages comprising silicic, calc-silicate and volcanogenic successions, or high-grade Neoproterozoic metasedimentary assemblages. Towards to NE, about 100km southwest of the Red River fault zone, the Song Da (Da River) has formed a deep valley in folded Palaeozoic and Triassic sediments. Upper Palaeozoic to Lower-Middle Triassic rocks are considered to have occurred in a subsident basin, the “Song Da rift”, together with basaltic volcanism and intrusions of Late Permian to Early Triassic in age, exposed North of the Yen Chau area. These Palaeozoic and Triassic rocks are thrust over Cretaceous red conglomerates and sandstones of the Yen Chau Formation (Lacassin *et al.*, 1998). Within the Upper Palaeozoic to Lower-Middle Triassic rocks involved in the nappes pile, the strike of the isoclinal fold axes and stretching mineral lineations is consistently around N-S and kinematic criteria indicate a top-to-the-north sense of shear.

These geological cross sections for NWVN reveal a clear sequence of geological processes that are easily linked to the sequence of events that occurred during Triassic and Cretaceous times. The tectonic style with nappe emplacement characterizes of the Triassic Indosinian orogeny northwestern Vietnam. It contrasts with the later strike-slip Cenozoic deformations with associated magmatism (Lepvrier *et al.*, 1997, Tran Trong Hoa *et al.*, 2008a) in the Truong Son belt and Phan Si Pan – Red River zone of Northern Vietnam.

### **2.3. Plate tectonics**

East and Southeast Asia comprise different terranes and blocks, which were derived from the northern margin of Gondwanaland (Leloup *et al.*, 1995, 2001; Findlay, 1997, Findlay & Phan Trong Trinh, 1997; Tran Ngoc Nam, 1998; Fan, 2000; Carter *et al.*, 2001; Golonka *et al.*, 2006a). Successive rifting and breakup formed several continental blocks during Palaeozoic and Mesozoic times. The northward movement of these blocks resulted in the amalgamation of present-day Southeast Asia. The closing of the Palaeotethys between the blocks led to the formation of several sutures like Song Ma, Song Da, Nan-Uttaradit and so on (Metcalf 1996a,b, 1999, 2006; Golonka *et al.*, 2006a).

Metcalf (1998, 2002) and Golonka *et al.* (2006a, c) distinguished a number of plates and terranes within Vietnam and adjacent areas (Fig. 1.4). The northwestern Vietnam (NWVN)

belongs to Indochina (ICB) and South China (SCB) blocks. The SCB includes southern part of China and northeastern fragment of Vietnam. It is separated from North China by the Quingling-Dabie suture, from Indochina by Song Ma suture, from the Sibumasu Plate by the Ailaoshan suture, from the Songpan-Ganzi accretionary complex by the Longmenshan suture. The southeastern margin of South China is a passive margin connected to South China Sea by extended continental crust. To the East SCB is bordered by the Taiwan foldbelt and the Okinawa trough passive margin. The SCB block was finally formed during Precambrian times.

The Indochina block (ICB) comprises the countries of Vietnam, Laos, Cambodia and western Thailand, perhaps also southeastern part of Malayan Peninsula, a fragment of Sumatra and the westernmost fragment of Borneo belong to ICB. To the West ICB is separated from the Sibumasu plate (from south to north) by Raub-Bentong, Phra Kaeo and Nan-Uttaradit sutures; to the northeast it is separated from the SCB by the Song Ma suture. The eastern margin of Indochina is a passive margin connected to South China Sea by extended continental crust.

The tectonic structure of Northwestern Vietnam results from three major collisional events that took place during the Palaeozoic, Permo-Triassic and Cenozoic (Khuong The Hung & Golonka, 2008). The large scale (~600 km) sinistral displacement along the Ailao Shan-Red River (ASRR) shear zone occurred during  $\sim 27 \pm 22$  Ma (Chung *et al.*, 1997) event. The suture between Indochina and South China is located along the Song Ma belt. The Song Ma belt is characterized by the occurrence of mafic and ultramafic masses originated in oceanic domain and metamorphosed into Lower Palaeozoic greenschists. They are unconformably covered in many localities by Devonian redbeds (Hutchison, 1989). These mafic-ultramafic rocks have been widely interpreted as ophiolitic fragments, derived from the Paleo-Tethys and obducted during the collision of Indochina with South China (*e.g.*, Golonka *et al.*, 2006a and references therein). Moreover, the Song Ma ophiolite can be correlated with the Shuanggou ophiolite cropping out in the south of the Ailao Shan range (Zhang *et al.*, 1994; Graciano *et al.*, 2008). These ophiolitic belts delineate the boundary between Indochina and South China. The collision time had previously been thought to be Silurian based on a greenschist metamorphic age of  $\sim 455$  Ma obtained by the K $\pm$ Ar method (Tran Van Tri, ed. 1979). Recent data about metamorphic terranes in Vietnam recorded that the Indosinian metamorphism occurred  $\sim 250$  Ma ago overprinting older events (Lepvrier *et al.*, 1997, 2004, 2008, Lepvrier & Maluski, 2008, Lan *et al.*, 2000; Tran Ngoc Nam, 1998). This implies that the final suturing between Indochina and South China took place in the earliest Triassic, during the early phase of the Indosinian orogeny that resulted in regional metamorphism and magmatism (Hutchison, 1989). However, the tectonic model that fully explains Indosinian orogeny still requires further detail geochemical and geochronological investigations on the constituent rocks.

#### **2.4. Tectonic subdivision of Northwestern Vietnam**

Fromaget (1937, 1941) first distinguished structural units in NNVN and gave those names such as Phu Hoat and Song Ma arcs, Song Da depression, Song Ca and Sam Nua synclines. He called structural units in north Laos and Dien Bien – Lai Chau fault zone the “Upper Laos element”, distinguishing Burmese element in the western Upper Laos. Dovjikov

(ed.) *et al.* (1965) defined the entire North Vietnam as the geosynclinal's domain turned into folded Mesozoic, distinguishing Sam Nua depression as a structural unit within the Truong Son folded region. Since 1965, Vietnamese geologists have followed these ideas researching geology of Vietnam. Tran Van Tri *et al.* (1977) conducted detail geological studies and described the NWNV area as the West Bac Bo Fold System, which extends between the Song Ma Suture and the Chay River fault. A deformed Upper Proterozoic and Lower Palaeozoic metamorphic belt occurs north of the Song Ma suture forming broad antiform unit, called the Song Ma Anticlinorium. Farther north, mafic and ultramafic rocks, intercalating Permian-Early Triassic terrigenous-carbonate sedimentary succession, form the strongly folded Song Da zone, which is unconformably overlain by Cretaceous red beds.

Based on present-day knowledge of plate tectonics, distinctive morphotectonic features, structure and lithostratigraphy, the general geology of northwestern Vietnam, depicted in Fig. 2.2, shows five geological entities, from the north to the south: Phan Si Pan-Song Hong, Tu Le, Song Da, Song Ma and Sam Nua regions.

**The Phan Si Pan-Song Hong (Red River) region**, which lies between the Song Chay and the Phong Tho faults and is dominated by a linear belt of highly strained high-grade schists assigned to the Proterozoic in Vietnamese geological maps. This region was referred to as the Phan Si Pan structural zone in Dovjikov (ed.) *et al.* (1965) or the Hoang Lien Son continental belt which belongs to the Tonkin – Yangtze – Cathaysia zone in Nguyen Xuan Tung and Tran Van Tri (1992). The northwestern part of this zone is occupied by the Phan Si Pan massif where the geology is dominated by migmatitic and granitic complexes offset sinistrally by major fault. Slivers of Cambrian to Devonian sedimentary sequences also occur in this zone and trend more or less northwest.

**The Tu Le region** was referred to as the Tu Le zone in Dovjikov (ed.) *et al.* (1965) or the Tu Le rift depression in Tran Van Tri (ed., 1977). It is located between the Song Da and the Phan Si Pan-Song Hong structures, and dominated by Jurassic to Cretaceous calc-alkaline volcanic units and continental sedimentary rocks.

**The Song Da region** is a part of the SCB; it is bordered to the northeast by the Van Yen-Nam Xe-Phong Tho fault and to the southeast by the Song Da fault. It was referred to as the Song Da rift depression in Tran Van Tri (ed., 1977) or the Song Da arc in Fromaget (1937, 1941). The Song Da terrane consists of Cambrian to Cretaceous sedimentary rocks ranging from marine carbonates to continental red beds, and includes a widespread series of Permian basalts and Permo-Triassic sedimentary series.

**The Song Ma region** is located between the Truong Son fold belt and the Song Da region. It is an arched northwest trending structure often referred to as the Song Ma Anticlinorium (*e.g.* Tran Van Tri, ed., 1979). It is dominated by low to high-grade unfossiliferous schists intruded by Devonian and Triassic granitoids, metagreywackes, greenschists, amphibolites, and marbles. The southern part of the structure contains serpentinitised ultramafic bodies referred to as ophiolites by Vietnamese geologists (*e.g.* Tran Van Tri, ed., 1979; Phan Cu Tien, ed., 1989 and references therein), and a gneissic plagiogranite called the Chieng Khuong complex. The Song Ma region also contains non-

schistose fossiliferous middle Cambrian limestones at Dien Lu and perhaps Permian Nui Nua ultramafic massif west of Thanh Hoa. The suture zone between the IDB and the SCB is located within the Song Ma region.

*The Sam Nua region (Truong Son fold belt)* is a part of the IDB within northwestern Vietnam; it is bordered to the northeast by Song Ma fault and limited westward by the border between Laos and Vietnam. This is a complex, faulted region with imbricated thrust fold and fault structures, dominated by Ordovician to Cretaceous sedimentary and subsidiary volcanic beds and contains possibly Cambrian but undated low to high-grade metamorphic rocks at Phu Hoat (Tran Van Tri, ed., 1977; Phan Cu Tien, ed., 1989). The Triassic to Cretaceous units in northern part of the fold belt could be correlated with those in the Song Da zone (Tran Van Tri, ed., 1977; Phan Cu Tien, ed., 1989).

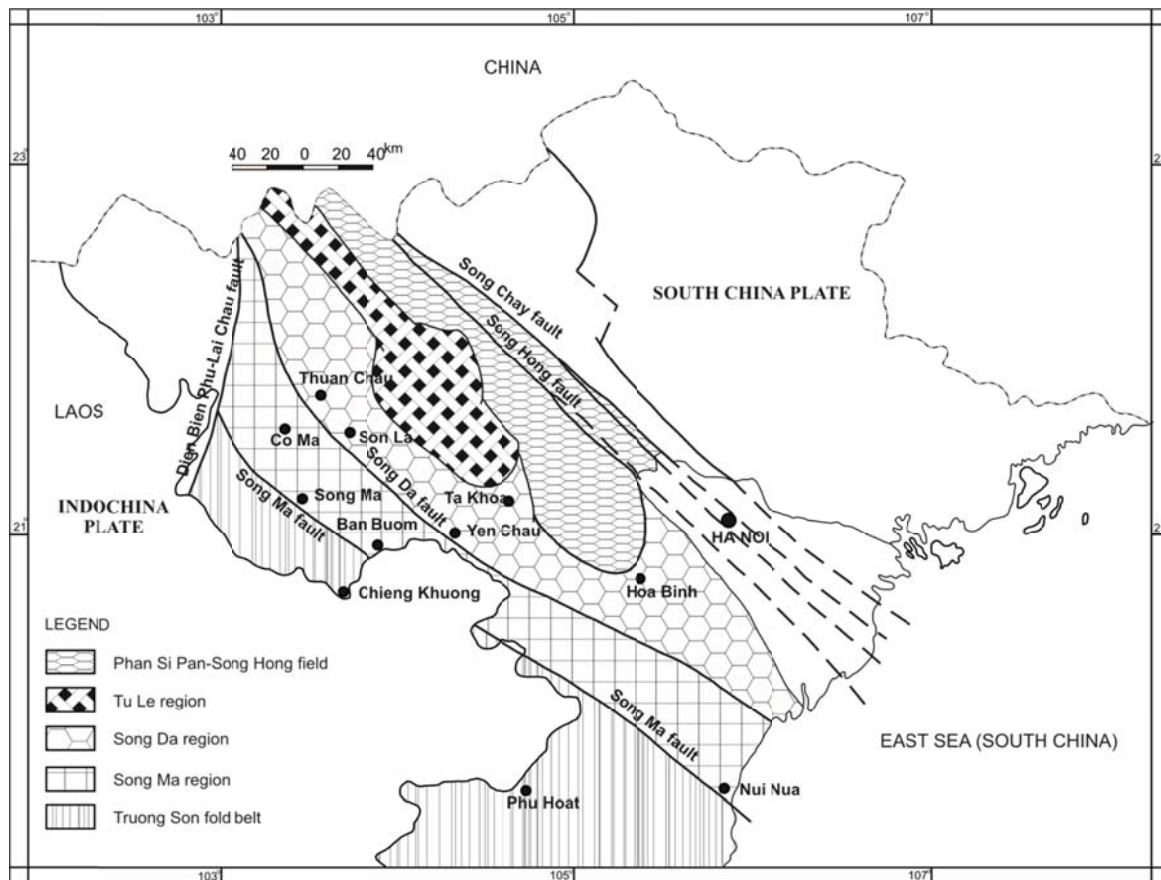


Fig. 2.3. Geological terrane map of the Northwest Vietnam (after Tran Van Tri ed., 1979).

### 3. METHODOLOGY

Detailed structural field work was done to establish a generalized geological map of the NWVN area. The structural features in this map include faults and lineaments. The structures factors were specified through geological map and National Remote Sensing Center's photogeological interpretation of SPOT HRV images (XS mode) on scale of 1:100,000, a

remote sensing image quotes from <http://earth.google.com> and Digital elevation model analysis was done for parts of this area.

### 3.1. Division of magmatic rocks

In the Northwestern Vietnam (NWVN), magmatic intrusions and effusions have mainly acid and minor mafic to ultramafic compositions (Fig. 2.1). They have been subdivided into 21 complexes and 5 formations through Proterozoic to Cretaceous times. The scientific research on the magmatic rocks of NWVN area applying new technology led to new results and different interpretation of the origins of geological events. Therefore, carrying out a synthetic review of the magmatic rocks is necessary in order to provide a comprehensive overview of the regional geology. This dissertation presents the overview of petrographic, geochemical and geochronological studies on different magmatic rock types from the NWVN area. It also attempts to explain mechanism responsible for magmatic processes and help to understand the magmatic characteristics and the tectonic implications. The author's research is combined with results obtained by the Department of Geology and Minerals of Vietnam (DGMV). The geochemical, mineralogical and geochronological data were given mainly by Tran Trong Hoa (1996, Tran Trong Hoa *et al.*, 1999). Some newest data were published by Pham Trung Hieu *et al.* (2008, 2009). The magmatism history of northwestern Vietnam is also supported by 1:50,000-1:200,000 geologic maps and other recent geological studies (Bui Cong Hoa, ed., 2004, Bui Phu My, ed. *et al.*, 1977, Dinh Minh Mong ed., 1977 and references therein). The paper's interpretation is focused on: 1. the relationships between the NWVN area (including Phan Si Pan-Song Hong, Tu Le, Song Da, Song Ma and Sam Nua areas) and adjacent areas; 2. the magmatic evolution of the NWVN as a whole.

The complexes of granitoids are closely related to tectonic setting; therefore one can successfully use the mineralogy, chemistry and trace element discrimination diagrams for the tectonic interpretation of granitoids (Pearce *et al.*, 1977; Condie, 1997). Various discrimination plots are presented which sequentially discriminate the different tectonic environments. These plots used the GeoPlot software and some elements in the CorelDraw software. GeoPlot is a free VBA macro program used in Excel for plotting geochemical data. It has the following major plotting functions: X-Y plot and triangular plot, normalized spidergram, discrimination diagram, and the related functions such as calculating formulas and CIPW norm. GeoPlot also contains many normalization values used for spidergram and many discrimination diagrams. Users can also add new normalization values for spider diagrams and the specification data for a new discrimination diagram into GeoPlot. GeoPlot has the advantage over the existing stand-alone plotting programs because it allows data to be plotted and visualized easily in the Excel environment, which geochemists use to organize and evaluate the data. A menu and a toolbar in Excel allow easy management of data and functions. In summary, GeoPlot is practical and enables geochemists to plot data professionally. The source codes are accessible to all users and can be modified for special use. The software is developed by Jibin Zhou from Guangzhou Institute of Geochemistry Chinese Academy of Sciences.

### 3.2. The method of mineralization analysis

Metallogenic patterns in NWVN were influenced by spatial, temporal, or process-related factors. No single set of factors can (or should) explain these variations; rather, they reflect a combination of influences (Barton, 1996). These combinations include regional and temporal differences in the composition, thickness, thermal structure, and state of materials, nature of material transport, and depositional environments.

Tectonic setting provides a first-order control on the localization of mineral deposits and controls other factors favorable for the formation of mineral deposits. These factors include, for example: the form and composition of the associated igneous bodies, the formation of sedimentary basins and the characteristics of sediments that fill the basins, the development of faults and shear zones that provide conduits for mineralizing fluids or places for ore localization (Misra, 1999).

Igneous-related mineralization is ubiquitous where epizonal environments are preserved, thus preservation (and exposure) form the first-order filter on metallogeny. Mineralization includes porphyry, skarn, epithermal, replacement and syngenetic deposits of widely varying styles, metal contents and links to magmatic heat and materials. Metal contents and alteration styles correlate closely with igneous compositions and are broadly independent of setting, although systematic regional variations in metal ratios are documented. Ore element suites vary from Cu- Au- Fe associated with (quartz) dioritic to monzonitic intrusive centres through Cu- Zn- Mo- Pb- Ag- W- Au associated with broadly granodioritic centres, and finally to Fe-Mo-Zn-W-Ag- Be associated with metaluminous to strongly peraluminous granitic centers (Barton, 1996).

Effusive-related mineralization include epithermal Au-Ag-(Pb-Zn-Cu) veins, high-silica rhyolite volcanic center with F±Mo, felsic volcanic hosted - Cu-Pb-Zn-Ag-Au, mafic volcanic hosted - Cu (-Zn, - Au) or mixed volcanic/sedimentary - Cu-Zn (-Au).

The age of mineralization is a critical piece of information required for understanding the genesis of any mineral deposit, because the age provides constraints on potential controls of ore emplacement, such igneous activity, tectonic setting, metamorphic remobilization, sources of ore fluids and ore constituents, etc. In the study area, the problem's age of mineralization requires us to further research on geochronological and geochemical data. Problem solving will discussed them from constraints revealed by stratigraphic relations, such as cross cutting veins or dikes and restriction of mineralization to certain stratigraphic interval, metamorphism, and deformation. Mineral deposits, especially those hosted by sediments, are often described as *syngenetic* – formed contemporaneously with (and essentially by the same process as) the host rocks or *epigenetic* – formed later than the host rocks. An example is vein. The first step in the formation of a vein is the fracturing or breaking of rock along a fault zone, at a depth ranging from surface to several kilometers below surface. The rock must be solid (lithified) and brittle, creating open spaces when it breaks. Hydrothermal solutions pass along the fault zone and deposit or precipitate the ore and gangue minerals within the open spaces. Thus, the vein is necessarily younger than the rocks that contain it.

In some cases, we cannot estimate the relationship between mineral deposit and stratigraphy and we try to estimate the age of mineralization by dating associated minerals of ore clusters. Particularly, we are going to carry out the Rb-Sr dating of the single grain pyrite from molybdenum mineral association, the resulted dating of grain pyrite is also considered as time of forming molybdenum mineralization. Moreover, using available data from Vietnamese literature will allow us to discuss correlation between mineralization and host rocks, for example to find intergrowth of hydrothermal quartz and ore mineral.

Additional field tests were carried out along main tectonic lines (Red River, Song Ma and Song Da fault zones). They led to understand the geological structures better, and distribution of mineral deposits.

Combination of the characteristics of geological formations, ore, together with geochemical and heavy mineral anomalies and the geological structure characteristics were used to discuss relationship between geological setting and mineralization, and metallogenic characteristics of the NWVN area.

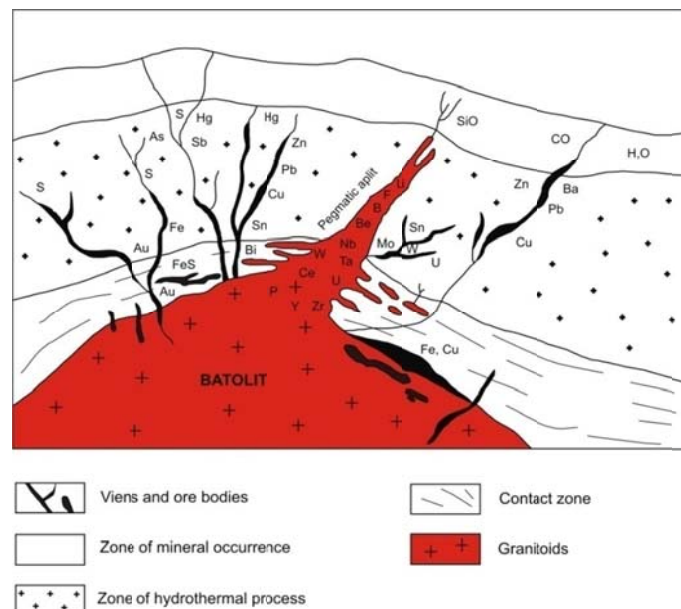


Fig. 3.1. Most of the ore deposits are formed in relation to magmatic intrusion (adapted from Barton, 1996).

### 3.3. Digital elevation model and remote sensing image

Digital elevation model (DEM, also called digital terrain model is a representation of the surface topography of a region of the Earth's surface, normally in vector format (i.e. stored like an image). DEMs are often obtained by digitizing map contours, or by stereo matching aerial photographs or satellite images. They can be used in the process of image classification, either as an extra 'feature' or, more commonly, to allow for the correction of atmospheric path and differential illumination effects. DEM construction is based on scanning the maps and digitization of contour line, or other elements of the terrain and then transformation from target

point to the X, Y, Z coordinate system and save data in files. Computer software, such as Surfer program, is designed for these purposes

Surfer can help us convert the contours to X, Y, Z data with onscreen digitizing. The Surfer's procedures include the loading the map file with the contours as a base map, selection of the map, and then choice within the Map/Digitize menu. The X, Y coordinates are displayed in the status bar (at the bottom of the Surfer window. Clicking on screen stores this coordinates in the edit window. The Z value is not stored automatically, but we can add the Z value in the Surfer worksheet. Once we have an X, Y, Z data file for contours, we can choose the Grid/Data menu command to interpolate a grid file from the X, Y, and Z data. Then, we can save results from Surfer in their Grid format (.GRD).

DEM representation of data is done using a regular grid, which is described as a density function  $Z = F(x,y)$  (Keckler, 1994) (Fig. 3.2). Surfer program is used to create a grid from X, Y, Z data. Interpolation and filling empty space between digital points is carried out by Kriging algorithm. Kriging is a geostatistical method and Surfer program provides an execution of kriging spatial analysis of data: the designation of average, median, estimating the Z value. In cartographic techniques we have options of the point or block kriging. The first option is estimating the value of a point by making use of a number of reference points nearby; the second one is estimating the value of a block from a set of nearby sample values (Li, Z. *et al.*, 2005). The program offers the Surfer kriging option without drift, with drift square or linear. The first applies when the data are evenly distributed, the second - when the data varies around the square trend, the last - if the data changes linearly (Keckler, 1994). In the case of level set, it seems that the first and third option is most appropriate. In order to reflect the morphology of the test site at work, the present author decided to try out various Kriging methods.

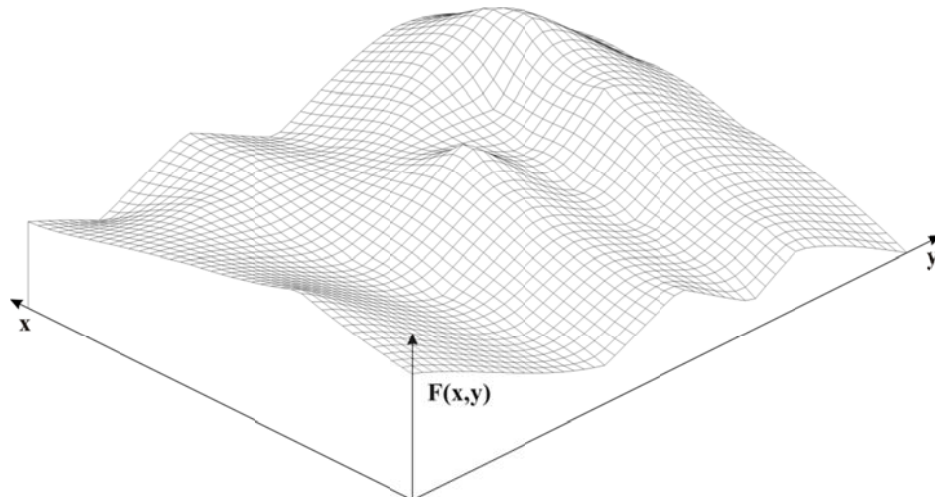


Fig. 3.2. Digital elevation model, regular grid composite of X, Y, Z point system.

Digital elevation model can be obtained from derivatives products as: transverse profiles, contour map, slope map, shaded relief image, and a spatial model (surface plot). Method based on mapping studies is indispensable in the case of mountainous areas, particularly useful in the analysis of lines of streams, ridges, discontinuities terrain type slopes, slopes and cliffs, and stagnant waters. DEM had been applied to analysis of regional (Ngo Van Liem *et al.*, 2006;

Nguyen Quoc Cuong, 2007; Hoang Quang Vinh, 2006), as well as local, several kilometers areas in size areas (Ngo Van Liem *et al.*, 2006; Nguyen Quoc Cuong, 2007). Digital elevation model strongly facilitated recognition of multiple forms of relief, which are difficult to capture in the field. The model allows direct transfer of topographical results of geological fieldwork and analysis of remote sensing image to one primer. Facilitated interpretation and verification of geological boundaries are based on the geomorphological relations, a mapping and inheritance issues with some geodynamic processes (Jordan, G., 2005, Struska, M., 2008).

The remote sensing image analysis is carried out on SPLOT image and other images obtained for example from <http://earth.google.com> combined with DEM analysis. It helps to better understand lineaments and recognize tectonic boundaries. Analysis of remote sensing images is performed in order to classify areas where geological features are very difficult to read. When remote sensing data are available in digital format, digital processing and analysis may be performed using a computer. Digital processing may be used to enhance data as a prelude to visual interpretation. Digital processing and analysis may also be carried out to automatically identify targets and extract information completely without manual intervention by a human interpreter. However, rarely is digital processing and analysis carried out as a complete replacement for manual interpretation. Often, it is done to supplement and assist the human analyst.

#### **3.4. Focal mechanism solution of earthquakes**

The seismic waves generated by earthquakes, when recorded at seismograph stations around the world, can be used to determine the nature of the faulting associated with the earthquake, to infer the orientation of the fault plane and to gain information on the state of stress of the lithosphere. The result of such an analysis is referred to as a focal mechanism solution or fault plane solution. The technique represents a very powerful method of analyzing movements of the lithosphere, in particular those associated with plate tectonics. Information is available on a global scale as most earthquakes with a magnitude in excess of 5.5 can provide solutions, and it is not necessary to have recorders in the immediate vicinity of the earthquake, so that data are provided from regions that may be inaccessible for direct study.

According to the elastic rebound theory, the strain energy released by an earthquake is transmitted by the seismic waves that radiate from the focus. Consider the fault plane shown in Figs 3.3 & 3.4 and the plane orthogonal to it, the auxiliary plane. The first seismic waves to arrive at recorders around the earthquake are P waves, which cause compression/dilatation of the rocks through which they travel. The shaded quadrants, defined by the fault and auxiliary planes, are compressed by movement along the fault and so the first motion of the P wave arriving in these quadrants corresponds to a compression.

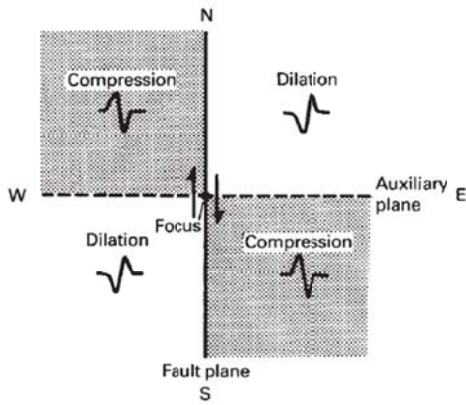


Fig. 3.3. Quadrantal distribution of compressional and dilational P wave first motions about an earthquake.

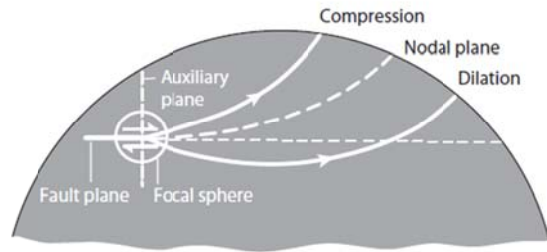


Fig. 3.4. Distribution of compressional and dilational first arrivals from an earthquake on the surface of a spherical Earth in which seismic velocity increases with depth.

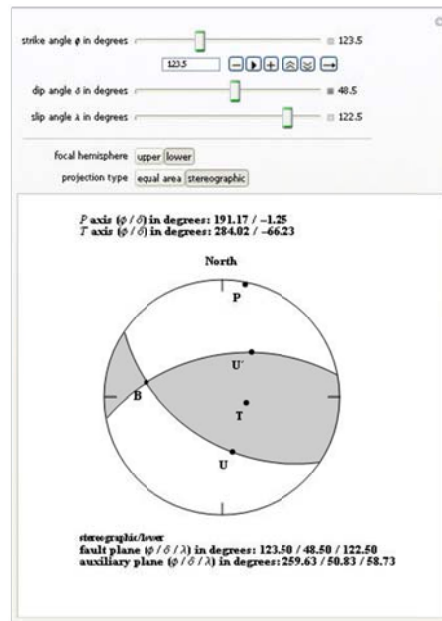


Fig. 3.5. Earthquake Focal Mechanism

The focal mechanism solution is presented as the “ball beach plot” symbol (Figs 3.5 & 3.6), which depicts also the stress orientation. This work requires delivery of the values of tension, pressure axis, and slip data, and then we put all the data into the software which is contributed by Scherbaum, F., Kuehn, N., & Zimmermann, B. (<http://demonstrations.wolfram.com/earthquakefocalmecanism>). “The beach ball symbol is the projection on a horizontal plane of the lower half of an imaginary, spherical shell (focal sphere) surrounding the earthquake source (A). A line is scribed where the fault plane intersects the shell. The stress-field orientation at the time of rupture governs the direction of slip on the fault plane, and the beach ball also depicts this stress orientation. In the schematic cartoon (Fig. 3.6), the gray quadrants contain the tension axis (T), which reflects the minimum compressive stress

direction, and the white quadrants contain the pressure axis (P), which reflects the maximum compressive stress direction. The computed focal mechanisms show only the P and T axes and do not use shading”.

These focal mechanisms are computed using a method that attempts to find the best fit to the direction of P-first motions observed at each station. For a double-couple source mechanism (or only shear motion on the fault plane), the compression first-motions should lie only in the quadrant containing the tension axis, and the dilatation first-motions should lie only in the quadrant containing the pressure axis. However, first-motion observations will frequently be in the wrong quadrant. This occurs because a) the algorithm assigned an incorrect first-motion direction because the signal was not impulsive, b) the earthquake velocity model, and hence, the earthquake location is incorrect, so that the computed position of the first-motion observation on the focal sphere (or ray azimuth and angle of incidence with respect to vertical) is incorrect, or c) the seismometer is mis-wired, so that "up" is "down". The latter explanation is not a common occurrence. For mechanisms computed using only first-motion directions, these incorrect first-motion observations may greatly affect the computed focal mechanism parameters. Depending on the distribution and quality of first-motion data, more than one focal mechanism solution may fit the data equally well.

For mechanisms calculated from first-motion directions as well as some methods that model waveforms, there is an ambiguity in identifying the fault plane on which slip occurred from the orthogonal, mathematically equivalent, auxiliary plane. We illustrate this ambiguity with four examples (B). The block diagrams adjacent to each focal mechanism illustrate the two possible types of fault motion that the focal mechanism could represent. Note that the view angle is 30-degrees to the left of and above each diagram. The ambiguity may sometimes be resolved by comparing the two fault-plane orientations to the alignment of small earthquakes and aftershocks. The first three examples describe fault motion that is purely horizontal (strike slip) or vertical (normal or reverse). The oblique-reverse mechanism illustrates that slip may also have components of horizontal and vertical motion.

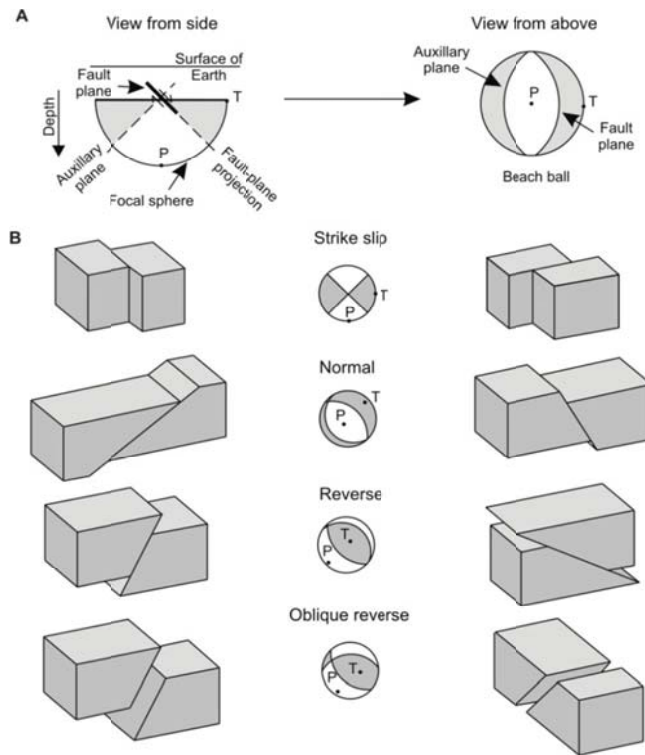


Fig. 3.6. Schematic diagram of a focal mechanism (after USGS, 1996)

In many cases, consideration of the local geology in the region of earthquake and in comparison with focal mechanism solution can be use to resolve the ambiguity of a fault plane solution.

## 4. MAGMATICS

### 4.1. The characteristics of magmatism in northwestern Vietnam

The petrographic, geochemical and geochronological characteristics of magmatic complexes of the NWVN are described in this chapter. Based on the present geochemical and geochronological data, six groups of magmatic rocks developed in different tectonic setting are recognized. These group and complexes are organized according to their age, from oldest to youngest. The results of this chapter were also published in the Journal of Annales Societatis Geologorum Poloniae (ASGP)/under the tile: “Overview of magmatism in Northwestern Vietnam”.

#### 4.1.1. Petrography and geochronology

##### *The first group – Proterozoic*

**The Bao Ha complex** was established by Izokh (in Dovjikov, ed. *et al.*, 1965). It comprises of small massifs (1-2 km<sup>2</sup>) in eastern part of the NWVN area, found mainly within the distribution area of metamorphic rocks of the Sinh Quyen Formation, in the Phan Si Pan-Red River structural

zone. These massifs are composed mainly of gabbros of ophitic texture, amphibolized and albitized gabbrodiabase and diabase, locally, melanocratic olivine gabbros near to lherzolite. These rocks were metamorphosed to epidote-amphibolite facies. Cu and Au mineralization of gabbros of the Dong An massif is related to hydrothermal alteration. The isotopic dating of gabbros indicated Proterozoic times, reaching 1777 Ma obtained by Rb-Sr method (Nguyen Van The, ed., 1999), and 1036 Ma by Ar-Ar method (Tran Trong Hoa *et al.*, 2000).

**The Xom Giau complex** was described by Phan Viet Ky (1977) (in Phan Cu Tien, ed. *et al.*, 1977). It is distributed in the Suoi Chieng, Sinh Quyen formations and belongs to the Phan Si Pan – Song Hong zone. Petrographic composition of this complex is fairly simple, consisting mainly of leucocratic microcline-rich arinite (biotite <5%) or biotite monzogranite ( $\geq 10\%$ ); locally pegmatitoid granite. Almost all rocks display regular-grained or weakly porphyritic texture and massive or striped gneissoid structure. The Xom Giau complex intrusives penetrate metamorphic rocks of the Suoi Chieng and Sinh Quyen Formations. The fragments of these metamorphic rocks are also present as xenoliths. The position of the Xom Giau complex indicates Neoproterozoic age. Similar magmatic intrusives situated in the Hanoi area gave isotopic ages from 1350 to 1386 Ma (Phan Cu Tien, ed. *et al.*, 1977).

**The Po Sen complex** was described by Tran Quoc Hai (1967). It includes granitoid massifs, distributed mainly in the middle of the Phan Si Pan-Song Hong structural zone, with a composition changing from diorite to granodiorite and biotite-amphibole granite. The greatest Po Sen massif with an area of 250 km<sup>2</sup> and other small massifs are scattered in the northwestern Phan Si Pan-Song Hong zone. The majority of granitoids of the Po Sen complex belongs to quartz diorite (tonalite) and granodiorite. According to Wang *et al.* (1999), the TIMS U-Pb age of zircon from Po Sen gneiss is 760 $\pm$ 25Ma. The SHRIMP U-Pb age of zircon is 751 $\pm$ 7Ma (Tran Ngoc Nam, 2003). According to Pham Trung Hieu *et al.* (2009), the LA-ICP-MS Lu-Hf ages of zircons from Po Sen complex are 723 $\pm$ 14 Ma and 760 $\pm$ 12 Ma, also Neoproterozoic.

#### *The second group – Devonian*

**The Song Chay complex** composed of the Song Chay, Nui Lang and Nui Bao massifs, was established by Izokh (in Dovjikov, ed. *et al.*, 1965). The Song Chay massif is distributed mainly in the Phan Si Pan-Song Hong structural zone with an area of 200 km<sup>2</sup>. It includes two mica, felsic and ultrametamorphic granites.

The Song Chay and Ha Giang formations cover conformably the Song Chay structural massifs. As was mentioned above, the Song Chay Formation was dated as Early Devonian (Tran Van Tri, ed., 1977), while biotite sample from the Nui Lang massif provided isotope age of 350 Ma. Remarkably, the Song Chay granite is similar the Dai Loc complex, which is distributed in the southern Vietnam, where intrusive granitoids penetrate the Cambrian-Ordovician formation and underlies the Devonian Tan Lap Formation.

#### *The third group – Permian*

**The Nui Nua complex** was established by Le Dinh Huu (in Phan Cu Tien, ed. *et al.*, 1977). This complex is composed of 4-5 km long and 300-400 m wide lentiform ultramafic bodies. They

are distributed in the Song Ma structural zone, along the Song Ma Fault. The Nui Nua complex is composed of harzburgite, dunite and pyroxenite; almost completely serpentinized or transformed into talc, chlorite and talc-carbonate rocks. Secondary minerals are represented by actinolite and widespread accessory minerals: magnetite, ilmenite and rutile (Fig. 4.1).

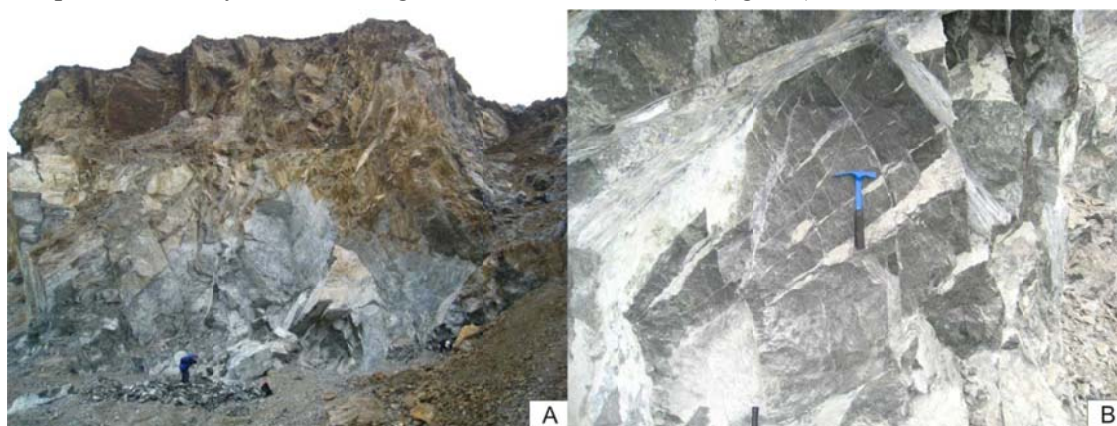


Fig. 4.1. The Nui Nua ultramafic block exposed in the right side of the road from Son La to Dien Bien area. Hammer is long 30 cm. A – The Nui Nua block, B – The Nui Nua ultramafic rock displaying serpentine alteration

Rocks of the Nui Nua complex lie conformably with metabasalt of the Huoi Hao Formation and are metamorphosed to the greenschist facies. The isotopic dating ( $^{206}\text{Pb}/^{238}\text{U}$ ) of metabasalt indicate  $254\pm 12$  Ma age (Pham Trung Hieu *et al.*, 2008), the LA-ICP-MS method indicates Late Permian times. These Permian rocks belong to the lower part of the ophiolite section, composed of ultramafic rocks (Nui Nua complex), metabasalt (Huoi Hao Formation) and gabbrodiabase (Bo Xinh complex).

**The Bo Xinh complex** was described by Dao Dinh Thuc (1976). It is composed of small bodies of gabbro, gabbrodiabase, gabbroic amphibole diabase, closely related in space and time to metamorphosed mafic effusives of the Huoi Hao Formation. Many dykes of gabbrodiabase penetrate greenschist (metabasite) of the Huoi Hao Formation along the Song Ma zone. This setting is similar to the area where the described below Chieng Khuong plagiogranite penetrates and causes the alteration to the metabasalt and metagabbro.

The Bo Xinh complex comprises amphibole gabbro, gabbrodiabase, gabbrodiorite and diabase. Amphibole gabbro is light to dark green in colour, small- to medium-grained, displaying compressed gneissoid structure. Along the Song Ma fault, it is strongly metamorphosed and transformed into gabbro-amphibolite. Gabbrodiabase is rather widespread and forms intrusive bodies of great size. It is usually schistose, greenish in colour, rarely of massive structure. Gabbrodiorite is small- to medium-grained, greenish-grey in colour, of granular texture, rather rich in plagioclase (80%), with prismatic, regularly arranged amphiboles. Diabase is small- to medium-grained, of residual diabasic texture and schistose, mostly actinolitized and transformed into greenschist, difficult to distinguish from metabasalt. Gabbroids of the Bo Xinh complex are closely related to Late Permian metabasalt of the Huoi Hao Formation (Pham Trung Hieu *et al.*, 2008). Thus, this complex has assumed Late Permian age.

**The Chieng Khuong complex** was described by Dao Dinh Thuc (1976). Plagiogranite of this complex is largely distributed in the Song Ma structural zone. It forms usually lentiform intrusive bodies stretching in the NE-SW direction, in coincidence with the structural trend of surrounding Neoproterozoic-Lower Cambrian rocks. This complex includes the Chieng Khuong and Ban Phung massifs and some small bodies located within the terrigeno-volcanic beds of the Bo Xinh group. They crop out along right side of the road from Ha Noi to the Song Ma province, and in the middle of Ma River (Fig. 4.2).



Fig. 4.2. Chieng Khuong plagiogranite complex. Hammer is long 30 cm. A – Granite rocks displaying very strong alteration; distance of 30m to the Nui Nua point; B, C – Heterogeneity of ultramafic (or mafic) assimilation in process of the intrusive massif - forming; D – Chieng Khuong block occurs in the middle of Ma river.

These rocks are greenish-grey, small- to medium-grained, weakly compressed. Mineral composition is as follows: 76-86% of plagioclase, 5-7% of hornblende, some biotite separated from hornblende, 5-8% of calcifeldspath; quartz from 5% in diorite to 20-30% in granodiorite. The rocks have residual granulo-hypidiomorphic texture, and directive structure. Plagiogranite forms the major part of massifs.

As was mentioned above, the rocks of the Chieng Khuong complex penetrate volcano-terrigenous, terrigeno-cherty and terrigeno-carbonate beds of the Bo Xinh Group causing their hornfelsification. The pebbles of plagiogranite from the basalt conglomerates of the Middle Cambrian Song Ma Formation of the Nam Co Anticline have petrochemical characteristics similar to rocks of the Chieng Khuong complex. They yield the isotopic (Rb-Sr) age of  $254 \pm 14$  Ma. Pham Trung Hieu *et al.*, (2008) supported the isotopic ( $^{206}\text{Pb}/^{238}\text{U}$ )  $262 \pm 8$  Ma age of Chieng Khuong plagiogranite using the LA-ICP-MS method. Based on these results, the Chieng Khuong complex can be Late Permian in age.

**The Huoi Hao Formation** was established by Pham Dinh Tuong (ed., 1999). It is an equivalent of the former “Lower Bo Xinh subsuite” (Phan Son, ed. *et al.*, 1978) and belongs to the Song Ma zone. The Bo Xinh metabasalt section along the Huoi Hao stream was chosen as

type section for the new Huoi Hao Formation (Pham Dinh Tuong, ed., 1999; Nguyen Van Thuat, ed., 1999).

The lower part of this formation is composed mainly of greenschists (metabasalt, metadiabase) and beds of altered tuffs. Three members were recognized in the section extending along Ma River from Nam Ma to Bo Xinh. The first member is represented by greenschist interbedded with quartz-sericite schist, second member by schistose greenschist, unclearly striped, locally massive greenschist, and the last one by greenschist interbedded with cherty schist and quartz-sericite schist. The lower boundary of the formation is unknown, while its upper part underlies conformably the Nam Ty Formation.

The LA-ICP method (Pham Trung Hieu *et al.*, 2008) follows results of  $^{206}\text{Pb}/^{238}\text{U}$  dating, giving the of  $254\pm 12$  Ma age of metabasalt samples from the Song Ma belt. The Late Permian age was established for Huoi Hao Formation according to these results.

**The Ban Xang complex** distributed in the Ta Khoa area belonging to the Song Da structural zone, was established by Dovjikow (ed.) *et al.* (1965). According to his description, the Ban Xang complex is located near the axis of the Ta Khoa anticline, and penetrates micaschist, biotite-muscovite hornfels, and actinolite-muscovite hornfels of the Nam Sap Formation. Intrusive massifs lay conformably with country rocks. Copper-nickel mineralization in the compact or disseminated form occurs often in the contact zone.

The petrology of the Ban Xang complex suggests ophiolitic, obducted origin. The massifs are composed mainly of strongly serpentinized dunite containing forsterite. Accessory minerals are represented by magnetite and chrome-spinel. The rock has panidiomorphic, medium- to coarse-grained texture. It is serpentinized, compact, near black in colour, of netted texture. Abundant olivine consists of nuclei surrounded by antigorite, forming lamellar, acicular assemblage; less numerous chrysotile forms micro-veins and transversal fibres. In some places, chrysotile is replaced by carbonate and some ore minerals.

The Late Permian age of the Ban Xang complex was assumed based on penetration of the sedimentary beds, which have yielded an age range from Devonian to Early Permian. The ophiolitic character contradicts this penetration. The relationship to the other ophiolites from this area suggests similar, Permian age.

**The Cam Thuy Formation** exposed west of the Son La Town and belonging to the Song Da structural zone was described by Dinh Minh Mong (ed., 1977). A section cutting through the Son La Pass comprises two members: the 350m thick member one is composed mainly of basalt, amygdaloidal basalt, porphyritic basalt with beds of basaltic tuffs and lavas (2-3 m thick); the 300 m thick member two contains mainly chocolate tuffaceous siltstone with beds of tuffs lavas and basalt. The studied rocks are exposed in the road to Dien Bien area (Fig. 4.3).



Fig. 4.3. Rocks of the Cam Thuy and Vien Nam formations. Hammer is long 30 cm, and book cover area of 20cm x 10cm. A, B – Basalt of the Cam Thuy Formation is weathered, and exposed in the road from Son La to Dien Bien area. C– Basalt block of the Cam Thuy Formation, D – Vien Nam rhyolitic rocks (photograph from Pająk *et al.*, 2006).

Krobicki and Golonka (2008) argued that basalts of the Cam Thuy Formation are loaf-shaped pillow lavas formed during submarine eruptions, due to rapid cooling of lava at the contact with seawater. Both the continental basalts and the pillow lavas indicating marine affinities were perhaps associated with back-arc spreading. Moreover, Tran Van Tri (ed., 1977) and Tran Trong Hoa *et al.* (1998) considered them as products of Song Da rift.

The Cam Thuy Formation covers the eroded surface of limestone containing *Neoschwagerina craticulifera* of the Carboniferous-Permian Bac Son Formation and underlies terrigenous-carbonate beds containing Late Permian brachiopods of the Yen Duyet Formation. The isotopic dating of five basalt samples from Cam Thuy Formation yield age  $283 \pm 21$  Ma (Nguyen Hoang *et al.*, 2004), corresponding to Early-Middle Permian.

**The Vien Nam Formation** was described by Phan Cu Tien, ed. *et al.* (1977). This formation is distributed in the Song Da and Song Ma zones forming long bands of NW-SE direction. Well studied sections are exposed along the Trat Stream, and along the road from Phu Yen to Muong Lang (Son La province). The formation in these sections is composed in the lower part of porphyritic basalt, aphyric basalt, high-magnesium basalt; in the upper part of porphyritic diabase, basaltic tuff, andesitobasalt, trachybasalt, andesitodacite, dacitic tuff, trachytic tuff, porphyritic trachite, rhyotrachyte, rhyolite, tuffaceous sandstone and tuffaceous siltstone. Tran Trong Hoa *et al.* (1995) and To Van Thu, ed. (1996) consider the Vien Nam Formation as basaltoids.

The Vien Nam Formation overlies unconformably the Bac Son Formation and unconformably underlies the Tan Lac Formation. Tran Xuyen *et al.* (1983) and Nguyen Hoang (2004) showed that volcanites of the Vien Nam Formation in its stratotype area penetrate the

Upper Permian Yen Duyet Formation. The Late Permian – Early Triassic age of the Vien Nam Formation can be established using these results.

*The fourth group – latest Permian-Triassic*

**The Dien Bien Phu complex** distributed mainly in the Sam Nua zone was described by Izokh (in Dovjikov, ed. *et al.*, 1965). A well exposed block of this formation is located in the Da River near the road from Muong Lay to Muong Te (Fig. 4.4). The complex is composed mainly of gabbro-diorite, diorite, quartz diorite and biotite-hornblende granite. According to the time of the formation process, the complex has been subdivided into 3 intrusive phases as follows: Phase 1 – gabbro-diorite and diorite; Phase 2 – quartz diorite and granodiorite; Phase 3 – variegated biotite-hornblende granite, rich in K-feldspath granite. The rocks of phase 2 are most widespread. Granitoid massif of the Dien Bien Phu complex penetrate the Nam Co, Ben Khe, Nam Pia, and Song Da formations forming hornfels bearing andalusite and amphibole in the contact aureole. These granitoids are covered by coal-bearing Suoi Bang Formation and penetrated by biotite granite of the Phia Bioc complex. Pb-Zn polymetal mineralization related to the Dien Bien Phu granitoids is expressed by placer dispersal aureoles, bearing pyromorphite, galenite and anglesite.



Fig. 4.4. Dien Bien Phu complex. Hammer is long 30 cm. A – Dien Bien Phu intrusive block exposed in the middle Da river, and crop out along left side of the road from Muong Lay (Lai Chau) to Muong Te area, B – The Dien Bien Phu block penetrated by veinstone.

Fromaget (1937) referred Dien Bien Phu granitoids as Hercynian granite. In the geological work on North Vietnam, Izokh (in Dovjikov, ed. *et al.*, 1965) dated them as post-Permian. Tran Van Tri and Nguyen Xuan Tung (1977) postulated three stages of their development Late Permian-Carnian times. Some isotopic values received from granitoids of the complex yield age 252-266 Ma (Tran Trong Hoa *et al.*, 2008a). These results and geological position indicate Late Permian - Early Triassic age.

**The Song Ma complex** was established by Dao Dinh Thuc *et al.* (1995). Subvolcanic massifs, developed mainly in the Sam Nua structural zone and related to Anisian felsic effusives, belong to the Song Ma complex. The Song Ma massif is the greatest intrusion of the area, having a clearly prolonged form in W-NW direction with a length of 80 km, a width of 5-10 km and an area of about 418 km<sup>2</sup>. It spreads mainly on the left side of the Ma River, along

the great fault, which separates the Song Ma and Sam Nua structural zones (Song Ma fault zone). In the east, the massif has tectonic contact with greenschist (metabasite) and quartz-sericite schist of the Upper Permian Bo Xinh Group and granodiorite of the Dien Bien Phu complex. In the southwest, it is closely related to Middle Triassic felsic-intermediate effusives of the Dong Trau Formation. Beside the intrusive massif, small satellite intrusions developed in the distributive area of effusives of the Dong Trau Formation. The Song Ma complex is composed mainly of biotite granite and biotite tonalite. In the northeast of the massif, biotite granite has the small-grained poikilitic texture and gradually transforms into porphyritic granite of effusive appearance. Two sides of the massif are bounded by faults, and, between them, large pieces of basal conglomerate of the Norian-Rhaetian Suoi Bang Formation occur, covering unconformably the intrusive massif.

On the geological, petrological and geochemical sides, the Song Ma complex is closely related in space and in origin to Middle Triassic felsic-intermediate effusive of the Dong Trau Formation. Its rocks are covered unconformably by coal-bearing beds of the Suoi Bang Formation, the basal conglomerate of which contains pebbles from granitoids of the Song Ma complex. The Rb- Sr whole rock isochron age yields  $232 \pm 11$  Ma age (Nguyen Minh Trung, 2007). The subvolcanic Song Ma complex can therefore be dated as Middle Triassic.

**The Phia Bioc complex** was described by Izokh (in Dovjikov, ed. *et al.*, 1965). In the studied area, the Phia Bioc complex is bounded in the west by faults. In the east, granite of the massif penetrates shales of the Lai Chau Formation causing its hornfelsification (the hornfels zone is 200 – 300m in width). It is covered by Upper Triassic coal-bearing beds of the Suoi Bang Formation in the south. The geological position of granitoids of the Phia Bioc indicates that this complex is younger than Middle-Upper Triassic rocks and older than Norian-Rhaetian coal-bearing formation.

#### *The fifth group – Jurassic-Cretaceous*

**The Suoi Be Formation** was described by Nguyen Xuan Bao (ed., 1970). This formation is distributed in the southeast margin of the Tu Le structural zone, forming a NW-SE oriented band which includes 2 parts. The lower part is represented by purple-chocolate to green tuffaceous conglomerates and gritstones, sandstones, silty sandstones, tuffs and lenses of aphyric basalt. The upper part contains different kinds of basalts, such as the plagiobasalt, andesitobasalt, and trachybasalt. These basalts form irregular flows, interbeds or lenses, interbedded with basalt tuff, lenses of agglomerate tuff, and crumpled black-green tuffaceous shale. Both parts are penetrated by small diabase bodies.

Post-effusive alterations are represented mainly by propylitization with high temperature facies (actinolite-epidote). In addition, medium temperature association (albite-epidote-chlorite) and low temperature association (calcite-albite-chlorite) occur. Au and Ag mineralization occurs within the formation.

The isotopic age of three basalt samples yield ages around  $117.3 \pm 0.6 \div 176.3 \pm 0.8$  Ma (Tran Tuan Anh *et al.*, 2004). Based on these results and Jurassic-Cretaceous flora fossils collected in the adjacent Thuan Chau area, the formation can be dated as Jurassic-Cretaceous.

**The Nam Chien complex** in the Tu Le structural zone was established by Phan Viet Ky (1977) (in Phan Cu Tien, ed. *et al.*, 1977). This complex is composed of amphibole gabbro and gabbrodiabase. Their mineral composition is rather simple with Cpx (amphibolized) + Plagioclase + Ilmenite + Apatite.

Their composition and origin are similar to those of subalkaline basalts of the Suoi Be Formation. Because of this similarity the age of gabbroids of the Nam Chien complex have been preliminarily assigned to Cretaceous.

**The Tu Le volcanic subcomplex** was established by Vu Khuc & Bui Phu My (eds., 1989). In the study area, the complex includes felsic-intermediate, subalkaline and alkaline effusives. It occurs in the Tu Le volcanic depression zone (Fig. 4.5). Rocks of the effusive facies play a predominant role in the composition of the subcomplex. They are accompanied by tuffaceous sandstones of eruptive facies and agglomerate tuffs of neck facies.



Fig. 4.5. Rhyolite subextrusive Tu Le complex, outcrop along the road to Sa Pa province.

From the petrographic point of view, the subcomplex consists of rhyodacite, rhyolite, and trachyrhyolite with a porphyritic trachyte. They usually display transitional relations with subvolcanites of the same composition. Almost all the rocks show results of compression, having banded structure and porphyritic texture. The phenocrystals consist mainly of kalifeldspath, a little plagioclase and quartz. Besides these, the compressed felsite and microfelsite also occur. Chromatic minerals in rhyodacite and rhyolite usually are biotite of titanium-high content and relatively iron-high content. In trachyte and trachyrhyolite, there is alkaline amphibole apart from biotite.

According to Lan (2000); the isotopic dating of 3 rhyolite samples is around  $58.603 \pm 0.2 - 79.30 \pm 0.3$  Ma. Based on these results, the subcomplex can be dated as Cretaceous.

**The Ngoi Thia volcanic subcomplex** distributed in the Tu Le volcanic depression zone was first distinguished by Nguyen Vinh (ed.) *et al.* (1977). Bui Cong Hoa (ed., 2004) described the subcomplex as mainly the subvolcanic facies with porphyritic rhyolite and comendite. Porphyritic rhyolite is light-grey in colour, massive, its texture is porphyritic with microgranular groundmass. Comendite contains alkaline chromatic mineral (riebeckite); it is grey, massive, porphyritic, with microgranular texture. The porphyritic rhyolite display micropoikilitic groundmass, massive structure, porphyritic texture with quartz surrounded by micropoikilitic groundmass. The Ngoi Thia subcomplex overlies unconformably the Suoi Bang

and Suoi Be formations, and occupies the uppermost position within the Tu Le structural zone. The Late Cretaceous age was assumed for this subcomplex.

**The Muong Hum complex** was described by Izokh (in Dovjikov, ed. *et al.*, 1965). Alkaline granitoid massif of this complex occurs in the Phan Si Pan mountain range and belongs to the Phan Si Pan-Song Hong structural zone. The main composition of the Muong Hum granitoid complex corresponds to granosyenite and granite. Main mineral composition includes quartz, feldspar K, plagioclase, amphibole, and biotite; alkaline pyroxene (aegyrine) and alkaline amphibole (arfvedsonite). Accessory minerals are represented by apatite, sphene, sometimes garnet.

Due to the Muong Hum granitoids appearance on the Phan Si Pan zone, the complex has been preliminarily dated as early Palaeozoic. The result of isotope dating of Nguyen Trung Chi (1999) shown that the Muong Hum granitoid complex reaches 75 Ma with TDM=0.6-0.8 Ga, and it can be dated as Cretaceous.

**The Phu Sa Phin complex** was described by Izokh (in Dovjikov, ed., *et al.*, 1965). This complex is composed of hypahyssal intrusive and subvolcanic bodies with kalifeldspath granite, granosyenite and syenite closely related in space, time and origin to Cretaceous rhyolite and comendite formations in the Tu Le zone. In the Phu Sa Phin mountainous area, these subvolcanic-intrusive bodies form the basement of the effusive cover. In some places within the Tu Le zone, these intrusive massifs are associated with effusive along the Phong Tho-Nam Pia fault zone.

The main rocks of the complex consist of alkaline feldspar granite, quartz porphyritic syenite, porphyritic granosyenite and granophyric granite. Average mineral composition of granite is as follows: kalium-natrium feldspar = 50 - 70%; plagioclase = 0 - 10%; quartz = 30 - 35%; biotite = 3 - 5%; amphibole and pyroxene = 1 - 5%. Accessory minerals are represented by fluorite, sphene, apatite, zircon and magnetite.

According to the field materials, petrochemical and geochemical characteristics, the co-magmatic relationship between Phu Sa Phin granitoids and Cretaceous Tu Le - Ngoi Thia effusives has been proved. Thus, the age of granitoids can be considered close to that of effusives. The rocks of the Phu Sa Phin complex were penetrated by biotite granite of the Ye Yen Sun complex and intrusions of the Pu Sam Cap complex. In addition, Ar-Ar age data yield the value 89-144 Ma to Phu Sa Phin granite (Tran Tuan Anh *et al.*, 2003), corresponding to Cretaceous. Therefore, the Cretaceous age of Phu Sa Phin complex is established.

#### *The sixth group – Palaeogene*

**The Ye Yen Sun complex** was established by Izokh (in Dovjikov, ed. *et al.*, 1965). The Ye Yen Sun batholith stretches over thousands square kilometers from the Vietnam-Chinese border in northwest to southeast through the Phan Si Pan range. Bui Phu My (ed.) *et al.* (1977) and Nguyen Trung Chi (1999) described northwestern and southeastern part of this massif. They distinguished granodiorite and biotite-amphibole granite, which belong to rather typical calc-alkaline series according to their petrographic characteristics.

Tran Tuan Anh (2003, 2004) has distinguished within the Ye Yen Sun complex, distributed around the O Quy Ho Pass (Fig. 4.6), two different types: leucocratic granite, with high-K calc-alkaline character of I-granite type in the west, and subalkaline biotite granite of A-granite type in the east. According to Zhang and Schärer (1999), the U-Pb age data gives the Ye Yen Sun granite an age of 35 Ma (the West Ye Yen Sun type) corresponding to Palaeogene.

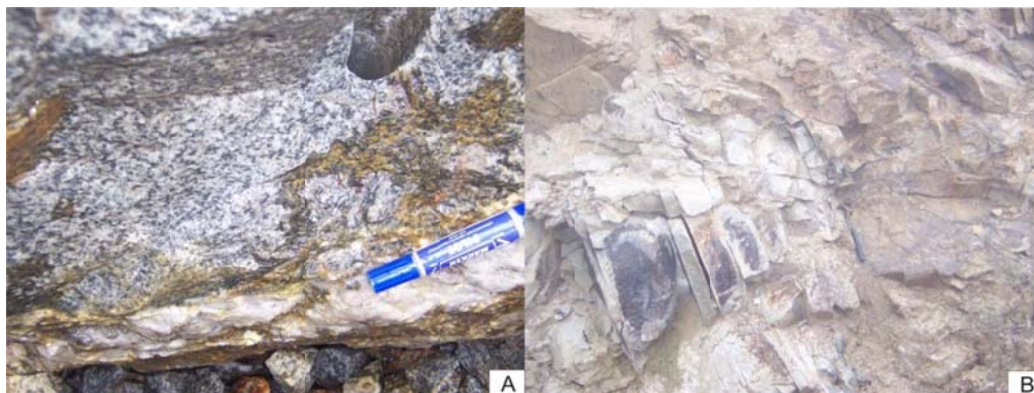


Fig. 4.6. Alkaline Ye Yen Sun complex. Hammer is long 30 cm. A – Molybdenum mineralization accompanied quartz veins bearing the Ye Yen Sun granite, B – The outcrop of Ye Yen Sun complex, 50 m to Bac waterfall.

**The Pu Tra Formation** was established by Tran Duc Luong & Nguyen Xuan Bao (1988). This formation occurs in the Song Da structural zone with a small distributive area (0.5-1 km<sup>2</sup>). It is composed of volcanogenic rocks of eruptive facies with the clay shale, trachytic tuff, porphyritic trachyte fragments. The formation can be subdivided into two members: member 1 – conglomerate interbedded with medium-grained sandstone, chocolate claystone, 15-20 m thick; member 2 – alkaline effusives, tuffs, agglomerate tuff, trachytic tuff, about 300 m thick. Agglomerate tuff contains many clasts of trachyte, porphyritic trachyte and porphyritic syenite. Their size ranges from few millimeters to 80 cm. The Pu Tra Formation lay unconformably upon the Upper Cretaceous Yen Chau Formation. In addition, a value of isotopic dating of 45±3 Ma confirms the Palaeogene age of the Pu Tra Formation.

**The Nam Xe-Tam Duong complex** was established by Izokh (in Dovjikov, ed. *et al.*, 1965). This complex includes small bodies distributed along the fault zone between the Song Da structural zone in the west and the Phan Si Pan zone in the east (Fig. 4.7).

The massifs are composed mainly of subalkaline to alkaline syenite and granosyenite. Characteristic paragenetic minerals include quartz, K-feldspar, plagioclase, pyroxene, amphibole, and biotite. The studied rocks have regular-grained structure. Pyroxenes are represented mainly by diopside, sometimes rich in aegirine-augite, amphiboles by high-alkaline hornblende or arfvedsonite. The rocks often contain of sphene and titanium-high garnet (melanite); the content of garnet sometimes reaches 5-10% in melanocratic syenite.

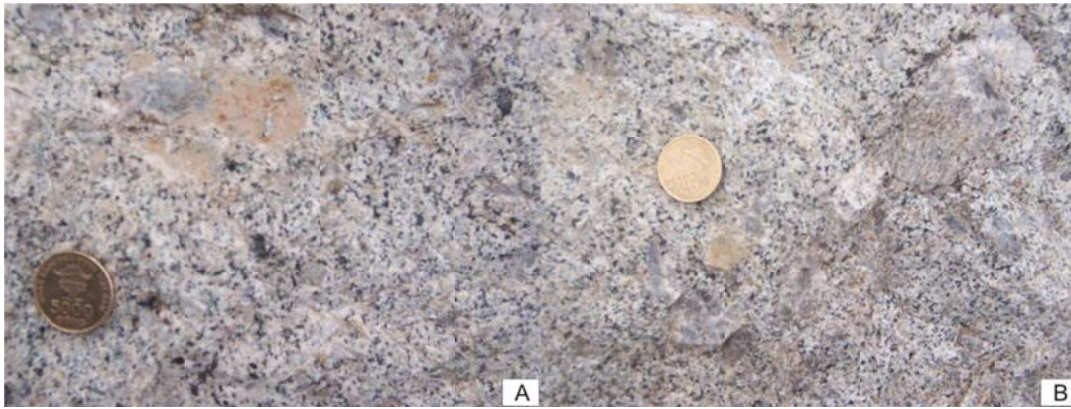


Fig. 4.7. A, B – Alkaline rocks of the Nam Xe-Tam Duong block exposed as boulders in the way to Sapa province.

The Palaeogene age of the Nam Xe-Tam Duong complex is derived from its geological setting. The Nam Xe-Tam Duong intruded volcanic trachytes of the Pu Tra Formation, the syenite bodies of the complex also penetrate granitoids of the Phu Sa Phin and Ye Yen Sun complexes. The Nam Xe deposit of radioactive ores and RRE and mineralization of lead-zinc, barite and fluorite are related to the Nam Xe syenite.

**The Pu Sam Cap complex** was described by Izokh (in Dovjikov, ed. *et al.*, 1965). This complex includes subvolcanic intrusions scattered in the Song Da structural zone. They are closely related to felsic-intermediate-alkaline volcanites (trachyte, trachyrhyolite) of the Pu Tra Formation, and together with them they form a very typical volcano-plutonic association.

The massifs of the studied rocks have a rather simple structure, almost entirely composed of leucocratic syenite and granosyenite. The melanocratic varieties, which have the composition corresponding to monzogabbro and shoshonite, or melanocratic syenite having clearly monzonitic texture (Fig. 4.8) occur in some massifs (Khuon Ha, Khao Cum). The isotopic dating (Ar-Ar method) yield two values of  $31.5 \pm 0.2$  and  $35.4 \pm 0.2$  Ma (Tran Trong Hoa *et al.*, 1999) indicating the Palaeogene age.



Fig. 4.8. Pu Sam Cap block.  
Book cover area of 20cm x  
10cm.

**The Coc Pia complex** includes mafic-potassic alkaline and potassic ultra-alkaline formations, composed of volcanites, neck intrusives and dykes largely developed in southeast of Tam Duong and Phong Tho areas in the Song Da zone. These rocks are best exposed southeast of Tam Duong (Coc Pia, Sin Cao) in the distribution area of intermediate-felsic-alkaline volcanites and

subvolcanites of the Pu Tra, Pu Sam Cap type described above, as well as of Triassic terrigeno-carbonate formations. They form rather typical volcano-plutonic associations with three manifestation forms: eruptive, intrusive neck form, dykes and veins (Tran Trong Hoa *et al.*, 1999).

The mafic-alkaline tuffaceous breccia can be usually observed in volcanic structure of pipe type, together with the trachytic tuff. It often corresponds in composition with alkaline andesitobasalt (absarokite-according to Lacroix, 1933), or lamproite tuff (cocite tuff). Absarokite tuff contains usually fragments of trachyte and trachyrhyolite. Sometimes, leucitite and similar variety as wyomingite have been observed.

The isotopic dating by Rb-Sr method of lamproite from the Dong Pao has yield the  $42 \pm 7$  Ma age (Tran Trong Hoa *et al.*, 1995), by Ar-Ar method of lamproite and absarokite from the Coc Pia and Sin Cao 29-34 Ma age (Tran Trong Hoa *et al.*, 1999). Based on these results, the complex has been dated as Palaeogene.

#### 4.1.2. Geochemistry

Representative chemical and trace element composition of different magmatic rock types from the NWVN are listed in Table 4.1 to Table 4.19. The nomenclatures of the plutonic rocks from the NWVN are deciphered on diagrams (Figs 4.9 - 4.27), including the TAS diagram of Cox *et al.*, (1997) (Fig. 4.9) and on the AS diagram of Dmitriev *et al.*, (1972) (Fig. 4.11).

The Bao Ha, Bo Xinh, Nam Chien mafic rocks are classified as gabbros. The Xom Giau, Po Sen, Song Chay, Chieng Khuong, Song Ma, Phia Bioc, Muong Hum, Ye Yen Sun, Nam Xe-Tam Duong and Phu Sa Phin rocks represent granites, sometimes granodiorites. The rocks from Pu Sam Cap are classified as syenite and nepheline syenite, Coc Pia as syeno-diorite and gabbro, and the Dien Bien Phu magmatic represent rocks changing from granite, gabbrodiorite to diorite, gabbro (Fig. 4.9).

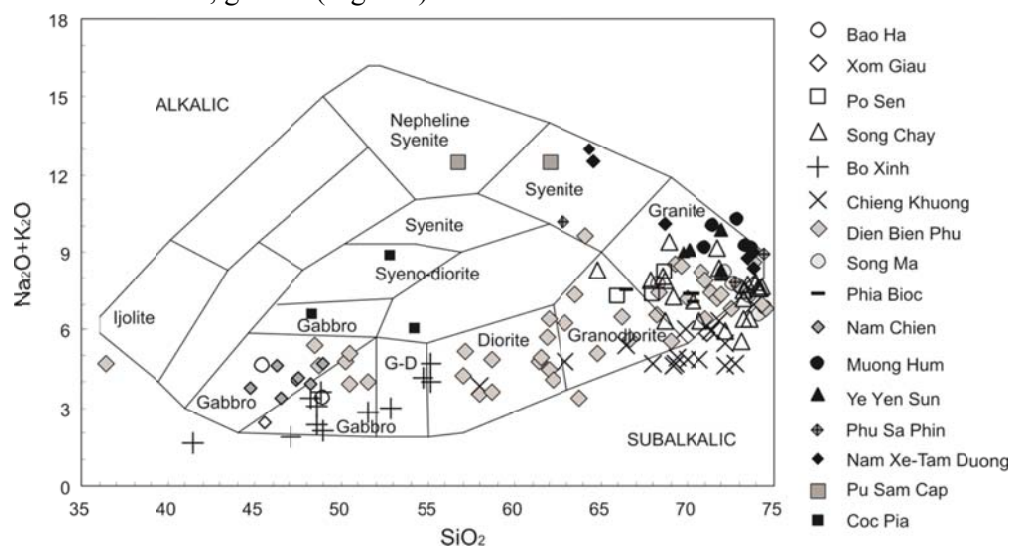


Fig. 4.9. Classification diagram for the NWVN plutonic rocks (applied method of Cox *et al.*, 1979).

On the AFM diagram of Irvine and Baragar (1971), gabbroic rocks belong to the tholeiitic series (TH), while the granites and dacites and others are calc-alkaline rocks, except the Dien Bien Phu magmatic rocks ranging from tholeiitic to calc-alkaline rocks (Fig. 4.12). The Nui Nua ultramafic rocks are classified as harzburgites sometimes lherzolites, while the Ban Xang ranges from clinopyroxenite, verlite and lherzolites (Fig. 4.11). On the AFM diagram of Irvine and Baragar (1971) (Fig. 4.13), ultramafic rocks belong to tholeiitic series (TH).

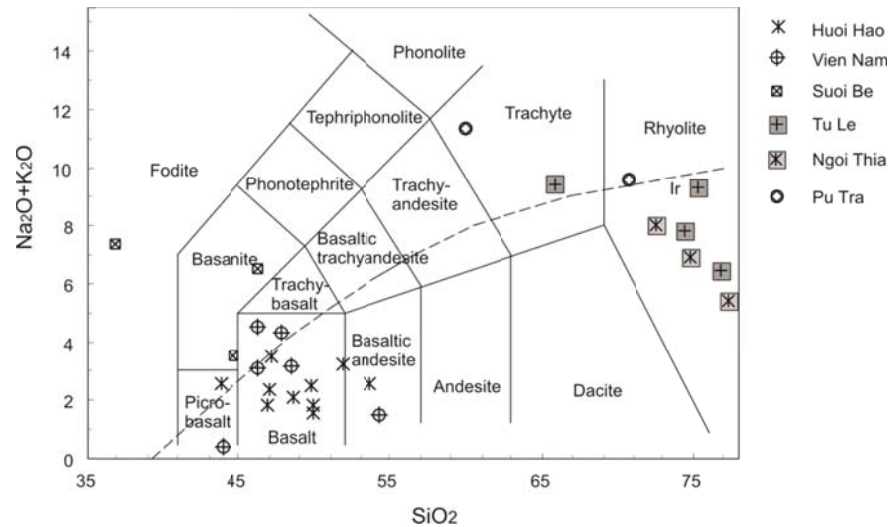


Fig. 4.10. Classification diagram for the NWVN volcanic rocks (applied method of Le Maitre, 1989).

The nomenclatures of the volcanic rocks from the NWVN are shown on the TAS diagram of Le Maitre *et al.*, (1989) (Fig. 4.10). It shows that the Huoi Hao, Vien Nam are classified as basalt; the Suoi Be is plotted in basanite sometimes fodite field; while the Tu Le, Ngoi Thia represent rhyolite, and the Pu Tra, rhyolite sometimes trachyte. On the AFM diagram of Irvine and Baragar (1971) (Fig. 4.13), rhyolite and trachyte belong to calc-alkaline series (CA), while basalt and basanite belongs to tholeiitic series (TH).

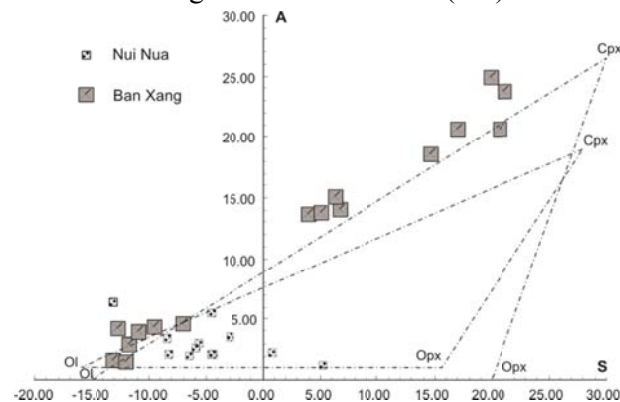


Fig. 4.11. Classification diagram for ultramafic rocks (applied method of Dmitriev *et al.*, 1972),  $A = Na_2O + K_2O + Al_2O_3 + CaO$ ;  $S = SiO_2 - (TiO_2 + Fe_2O_3 + FeO + MnO + MgO)$ .

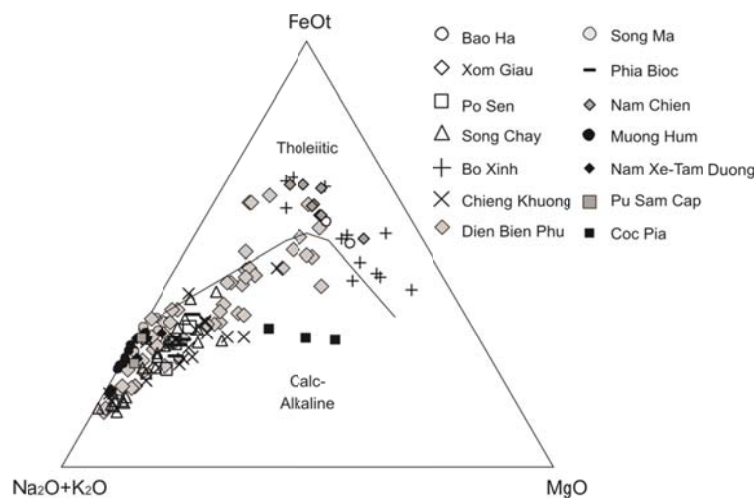


Fig. 4.12. A subdivision diagram showing the boundary between the calc-alkaline field and tholeiitic field of NWVN plutonic rocks (applied method of Irvine & Baragar, 1971).

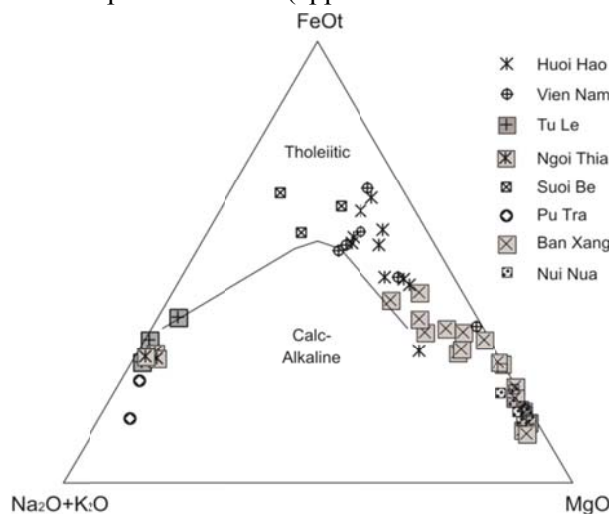


Fig. 4.13. A subdivision diagram showing the boundary between the calc-alkaline field and tholeiitic field of NWVN volcanic rocks (applied method of Irvine & Baragar, 1971).

The serpentized harzburgite of the Nui Nua complex are poor in silica ( $\text{SiO}_2=36.08-46.36\%$ ), alkali ( $\text{Na}_2\text{O}+\text{K}_2\text{O} < 2\%$ ), and in aluminum ( $\text{Al}_2\text{O}_3 = 0.21-2.12\%$ ), but rich in magnesium ( $\text{MgO} = 34.39-38.8\%$ ); with the  $\text{MgO}/\text{FeO}$  ratio: 7-29 (Table 4.5). The  $\text{Mg}/\text{Fe}$  ratios: 8.9-12.8 (Nguyen Van Chien, 1964) indicate that this complex was crystallized from peridotite magmatic source. The serpentized dunite of the Ban Xang complex are poor in silica ( $\text{SiO}_2=34.3-45.82\%$ ), very rich in calcium ( $\text{CaO}=0.24-10.6\%$ ), with sodium > potassium (Table 4.10). On the  $\text{FeOt}-\text{MgO}-\text{Al}_2\text{O}_3$  diagram of Pearce *et al.*, (1977) (Fig. 4.19), most of all the ultramafic rocks corresponding to the ocean ridge-floor (ORF). According to the DGMV (unpublished data), the content of Ba, Rb, Sr, Y, Yb, Th, Ce, Zn, and Zr is 1-14 times higher than Clarke; specifically the ore forming elements Cu, V and Pt are 3-8 times higher than Clarke. On the  $\text{Na}_2\text{O}-\text{K}_2\text{O}-\text{CaO}$  diagram of Green & Poldervaart (1958) (Fig. 4.15), the Nui Nua and Ban Xang complexes belong to sodic rock types. On the  $\text{FeOt}-\text{MgO}-\text{Al}_2\text{O}_3$  diagram of Pearce *et al.*, (1977), they also belong to ocean ridge-floor (ORF) magmatic rock types.

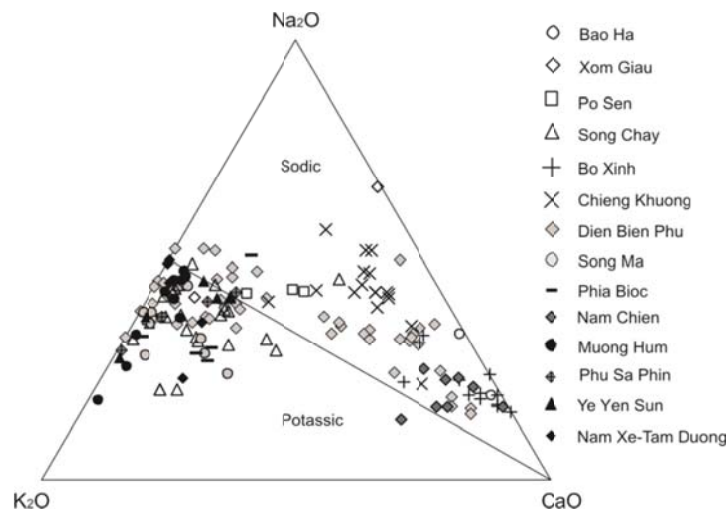


Fig. 4.14. Na<sub>2</sub>O-K<sub>2</sub>O-CaO diagram for the NWVN plutonic rocks (applied method of Green & Poldervaart, 1958).

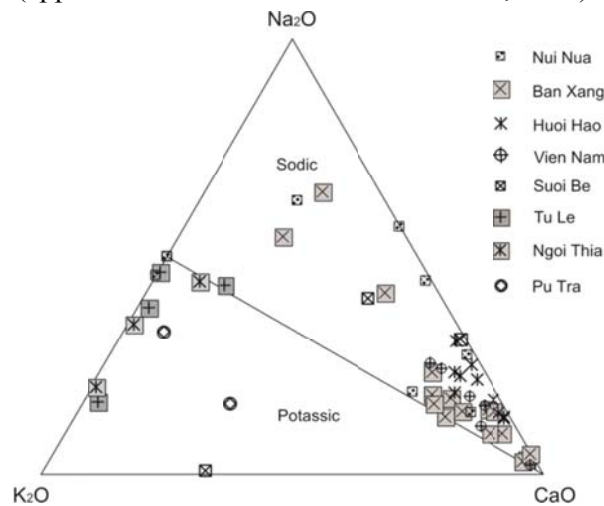


Fig. 4.15. Na<sub>2</sub>O-K<sub>2</sub>O-CaO diagram for the NWVN ultramafic and volcanic rocks (applied method of Green & Poldervaart, 1958).

Geochemically, all study plutonic rocks samples from the NWVN, except for serpentinized harzburgite and dunite of the Nui Nua and Ban Xang complexes, are fairly subdivided into three series. The first series contains the mafic plutonics of the Bao Ha, Bo Xinh, and Nam Chien gabbroic samples, which are silica undersaturated rocks ( $\text{SiO}_2=41.4\text{-}55.14\%$ ) with low alkalinity (total  $\text{Na}_2\text{O}+\text{K}_2\text{O}=2.49\text{-}4.77\%$ ).  $\text{Na}_2\text{O}$  content is higher than  $\text{K}_2\text{O}$  content. On the  $\text{Na}_2\text{O}-\text{K}_2\text{O}-\text{CaO}$  diagram of Green & Poldervaart (1958) (Fig. 4.14), they belong to sodic types. On the  $\text{Nb}^*2 - \text{Zr}/4\text{-Y}$  ternary diagram of Meschede (1986) (Fig. 4.18), the Bao Ha complex belongs to intraplate alkaline and tholeiite gabbros, while the Nam Chien complex plot in intraplate alkaline field. On the other hand, on the  $\text{FeOt}-\text{MgO}-\text{Al}_2\text{O}_3$  diagram of Pearce *et al.*, (1977) (Fig. 4.19), the Bao Ha belong to island ocean field (IO), while the Nam Chien fall into continental ocean types (CO). The Bo Xinh complex display a wide range of mafic rock types, but mainly island ocean (IO) and ocean ridge-floor (ORF). Particularly, the

chemical composition of the Bao Ha complex characterizes the rock type relatively high in titanium ( $\text{TiO}_2=1.32\text{-}2.66\%$ ), medium in magnesium ( $\text{MgO}=6.73\text{-}7.32\%$ ), relatively low in aluminum ( $\text{Al}_2\text{O}_3=13.11\text{-}14.59\%$ ) (Table 4.1). These rocks are rather poor in Cu (55-73 ppm), Cr (146-271 ppm), and relatively rich in V (316-402 ppm). Their content of Rb is relatively poor (2.1-4.3 ppm), however Nb, Zr and Y are rather stable in high level in comparison with the low-alkali tholeiite type. They are rich in rare earth elements (REE), especially the light rare earth elements (LREE) (Fig. 4.20-1). The distributive characteristics of Rb, Sr, Nb and REE show that gabbroids of the Bao Ha complex belong to within-plate (intraplate) type (Fig. 4.26). The origin of this complex was related to the spreading process of the continental margin. The described rocks of the Bo Xinh complex are low in  $\text{TiO}_2=0.8\text{-}2.1\%$ , their chemical composition displaying a mantle origin (oceanic crust of the IO or ORF type). The Cu, Ni, Cr, Ti and V elements are higher than Clarke (Table 4.6). Chemical composition of the Nam Chien complex has following characteristics: high in titanium ( $\text{TiO}_2=2.02\text{-}3.63\%$ ); relatively high in calcium ( $\text{CaO}=7.47\text{-}11.22\%$ ) (Table 4.14). The rocks are all rich in Rb, Ba, Th, LREE, belonging to tholeiite within-plate (intraplate) series of the mid-ocean ridges (Figs 4.18 & 4.26).

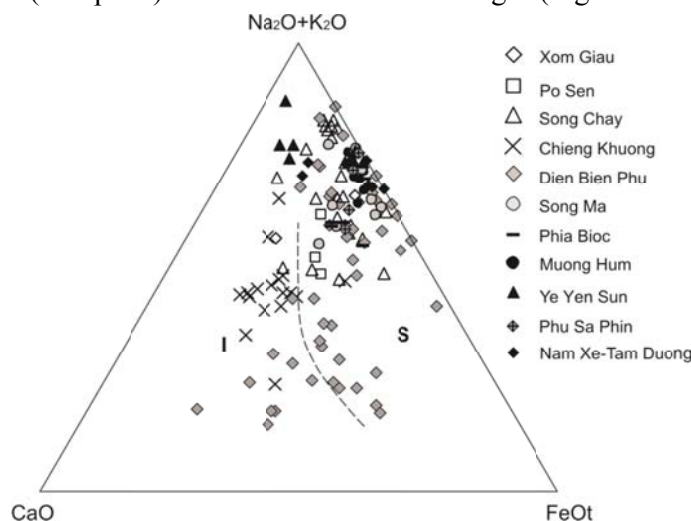


Fig. 4.16.  $\text{Na}_2\text{O}+\text{K}_2\text{O}$ - $\text{FeOt}$ - $\text{CaO}$  diagram classifying for the NWVN granitoid types (I, S) (applied method of Chappell *et al.*, 1974).

The second series contains the felsic plutonics from the Xom Giau, Po Sen, Song Chay, Chieng Khuong, Dien Bien Phu, Song Ma, Phia Bioc, and Muong Hum, Ye Yen Sun, Nam Xe-Tam Duong, Phu Sa Phin complexes. These plutonics are granites sometimes granodiorites. They show a wide range of  $\text{SiO}_2$  (57.94-78.15), and are rich in the alkalis ( $\text{Na}_2\text{O}+\text{K}_2\text{O}=3.89\text{-}13.0$ ). On the  $\text{Na}_2\text{O}$ - $\text{K}_2\text{O}$ - $\text{CaO}$  diagram of Green & Poldervaart (1958) (Fig. 4.14), most of them belong to potassic types, except the Xom Giau, Po Sen, Chieng Khuong complexes, which belong to sodic types. On the  $\text{Na}_2\text{O}+\text{K}_2\text{O}$ - $\text{FeOt}$ - $\text{CaO}$  diagram classifying granite types (I, S) of Chappell *et al.*, (1974) (Fig. 4.16), granitoids of the Xom Giau, Po Sen, Song Ma, Phia Bioc, Muong Hum, Phu Sa Phin, Nam Xe-Tam Duong complexes belong to S-granite types, while the Chieng Khuong complex belong to I-granite type. The Song Chay, Dien Bien Phu, and Ye Yen Sun complexes represent the I-granite changing to the S-granite, respectively. Chemical

composition of biotite from the Xom Giau complex places it in the type low in titanium ( $\text{TiO}_2=1.3\%$ ), relatively high in aluminum ( $\text{Al}_2\text{O}_3=15.7\%$ ) and high in iron ( $\text{FeO}=19.5\%$ ). It displays intermediate characteristics between biotite from S-granite and A-granite (Nguyen Van The, ed., 1999). The studied rocks characterize the type rich in Rb (170 ppm), Zr (476 ppm), Th (55 ppm), U (9 ppm), but rather poor in Nb (8.5 ppm), Ta (1.65 ppm) (Table 4.2). They are very rich in REE, especially LREE, with La=102-240 ppm, Ce=132-140 ppm, Nb=43.3-102 ppm. Based on the distribution of Rb, Sr, Zr, Nb, Ta Th, and REE (Fig. 4.19-2), granitoids of the Xom Giau complex bear the intermediate characteristics between S-granite and A-granite. The shortage of Nb, Ta and other elements as well as its close spatial (possibly even time) relationship with calc-alkaline granitoids of Ca Vinh type indicate that origin of Xom Giau granitoids is related to subduction. The chemical composition of the Po Sen complex (Table 4.3) is rather rich in Rb (67-84 ppm), Sr (429-548 ppm) and LREE; expressing a weak Eu min. The distribution of REE is typical for calc-alkaline series (I-granite). The rocks are all relatively poor in Nb, Ta, Hf, Zr, Sm, Y and Yb in comparison with granite of chondrite and ocean island (Figs 4.20-3, 4.20-4). Based on these characteristics and the Rb vs Y+Nb correlation, the Po Sen granitoids correspond to volcanic arc granites (Fig. 4.25), and were perhaps formed in the active continental margin tectonic setting. Lan (2000) argues that the granitic rocks originated by melting of older crustal sources, but with a significant input of mantle component during magma genesis. Pham Trung Hieu *et al.* (2009) using the Hf isotopic ratios  $\epsilon\text{Hf}(t) = -16.1$  to  $+3.4$ , and wide range of isotopic ages  $\text{TDM1}(\text{Hf}) = 1186$  to  $1945\text{Ma}$  demonstrated participation of both mantle materials and newly-formed components of continental crust in this complex. The mixing crust-mantle model best explains the origin of the Po Sen complex. Basically, the Sn, Pb, Sb, Zr, Y bearing rocks are prevailing in the Song Chay complex. Zr is 10 times and Y 9-10 higher than Clark index. The Song Chay granitoid complex is depicted as S-type post orogenic granite in tectonic classification diagram (Figs 4.22-4, 4.22-5). Rocks of the Chieng Khuong complex have high aluminum content ( $\text{Al}_2\text{O}_3= 13.8-16.35\%$ ). In comparison with Clarke, the rock making micro-elements (Sr, Mn, Ti, V, Cr) are higher from 1.2 to 5 times. Cu is 8.9 times higher than Clarke, Pb-1.5; Zn-1.8 and As-10 times higher than Clarke. The ratios  $\text{Ba}/\text{Sr}=2.7$ ;  $\text{La}/\text{Ba}=1.03$ ;  $\text{Nd}/\text{Sm}=3.97$ ;  $\text{La}/\text{Sr} = 0.08$ ;  $^{87}\text{Sr}/^{86}\text{Sr}=0.669$  (After DGMV, 1999).

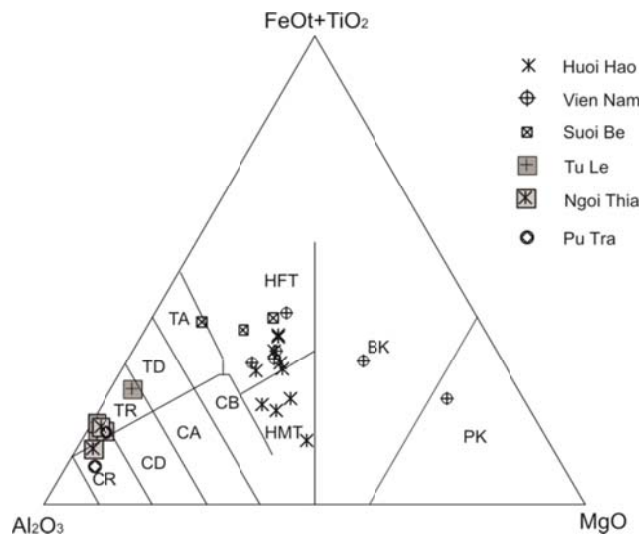


Fig. 4.17. Discrimination diagram for the NWVN volcanic rocks (applied method of Jensen & Rickwood, 1989). BK – Komatiitic basalt; PK – Komatiite; HFT – High iron tholeiite; HMT – High magnesium tholeiite; TA – Andesitic tholeiite; TD – Dacitic tholeiite; TR – Rhyolitic tholeiite; CB – Basaltic calc-alkaline; CA – Andesitic calc-alkaline; CD – Dacitic calc-alkaline; CR – Rhyolitic calc-alkaline.

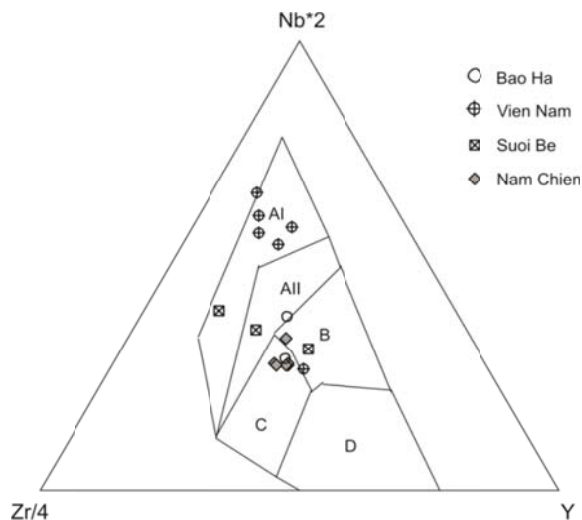


Fig. 4.18. Nb\*2 - Zr/4-Y ternary diagram for the NWVN mafic rocks (applied method of Meschede, 1986), AI – Intraplate alkali basalts; AII – Intraplate alkaline and tholeiite basalts; B – MORB-E type – Enriched tholeiites of mid-ocean ridges and tholeiites of intraplate structures; C – Intraplate alkaline; D – MORB-N type – Depleted tholeiites of mid-ocean ridges.

The granitic rocks of the Song Ma and Phia Bioc complexes are similar to the granites generated in volcanic arc-related tectonic setting (Figs 4.24 & 4.25), while the rocks of the Dien Bien Phu complex are mainly of the I-granite (early phases) changing to the S-granite (late phase) (Fig. 4.16). Their magmatic mixed nature originated during their forming process related to the subduction zone (Tran Trong Hoa, 1999). They can be correlated to syn-collision granite type.

Particularly, the Song Ma complex represents volcanic assemblage formed during the magmatic Triassic in a dynamic environment of post-collision, bearing characteristics of volcanic arc granite type (VAG). Based on the geochemical characteristics of trace element group (Fig. 4.21-1), the described rocks of the Phia Bioc complex have clearly higher content of light rare earth elements (LREE), comparing with heavy rare earth elements (HREE), without the negative Eu anomaly. Besides, they have high content of lithophilous element group (Rb, Ba, Th, K, etc.) and low content of elements having stable field (Ta, Nb, Zr, Th). More specifically, they have an extreme low content of Ti, Y and Yb, very characteristic for magmatic association forming in the convergent margin - post collisional tectonic setting (Fig. 4.22-6).

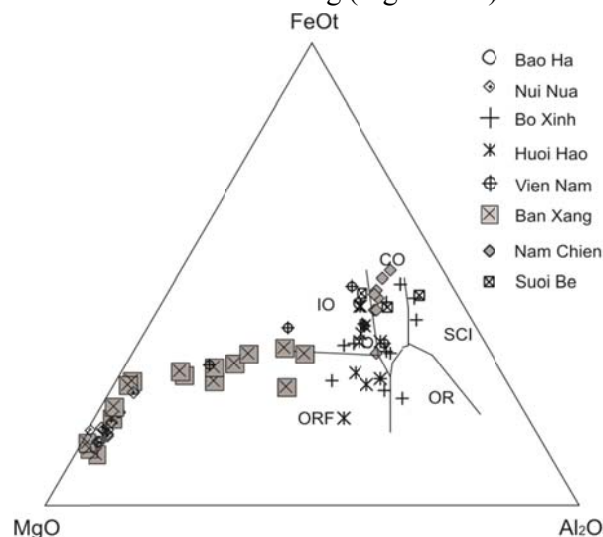


Fig. 4.19. FeOt-MgO-Al<sub>2</sub>O<sub>3</sub> diagram subdividing the NWVN ultramafic and mafic rocks (applied method of Pearce *et al.*, 1977), IO – Island ocean, CO – Continental ocean, SCI – Spreading center-island, OR – Orogenic ridge, ORF – Ocean ridge-floor.

The Muong Hum granitoids are relatively rich in Ba (285-3854 ppm), Rb (110-210 ppm), and rich in Nb (83-252 ppm), Ta (5.88-21.28 ppm), Zr (668-1384 ppm), Y (50.95-346.8 ppm), Hf (16.01-41.14 ppm) and very poor in Sr (19.06-180 ppm); except for the H-906 sample. The K/Rb ratio is relatively low (1653.2-451.9), Rb/Sr (0.09-9.70), and Rb/Ba (0.07-0.67). They are rich in REE especially the LREE, their content is 200 to 1000 times higher than that of chondrite (Sun & McDonough, 1989) (Fig 16-3). The (La/Sm)<sub>N</sub> ratio is (6.18-44.00) and based on the REE characteristics, the Muong Hum granitoids correspond to the A-granite and quite express the picks of Eu anomalies (Eu/Eu\*=0.14-0.39) (Table 4.16). Based on characteristics of high in alkali (potassic alkali type), rich in Rb, Zr, Nb and rare elements, Tran Trong Hoa (1995) inferred that the Muong Hum granitoids correspond to the A-granite representing the formation and evolution of the Tu Le depression (144-73 Ma). Perhaps, it is a product of within-plate (intraplate) magmatic activity, related to the collision between the Izanagi Plate (proto-Pacific Ocean) and South China blocks during Jurassic - Cretaceous times. The development of Red River strike-slip influenced the Muong Hum granitoids, producing “fish-tectonics”, and metamorphism manifested in the granite gneisses widespread in the southeastern Phan Si Pan-Song Hong zone. For the Phu Sa Phin complex, based on the (K<sub>2</sub>O+Na<sub>2</sub>O)/CaO-(Zr+Nb+Ce+Y) and Fe<sup>\*</sup>/MgO-(Zr+Nb+Ce+Y)

correlations, they correspond to the A-granite type. They represent within-plate (intraplate) magmatism related to intracontinental spreading (Table 4.16, Fig. 4.26).

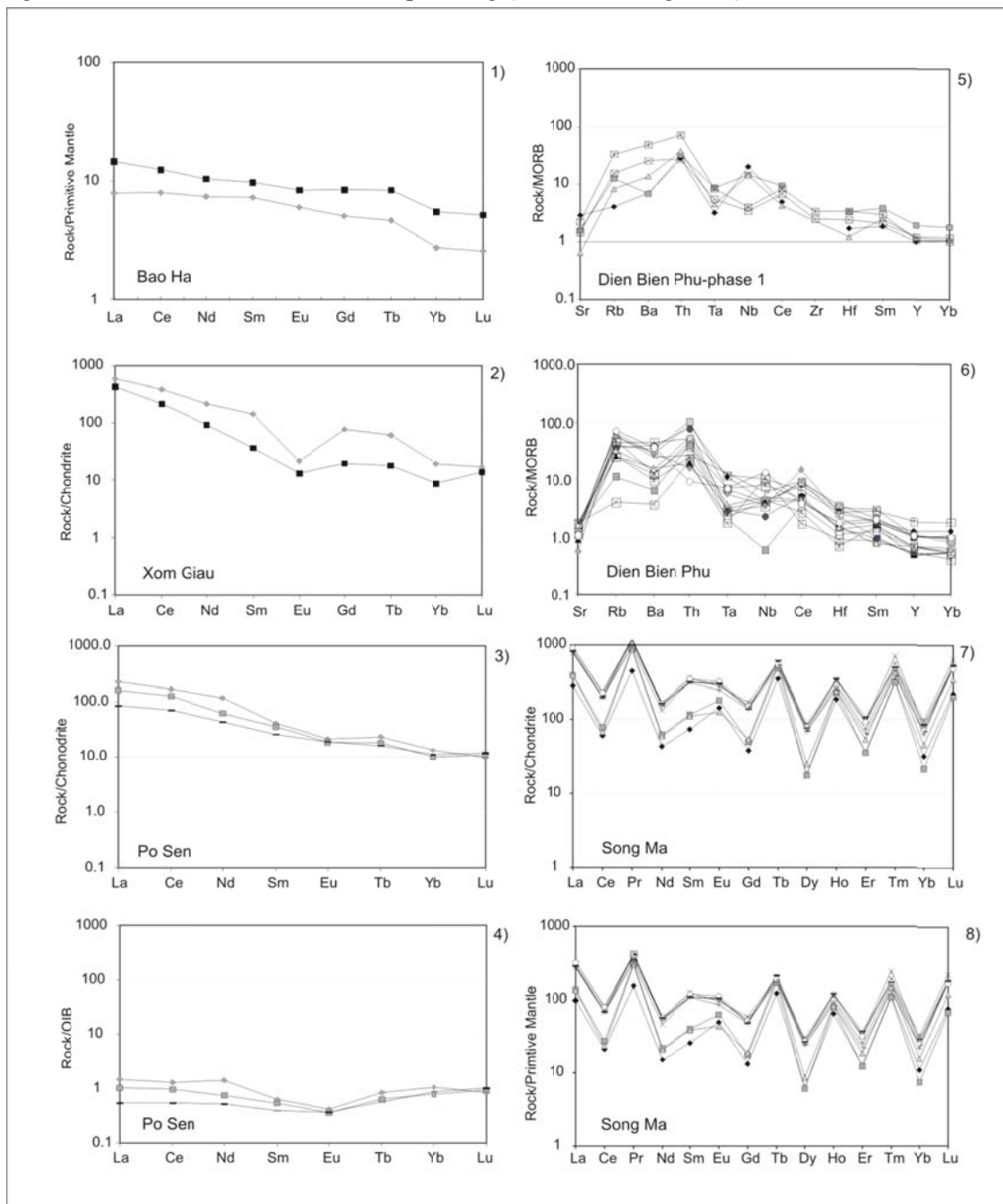


Fig. 4.20. Primitive mantle, chondrite-normalized, ocean island-normalized, and mid-ocean ridge basalt (applied method of Sun & McDonough, 1989) REE distribution patterns for the NWVN igneous rocks.

The subalkaline biotite granite of the Ye Yen Sun complex in the east, based on the following characters: rich in potassium, in Rb, Zr, Nb, Ta and rare earth Th, U elements, poor in Sr, Ba, is completely close to the subalkaline granite of the Phu Sa Phin complex, and bears the characteristics of within-plate (intraplate) magmatic activity (Table 4.17, Fig. 4.26). The

leucocratic granite in the west of the pass is characterized by its relatively high alkalinity of the potassium-sodium type; it is rich in Rb, Sr, Ba and relatively poor in Nb, Ta, Hf, and Zr, bearing complex characteristics of magmatic activities of continental arc or post-collisional, related to the compressional movement caused by the Eurasia-India collision. The Ye Yen Sun complex needs further detailed studies on isotopes in association with isotopic dating for clarifying the problem of its exact setting.

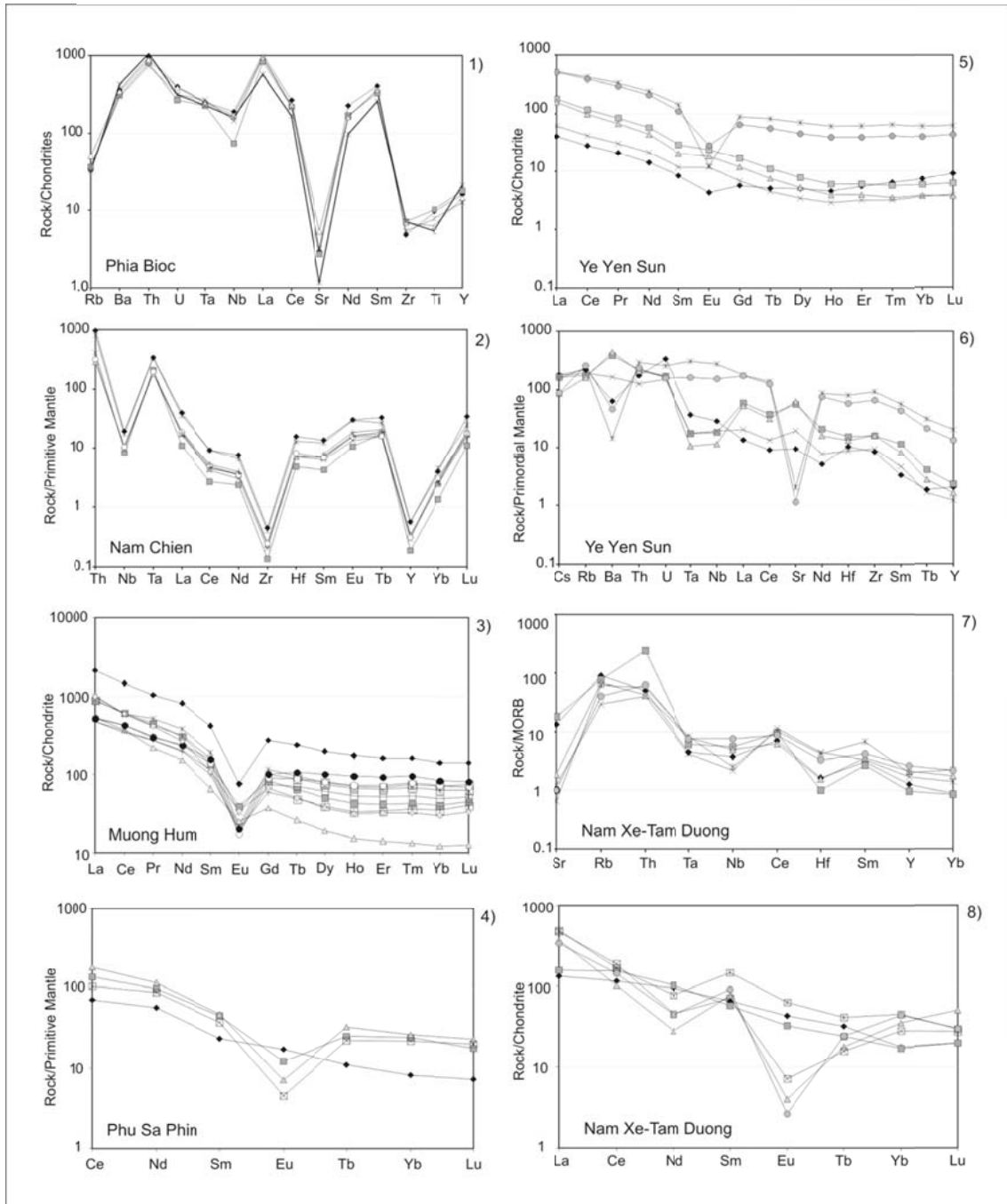


Fig. 4.21. Primitive mantle, chondrite-normalized, ocean island-normalized, and mid-ocean ridge basalt (applied method of Sun & McDonough, 1989) REE distribution patterns for the NWVN igneous rocks.

The content and distributive characteristics of REE are different in the studied granites (Table 4.17, Figs 4.21-5, 4.21-6). In the east, granite is very rich in REE, especially LREE with the ratio  $(La/Yb)_N = 8.65-12.88$ . The western granite is relatively poorer in REE with strongly changing ratio  $(La/Yb)_N = 5.38-41.46$ . The eastern granite is characterized by strong negative Eu anomaly ( $Eu/Eu^* = 0.11-0.30$ ), while the western granite has positive Eu anomaly or weak negative Eu anomaly ( $Eu/Eu^* = 0.62-1.30$ ). The absence of negative Eu anomaly and the relative richness in HREE is a particular feature of the western granite that needs further studies.

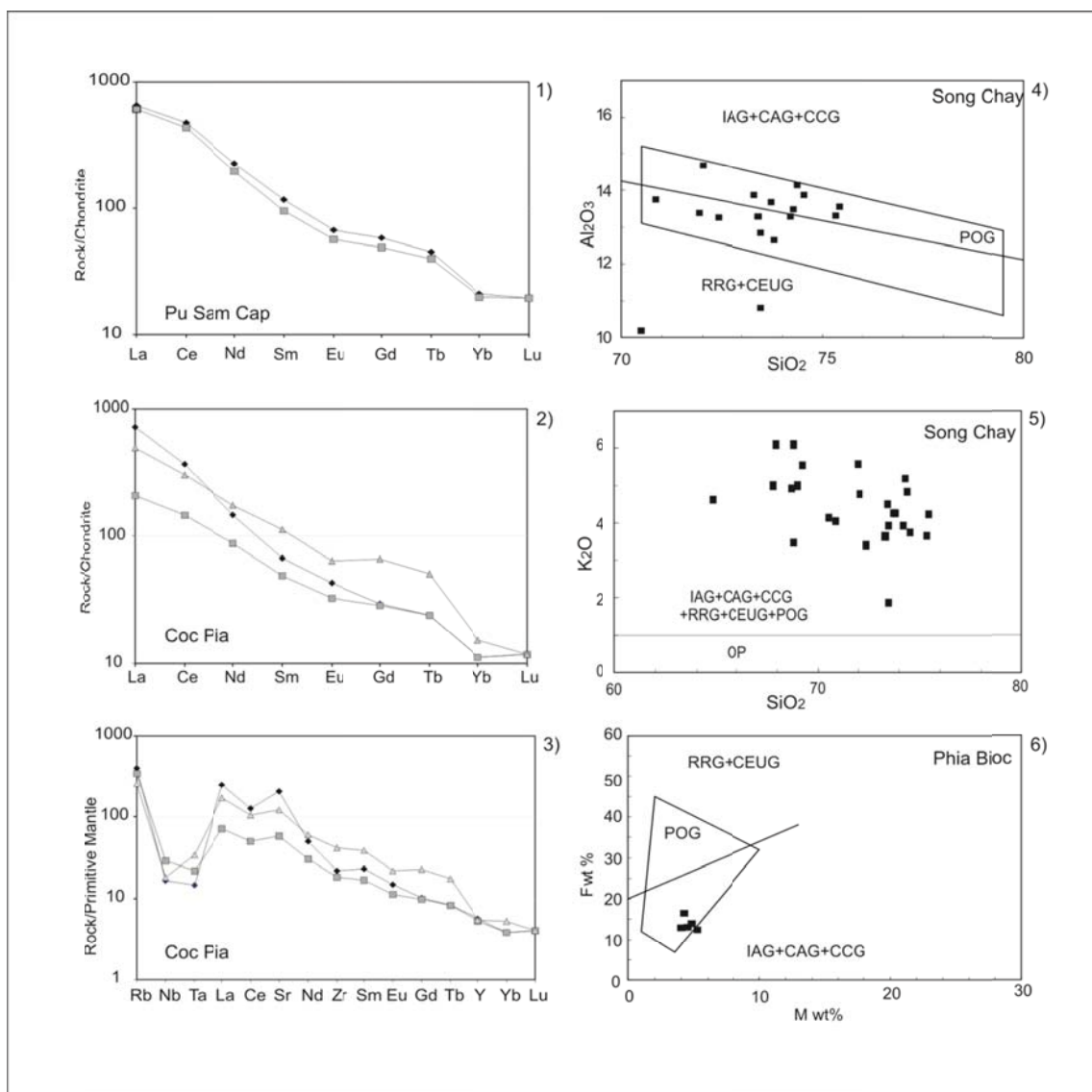


Fig. 4.22. Primitive mantle, chondrite-normalized (applied method of Sun & McDonough, 1989) REE distribution patterns (1-3); the correlated diagrams between SiO<sub>2</sub> and Al<sub>2</sub>O<sub>3</sub>; SiO<sub>2</sub> and K<sub>2</sub>O (4, 5); and discrimination diagram of granitoids (applied method of Maniar & Piccoli, 1989). IAG – Island arc granitoids; CAG – Continental arc granitoids; CCG – Continental collision granitoids, POG – Post-orogenic granitoids; RRG – Rift related granitoids; CEUG – Continental epeirogenic uplift granitoids, OP – Oceanic plagiogranites.

The studied rocks of the Nam Xe-Tam Duong complex are rich in Rb (59.4-180 ppm), very rich in Ba (35.3-796 ppm), Sr (78.5-2169 ppm), Y (29-78.4 ppm), but relatively poor in Zr (73-92 ppm), Nb (7.61-19.3 ppm), Ta (0.8-1.48 ppm). The content of REE in Nam Xe-Tam Duong granite is rather high, but not reaching the characteristics of calc-alkaline granitoid series. The characteristics of distribution of REE and the shortage of Nb, Ta, Zr and Hf (Table 4.19, Fig. 4.21-7, 4.21-8) correspond to granitoids related to the post-collision tectonic setting, belonging to the within-plate (intraplate) granite (Figs 4.24, 4.25).

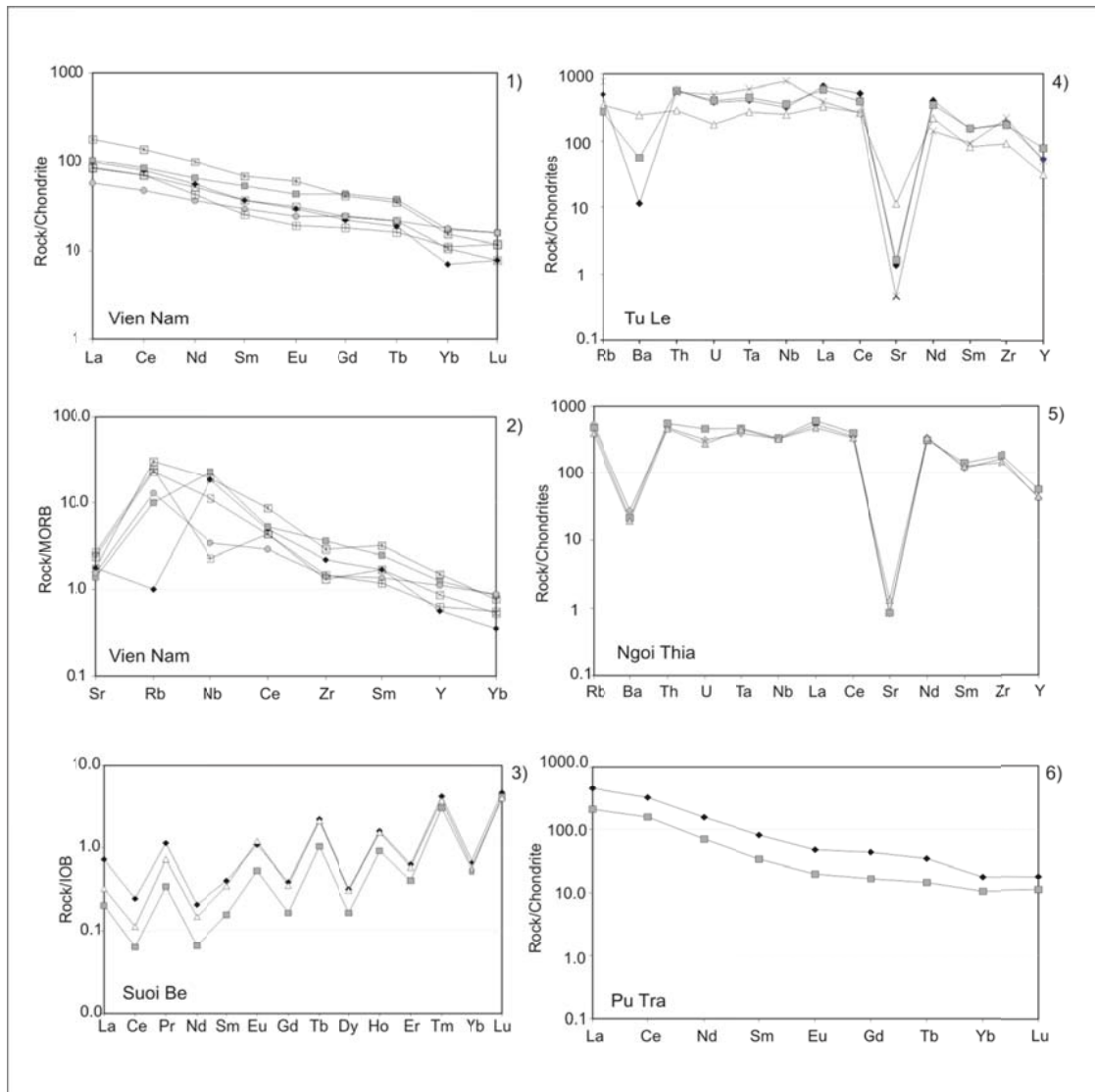


Fig. 4.23. Chondrite-normalized, ocean island-normalized, and mid-ocean ridge basalt (applied method of Sun & McDonough, 1989) REE distribution patterns for the NWVN volcanic rocks.

Other series includes syenite and nepheline syenite of the Pu Sam Cap complex, and syeno-diorite and gabbro of the Coc Pia complex. Rocks of the Pu Sam Cap complex are characterized by high and very high alkalinity ( $\text{Na}_2\text{O}+\text{K}_2\text{O}=12.46-12.47\%$ ), and belong to the potassic and ultrapotassic series ( $\text{K}_2\text{O}/\text{Na}_2\text{O}>2-4.4$ ). They are rich in Rb (241.6-265.7 ppm), Sr (2535-3989 ppm), Zr (521.8-559.1 ppm), Y (43.52-47.1 ppm), but rather poor in Nb (32.2-32.8

ppm), and Ta (1.5 ppm). They are also rich in LREE, as well as Th and U (Table 4.19), and the curve of their distribution has an unclear Eu min. In general, the characteristics of distribution of rare elements represent oceanic ridge granite and are similar to granitoids of the Nam Xe-Tam Duong complex with well manifested shortage of Nb and Ta (Fig. 4.22-1). As mentioned above, the characteristics of the Nb-Zr, Nb-Y and so on, indicate that alkaline granitoids of the Pu Sam Cap complex (A-granite) were formed in the within-plate (intraplate) (Figs 4.24, 4.25) extension environment which perhaps related to the strike-slip Ailao Shan - Red River fault zone during Palaeogene. In addition, the rocks of the Coc Pia complex (including all volcanites, intrusives, dykes and veins) correspond mainly to mafic group ( $\text{SiO}_2 = 48.32\text{-}54.26\%$ ). They are also rich in Rb (163-253 ppm), Sr (1226-4318 ppm), Zr (206-469 ppm) and REE, but relatively poor in Nb (12-20 ppm), Ta (0.6-1.4 ppm), and  $\text{TiO}_2$  (0.5-0.8 ppm) (Table 19). The characteristics of distribution of rare elements and REE of lamproite and absarokite show similarities of rocks within the Coc Pia complex (Figs 4.22-2, 4.22-3). The geochemical characteristics indicate that the magmatic fluid originated from materials of mantle basement that are enriched by lithophilous matters and other incompatible elements by latter metasomatism. However, the exhausted manifestations of Nb, Ta, and Ti show properties of a subduction zone during the forming process of potassic alkaline and potassic ultra-alkaline rocks of the Coc Pia complex. In general, the mafic-potassic alkaline and potassic ultra-alkaline rocks of the Copia complex are products of within-plate (intraplate) extension (Figs 4.24, 4.25) related to the strike-slip process of the Ailao Shan - Red River fault zone, which was caused by the collision between the Indian and Eurasian blocks (Chung *et al.*, 1997; and references therein).

The geochemical volcanic rocks from the NWVN area are also distinguished into mafic and felsic series (Figs 4.10, 4.13). Volcanic mafic series comprise mainly of basalts of the Huoi Hao, Vien Nam formations, basanite and fomite of the Suoi Be Formation, which are characterized by silica undersaturation ( $\text{SiO}_2=36.82\text{-}54.29\%$ ), low alkalinity ( $\text{Na}_2\text{O}+\text{K}_2\text{O}=0.38\text{-}7.29\%$ ),  $\text{K}_2\text{O}/\text{Na}_2\text{O}$  ratio is often lower than 1, except the T931344 sample of the Suoi Be Formation, and high in titanium ( $\text{TiO}_2=0.4\text{-}3.26\%$ ). On the  $\text{Na}_2\text{O}-\text{K}_2\text{O}-\text{CaO}$  diagram of Green & Poldervaart (1958) (Fig. 4.15), they belong to sodic rock type, except a sample of the Suoi Be Formation, which is plotted in the potassic field. On the discriminated diagram of Jensen & Rickwood (1989) (Fig. 4.17), the rocks of Suoi Be Formation are mainly high iron tholeiite (HFT), while the Huoi Hao Formation is plotted in high iron tholeiite (HFT) and high magnesium tholeiite (HMT). The Vien Nam basalts also display a wide range of komatite (PK), komatitic basalt (BK) to high iron tholeiite (HFT). Moreover, on the  $\text{FeO}t\text{-MgO}-\text{Al}_2\text{O}_3$  diagram of Pearce *et al.*, (1977) (Fig. 4.19), the Huoi Hao basalts fall into island ocean (IO) and ocean ridge-floor (ORF) type, the Vien Nam Formation are mainly island ocean (IO), while the Suoi Be basalts belong to continental ocean (CO). Particularly, rocks of the Vien Nam Formation are all relatively poor in Cu, Ni and Co, but rather rich in V, lithophile elements (Rb, Sr, Zr, Nb) and LREE (Table 4.9, Figs 4.23-1, 4.23-2). Based on the characteristics of distribution of REE and the Zr vs. Y-Zr, the mafic-ultramafic volcanites of the Then Sin-Phong Tho band can be considered as subalkaline association of within-plate (intraplate) magmatism (Fig. 4.26).

Moreover, the described rocks of the Suoi Be Formation have the content of Ti, Mn, Pb-Zn, Au, V and Co is higher than Clarke (Table 4.13). The rocks correspond to within-plate (intraplate) magmatism (Fig. 4.26).

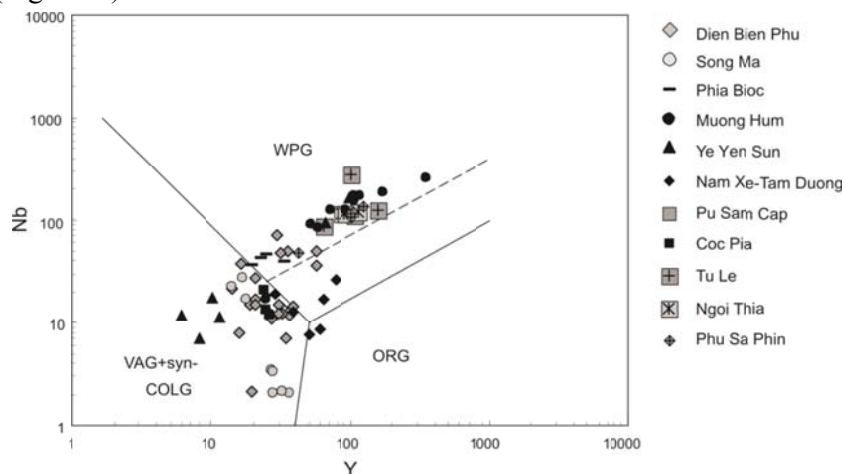


Fig. 4.24. Nb vs. Y binary diagram for the NWVN granitoids (applied method of Pearce *et al.*, 1984). ORG – Ocean ridge granitoids; Syn-COLG – Syn-collision granitoids; VAG – Volcanic arc granitoids; WPG – Within-plate (intraplate) granitoids.

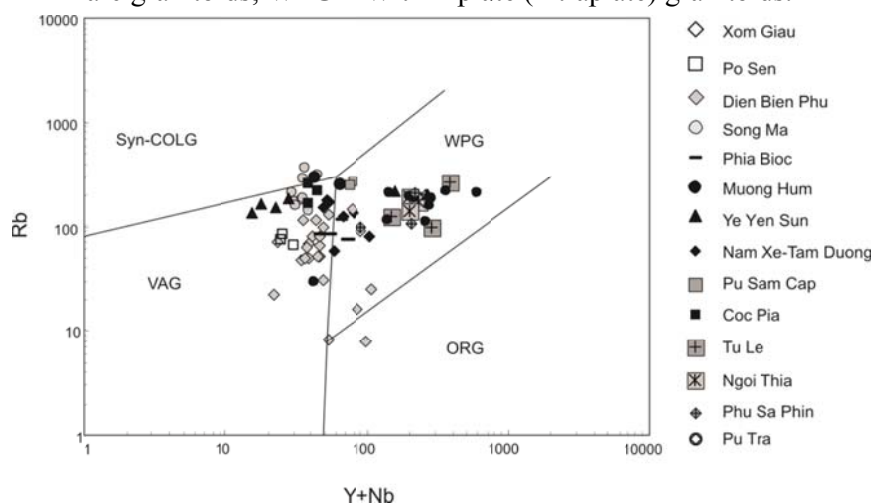


Fig. 4.25. Rb vs. Y+Nb binary diagram for the NWVN granitoids (applied method of Pearce *et al.*, 1984). ORG – Ocean ridge granitoids; Syn-COLG – Syn-collision granitoids; VAG – Volcanic arc granitoids; WPG – Within-plate (intraplate) granitoids.

Finally, the third series, which comprise the Tu Le, Ngoi Thia, and Pu Tra formations, is represented mainly by rhyolites and some trachytes. They are characterized by high contents of  $\text{SiO}_2$  (59.55-77.56%), and total  $\text{Na}_2\text{O}+\text{K}_2\text{O}$  (5.27-11.4%) with potassium prevailing sodium ( $\text{K}_2\text{O}/\text{Na}_2\text{O} = 0.96-4.84$ ). On the  $\text{Na}_2\text{O}-\text{K}_2\text{O}-\text{CaO}$  diagram of Green & Poldervaart (1958) (Fig. 4.15), they belong to potassic rock type. On the discriminated diagram of Jensen & Rickwood (1989) (Fig. 4.17), the Tu Le, Ngoi Thia, and Pu Tra volcanic rocks belong to the rhyolitic tholeiite type (TR). Both of the Tu Le and Ngoi Thia formations also displaying the characteristics of distribution of rare elements in rhyolite from the Binh Lu area are completely similar to that from the Tu Le, Tram Tau areas and to granite (A-granite) of Phu Sa Phin

complex (Fig. 4.21-4, Figs 4.23-4, 4.23-5). They indicate the products of within-plate (intraplate) magmatism (Table 4.15, Figs 4.24–4.26) and have isotopic characteristics:  $^{143}\text{Nd}/^{144}\text{Nd}=0.512562$ ;  $\epsilon\text{Nd}(0)=-1.48$  (original ratio  $\epsilon\text{Nd}(T)=0.6$ ) (Lan, 2000 and references therein). In addition, the Pu Tra volcanic rocks are rich in Rb, Ba, Sr, Zr and LREE (Table 18, Fig. 18-6). Due to the limited data of analyzed samples, we cannot identify certain tectonic setting for the Pu Tra Formation, but both characteristics of the Nb vs. Y+Nb, and Zr vs. Zr-Y suggest that the Pu Tra Formation may be related to within-plate (intraplate) setting (Fig. 4.26).

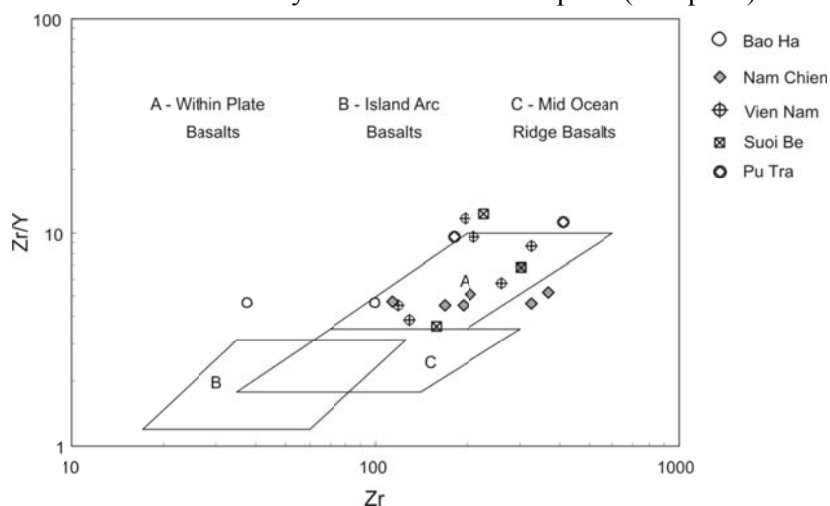


Fig. 4.26. The Zr/Y vs. Zr correlation for the NWVN magmatic rocks (applied method of Pearce & Norry, 1979).

## 4.2. Discussion

The detailed magmatic units and their relationship to tectonics are presented in Table 4.20. Six groups of magmatic rocks are related to the tectonic events. The first, Proterozoic group corresponds to the major episodes of crustal formation in the South China block, or is linked with the formation of Gondwana. The tectonic environment of the Northwest Vietnam changed from a subduction-related magmatism (orogenic) to a matured continental intraplate magmatism (anorogenic) in the time span between the Palaeozoic-early Triassic and Cretaceous (Fig. 4.27, Table 4.20).

The second group comprises the Devonian Song Chay granitoids, coeval with the Palaeozoic orogenic event. The third group contains Permian magmatic rocks – ophiolites of the Nui Nua, Bo Xinh, Chieng Khuong complexes, ultramafic Ban Xang complex and Huoi Hao Formation as well as extrusives of Cam Thuy, Vien Nam formations formed in intraplate setting, related to back-arcs spreading.

The fourth group is related to Triassic Indosinian orogeny and includes granitoids of the Dien Bien Phu, Song Ma and Phia Bioc complexes. The granitoids of Dien Bien Phu complex were formed in syn-collisional, while the granitoids of the Song Ma and Phia Bioc complexes in post-collisional tectonic setting.

The fifth group comprises the mafic effusive of Suoi Be Formation, gabbroic Nam Chien complex, acidic volcanics from the Tu Le, Ngoi Thia complexes, granosyenite and granite from

Phu Sa Phin and Muong Hum complexes, and biotitic granite of East Ye Yen Sun complex. They were formed during Jurassic-Cretaceous intraplate magmatism activity, linked to the Yanshanian tectonic cycle, related to the collision between Izanagi Plate (proto-Pacific Ocean) and South China.

The last group comprises the West Ye Yen Sun leucocratic granite, subalkaline to alkaline Nam Xe-Tam Duong granites, syenite and granosyenite from Pu Sam Cap, mafic-potassic alkaline Coc Pia complexes and rhyolite from the Pu Tra Formation. These rocks were formed during Cenozoic times, as an effect of strike-slip faulting related to the collision of India and Eurasia plates.

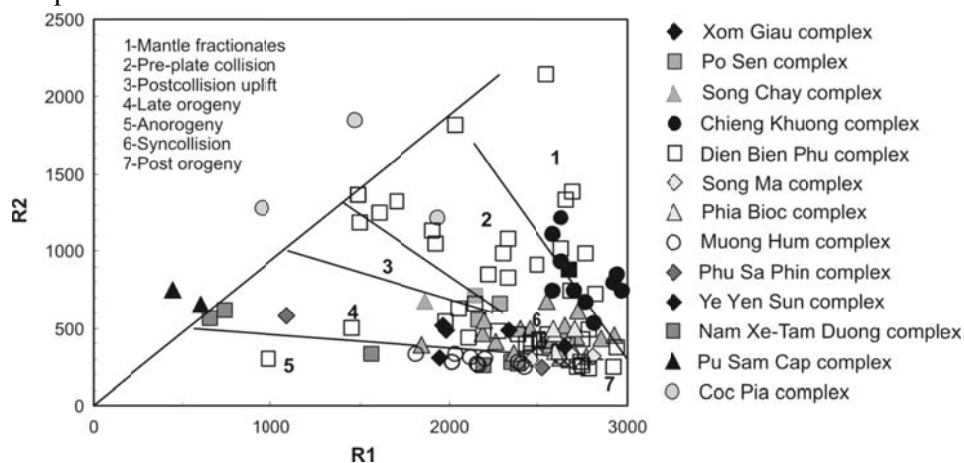


Fig. 4.27. The R1–R2 discriminated diagram for granitoids (applied method of Batchelor & Bowden, 1985).  $R1 = 4Si - 11(Na + K) - (Fe + Ti)$ ;  $R2 = 6Ca + Al$ .

Table 4.20. The magmatic rocks and their relationship to the tectonic setting of NWVN area

Erathem Era	System Period	Lithological complexes	Symbol	Magmatic rocks		Probable tectonic setting
				Intrusive	Effusive	
Cenozoic	Palaeogene	Pu Tra	26		x	<i>intraplate extension</i>
		Coc Pia	25	x		<i>intraplate extension</i>
		Pu Sam Cap	24	x		<i>intraplate extension</i>
		Nam Xe-Tam Duong	23	x		<i>intraplate extension</i>
		West Ye Yen Sun	22	x		<i>intraplate extension</i>
Mesozoic	Cretaceous	East Ye Yen Sun	21	x		<i>intraplate magmatism</i>
		Phu Sa Phin	20	x		<i>intraplate magmatism</i>
		Muong Hum	19	x		<i>intraplate magmatism</i>
		Ngoi Thia	18		x	<i>intraplate magmatism</i>
		Tu Le	17		x	<i>intraplate magmatism</i>
		Nam Chien	16	x		<i>intraplate magmatism</i>
	Permian-Triassic	Suoi Be	15		x	<i>intraplate magmatism</i>
		Phia Bioc	14	x		<i>post-orogenies</i>
		Song Ma	13	x		<i>post-orogenies</i>
		Dien Bien Phu	12	x		<i>syn-collision related to the subduction zone</i>
Palaeozoic	Permian-Triassic	Ban Xang	11		x	<i>ophiolite</i>
		Vien Nam	10		x	<i>intraplate extension</i>
		Cam Thuy	9		x	<i>intraplate extension</i>

Erathem Era	System Period	Lithological complexes	Symbol	Magmatic rocks		Probable tectonic setting
				Intrusive	Effusive	
		Huoi Hao	8		x	<i>ophiolite belt</i>
		Chieng Khuong	7	x		<i>ophiolite belt</i>
		Bo Xinh	6	x		<i>ophiolite belt</i>
		Nui Nua	5	x		<i>ophiolite belt</i>
		Song Chay	4	x		<i>post orogenic granite</i>
		Proterozoic		Po Sen	3	x
Xom Giau	2	x			<i>volcanic arc granite to subduction</i>	
Bao Ha	1	x			<i>active continental margin</i>	

Table 4.1 Representative chemical and trace element composition of gabbroids of the Bao Ha complex (data from Nguyen Van The, ed., 1999, Tran Trong Hoa *et al.*, 1999).

Sample	SiO <sub>2</sub>	TiO <sub>2</sub>	Al <sub>2</sub> O <sub>3</sub>	Fe <sub>2</sub> O <sub>3</sub>	MnO	MgO	CaO	Na <sub>2</sub> O	K <sub>2</sub> O	P <sub>2</sub> O <sub>5</sub>	
LY.835	48.98	1.32	14.59	11.72	0.17	7.32	12.3	3.06	0.30	0.12	
LY.10523	45.46	2.66	13.11	15.31	0.18	6.73	8.53	4.47	0.11	0.23	
	Cu	Ni	Co	Cr	V	Rb	Sr	Zr	Nb	Y	Ta
LY.835	73	76	32	271	316	4.3	140	37.7	3.6	8.2	0.5
LY.10523	5	115	50	146	402	2.1	51.2	100	14.6	21.5	0.5
	Th	Hf	La	Ce	Nd	Sm	Eu	Gd	Tb	Yb	Lu
LY.835	0.6	1.5	5.4	14	10	3.2	1	3	0.5	1.35	0.19
LY.10523	0.9	3.1	10	22	14	4.3	1.4	5	0.9	2.7	0.38

Table 4.2 Representative chemical and trace element composition of microcline-rich biotite granite of the Xom Giau complex (data from Nguyen Van The, ed., 1999, Tran Trong Hoa *et al.*, 1999).

Sample	SiO <sub>2</sub>	TiO <sub>2</sub>	Al <sub>2</sub> O <sub>3</sub>	Fe <sub>2</sub> O <sub>3</sub>	MnO	MgO	CaO	Na <sub>2</sub> O	K <sub>2</sub> O	P <sub>2</sub> O <sub>5</sub>
LY.3916	73.76	0.32	12.83	3.35	0.03	0.27	0.72	3.47	4.16	0.03
LY.5414	71.06	0.10	14.01	1.9	0.04	0.56	2.80	5.71	0.05	-
	Rb	Sr	Zr	Nb	Y	Th	U	Ta	Hf	
LY.3916	170	105	476	8.5	44	55	9	1.65	14	
LY.5414	-	-	-	-	-	-	-	-	-	
	La	Ce	Nd	Sm	Eu	Gd	Tb	Yb	Lu	
LY.3916	140	240	102	22	1.25	16	2.30	3.30	0.43	
LY.5414	102	132.7	43.3	5.6	0.76	4.03	0.67	1.47	0.35	

Table 4.3 Representative chemical and trace element composition of granitoids of the Po Sen complex (data from Lan *et al.*, 2000)

Sample	SiO <sub>2</sub>	TiO <sub>2</sub>	Al <sub>2</sub> O <sub>3</sub>	Fe <sub>2</sub> O <sub>3</sub>	MnO	MgO	CaO	Na <sub>2</sub> O	K <sub>2</sub> O	P <sub>2</sub> O <sub>5</sub>
RR28A	66.08	0.54	15.88	4.13	0.06	1.25	3.09	4.35	2.71	0.18
RR28B	60.05	0.49	15.44	3.43	0.05	1.05	2.81	4.28	2.87	0.14
RR29	68.73	0.48	14.94	2.79	0.03	1.18	1.88	4.17	3.77	0.14
	Rb	Sr	Nb	Zr	Y	Th	U	Ta	Hf	La
RR28A	67	548	11.1	196	19	5.7	1.3	0.77	6.6	54.1
RR28B	75	433	9.4	163	15	6.7	1.7	0.76	5.8	37.8
RR29	84	42.9	9.8	169	16	6.0	2.4	0.70	6.0	36.5
	Ce	Nd	Sm	Eu	Tb	Yb	Lu			
RR28A	102.2	54.3	6.20	1.23	0.87	2.26	0.25			
RR28B	76.4	28.6	5.36	1.07	0.67	1.70	0.28			
RR29	73.2	47.3	5.00	1.08	0.68	0.70	0.28			

Table 4.4 Representative chemical composition of granitoids of the Song Chay complex (data from Tran Duc Luong & Nguyen Xuan Bao, 1995).

Sample	NT38	71/3	NTCB37	TH71/1	2674A	71/4	73/50	10552	NT2265
SiO <sub>2</sub>	64.76	67.78	67.92	68.68	68.8	68.8	68.98	69.19	70.49
TiO <sub>2</sub>	0.43	0.39	0.39	0.25	0.35	0.4	0.14	0.41	0.25
Al <sub>2</sub> O <sub>3</sub>	14.45	16.43	16.94	16.47	16.94	15.68	16.65	16.67	10.19
Fe <sub>2</sub> O <sub>3</sub>	1.91	1.08	0.8	1.14	0.8	1.32	0.78	0.17	2.41
FeO	4.09	2.12	2.2	1.29	2.2	2.2	0.96	3.05	1.66
FeOt	6	3.2	3	2.43	3	3.52	1.74	3.22	4.07
MnO	0.13	0.07	0.11	0.06	0.11	0.06	0.05	0.04	0.18
MgO	1.01	0.71	0.75	0.68	0.75	0.78	0.36	0.8	2.42
CaO	3.23	1.04	1.2	0.5	1.2	1.29	0.45	1.45	3.32
Na <sub>2</sub> O	3.7	3.15	1.89	3.185	1.89	3.04	4.37	1.81	3.1
K <sub>2</sub> O	4.61	5	6.11	4.91	6.11	3.48	5	5.55	4.15
P <sub>2</sub> O <sub>5</sub>	0.15	0.31	0.06	0.22	0.06	0.18	0.33	0.02	0.39
Sample	72/3	H4658/2	H4341	H4662/3	41M	H4337/5	2268	NT2150	H4339/1
SiO <sub>2</sub>	70.84	71.92	72.02	72.38	73.3	73.4	73.45	73.47	73.72
TiO <sub>2</sub>	0.57	0.02	0.21	0.04	0.46	0.29	0.25	0.01	0.12
Al <sub>2</sub> O <sub>3</sub>	13.77	13.39	14.68	13.28	13.89	13.3	10.83	12.86	13.7
Fe <sub>2</sub> O <sub>3</sub>	1	0.63	0.54	4.83	1.22	1.13	2.4	2.24	0.55
FeO	2.9	0.79	1.05	0.44	1.71	1.36	0.5	0.07	0.69
FeOt	3.9	1.42	1.59	5.27	2.93	2.49	2.9	2.31	1.24
MnO	0.07	0.29	0.03	0.14	0.16	0.05	0.05	0.01	-
MgO	0.89	0.5	0.46	1.37	1.33	0.81	0.2	0.5	0.05
CaO	1.09	2.48	0.28	1.19	1.01	0.71	3.64	1.54	0.35
Na <sub>2</sub> O	2.46	3.58	3.65	2.76	2.16	3.13	4.65	3.4	3.57
K <sub>2</sub> O	4.06	5.58	4.78	3.4	3.64	4.49	1.9	3.92	4.26
P <sub>2</sub> O <sub>5</sub>	0.21	-	0.17	-	-	0.2	0.28	0.54	0.22
Sample	H4345	NT.HG4	H4347	73/4a	73/5	H4663	46M		
SiO <sub>2</sub>	73.8	74.19	74.26	74.37	74.54	75.32	75.42		
TiO <sub>2</sub>	0.37	0.08	-	0.16	0.06	0.02	-		
Al <sub>2</sub> O <sub>3</sub>	12.66	13.3	13.49	14.14	13.88	13.32	13.57		
Fe <sub>2</sub> O <sub>3</sub>	1.46	1.23	0.53	0.89	0.79	2.86	0.79		
FeO	1.55	0.12	0.88	0.69	0.83	0.46	0.56		
FeOt	3.01	1.35	1.41	1.58	1.62	3.32	1.35		
MnO	0.05	0.09	0.03	0.05	0.03	0.11	0.2		
MgO	0.77	0.29	0.51	0.46	0.18	1.23	0.26		
CaO	-	1.05	0.14	0.2	0.4	0.2	0.36		
Na <sub>2</sub> O	2.33	4	2.5	2.89	4	2.15	3.45		
K <sub>2</sub> O	4.26	3.93	5.2	4.82	3.75	3.67	4.24		
P <sub>2</sub> O <sub>5</sub>	0.19	0.3	0.13	0.17	0.27	-	-		

Table 4.5 Representative chemical composition of the ultramafic Nui Nua complex (data from Phan Son *et al.*, 2005-in the Son Lasheet group at 1:200,000 scale)

Sample	S.7270/1	S.7268/1	S.5071	SL.6052	SL.5069/1	S.9101
SiO <sub>2</sub>	36.08	38.23	38.36	39.08	39.14	39.74
TiO <sub>2</sub>	0.07	0.04	0	0	0	0.11
Al <sub>2</sub> O <sub>3</sub>	2.02	1.27	1.63	2.04	1.43	1.57
Fe <sub>2</sub> O <sub>3</sub>	10.18	5.98	6.98	5.28	5.58	6.78

<b>FeO</b>	0	0	2.73	1.72	1.87	1.57
<b>MnO</b>	0	0	0.11	0.12	0.15	0.09
<b>MgO</b>	38.80	36.66	36.74	37.83	37.92	36.78
<b>CaO</b>	2.24	2.86	0	0	0	0
<b>Na<sub>2</sub>O</b>	1.83	1.10	0.11	0.13	0.13	0.99
<b>K<sub>2</sub>O</b>	0.05	0.05	0.13	0.13	0.13	0.16
<b>P<sub>2</sub>O<sub>5</sub></b>	0.11	0.06	0.04	0.03	0.05	0.12
<b>MKN</b>	8.40	13.20	12.28	12.52	12.44	11.47
<b>Sample</b>	<b>SL.5124/3</b>	<b>SL.5203</b>	<b>SL.74/2</b>	<b>S.2511/2</b>	<b>SL.4007/3</b>	<b>SL.1806/5</b>
<b>SiO<sub>2</sub></b>	39.82	39.96	40.26	40.68	42.96	46.36
<b>TiO<sub>2</sub></b>	0	0	0	0.06	0	0
<b>Al<sub>2</sub>O<sub>3</sub></b>	1.63	1.85	1.73	2.12	0.93	0.21
<b>Fe<sub>2</sub>O<sub>3</sub></b>	4.96	5.59	4.38	7.29	4.10	3.23
<b>FeO</b>	1.29	1.22	3.02	5.18	3.02	3.38
<b>MnO</b>	0.11	0.13	0.05	0.07	0.11	0.09
<b>MgO</b>	37.92	35.82	37.21	36.35	34.89	34.39
<b>CaO</b>	0	0.28	0.14	0.63	0.84	0.28
<b>Na<sub>2</sub>O</b>	0.13	0.90	0	0.18	0.15	0.37
<b>K<sub>2</sub>O</b>	0.13	0.25	0	0.16	0.08	0
<b>P<sub>2</sub>O<sub>5</sub></b>	0.05	0.16	0.08	0.04	0.13	0.04
<b>MKN</b>	12.73	13.15	12.26	5.12	11.443	9.73

Table 4.6 Representative chemical composition of the gabbroic Bo Xinh complex (data from Phan Son *et al.*, 2005-in the Son La sheet group at 1:200,000 scale)

<b>Sample</b>	<b>SL.4009</b>	<b>SL.4009/4</b>	<b>SL.5340</b>	<b>SL.4010/6</b>	<b>S.1305</b>	<b>SL.4007/6</b>
<b>SiO<sub>2</sub></b>	41.4	47.08	48.18	48.6	48.6	48.78
<b>TiO<sub>2</sub></b>	2.1	1.2	0.9	1.1	1.72	1.6
<b>Al<sub>2</sub>O<sub>3</sub></b>	16.69	14.88	14.36	16.81	14.7	12.57
<b>Fe<sub>2</sub>O<sub>3</sub>t</b>	3.7	3.3	2.06	2.94	15.36	2.45
<b>FeO</b>	10.96	6.75	5.82	5.23	0	8.8
<b>MnO</b>	0.24	0.2	0.15	0.15	0	0.2
<b>MgO</b>	10.33	12.23	6.78	7.82	4.8	8.62
<b>CaO</b>	7.67	8.37	11.1	9.49	10.22	8.93
<b>Na<sub>2</sub>O</b>	1.56	1.77	3.44	2.29	2.6	2.84
<b>K<sub>2</sub>O</b>	0.17	0.17	0	0.09	0.52	0.8
<b>P<sub>2</sub>O<sub>5</sub></b>	0.27	0.13	0.27	0.11	0.27	0.2
<b>MKN</b>	0.48	2.72	2.69	2.69	0.43	3.74
<b>Sample</b>	<b>SL.4008/5</b>	<b>SL.1802</b>	<b>SL.4012/1</b>	<b>S.1632/1</b>	<b>S.8515/1</b>	<b>S.7214</b>
<b>SiO<sub>2</sub></b>	48.94	51.48	52.72	54.68	55.06	55.14
<b>TiO<sub>2</sub></b>	0.8	1.1	1	1.1	1.68	1.9
<b>Al<sub>2</sub>O<sub>3</sub></b>	17.92	15.16	15.22	13.98	14.48	12.84
<b>Fe<sub>2</sub>O<sub>3</sub>t</b>	3.18	2.45	2.34	2.49	2.62	2.43
<b>FeO</b>	4.28	8.23	7.9	10.85	9.14	12.03
<b>MnO</b>	0.15	0.21	0.2	0.29	0.11	0.17
<b>MgO</b>	6.82	6.12	5.82	2.41	2.94	2.78
<b>CaO</b>	12	9.77	8.93	5.95	6.73	6.14
<b>Na<sub>2</sub>O</b>	2.19	2.31	2.31	3.16	3.74	2.27
<b>K<sub>2</sub>O</b>	0	0.58	0.75	1	0.97	1.8
<b>P<sub>2</sub>O<sub>5</sub></b>	0.13	0.27	0.17	0.83	0.16	0.35
<b>MKN</b>	2.24	1.55	1.64	1.52	1.02	0

Table 4.7 Representative chemical composition of plagiogranite of the Chieng Khuong complex  
(data from Phan Son *et al.*, 2005-in the Son La sheet group at 1:200,000 scale)

Sample	SL.24	SL.6121	SL.1805/4	SL.1805	SL.6122	SL.2511/2	SL.2511/1	SL.6106/1	S.540/5
SiO <sub>2</sub>	57.94	62.82	66.4	67.88	69	69.12	69.12	69.28	69.76
TiO <sub>2</sub>	0.6	0.1	0.1	0.1	0.1	0.4	0.4	0.2	0.58
Al <sub>2</sub> O <sub>3</sub>	17.77	18.78	18.37	17.03	16.52	16.35	16.35	16.14	15.57
Fe <sub>2</sub> O <sub>3</sub>	0.49	0.5	0.14	0.75	0.25	1.11	0.11	0.42	0.68
FeO	4.96	2.55	1.87	1.9	1.62	1.9	1.9	1.9	2.18
MnO	0.12	0.02	0.05	0.05	0.05	0.02	0.02	0.04	0.03
MgO	2.39	2.21	1	1.2	0.9	1.1	1.1	1	0.85
CaO	6.94	5.86	4.88	4.19	4.03	3.77	3.77	3.47	3.63
Na <sub>2</sub> O	2.36	3.75	4.25	3.75	3.44	3.64	3.64	3.75	5.06
K <sub>2</sub> O	1.53	1.06	1.15	0.96	1.25	1.13	1.13	1.25	0.98
P <sub>2</sub> O <sub>5</sub>	0.29	0.2	0.17	0.16	0.16	0	0	0.17	0
MKN	2.65	0.49	0.42	0.5	0.73	0.1	0.07	0.41	0.11
<b>Sample</b>	<b>S.7251</b>	<b>S.3321</b>	<b>S.540</b>	<b>SL.1806c</b>	<b>SL.1806A</b>	<b>S.4219</b>	<b>S.1481/1</b>	<b>SL.1806B</b>	
SiO <sub>2</sub>	69.9	70.58	71.22	71.7	72.06	72.12	72.62	73.66	
TiO <sub>2</sub>	0.32	0.35	0.31	0.1	0.1	0.27	0.09	0	
Al <sub>2</sub> O <sub>3</sub>	15.7	15.21	15.18	15.59	14.36	13.8	14.59	14.62	
Fe <sub>2</sub> O <sub>3</sub>	0.77	0.67	0.74	0.4	0.39	2.3	0.69	0.16	
FeO	2.31	2.08	2.12	1.36	2.37	0	2.88	1.29	
MnO	0.03	0.07	0.02	0.05	0.07	0	0.06	0.01	
MgO	1.1	1	0.8	0.6	1.7	0.2	0.49	0.1	
CaO	3.2	3.4	3.77	3.07	3.11	4.76	1.77	2.23	
Na <sub>2</sub> O	3.82	3.89	5.06	4.09	3.33	4.37	3.68	3.75	
K <sub>2</sub> O	1.05	1	0.91	2.29	1.34	1.1	1.02	3.23	
P <sub>2</sub> O <sub>5</sub>	0	0	0	0.08	0.08	0	0	0.04	
MKN	0.46	1.23	0.07	0.29	0.4	1.07	0.5	0.13	

Table 4.8 Representative chemical composition of metabasalts of the Huoi Hao Formation  
(data from Phan Son *et al.*, 2005-in the Son Lasheet group at 1:200,000 scale)

Sample	SL.4007/4	SL.90KT	SL.88KT/2	SL.1585	SL.5194	SL.6058
SiO <sub>2</sub>	43.86	46.94	47.03	47.24	48.64	49.76
TiO <sub>2</sub>	1	1.8	1.7	2.6	1.4	2.1
Al <sub>2</sub> O <sub>3</sub>	16.45	13.89	13.34	13.23	14.97	12.32
Fe <sub>2</sub> O <sub>3</sub>	0.94	5.12	3.3	3.51	3.87	1.98
FeO	8.15	7.62	8.24	9.23	5.9	12.29
MnO	0.2	0.21	0.18	0.18	0.18	0.29
MgO	7.82	7.58	7.58	6.72	9.38	6.42
CaO	6.14	11.1	10.55	9.07	11.38	7.83
Na <sub>2</sub> O	2.05	1.72	2.19	2.84	1.88	2.25
K <sub>2</sub> O	0.5	0.13	0.19	0.67	0.23	0.25
P <sub>2</sub> O <sub>5</sub>	0.27	0.27	0.27	0.17	0.2	0.24
MKN	11	2.08	2.87	2.81	0.48	2.43
<b>Sample</b>	<b>SL.94KT</b>	<b>SL.88KT/3</b>	<b>SL.6062/1</b>	<b>SL.4007/1</b>	<b>SL.94KT</b>	
SiO <sub>2</sub>	49.88	49.94	51.84	53.72	49.88	
TiO <sub>2</sub>	2.2	0.9	1.3	0.4	2.2	
Al <sub>2</sub> O <sub>3</sub>	12.3	16.52	14.06	12.72	12.3	
Fe <sub>2</sub> O <sub>3</sub>	4.18	2.13	2.67	0.43	4.18	

<b>FeO</b>	10	6.91	8.3	4.63	10
<b>MnO</b>	0.21	0.13	0.25	0.12	0.21
<b>MgO</b>	6.29	9.18	5.93	9.43	6.29
<b>CaO</b>	9.58	5	8.79	5.3	9.58
<b>Na<sub>2</sub>O</b>	1.41	1.72	2.25	2.41	1.41
<b>K<sub>2</sub>O</b>	0.13	0.13	1	0.17	0.13
<b>P<sub>2</sub>O<sub>5</sub></b>	0.36	0.29	0.11	0.24	0.36
<b>MKN</b>	0.92	5.31	1.56	8.97	0.92

Table 4.9 Representative chemical composition of picrite (P.18), microbasalt (H.639), basalt (H.615); andesitobasalt (T1500), basaltolivine (T1648) of the Cam Thuy, and Vien Nam Formations. (H – Sample from the Institute of Geosciences (ASTVN); P, T – Sample from the Phong Tho sheet group at 1:50 000 scale)

Sample	SiO <sub>2</sub>	TiO <sub>2</sub>	Al <sub>2</sub> O <sub>3</sub>	Fe <sub>2</sub> O <sub>3</sub>	MnO	MgO	CaO	Na <sub>2</sub> O	K <sub>2</sub> O	P <sub>2</sub> O <sub>5</sub>
<b>P.18</b>	43.89	2.14	6.55	12.76	0.19	22.91	10.22	0.21	0.17	0.27
<b>P.181/89</b>	47.85	2.64	15.03	11.4	0.16	6.04	8.96	3.25	1.07	0.37
<b>H639</b>	46.27	2.31	9.04	13.23	0.22	12.16	12.78	2.49	0.63	0.25
<b>H615</b>	46.27	2.35	14.02	13.87	0.24	7.32	8.24	3.29	1.25	0.2
<b>T1500</b>	54.29	3.26	10.33	14.41	0.18	5.77	6.79	0.9	0.57	0.39
<b>T1648</b>	48.47	1.58	14.64	13.93	0.23	7.4	10.31	2.39	0.79	0.18
	<b>Ni</b>	<b>Co</b>	<b>Cu</b>	<b>Cr</b>	<b>V</b>	<b>Rb</b>	<b>Sr</b>	<b>Nb</b>	<b>Zr</b>	<b>Y</b>
<b>P.18</b>	-	-	-	-	-	2	212	65	197	17
<b>P.181/89</b>	79	30		390	390	20	166	80	324	37.5
<b>H639</b>	297	67	87	848	227	62	689	59	209	22
<b>H615</b>	95	59	163	125	285	46	287	39	118	26
<b>T1500</b>	91	41	118	263	249	61	210	67	260	45
<b>T1648</b>	320	54	30	240	240	25.8	186	11.9	128.4	33.3
	<b>La</b>	<b>Ce</b>	<b>Nd</b>	<b>Sm</b>	<b>Eu</b>	<b>Gd</b>	<b>Th</b>	<b>Yb</b>	<b>Lu</b>	
<b>P.18</b>	23.6	49	26	5.6	1.7	4.5	0.7	1.2	0.2	
<b>P.181/89</b>	24.8	52.3	30.6	8.2	2.5	8.9	1.4	2.9	0.4	
<b>H639</b>	33	68	36	7.4	2.2	5.4	0.8	1.7	0.2	
<b>H615</b>	20.4	43	24	5.6	1.8	4.9	0.8	1.8	0.2	
<b>T1500</b>	43	86	47	10.5	3.5	8.4	1.3	2.6	0.3	
<b>T1648</b>	13.6	29	17	4.5	1.4	5	0.8	3	0.4	

Table 4.10 Representative chemical composition of the ultramafic Ban Xang complex (data from Nguyen Xuan Bao *et al.*, 2005-in the Van Yen sheet group at 1:200,000 scale)

Sample	844	920/78	P.191	844/78	862/78	861/78	886/78	VY.6522
<b>SiO<sub>2</sub></b>	34.3	34.45	35.2	35.44	36.4	37.4	38.05	40.62
<b>TiO<sub>2</sub></b>	0.08	0.05	0.04	0.14	0.14	0.13	0.08	0.6
<b>Al<sub>2</sub>O<sub>3</sub></b>	1	0.95	0.5	1.43	1.2	1.3	1.9	4.79
<b>Fe<sub>2</sub>O<sub>3</sub></b>	8.86	3.06	4.04	3.48	3.72	3.52	2.33	4.16
<b>FeO</b>	1.48	2.68	2.4	5.45	9.34	9.34	2.77	7.26
<b>MnO</b>	0.12	0.01	0.08	0.01	0.16	0.15	0.01	0.18
<b>MgO</b>	36.85	40.4	40.7	37.35	35.75	33.77	39.9	24.47
<b>CaO</b>	0.62	0.43	0.24	1.89	2.94	2.67	1.33	5.86
<b>Na<sub>2</sub>O</b>	0.02	1.12	0.67	0.45	0.09	0.28	1.17	2.08
<b>K<sub>2</sub>O</b>	0.01	0.5	0.12	0.25	0.08	0.1	0.3	0.94
<b>P<sub>2</sub>O<sub>5</sub></b>	0.01	0.01	0.03	0	0.1	0.09	0	0.2
<b>Sample</b>	<b>VY.9536/2</b>	<b>VY.968/1</b>	<b>VY.9505/1</b>	<b>VY.4156/2</b>	<b>VY.4156/d</b>	<b>VY.9515/1</b>	<b>VY.904</b>	<b>VY.4154</b>
<b>SiO<sub>2</sub></b>	41.82	41.82	42.18	43.98	44.02	44.36	45.38	45.82
<b>TiO<sub>2</sub></b>	0.7	0.8	1.1	1.7	1.9	1.1	1.4	0.6

Sample	844	920/78	P.191	844/78	862/78	861/78	886/78	VY.6522
Al <sub>2</sub> O <sub>3</sub>	4.2	7.46	6.75	6.99	6.86	8.61	11.32	11.42
Fe <sub>2</sub> O <sub>3</sub>	2.72	2.51	2.17	3.05	2.33	3.16	2.31	2.98
FeO	8.98	8.69	10.2	7.54	8.19	7.44	9.3	6.04
MnO	0.21	0.16	0.17	0.17	0.17	0.17	0.23	0.15
MgO	24.27	22.95	22.26	16.85	14.44	11.85	12.27	14.94
CaO	7.11	6.38	6.84	8.05	10.6	10.04	9.58	10.46
Na <sub>2</sub> O	1.25	0.31	1.25	2.13	2	1.75	2.19	1.15
K <sub>2</sub> O	1.26	0	0.31	1.5	1.23	0.31	1.88	0.75
P <sub>2</sub> O <sub>5</sub>	0.24	0.17	0.24	0.33	0.36	0.2	0.24	0.13

Table 4.11a. Representative chemical composition of granitoids of the Dien Bien Phu complex (data from Tran Dang Tuyet *et al.*, 2005- in the Khi Su-Muong Te sheet group at 1:200,000 scale)

Sample	M.301	M.63/4	M.8005	M.64/2	M.302	M.1532	M.5017	M.1039/3	M.1500	M.67/1
SiO <sub>2</sub>	48.54	48.74	50.3	50.58	50.58	51.64	57.08	57.26	58.03	58.74
TiO <sub>2</sub>	2.1	0.2	1.3	1.9	1.08	1.33	0.6	1.4	0.76	0.7
Al <sub>2</sub> O <sub>3</sub>	14.75	14.77	14.87	15.59	15.04	17.09	16.47	16.69	17.5	16.4
Fe <sub>2</sub> O <sub>3</sub>	2.29	3.95	1.92	7.62	3.55	3.65	3.31	2.48	3.45	2.87
FeO	8.66	9.27	6.03	3.5	9.38	6.2	4.49	7.61	3.65	4.35
MnO	0.24	0.27	0.15	0.25	0.24	0.13	0.16	0.13	0.1	0.17
MgO	5.91	5.84	5.95	4.43	4.11	1.56	3.33	5.11	0.82	3.33
CaO	7.25	6.17	6.87	6.17	5.86	13.14	5.47	4.32	8.84	4.63
Na <sub>2</sub> O	3.06	3.75	3.57	3.59	3.47	2.75	3.21	4.75	2.3	3.04
K <sub>2</sub> O	2.34	0.87	1.25	1.53	0.47	1.26	1	0.42	1.2	1.87
P <sub>2</sub> O <sub>5</sub>	0.4	0.55	0.31	0.58	0.4	0.26	0.29	0.31	0.24	0.29
Sample	M.1506	M.6128	M.1039/3	M.1500	M.67/1	M.1506	M.6128	M.6142	M.6135/1	M.6121
SiO <sub>2</sub>	58.82	61.5	57.26	58.03	58.74	58.82	61.5	61.58	61.98	62.02
TiO <sub>2</sub>	0.97	0.4	1.4	0.76	0.7	0.97	0.4	0.4	0.4	0.3
Al <sub>2</sub> O <sub>3</sub>	16.68	17.43	16.69	17.5	16.4	16.68	17.43	16.33	15.51	16.6
Fe <sub>2</sub> O <sub>3</sub>	3.66	1.71	2.48	3.45	2.87	3.66	1.71	2.03	2.35	1.71
FeO	3.6	3.88	7.61	3.65	4.35	3.6	3.88	3.73	3.44	2.66
MnO	0.1	0.12	0.13	0.1	0.17	0.1	0.12	0.13	0.13	0.15
MgO	0.89	1.7	5.11	0.82	3.33	0.89	1.7	2.19	2.1	1.3
CaO	9.43	16	4.32	8.84	4.63	9.43	16	4.44	3.89	5.83
Na <sub>2</sub> O	2.16	3.06	4.75	2.3	3.04	2.16	3.06	3.21	3.21	3.25
K <sub>2</sub> O	1.43	1.71	0.42	1.2	1.87	1.43	1.71	1.72	2.5	1.25
P <sub>2</sub> O <sub>5</sub>	0.2	0.16	0.31	0.24	0.29	0.2	0.16	0.16	0.16	0.16
Sample	M.6117	M.5	M.6129	M.6158	M.6144/1	TD.68	M.6138	M.68	M.1038	
SiO <sub>2</sub>	62.02	63.02	62.26	63.54	63.82	64.14	64.86	66.34	66.78	
TiO <sub>2</sub>	0.3	0	0.2	0.4	0.2	0.5	0.3	1.3	0.4	
Al <sub>2</sub> O <sub>3</sub>	16.55	14.8	16.96	15.51	15.42	15.46	15.62	13.31	15.34	
Fe <sub>2</sub> O <sub>3</sub>	1.32	2.23	1.3	2.02	1.32	1.93	1.72	2.16	1.01	
FeO	3.66	3.8	3.66	2.87	2.66	1.94	3.95	3.06	3.09	
MnO	0.18	0.15	0.17	0.16	0.12	0.07	0.12	0.09	0.08	
MgO	2.51	1.68	1.6	2.19	1.5	0.69	1.91	1.91	1.6	
CaO	1.95	4.42	5.27	1.94	6.66	1.52	4.46	0.42	3.35	
Na <sub>2</sub> O	3.5	3.75	3.06	3.21	2.5	4.14	3.19	2.81	3.33	
K <sub>2</sub> O	2.97	2.5	1.05	4.17	0.91	5.5	1.93	3.75	2.32	
P <sub>2</sub> O <sub>5</sub>	0.16	0.17	0.2	0.11	0.11	0.16	0.16	0.45	0.17	

Table 4.11b. Representative trace element composition of granitoids of the Dien Bien Phu complex (data from Tran Dang Tuyet *et al.*, 2005- in the Khi Su-Muong Tesheet group at 1:200,000 scale)

Sample	N.7113/1	MT.7085	N.7109	MT.27/1	MT.303	MT.53/1	MT.47	MT.46
	Dien Bien 1					Dien Bien 2		
La	18	39.9	44.8	26	34.8	12	8.6	17.9
Ce	48.9	93.4	41.9	66.7	82.7	33	22	32
Pr	-	-	-	-	-	-	-	-
Nd	19.5	25.5	18.3	33.9	46.5	17.9	14	22.6
Sm	6.04	12.6	8.2	6.7	9.7	4	3.5	6
Eu	1.66	1.3	1.02	1.8	1.8	1.1	1	1.1
Gd	-	-	-	8.2	8.2	4.6	4.4	6.4
Tb	0.94	1.43	0.47	1.2	1.1	0.7	0.76	0.97
Dy	-	-	-	8	6.8	4.6	5	6.66
Ho	-	-	-	1.08	1.2	0.94	1	1.4
Er	-	-	-	5	3.6	2.7	2.9	4.21
Tm	-	-	-	-	-	-	-	-
Yb	3.49	6	3.6	4	3.4	2.2	2.5	3.9
Lu	0.15	0.22	0.16	0.5	0.58	0.37	0.33	0.51
Y	29.9	57.1	34.9	36	32	19	25.9	33.7
Nb	70	50.3	49.3	12	14	14.9	12.5	7
Ga	-	-	-	26.9	14.8	7	7.8	12.9
Zr	-	-	-	221	300	98	200	135
Sr	343	188	78.1	177	267	76.7	157	121
Th	5.53	6.34	7.58	5.4	14.5	2.1	2	1.9
Cr	18.6	65.7	53	64.5	16.4	328	35	325
U	0.44	0.75	1.5	0.4	4.4	0.2	0.5	0.3
Rb	8.02	24.9	16.4	30.8	66.6	48	49.3	80
Ba	139	135	271	511	984	121	520	353
Hf	4.06	7.82	2.91	5.8	8.1	2.2	4.8	3
Zn	190	102	71.2	728	306	86	88.5	137
Ta	0.57	1.54	0.8	0.99	1.5	0.3	0.5	0.1
Sb	2.14	1.36	0.24	3.1	1	0.1	0.7	0.4
Sample	MT.32/2	MT.50	MT.49	MT.305	MT.7085/1	N.7112	MT.304/1	N.7111
	Dien Bien 2		Dien Bien 3					
La	45.8	37	47.5	18.5	104	30.3	29.8	45.8
Ce	88.4	78.6	89.6	42.7	92.9	46.7	51.2	64.3
Pr	-	-	-	-	-	-	-	-
Nd	29	8.48	46.5	22.6	16.2	11.7	19.1	13.3
Sm	5.01	6	6.9	5.9	9.93	5.18	3.1	9.17
Eu	1.2	1.03	0.94	1	0.63	0.55	0.5	1.93
Gd	5.9	6.99	7.7	5.2	-	-	2.8	-
Tb	2.8	1	0.95	0.8	0.55	0.26	0.5	0.94
Dy	5.2	7.4	6.5	5.6	-	-	3.5	-
Ho	1.1	1.54	1.4	1.2	-	-	0.75	-
Er	3.19	4.64	4.2	3.6	-	-	2.08	-
Tm	-	-	-	-	-	-	-	-
Yb	2.9	4.2	2.74	3.5	3.12	1.94	1.8	6.23
Lu	0.3	0.45	0.47	0.5	0.39	0.57	0.28	0.75
Y	27	38	32	30.2	32.4	21	15.7	55.7
Nb	11	14.7	14	15	12.1	27.5	7.9	35.5
Ga	13.7	26	15	7.6	-	-	6	-
Zr	223	289	320	176	-	-	135	-

<b>Sr</b>	231	165	167	111	207	142	176	139
<b>Th</b>	16	18.2	20.7	3.9	8.76	7.65	15.6	10.3
<b>Cr</b>	66.9	4.8	656	226	9.99	13.1	3.8	15.2
<b>U</b>	2.2	3.9	3.6	0.2	1.97	1.15	3.3	1.63
<b>Rb</b>	68.7	129	80	51.8	51	96.5	72.2	90.4
<b>Ba</b>	1347	563	667	312	249	254	800	892
<b>Hf</b>	5.6	7.1	8.6	4	7.63	3.3	3.4	6.39
<b>Zn</b>	166	430.1	149	80	29.9	20.1	58.5	44
<b>Ta</b>	0.3	2	1.2	0.4	0.5	1.27	0.53	2.15
<b>Sb</b>	1.5	92.6	0.8	1.2	0.58	1.02	0.4	0.98
<b>Sample</b>	<b>MT.7122</b>	<b>MT.7109/1</b>	<b>MT.7109/2</b>	<b>MT.7082/3</b>	<b>N.7119/2</b>	<b>N.7119/1</b>	<b>MT.7082/2</b>	<b>N.7075</b>
	<b>Dien Bien 3</b>							
<b>La</b>	31.6	44.17	54.8	41.5	14.8	20.1	37.2	26.9
<b>Ce</b>	92.3	53	146.8	34.7	44.2	17.3	27.5	38.3
<b>Pr</b>	-	10.07	-	-	-	-	-	-
<b>Nd</b>	18.1	22.38	22.9	7.49	4.52	4.82	9.96	7.7
<b>Sm</b>	3.43	4.88	6.05	4.12	2.61	2.86	4.83	6.79
<b>Eu</b>	1.45	0.51	1.22	0.5	0.96	0.43	0.34	1.21
<b>Gd</b>	-	3.95	-	-	-	-	-	-
<b>Tb</b>	0.35	0.64	0.77	0.31	0.35	0.23	0.24	0.98
<b>Dy</b>	-	3.56	-	-	-	-	-	-
<b>Ho</b>	-	0.63	-	-	-	-	-	-
<b>Er</b>	-	2.47	-	-	-	-	-	-
<b>Tm</b>	-	0.43	-	-	-	-	-	-
<b>Yb</b>	1.8	1.84	3.31	1.77	2.14	1.4	1.8	3.4
<b>Lu</b>	0.51	0.29	0.49	0.32	0.08	0.27	0.59	0.37
<b>Y</b>	14.2	14.17	30.7	19.7	20.5	16.3	20.9	31.6
<b>Nb</b>	21.3	-	12.3	2.12	17.2	37.2	15.2	46.9
<b>Ga</b>	-	-	-	-	-	-	-	-
<b>Zr</b>	-	-	-	-	-	-	-	-
<b>Sr</b>	168	-	69	176	189	209	150	131
<b>Th</b>	5.22	-	3.14	7.88	10.9	4.01	4.86	1.89
<b>Cr</b>	26.5	-	11.8	5.94	9.94	3.33	4.8	14
<b>U</b>	1.2	-	0.66	1.73	2.36	0.63	1.34	0.74
<b>Rb</b>	116	-	113	22.4	64.2	8.15	50.6	144
<b>Ba</b>	500	-	579	128	307	73.5	193	738
<b>Hf</b>	5.22	-	6.13	2.73	3.56	2.21	1.7	4.37
<b>Zn</b>	58	-	48.6	23.5	83.1	11.4	13.5	62
<b>Ta</b>	2.35	-	0.99	0.37	0.65	0.32	0.54	1.27
<b>Sb</b>	1.56	-	0.91	0.02	1.37	0.3	1.08	0.63

Table 4.12 Representative chemical and trace element composition of granitoids of the Song Ma complex (data from RIGMR & DGMV, 2007).

Sample	26	27	28	29	30	31	32	33	34
<b>SiO<sub>2</sub></b>	68.34	72.16	72.66	73.12	73.54	74.2	74.58	75.18	76.29
<b>TiO<sub>2</sub></b>	0.8	0.23	0.45	0.4	0.3	0.3	0.33	0.8	0.35
<b>Al<sub>2</sub>O<sub>3</sub></b>	14.45	13.27	14.12	12.33	12.68	12.2	12.5	12.65	12.78
<b>Fe<sub>2</sub>O<sub>3</sub></b>	0.05	1.39	1.13	1.24	0.99	0.89	1.2	1.28	0.6
<b>FeO</b>	2.95	1.62	1.17	2.87	2.59	2.25	2.08	0.57	2.73
<b>MnO</b>	0.09	0.22	0.16	0.12	0	0.03	0.06	0.08	0
<b>MgO</b>	1.4	0.15	0.63	0.22	0.44	0.04	0.05	0.3	0.48
<b>CaO</b>	1.4	0.22	0.07	0.29	0.39	1.45	2.25	0.56	0.44
<b>Na<sub>2</sub>O</b>	2.9	3.19	2.98	2.82	2.84	2.3	2.16	2.5	2.86

Sample	26	27	28	29	30	31	32	33	34
<b>K<sub>2</sub>O</b>	4.82	5	4.77	4.81	4.48	4.32	4.66	5.88	3.18
<b>P<sub>2</sub>O<sub>5</sub></b>	0.27	0.02	0.03	0.02	0.04	0.3	0	0.17	0
<b>La</b>	67.15	92.7	91.67	184.85	215.76	216.67	187.27	196.67	195.45
<b>Ce</b>	37.13	47.92	41.44	120.45	143.18	139.77	120.45	127.27	120.45
<b>Pr</b>	42.32	84.02	81.43	88.13	115.18	110.71	109.82	114.29	96.43
<b>Nd</b>	20.2	29.07	27.88	62.33	77.83	76.17	73	71.83	76.17
<b>Sm</b>	11.27	17.62	16.96	48.78	55.25	52.87	47.73	48.56	48.4
<b>Eu</b>	8.26	10.43	7.25	17.39	16.09	18.7	14.35	17.1	17.54
<b>Gd</b>	7.79	10.24	11.2	29.96	34.38	30.84	28.11	30.36	28.43
<b>Tb</b>	13.19	18.3	20.64	21.49	22.13	20.21	18.51	20	22.77
<b>Dy</b>	4.55	4.43	6.3	19.07	21.72	20.03	17.43	17.81	19.5
<b>Ho</b>	10.57	13	13.57	18.86	19.57	16.14	15.43	14	19.71
<b>Er</b>	5.95	5.85	8.85	16.05	15.55	15.15	12.15	10.55	17.7
<b>Tm</b>	8.33	8	11	18	14	12.67	11.67	9.67	12.67
<b>Yb</b>	5.35	3.65	7.65	13.25	16	12	10.55	11.65	14.25
<b>Lu</b>	5.59	5	8.82	13.53	16.47	12.35	13.53	13.82	13.53
<b>Sr</b>	155	163	129.7	111	63.2	143	93.9	86.2	192
<b>Rb</b>	310.5	361.8	284.4	180.1	141	208.8	172	156	187
<b>Ba</b>	1063	755.5	711.8	672	643	924	846	850	909
<b>U</b>	2.43	2.65	2.86	3.11	2.79	4.33	3.56	4.12	4.17
<b>Th</b>	24	24.85	18.98	25.8	38.3	29.6	26.6	24	22.6
<b>Ta</b>	2.7	2.11	1.53	0.17	0.16	0.16	0.12	0.08	0.1
<b>Nb</b>	27.55	22.18	16.96	2.11	2.05	2.01	3.51	3.32	2.11
<b>Zr</b>	333.06	174.59	230.85	15.55	37.57	16.96	21.5	12.28	12.87
<b>Hf</b>	7.12	5.23	5.41	0.52	0.55	0.51	0.46	0.47	0.52
<b>Y</b>	16.64	14.28	17.75	32.12	35.84	27.51	26.73	27.78	32.67
<b>Ti</b>	3838.7	4307.5	3233.8	2990.8	2243.1	2422.5	2894.8	5735.5	2989.4
<b>V</b>	59	93.5	55.6	252.2	122.3	118.6	254.8	475.2	297.6
<b>Cr</b>	61	44.7	75.4	171.6	176.5	139	166.1	329.1	171.5
<b>Co</b>	12.4	10.8	9	26.5	27.6	33.2	37.4	18.8	21.6

Table 4.13 Representative chemical and trace element composition of granitoids of the Phia Bioc complex and Suoi Be Formation (data from RIGMR & DGMV, 2007).

Sample	35	36	37	38	39	T931331	T931344	T931352
	Phia Bioc					Suoi Be		
<b>SiO<sub>2</sub></b>	66.4	70.08	70.34	70.36	71.96	46.5	36.82	44.79
<b>TiO<sub>2</sub></b>	0.62	0.61	0.44	0.53	0.38	3.13	2.75	3.15
<b>Al<sub>2</sub>O<sub>3</sub></b>	15.22	13.18	13.61	13.34	12.79	15.05	20.76	12.37
<b>Fe<sub>2</sub>O<sub>3</sub></b>	1.48	1.07	1.2	0.8	0.91	8.97	15.27	8.58
<b>FeO</b>	3.27	2.48	2.08	2.44	2.23	5.93	4.39	6.82
<b>MnO</b>	0.09	0.05	0.07	0	0.01	0.31	0.29	0.34
<b>MgO</b>	1.21	1.21	1.01	1.11	1.31	4.97	3.12	5.85
<b>CaO</b>	1.4	1.4	1.68	1.68	0.28	5.27	3.45	7.16
<b>Na<sub>2</sub>O</b>	4.53	2.5	2.71	2.36	2.64	4.78	0.05	3.3
<b>K<sub>2</sub>O</b>	2.97	4.88	4.69	4.72	5.25	1.7	7.24	0.08
<b>P<sub>2</sub>O<sub>5</sub></b>	0.2	0.24	0.27	0.18	0.24	0.7	0.52	1.31
<b>LOI</b>	-	-	-	-	-	2.76	5.4	6.69
<b>Total</b>	97.39	97.7	98.1	97.52	98	100.07	100.06	100.44
<b>Sc</b>	-	-	-	-	-	25	32	28
<b>V</b>	-	-	-	-	-	395	353	236
<b>Cr</b>	121.1	111.7	76.2	95.4	64.7	34	139	84

Sample	35	36	37	38	39	T931331	T931344	T931352
	Phia Bioc					Suoi Be		
Co	-	-	-	-	-	49	43	43
Ni	-	-	-	-	-	19	121	34
Cu	-	-	-	-	-	9	72	13
Zn	-	-	-	-	-	201	343	167
Ga	-	-	-	-	-	24.3	35.8	19
Rb	75	83.9	116	85.1	74.1	45.4	358	2.1
Sr	21.9	20	38.9	23.5	8.5	250	18	97
Y	24.9	27.8	22.6	19.8	33.3	45	19	44
Zr	18.7	27.5	26.7	20.9	27.3	304	230	159
Nb	46.66	18.16	42.21	35.58	39.74	33	25.4	18.8
Ba	878.7	756.7	843.8	711.1	1022.5	858	654	37
La	242.73	196.97	224.85	223.33	135.45	66.53	18.69	30.05
Ce	163.64	135.23	142.05	135.23	101.59	147.57	37.77	67.88
Pr	129.46	112.5	110.05	118.75	76.43	14.45	4.41	9.29
Nd	106.5	79.5	76.33	76.83	45.67	58.3	18.54	41.59
Sm	62.98	50.83	55.8	55.14	39.78	10.58	4.13	9.18
Eu	24.49	13.33	14.93	15.36	9.42	3.32	1.62	3.66
Gd	44.58	35.26	38.23	35.26	28.39	10.89	4.63	9.95
Tb	30.21	20.43	25.53	28.3	22.13	1.55	0.73	1.47
Dy	28.78	22.3	22.89	22.39	19.77	8.13	4.22	7.89
Ho	25.43	21.14	19.43	20.29	19.14	1.69	0.98	1.63
Er	23.9	18.9	19.9	19.95	18.9	4.92	3.16	4.57
Tm	17.67	20.67	16	17	16.67	0.66	0.48	0.59
Yb	21.05	17.05	17.97	18.35	18.75	4.38	3.43	3.77
Lu	20	15.88	18.24	17.06	16.76	0.63	0.56	0.54
Hf	3.84	4.57	3.61	5.06	4.97	6.67	4.81	3.28
Ta	3.56	3.18	3.46	3.83	3.22	2.02	1.59	1.17
Pb	-	-	-	-	-	11	15	8
Th	27.6	23.3	25.6	21.3	30.7	8.5	5.3	2.8
U	3.22	2.15	3.12	2.54	2.51	0.5	2.4	0.7
Ti	4207.9	4522.1	2767.9	3442.1	2378.9	-	-	-

Table 4.14 Representative chemical and trace element composition of gabbros of the Nam Chien complex (data from Nguyen Xuan Bao *et al.*, 2005-in the Van Yen sheet group at 1:200,000 scale).

Sample	H154	H155	H156	H158	H161	H167	H168	H170
SiO <sub>2</sub>	48.98	45.56	46.58	47.45	48.27	44.78	46.35	47.58
TiO <sub>2</sub>	3.47	2.02	3.3	2.66	3.63	2.78	3.29	2.65
Al <sub>2</sub> O <sub>3</sub>	11.86	15.65	12.85	13.36	11.78	12.1	13.22	13.62
Fe <sub>2</sub> O <sub>3</sub>	4.72	2.77	4.61	4.34	4.72	2.42	15.64	14.19
FeO	10.59	8.42	10.76	9.38	10.28	10.93	-	-
MnO	0.24	0.18	0.22	0.19	0.21	0.2	0.23	0.21
MgO	2.98	7.28	4.76	5.34	3.66	4.44	5.2	5.58
CaO	7.98	11.22	9.47	9.47	8.62	9.22	7.47	8.77
Na <sub>2</sub> O	1.77	2.33	2.8	3.26	2.16	2.24	3.17	3.02
K <sub>2</sub> O	3	0.16	0.59	0.88	1.8	1.57	1.51	1.2
P <sub>2</sub> O <sub>5</sub>	1.47	0.36	0.69	0.45	1.48	0.55	0.62	0.52
LOI	2.77	3.79	3.2	2.81	2.88	8.9	-	-
Total	99.83	99.74	99.83	99.59	99.49	100.13	96.7	97.34
Sc	25	29	34	38	29	43	-	-
V	204	264	433	436	258	347	-	-

Sample	H154	H155	H156	H158	H161	H167	H168	H170
Cr	11	155	44	106	13	73	-	-
Co	27	60	43	43	45	39	-	-
Ni	7	146	23	35	9	27	-	-
Cu	17	108	19	36	68	45	-	-
Zn	149	112	151	129	138	162	-	-
Ga	22.6	15.7	20.1	19	23.2	17.9	-	-
Rb	152	3.4	21.1	22	79	96	-	-
Sr	408	276	299	401	387	169	-	-
Y	71	24	43	37	70	40	-	-
Zr	370	113	194	169	325	206	-	-
Nb	32.1	13.4	17.5	15.5	28.9	17.4	-	-
Ba	1884	78	228	369	1015	240	-	-
La	68.67	18.81	30.45	28.67	61.32	32.08	31	28
Ce	122.27	35.34	59.07	55.5	121.52	66.16	70	61
Pr	-	-	-	-	-	-	-	-
Nd	74.73	23.33	34.86	29.62	64.59	33.75	39	36
Sm	15.92	4.91	8.03	7.26	14.43	7.94	9.3	8.6
Eu	5.17	1.82	2.8	2.3	5.09	2.65	3.15	2.76
Gd	-	-	-	-	-	-	9.8	8.5
Tb	2.38	1.26	1.25	1.14	1.95	1.16	1.5	1.36
Yb	5.89	2	3.71	4.28	6.77	4.61	3.9	3.6
Lu	1.16	0.37	0.67	0.6	0.84	0.59	0.56	0.52
Hf	9.98	3.04	4.45	4.51	8.11	5.15	-	-
Ta	1.81	1.11	0.97	1.07	1.81	1.04	-	-
Pb	7	6	5	6	10	7	-	-
Th	9.8	<0.5	2.9	4.1	8.1	3.2	-	-
U	1.2	<0.5	<0.5	0.6	<0.5	0.6	-	-

Table 4.15 Representative chemical and trace element composition of rhyolite of the Tu Le, and Ngoi Thia subvolcanic complex (data from Tran Tuan Anh *et al.*, 2004).

Sample	T929	T985	RR30	LY.918	H152	H187	H198
	Tu Le				Ngoi Thia		
SiO <sub>2</sub>	77.06	74.68	65.64	75.5	75.07	77.56	72.69
TiO <sub>2</sub>	0.25	0.23	0.79	0.26	0.24	0.22	0.31
Al <sub>2</sub> O <sub>3</sub>	11.21	12.33	14.03	11.27	11.9	12.26	12.25
Fe <sub>2</sub> O <sub>3</sub>	0.79	1.09	3.64	3.12	0.79	1.07	1.16
FeO	2.3	1.96	2.46		2.19	1.14	2.11
MnO	0.12	0.05	0.21	0.05	0.11	0.04	0.11
MgO	0.08	0.2	0.59	0.1	0.36	0.34	0.23
CaO	0.21	0.17	1.65	0.01	0.07	0.07	0.8
Na <sub>2</sub> O	1.1	3.07	4.85	4.38	1.39	1.84	3.91
K <sub>2</sub> O	5.32	4.78	4.67	4.97	5.43	3.43	4.05
P <sub>2</sub> O <sub>5</sub>	0.01	0	0.14	0.03	0.01	0.01	0.02
LOI	2.14	0.81	1.16	-	2.04	1.81	1.88
Total	100.59	99.37	99.83	-	99.6	99.79	99.52
Sc	0	0		-	1	<1	2
V	<2	3	24	-	5	<1	<2
Cr	23	11	4	-	7	4	6
Co	2	<1	2	-	<1	3.6	<1
Ni	3	6	4	-	4	3	2
Cu	3	1	5	-	2	<1	1

Sample	T929	T985	RR30	LY.918	H152	H187	H198
	Tu Le				Ngoi Thia		
Zn	180	170	175	-	58	74	40
Ga	23.1	30.5	29.5	-	28.8	31.2	32.8
Rb	176	97	123	270	190	168	139
Sr	15	18	123	5.2	9.2	9.4	14.6
Y	107	156	63	101	84	114	89
Zr	1038	975	514	1221	929	1023	818
Nb	112.1	125.4	87.8	275	114.7	117.3	113.5
Ba	43	211	936	-	105	81	73
La	207.6	185.7	104.4	123	167.13	191.63	149.66
Ce	419.8	321.8	218.4	215	287.33	326.48	272.73
Nd	243.3	209.4	131.3	84	204.24	185.65	202.62
Sm	28.8	29.7	15.7	17.9	23	27.55	24.26
Eu	0.72	1.67	3.21	0.62	0.82	1.23	1.39
Gd	-	-	-	18	-	-	-
Tb	3.17	3.76	1.84	2.9	2.37	2.99	2.78
Yb	12	9.29	6.54	10	10.65	15.14	10.18
Lu	1.43	1.43	1.06	1.5	1.4	1.59	1.42
Hf	25.6	23.9	18.4	26	25.67	29.43	24.04
Ta	8.13	8.99	5.46	12	7.89	9.35	8.99
Pb	-	-	-	-	2	6	3
Th	29	28.4	14.4	27	24	27.7	23.1
U	5	5.3	2.3	6.5	4.1	6	3.6

Table 4.16 Representative chemical and trace element composition of granitoids of the Muong Hum and Phu Sa Phin complexes (data from Tran Trong Hoa *et al.*, 2004).

Sample	H-902	H-903	H-906	H10/92	H12/92	H17/92	SH-1317
	Muong Hum						
<i>Analysis by XRF method</i>							
SiO <sub>2</sub>	71.52	71.07	73.37	75.21	76.14	73.67	71.51
TiO <sub>2</sub>	0.33	0.3	0.27	0.29	0.39	0.26	0.35
Al <sub>2</sub> O <sub>3</sub>	11.66	11.06	12.3	10.74	12.35	10.72	13.65
Fe <sub>2</sub> O <sub>3</sub>	3.15	4.18	2.85	3.4	4.04	3.05	3.64
FeO	-	-	-	-	-	-	-
MnO	0.05	0.05	0.08	0.03	0.13	0.07	0.12
MgO	0.06	0.19	0.18	0.15	0.04	0.05	0
CaO	0.38	0.91	0.5	0.18	0.52	0.36	0.59
Na <sub>2</sub> O	2.65	3.67	4.39	3.05	4.59	4.29	4.3
K <sub>2</sub> O	7.34	5.45	4.83	6.01	4.81	4.84	5.63
P <sub>2</sub> O <sub>5</sub>	0.03	0.02	0.01	0.02	0.03	0.02	0.03
LOI	-	-	-	0.13	0.07	0.34	-
Total	97.14	96.88	98.79	99.21	103.11	97.67	99.82
<i>Analysis by ICP-MS method</i>							
Ba	1880	3854	450.9	285.6	1325	420.4	409.4
Rb	205.1	194.4	29.32	110.4	158.6	187.5	115.4
Sr	171	180	309.5	76.97	85.3	70.34	22.34
Cs	1.29	0.63	1.16	0.51	0.36	1.09	0.49
Ta	21.28	9.78	0.86	12.08	14.96	14.14	5.58
Nb	252.6	125.8	17.08	154.2	169.6	168.3	83.44
Hf	41.16	22.91	5.49	29.87	30.16	30.24	16.01
Zr	1384	874.3	187.3	1008	911.4	890.5	668.9
Y	346.8	72.18	24.42	108.9	108.4	117.6	58.15

<b>Th</b>	60.57	24.6	18.73	30.35	29.19	32.02	17.61
<b>U</b>	10.8	6.91	11.41	5.74	8.98	6.83	3.05
<b>Cr</b>	0.87	1.68	6.26	2.18	4.18	1.2	-
<b>Ni</b>	0.76	-	4.26	0.59	0.27	-	-
<b>Co</b>	1.99	2.06	6.84	1.46	3.19	2.1	-
<b>Sc</b>	14.49	4.91	12.7	22.36	7.62	12.55	11.89
<b>V</b>	9.11	-	11.38	3.05	8.82	9.03	-
<b>Cu</b>	15.65	10.61	365	4.91	4.65	6	0.88
<b>Pb</b>	38.32	22.95	4.01	6.54	5.73	19.76	6.33
<b>Zn</b>	267.5	218.4	18.15	195	47.32	152.6	112.4
<b>La</b>	503.6	205.1	127.6	239.9	212.3	126.3	113.6
<b>Ce</b>	891.9	374.5	226.2	361.4	364.8	262	220.4
<b>Pr</b>	98.31	42.51	20.83	49.2	40.13	28.85	26.38
<b>Nd</b>	379.3	141.8	71.07	178.7	147.1	108	92.07
<b>Sm</b>	64.03	20.7	10.03	28.83	24.63	21.41	15.26
<b>Eu</b>	4.35	2.25	1.46	1.27	1.9	1.01	1.18
<b>Gd</b>	55.91	16.84	7.64	23.47	20.98	18.4	12.11
<b>Tb</b>	8.9	2.39	0.97	3.55	3.27	3.29	1.82
<b>Dy</b>	50.41	12.6	4.83	20.05	18.63	20.13	9.87
<b>Ho</b>	9.82	2.37	0.86	3.93	3.74	4.1	1.88
<b>Er</b>	26.54	6.87	2.33	11.34	10.62	11.8	5.57
<b>Tm</b>	4.12	1.09	0.34	1.9	1.75	1.98	0.92
<b>Yb</b>	23.93	6.81	2.08	12.07	10.57	12.09	5.98
<b>Lu</b>	3.58	1.14	0.32	1.89	1.58	1.75	1.02
<b>Ga</b>	-	-	-	-	-	-	-
<b>Sample</b>	<b>SH-1318</b>	<b>SH-1319</b>	<b>SH-1320</b>	<b>H178</b>	<b>H182</b>	<b>V188</b>	<b>T962</b>
	<b>Muong Hum</b>			<b>Phu Sa Phin</b>			
<i>Analysis by XRF method</i>							
<b>SiO<sub>2</sub></b>	75.54	75.35	72.91	62.87	72.9	74.5	77.23
<b>TiO<sub>2</sub></b>	0.25	0.24	0.28	1	0.33	0.34	0.22
<b>Al<sub>2</sub>O<sub>3</sub></b>	11.97	11.96	12.46	16.06	12.77	11.88	11.02
<b>Fe<sub>2</sub>O<sub>3</sub></b>	3.39	2.56	3.09	2.36	1.19	0.97	1.22
<b>FeO</b>	-	-	-	2.82	2.32	1.78	1.07
<b>MnO</b>	0.07	0.03	0.05	0.19	0.08	0.12	0.05
<b>MgO</b>	0	0	0	0.93	0.45	0.13	0.24
<b>CaO</b>	0.39	0.29	0.22	2.03	1.11	0.07	0.36
<b>Na<sub>2</sub>O</b>	4.29	3.89	1.85	5.21	3.65	2.63	2.63
<b>K<sub>2</sub>O</b>	4.38	4.95	8.37	4.97	4.21	6.27	4.12
<b>P<sub>2</sub>O<sub>5</sub></b>	0.01	0.01	0.03	0.27	0.02	0.01	0
<b>LOI</b>	--	-	-	1.13	1.58	1.66	1.24
<b>Total</b>	100.29	99.27	99.27	99.84	100.61	100.36	99.4
<i>Analysis by ICP-MS method</i>							
<b>Ba</b>	327.2	1127	1940	1245	277	91	69
<b>Rb</b>	220.1	184.8	210.4	98	108	202	209
<b>Sr</b>	25.33	19.06	121.9	196	26	7	13
<b>Cs</b>	0.73	0.74	0.65	-	-	-	-
<b>Ta</b>	15.64	9.13	9.37	2.93	7.58	12.1	10.5
<b>Nb</b>	185.3	124.9	91.41	47.3	106.2	133.6	116.9
<b>Hf</b>	35.93	19.96	20.69	8.42	24.9	31.5	27.8
<b>Zr</b>	1167	759	734.3	320	877	1187	1002
<b>Y</b>	172	93.14	50.95	42	100	124	101
<b>Th</b>	31.49	27.57	13.81	7	24.6	38.3	23.4
<b>U</b>	7.71	5.95	3.26	2.8	4.3	7.7	5.8
<b>Cr</b>	1.65	-	1.1	7	23	4	8

<b>Ni</b>	1.08	-	-	3	4	4	4
<b>Co</b>	0.24	-	0.51	5	<1	1	4
<b>Sc</b>	20.46	10.33	20.64	8	0	0	3.41
<b>V</b>	2.24		10.86	33	<2	6	5
<b>Cu</b>	7.93	4.97	14.86	5	2	16	1
<b>Pb</b>	20.08	25.73	39.76	9	-	-	-
<b>Zn</b>	250.9	188.6	89.1	164	54	295	42
<b>La</b>	121.7	111.4	234.2	62.4	120.7	166.7	88.7
<b>Ce</b>	258.6	209.5	366.2	128.7	248.9	327.8	190.6
<b>Pr</b>	28.06	26.42	39.43	-	-	-	-
<b>Nd</b>	111.1	94.06	124.1	78.7	134.9	160.6	121.8
<b>Sm</b>	23.72	17.83	16.51	10.6	20.4	21.4	16.9
<b>Eu</b>	1.15	1	1.96	2.95	2.07	1.2	0.76
<b>Gd</b>	20.61	15.08	13.78	-	-	-	-
<b>Tb</b>	3.99	2.62	1.85	1.2	2.78	3.6	2.44
<b>Dy</b>	25.73	15.3	9.53	-	-	-	-
<b>Ho</b>	5.36	2.98	1.78	-	-	-	-
<b>Er</b>	15.24	8.51	5.28	-	-	-	-
<b>Tm</b>	2.43	1.36	0.83	-	-	-	-
<b>Yb</b>	14.13	8.3	5.1	4.06	12.2	13.2	11
<b>Lu</b>	2.04	1.31	0.84	0.54	1.33	1.74	1.52
<b>Ga</b>	-	-	-	26	28.3	21.4	34.1

Table 4.17a Chemical composition of biotite from granite in the O Quy Ho Pass  
(data from Tran Trong Hoa *et al.*, 1995)

<b>Samples</b> <b>Oxides</b>	<b>V-9274</b>	<b>V-9272</b>	<b>V-9263</b>
SiO <sub>2</sub>	38.97	39.05	42.04
TiO <sub>2</sub>	1.10	0.83	2.41
Al <sub>2</sub> O <sub>3</sub>	14.92	13.71	9.27
FeO*	18.27	19.20	15.91
MnO	0.42	0.75	0.93
MgO	11.83	13.10	13.10
CaO	0.00	0.01	0.02
Na <sub>2</sub> O	0.11	0.09	0.13
K <sub>2</sub> O	10.00	10.10	10.40
Si <sup>4+</sup>	6.66	5.94	6.02
Al <sup>3+</sup>	2.71	2.46	1.73
Ti <sup>4+</sup>	0.13	0.10	0.29
Fe <sup>2+</sup>	2.36	2.44	2.11
Mn <sup>2+</sup>	0.06	0.01	0.13
Mg <sup>2+</sup>	2.72	2.97	3.10
Ca <sup>2+</sup>	0	0.002	0.003
Na <sup>+</sup>	0.033	0.027	0.04
K <sup>+</sup>	1.97	1.96	2.10

Table 4.17b Representative chemical composition of granitoids from the Ye Yen Sun complex  
(data from Tran Tuan Anh *et al.*, 2002)

<b>Sample</b>	<b>SH.1326</b>	<b>SH.1327</b>	<b>SH.1328</b>	<b>SH.1329</b>	<b>SH.1331</b>	<b>SH.1332</b>
	<b>West O Quy Ho</b>				<b>East O Quy Ho</b>	
<b>SiO<sub>2</sub></b>	75.74	69.75	70.1	71.99	78.15	71.9
<b>TiO<sub>2</sub></b>	0.08	0.22	0.2	0.17	0.27	0.36
<b>Al<sub>2</sub>O<sub>3</sub></b>	14.89	16.27	16.56	16.1	11.48	14.25
<b>Fe<sub>2</sub>O<sub>3</sub></b>	0.35	1.33	1.19	0.8	2.66	2.92

Sample	SH.1326	SH.1327	SH.1328	SH.1329	SH.1331	SH.1332
	West O Quy Ho				East O Quy Ho	
MnO	0	0.04	0.02	0.02	0.01	0.05
MgO	0	0.13	0	0.07	0	0.22
CaO	0.81	1.75	1.45	1.6	0.11	0.17
Na <sub>2</sub> O	4.04	4.44	4.34	4.12	2.16	3.73
K <sub>2</sub> O	4.03	4.56	4.72	4.17	5.55	6.13
P <sub>2</sub> O <sub>5</sub>	0.01	0.07	0.03	0.04	0.02	0.04
Cu	1.826	4.892	7.541	4.064	4.825	4.515
Co	-	0.995	0.321	0.508	-	-
Cr	-	2.717	-	1.041	-	-
Pb	39.39	30.01	32.56	29.31	16.74	11.13
Cs	3.348	3.092	1.642	3.319	2.869	1.681
Rb	187.6	150.4	135.3	163	201.4	219.3
Sr	216.7	1289	1447	448.6	46.7	26.02
Y	10.21	11.58	8.1	6.051	97.52	64.37
Zr	92.89	177.2	178.3	103.6	1013	728.8
Nb	17.9	11.35	7.148	11.91	167.7	94.12
Ba	481.1	2890	3319	1229	109.2	349.3
La	9.57	42.32	37.42	14.62	124.5	121.5
Ce	17.15	71.63	60.06	25.44	259.2	238.4
Pr	1.981	7.945	6.364	2.896	31.92	28.27
Nd	6.61	26.89	20.5	9.875	112.1	97.27
Sm	1.278	4.419	3.117	1.796	21.78	16.7
Eu	0.249	1.38	1.057	0.68	0.707	1.637
Gd	1.163	3.462	2.44	1.412	18.1	13.41
Tb	0.19	0.416	0.282	0.167	3.056	2.08
Dy	1.272	1.98	1.329	0.865	17.84	11.54
Ho	0.257	0.339	0.221	0.163	3.45	2.219
Er	0.916	1	0.651	0.525	10.18	6.511
Tm	0.165	0.146	0.09	0.082	1.659	1.061
Yb	1.259	1.002	0.645	0.62	10.19	6.692
Lu	0.236	0.159	0.095	0.1	1.555	1.083
Hf	3.612	5.382	4.643	3.007	28.06	20.32
Ta	1.594	0.751	0.454	0.762	12.98	6.858
Th	16.61	20.97	19.67	12	27.52	22.1
U	8.978	4.524	4.514	4.036	6.862	4.213
K/Rb	178.33	251.58	289.29	212.52	228.68	232
Rb/Sr	0.87	0.12	0.09	0.36	4.31	8.43
Rb/Ba	0.39	0.05	0.04	0.13	1.84	0.63
Eu/Eu*	0.62	1.04	1.17	1.3	0.11	0.33
(La/Yb) <sub>N</sub>	5.38	29.99	41.46	16.73	8.65	12.88

Table 4.18 Content of main components of rare and trace elements of trachyte and trachyrhyolite of the Pu Tra Formation (T – Sample from the Institute of Geosciences (VAST), P – Sample from the Phong Tho sheet group at 1:50,000 scale).

Sample	SiO <sub>2</sub>	TiO <sub>2</sub>	Al <sub>2</sub> O <sub>3</sub>	Fe <sub>2</sub> O <sub>3</sub>	MnO	MgO	CaO	Na <sub>2</sub> O	K <sub>2</sub> O	P <sub>2</sub> O <sub>5</sub>
T.776	59.55	0.48	15.21	3.58	0.07	0.57	4.77	2.61	8.79	0.25
P.175	70.79	0.20	15.01	1.72	0.03	0.74	0.82	3.44	6.17	0.11
	Rb	Sr	Nb	Zr	Y	La	Ce	Nd	Sm	
T.776	259.6	1777	25.99	413.7	37.3	106.3	196.2	72.9	12.4	
P.175	296.3	614.7	23.39	180.2	18.9	49.5	96.6	32.9	5.2	
	Eu	Gd	Tb	Yb	Lu	Th	U	Ta	Hf	

<b>T.776</b>	2.77	8.95	1.29	3.02	0.45	25.8	7.33	1.356	9.6	
<b>P.175</b>	1.15	3.46	0.55	1.81	0.28	24.8	11.67	1.77	5.09	

Table 4.19 Representative chemical and trace element composition of alkaline granite of the Nam Xe-Tam Duong, Pu Sam Cap and Coc Pia complexes (data from Tran Trong Hoa, 1996 & 1999)

Sample	H.43	H.45	MT. 7077/4	MT. 7076/3	MT. 7076/2	N. 7107/1	T.770	V-III	P.45	T.1591	T.1737
	Nam Xe-Tam Duong						Pu Sam Cap		Coc Pia		
SiO <sub>2</sub>	64.29	64.51	68.62	73.53	73.78	73.86	56.87	62.15	48.32	54.26	52.88
TiO <sub>2</sub>	0.3	0.22	0.2	0	0	0	0.54	0.41	0.63	0.54	0.8
Al <sub>2</sub> O <sub>3</sub>	16.81	17.38	14.32	12.5	12.38	12.12	16.24	15.63	11.03	10.02	15.36
Fe <sub>2</sub> O <sub>3</sub>	2.84	2.59	3.3	0.22	2.82	3.17	5.35	4.01	6.52	5.14	6.73
FeO	-	-	1.15	3.52	0.32	0.86	-	-	-	-	-
MnO	0.06	0.08	0.07	0.3	0	0	0.09	0.14	0.14	0.11	0.15
MgO	0.17	0.17	0.3	0	0.3	0.6	0.21	0.49	9.25	6.07	5.59
CaO	2.52	1.96	0.28	0.28	0	0	3.93	2.98	10.99	6.73	6.52
Na <sub>2</sub> O	3.57	5.23	4.64	4.1	4.5	4.1	2.29	4.2	0.3	1.04	2.61
K <sub>2</sub> O	9.4	7.33	5.42	4.64	4.5	4.25	10.17	8.27	6.25	4.98	6.23
P <sub>2</sub> O <sub>5</sub>	0.08	0.06	0.08	0.05	0.11	0.11	0.18	0.18	0.57	0.3	0.53
Rb	180	154	136	59.4	124	80.6	265.7	241.6	253	218	163
Sr	1606	2169	224	147	78.5	120	3989	2535	4318	1226	2555
Nb	13.01	19.3	17.2	7.61	8.74	26.4	32.89	32.27	11.9	20.6	13.1
Zr	91.8	72.9	-	-	-	-	521.8	559.1	246	206	469
Y	37.9	28.8	63.5	50.4	59.4	78.4	47.11	43.52	26	24.2	25
Th	10.1	48.1	8.51	8.11	11.4	12.5	37.4	38.1	-	-	-
U	70.5	93.9	2.68	1.64	1.58	1.66	1.1	9.3	-	-	-
Ta	0.8	1.1	1.42	0.75	1.48	1.36	1.5	1.5	0.6	0.9	1.4
Hf	3.9	2.4	3.7	10.6	10	7.89	12.5	13.3	-	-	-
La	31.5	37	85.9	110	114	79	156.3	146.1	170	49	117
Ce	70.5	93.9	62.2	114	102.1	87.5	292.8	268.2	224	89	185
Nd	44.1	47.8	13.1	21.2	36	20.8	105.9	91.8	68	41	81
Sm	10	8.8	11.7	10.9	22.3	13.9	17.9	14.6	10.3	7.5	17.2
Eu	2.5	1.9	0.23	0.41	3.65	0.15	3.9	3.3	2.5	1.9	3.7
Gd	3.3	2.9	-	-	-	-	12	10.1	6.1	5.9	13.6
Tb	1.2	0.9	0.67	0.59	1.54	0.91	1.7	1.5	0.9	0.9	1.9
Yb	3	2.9	5.99	4.79	7.64	7.44	3.6	3.4	1.9	1.9	2.6
Lu	0.5	0.5	1.29	0.7	0.75	0.76	0.5	0.5	0.3	0.3	0.3
Sb	-	-	0.58	0.21	1.09	0.3	-	-	-	-	-
Cr	-	-	3.55	6.85	16.5	6.35	-	-	863	335	169
Ba	-	-	94.6	137	796	35.3	-	-	-	-	-
Zn	-	-	20.4	16.9	12	39.4	-	-	-	-	-
Cu	-	-	-	-	-	-	-	-	73	64	61
Ni	-	-	-	-	-	-	-	-	346	149	76
Co	-	-	-	-	-	-	-	-	39	15	28
V	-	-	-	-	-	-	-	-	128	107	118

## 5. GEOMORPHOTECTONIC MODELING

The model for tectonic geomorphology of NWVN area is based on the defined spatial controls using analysis of Digital Elevation Modeling (DEM) and remote sensing images. It helps to recognize the tectonic boundaries and better understanding recent tectonics of the area.

## 5.1. Geomorphic introduction

The India-Eurasia continental collision is the most spectacular example of active mountain building, plateau development and continental-scale strike-slip faulting on Earth, with deformation extending well beyond the Himalaya and the Tibetan plateau, deep into the Asian continent, including the northwestern Vietnam. These processes made the NWVN a mountainous region dominated by a number of high elevation ranges – Hoang Lien Son, Phi Si Lung and Phu Den Dinh. This montane region contains relatively large area of uplands above 2,000 m, with broad valleys interposed as the Red River, Da River, and Chan Nua valleys etc. The study area also comprises plateaus, including those at the Son La and Moc Chau provinces with elevation up to 1,500-1,700 m a.s.l.

Morphotectonic analysis of displaced landforms along the Vietnamese segment of the NWVN covered an area comprised between the Red River fault and Sam Nua zones (Fig. 5.1).

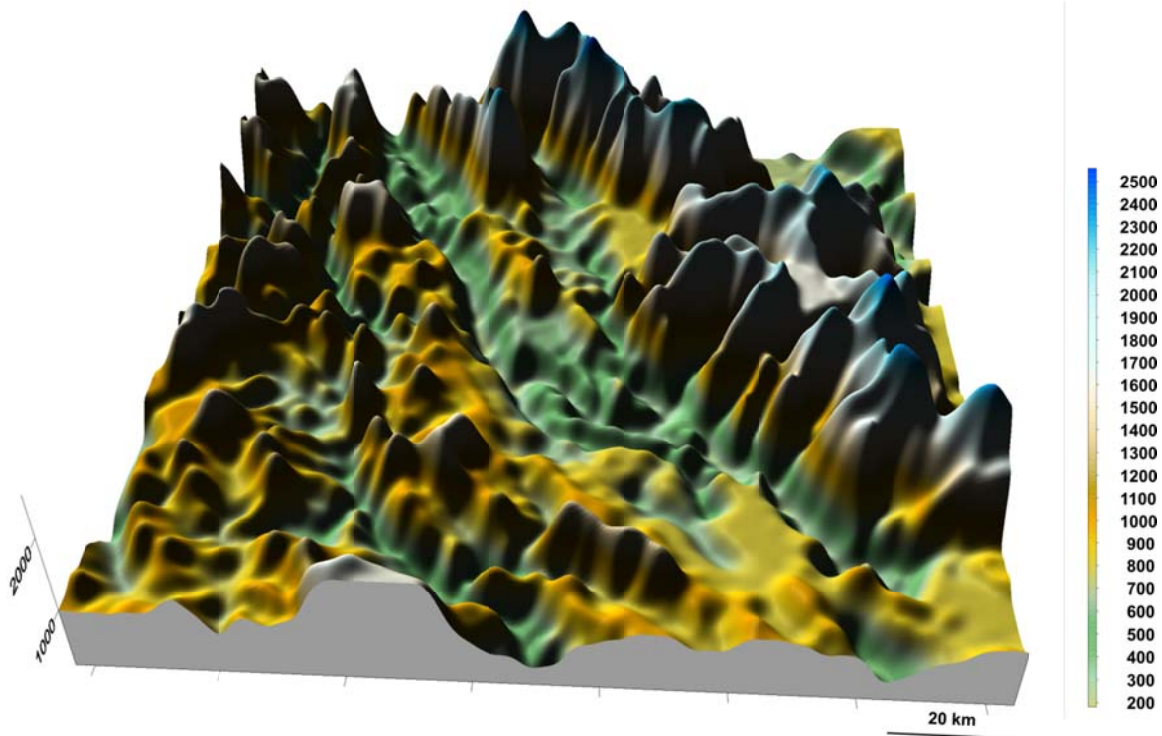


Fig. 5.1. Digital elevation model of the NWVN area.

This analysis consisted of examination of some the Spot images at 1:100,000 scale, and 1:100,000 topographic maps.

## 5.2. Lineament models

### 5.2.1. Literature review

Lineaments are more or less rectilinear alignments that can be seen on satellite images, aerial photographs and digital elevation models (Ollier, 1981; Panizza *et al.*, 1987). These

linear features may represent natural morphological alignments or those of anthropogenic nature (roads, aqueducts, crops, etc.). Structural discontinuities of rocks and other features related to tectonic activity often results in morphological lineaments (fault scarps, joints, fold axis, etc.; (Ramsay and Huber, 1987). These lineaments can be expressed as linear valleys, linear slope breaks or linear ridgelines (Jordan *et al.*, 2005).

There are many specific landforms associated with faults which allow the fault type recognition (Burbank and Anderson, 2001; Keller and Pinter, 1996). Fault scarps are the most clear fault features (Ollier, 1981). They are very steep slopes with the same aspect parallel to the fault trace. The size of fault scarps could vary between a few meters up to hundreds of kilometers of length (Burbank and Anderson, 2001) and between fraction of meter and hundreds of meters of height. As normal and strike slip faults usually present high dip angle they are not affected by topography and tend to be a straight line in plan view, although they may be curved or sinuous (Burbank and Anderson, 2001; Ollier, 1981). Thrust and reverse faults have low dip angles and in this way they present more complex topographic expressions and they are more difficult to recognize in remote sensed images (Burbank and Anderson, 2001; Ollier, 1981).

However, not only fractures and faults have linear topographic expressions. Lithological contacts, intersection of bedding and topography, some wind erosion and glacial features could also appear as lineaments in images (Jordan *et al.*, 2005; Smith and Clark, 2005). In this way, discrimination between tectonic and non-tectonic features can only be stated using geological and other ancillary information.

Tectonic geomorphologic studies and drainage network analysis are nowadays being analyzed in a fast and easier way by means of digital elevation data and geographical information systems (Jamieson *et al.*, 2004; Jordan, 2003).

Shaded relief maps have been largely used to identify faults and lineaments from digital elevation data (Ganas *et al.*, 2005; Onorati *et al.*, 1992). Onorati *et al.* (1992) compared geological data with two visual interpretations of shaded relief maps. Both of them used orthogonal illumination with respect to the known tectonic trends. They defined the accuracy in terms of detectability, length and displacement of features with respect to the truth.

### **5.2.2. Digital elevation model and remote sensing image**

Implementation of digital elevation model (DEM) by a Surfer software is based on the existing topographic maps at 1: 100,000 scale; they are sheets of the Lai Chau (F-48-39), Lao Cai (F-48-40), Pho Lu (F-48-41), Muong Lay (F-48-51), Than Uyen (F-48-52), Lien Son (F-48-53), Dien Bien Phu (F-48-63), Son La (F-48-64), Hat Lot (F-48-65). DEM construction is based on scanning maps, then loading scanning map as a base map in the Surfer program (version 8.0) and then carrying out digitization. The study area is very broad, it covers around 23,100 km<sup>2</sup>. Such a large area requires a selection of areas for detailed studies, because the DEM construction for entire area based on the basic topography maps at scale of 1:100,000 would be too time consuming for one person. Selected areas like the Pho Lu (Cam Duong) and Lai Chau-Muong Lay regions corresponding to a part of the Red River and Dien Bien-Lai Chau fault

zones, respectively were studied using interval between contour lines of 40m - to satisfy techniques for acquisition of DEM source data (Li, Z. *et al.*, 2005). For the remaining area, intervals of 200m were used, and a remote sensing image will be used to help for detail study.

The obtained model of DEM construction covers an area of 23,100 km<sup>2</sup> and 153 m to 3,143 m above sea level. Extracted lineament is based on a change in the angle of illumination shaded relief map (Fig. 5.2), contour map is interval of every 40 m (Figs 5.3, 5.4) and the spatial model (3D surface) (Fig. 5.1).

	Entire area	Lai Chau-Muong Lay	Pho Lu (Cam Duong)
Number of digitized parameters	660778	87080	120270
Z Minimum	153	110.77	54.36
Z Maximum	3143	2048.7	2458.34
Z Mean	907	833.3	463.56
Z Median	800	802.04	316.64
Z Standard Deviation	474.5	389.48	405.8
Interpolated type	Kriging point	Kriging point	Kriging point
Drift	linear	linear	linear
Grid Size	100/97	100/97	100/97

Table 5.1. Parameters of digitized values and digital elevation model (DEM) interpolation.

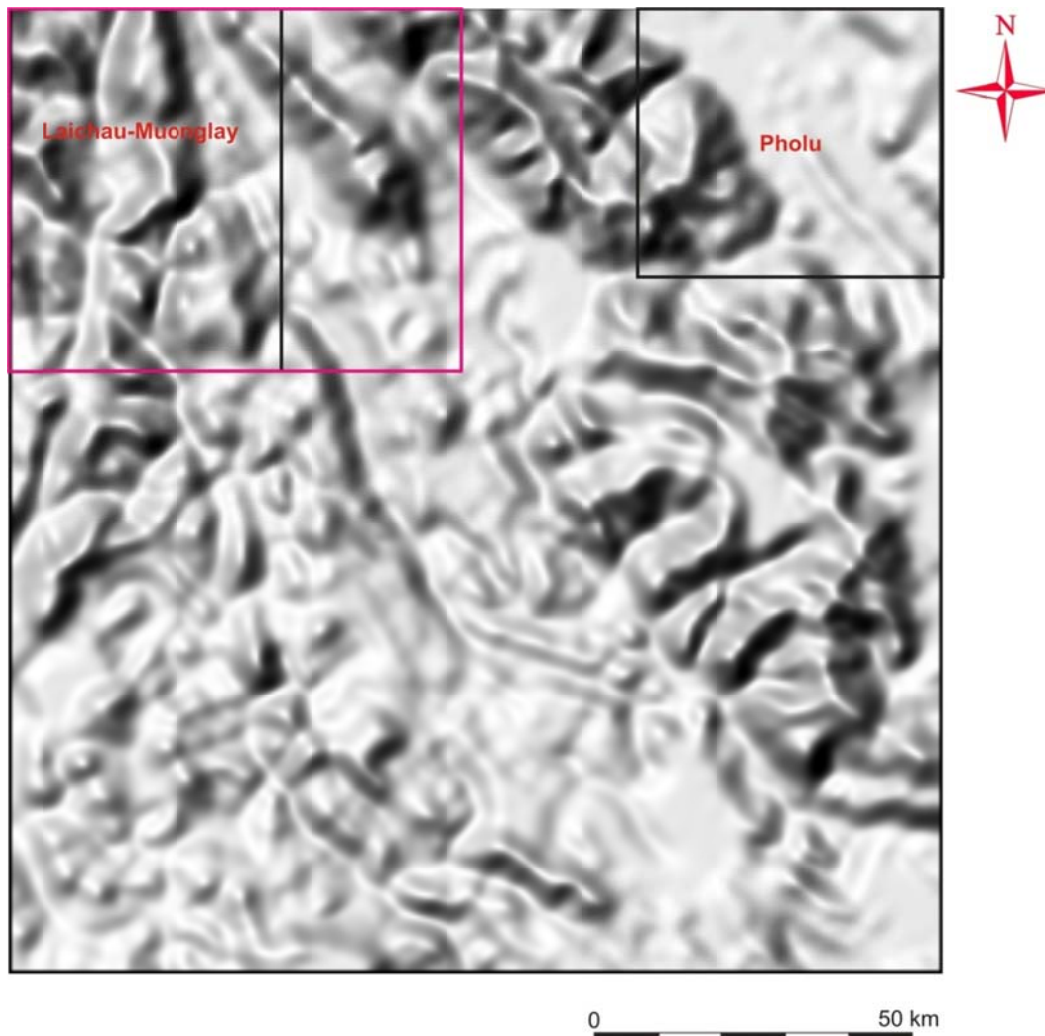


Fig. 5.2. Shaded relief map of the NWVN area, light position angles horizontal  $138^\circ$ , vertical  $65^\circ$ . Both the black rectangles indicates two areas with contour lines intervals of 40 m; and other (red rectangle) indicate area cover by SPOT HRV image.

Contour maps are also commonly called topographic maps or topo maps. As the name suggests, this is interpretation of terrain. Terrain height and morphological information are represented by contour lines. Contour density in the contour map is taken into account and concentrated in contour lines when dealing with linear structures (Figs 5.3, 5.4). The method has been used by Struska (2008) for the Orava valley to determine the zones of discontinuity. By appointing a number of discontinuities of the NNW-SSE, NNE-SSW, and NS directions, it was possible to depict the existence of a relationship between course of straight sections of river valleys and fault occurrence. Furthermore, Zuchiewicz and Nguyen Quoc Cuong (2004; 2007) have been used the method for analysis of geomorphotectonic features of the Dien Bien-Lai Chau and Red River fault zones. These methods have been used also by present author for interpretation of the study area.

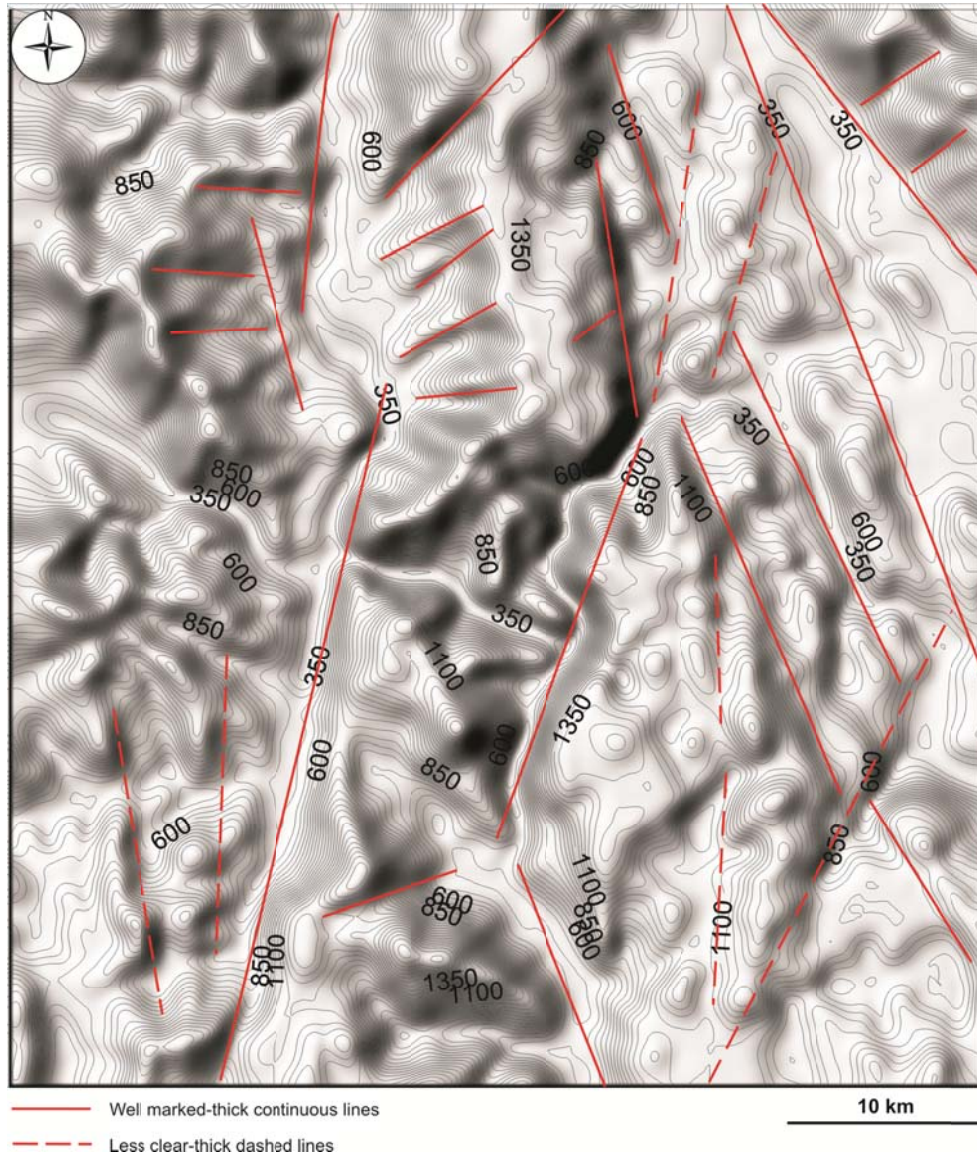


Fig. 5.3. Shaded relief map combined with contour lines intervals of every 40m for the Lai Chau-Muong Lay area, light position angles horizontal 138°, vertical 65°.

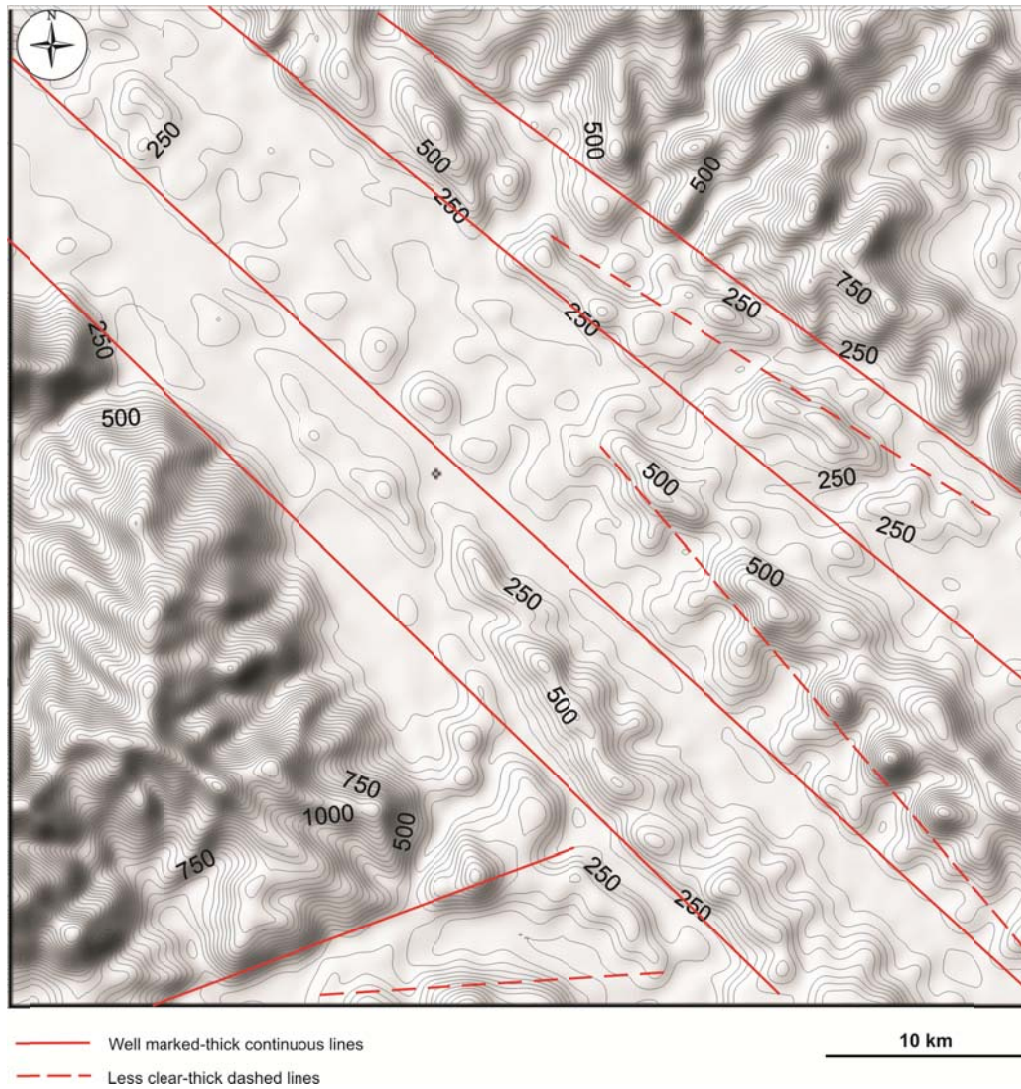


Fig. 5.4. Shaded relief map combined with contour lines intervals of every 40m for the Pho Lu area, light position angles horizontal 138°, vertical 65°.

Performed interpretation of Splot images at 1:100,000 scales covered an area of 527.53 km<sup>2</sup> is, it consists of two images of the Lai Chau and Lao Cai areas (Fig. 5.5), and the obtained results are treated as a complement to photo-interpretation digital elevation model. Moreover, the method has been used by Phan Trong Trinh (2004) for analysis of active faults in the Hoa Binh, and Son La areas.

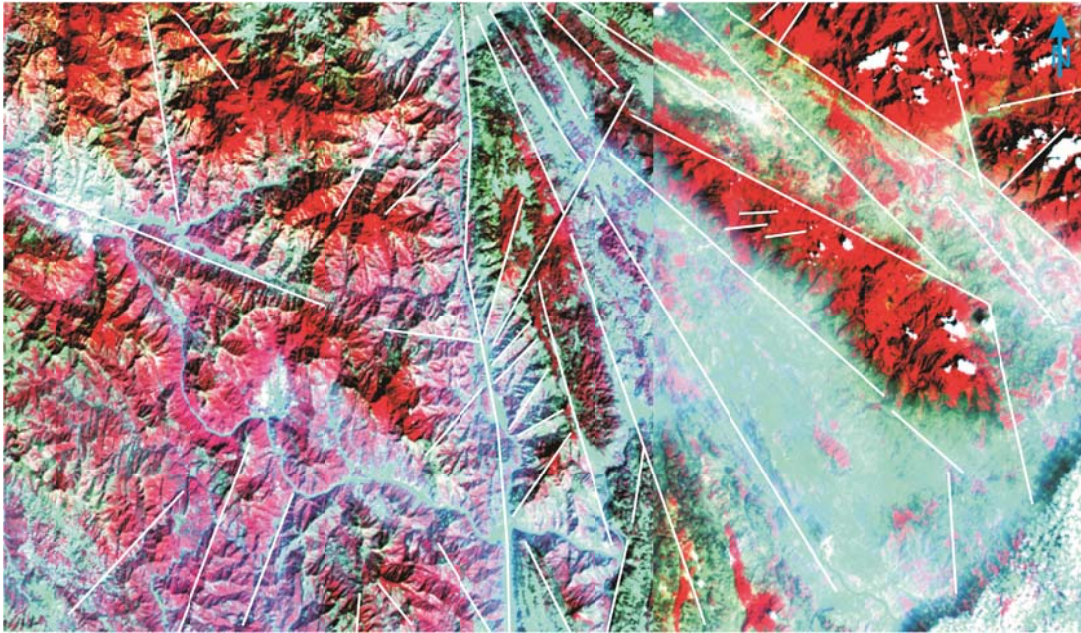


Fig. 5.5. The SPOT HRV images (XS mode) of the Lai Chau-Lao Cai area on scale of 1:100,000. The white-lines indicate tectonic lineaments.

### 5.2.3. Criteria adopted for determining the tectonic lineaments

The study area include a mountainous region where built up by Mesozoic sedimentary sequences consisting of acidic volcanic rocks, carbonates and terrigenous sedimentary rocks. Minor lithologies are Proterozoic, Palaeozoic and Cenozoic rocks consisting of flysch, carbonates sedimentary rocks, schists, phyllites and basalts. Quaternary sediments also occur, but usually are not consolidated, and dominated along basins and rivers, they also reflect the structures and lineaments. According to the criteria of Gupta (2002) and Struska (2008) tectonic lineaments may be shown by:

- 1) Drainage - upright sections of rivers and tributaries and the specific system, such as dendrite; rectangular and angulated; parallel; and rectilinear patterns (Fig. 5.6).
- 2) Incision and surface uplift recorded by the river- buttresses, ridges and indentations of erosion (Fig. 5.7).
- 3) Drainage offset – since they either displace or deflect river courses (Fig. 5.8).
- 4) Alignment of seams and basins – indicated fault trace.
- 5) Linear river segments or linear valleys extending for several kilometers suggest faulting (Fig. 5.7).
- 6) Topographic relief along a fault - fault a scarp gives a direct indication of dip slip and forms triangular faces; beheaded valley, and shutter ridge.
- 7) Linear features marked by contrasting topography, tone, texture and vegetation.
- 8) Groups of various elements listed from 1 to 7.

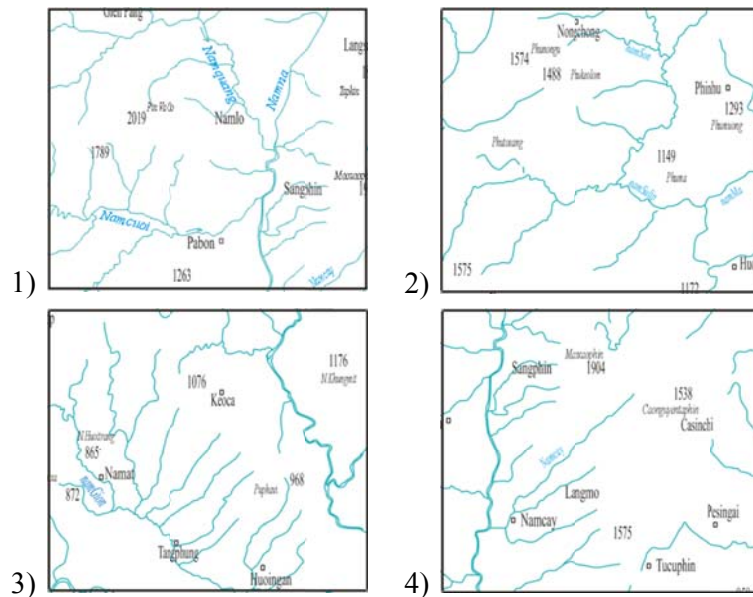


Fig. 5.6. Examples of important types of drainage patterns in the study area: 1) dendrite; 2) rectangular and angulated; 3) parallel; 4) rectilinear (see also Gupta, 2002).

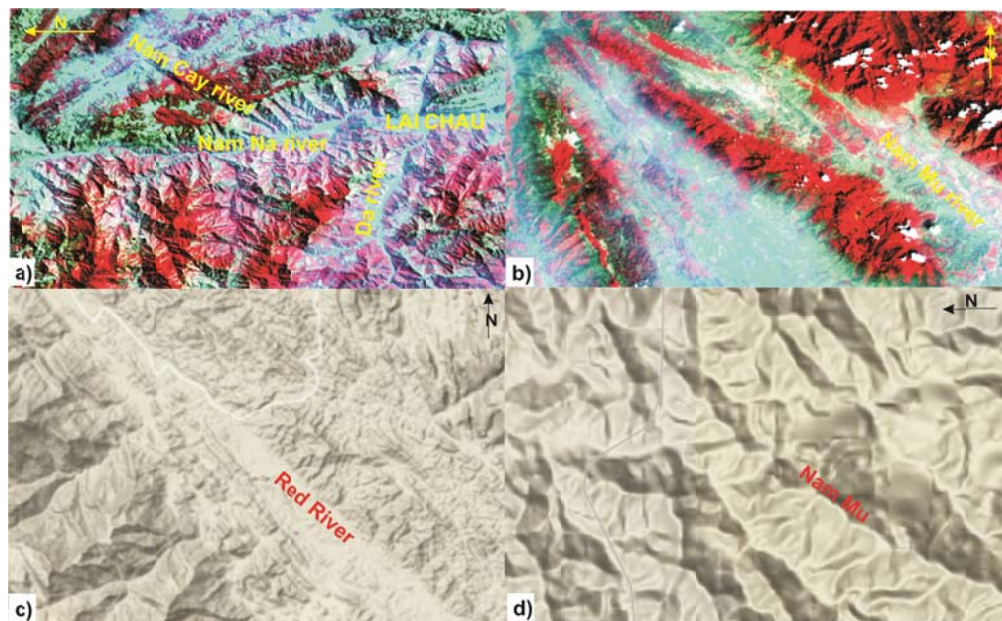


Fig. 5.7. Linear landforms, the example from Nam Na, Nam Cay rivers (a), Nam Mu river (b, d), and Red River (c).

Lineaments reflect the faults or fracture zones identified on the basis of the terrain (topolineament), digital elevation model (DEM) and remote sensing image analysis. Please note that in relation between faults, which developed in remote sensing and digital elevation methods (DEM) can only point to one parameter - line fault, a fault trace on the surface area (Struska, 2008).

#### **5.2.4. Lineament extraction by drainage network analysis**

Drainage network analysis is a fundamental tool in tectonic geomorphology. Fractures represent zones of rock weaknesses prone to intense erosion and hence valleys form along fault lines. Consequently, flow path routing and drainage network used in hydrological model can be applied for the purpose of morphological fracture tracing and network analysis. River acts as erosion or depositional, but their arrangement often depends on geological structure and tectonics of the area in which its network was developed. Generally, close-range in density or river-channel direction indicates similar rock types and also tectonic conditions are similar. These factors are based on the hydrological network of designated boundaries (Fig. 5.8) reflecting the diverse lithology, structure, and sloped terrain. This study focuses on utilizing drainage network extracted from several topographic maps at 1:100,000 scale in order to constrain the structure of the NWVN area. Topographic base was derived from the compilation by State Department for Cartography, and Geodesy and Cartographic Department of General Staff of the Vietnam published from 1990 to 1994.

Drainage network of the NWVN area has preserved good geological record of the movement, displacement, regional uplifts and erosion of tectonic units, simple linear patterns are arranged reflecting linear subsurface structures. We are dealing here with the Red River, Da River, Nam Na River, and Ma River. They are mainly playing a key role controlling drainage network of the area and are considered as old rivers, which more or less reflected actual offset of the faults. Common is the linear deflection of several rivers in a certain direction, visible in the tributaries of the Red, Da, Ma, and Nam Na Rivers. Perhaps the lineaments along main Red, Da, and Nam Na Rivers designated dislocations within the area. In addition, there are many straight stretches of river valleys, often contracted along a line zone, such as the Nam Cay, Nam Kim, Nam Co, Nam Khai, Ngoi Bo, Du Cang Thang streams. Their stream courses often coincide with the occurrence of many small tectonic lineaments (Fig. 5.7) and indicate a similar course. This type of elements is dominated on the lines of Red, Da, Nam Na, and Ma rivers.

The collinear stream lines from northeastern to northwestern part of the investigated area represent a large valleys that are known as a members of the Red River fault system running as long as 55km in the northeastern part of the area. Red and Nam Ma Rivers are oriented by Red River and Dien Bien - Lai Chau fault. The drainage network is transformed into lineament map (Fig. 5.8). In this experiment, 166 lineaments are identified basing on analysis of the individual river. The minimum and maximum lengths recorded are 3.09 and 55.468 km. The mean length of the lineaments is 17.679 km, and the total sum of their lengths is 2,917.1 km. They are divided into four groups by terms of direction, namely ESE-WNW, SSE-NNW, NNE-SSW, and ENE-WSW directions (Fig. 5.9). Among them, the lineament group of ESE-WNW direction is dominating and often set along the main rivers and streams in the area. Second one is lineament group of SSE-NNW direction which cut and moves lineaments of the NNE-SSW and ENE-WSW systems. With regard to the extent of the Red river valley lineament, these are arranged obliquely. The Chay River, Red River, Phong Nien, and Mai Dao-Lang Vai oblique lineaments extend from adjacent areas into the Red River

valley. Lineament elongated in SSE-NNW direction determines coverage fault border on valley.

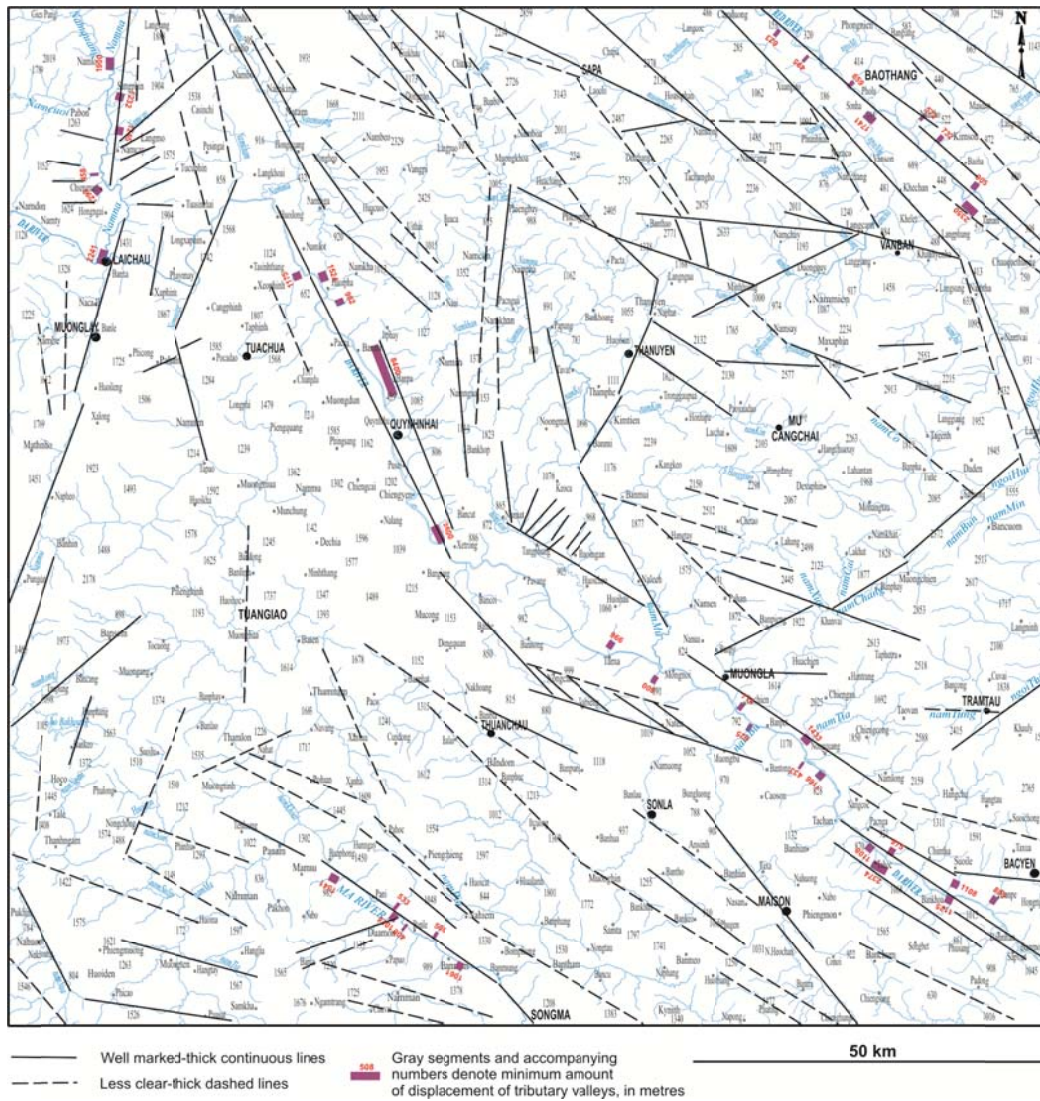


Fig. 5.8. Lineaments extracted from the drainage network analysis.

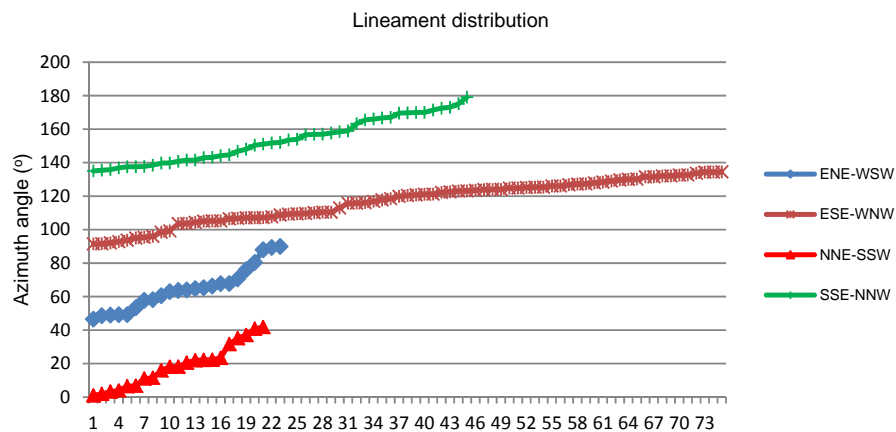


Fig. 5.9. Distribution of lineament groups extracted from the drainage network analysis.

### 5.2.5. Lineament extraction by terrain analysis

Limited coverage of the NWVN area indicated by a digital elevation model and remote sensing image of the site matches the description presented above. The study area comprises the Lai Chau, Son La, Hoa Binh provinces and part of the Lao Cai, Yen Bai and Thanh Hoa provinces.

Lineament terrain map presents lineament accumulation derived from analysis of selected SPLOT HRV images, and digital elevation model (shaded relief, contour maps and spatial model). Moreover, lineament map also can be attributed to the fractures that are recognizable on the satellite image (<http://earth.google.com>). Most lineaments were designated by individual model, then they were compared with each, chosen according to similar direction, aligned, averaged and affixed to one foundation forming shaded relief image (Fig. 5.11). The advantage of this method is that interpretation of results reveals tectonic lineaments, which are not visible on the area surface, and therefore not marked on the available geological maps at 1:200,000 scale. However, some of the designated lineaments are recognized in the field as the Red River and Dien Bien-Lai Chau fault zones. Analysis of the digital elevation model in comparison with the drainage network produces a better result in the lineament interpretation. It is possible to designate not only the lineament directions, but also their lengths. The obtained results from splot and remote sensing images interpretation have demonstrated the usefulness of digital elevation model in lineament map (Fig. 5.11). A total of 222 lineaments were extracted from the terrain model with length range from 2.543 km to 53.298 km, and average values of their lengths are 14.739 km.

Interpretation of the direction and spatial distribution of lineaments in Figure 5.11 demonstrate that four main directions dominate. These directions also influence lineaments' density. Analyzing the drainage network, we are dealing here with lineaments trending NNE-SSW, ENE-WSW, SSE-NNW and ESE-WNW (Fig. 5.12). The group of lineaments trending in SSE-NNW direction dominates in the area, showing also arrangement in faults. Some of these lineaments form a system of linear extension arranged in the Red River valleys along slopes of the Con Voi mountain range, they indicate a part of the Red River fault zone. Second group of lineaments shows the ESE-WNW direction. These lineaments are distributed mainly in the Tu Le volcanic zone, they cut and move the SSE-NNW lineament group. In the northwestern area, another group of lineaments of the NNE-SSW direction (sublongitudinal) occur with a length of 69.86 km, they indicate the Dien Bien-Lai Chau fault zone. Tectonic lineaments distributed in the central area are closely related to boundary of the Tu Le volcanic and Da River zones, they also suggest a combination with the Nam Xe-Van Yen-Phong Tho, and Da River fault systems, respectively. However, some of tectonic lineaments of the ESE-WNW directions are distributed in the southwestern area and display a pattern corresponding to the Ma River and Dien Bien-Sop Cop faults.

Moreover, the central part of NWVN area is covered by a few lineaments trending in SSE-NNW and ENE-WSW directions, they are similar in orientation to the lineaments and fotolineaments which were designated by Phan Trong Trinh *et al.* (2004, 2006) in the Son La, Hoa Binh areas (Fig. 5.10).

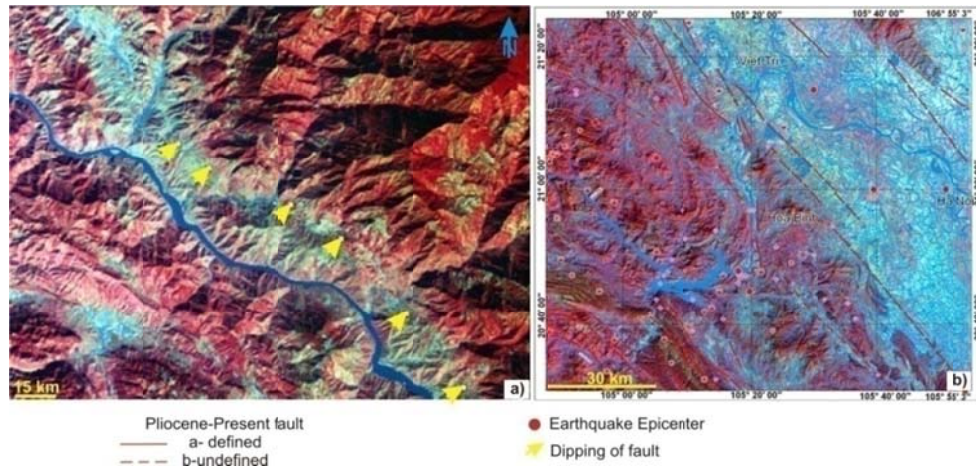


Fig. 5.10. a) Normal active fault in Son La area, dipping to SE, observed from SPOT image; b) Active fault systems in Hoa Binh and adjacent area on Landsat satellite image (after Phan Trong Trinh & Hoang Quang Vinh, 2004; 2006)

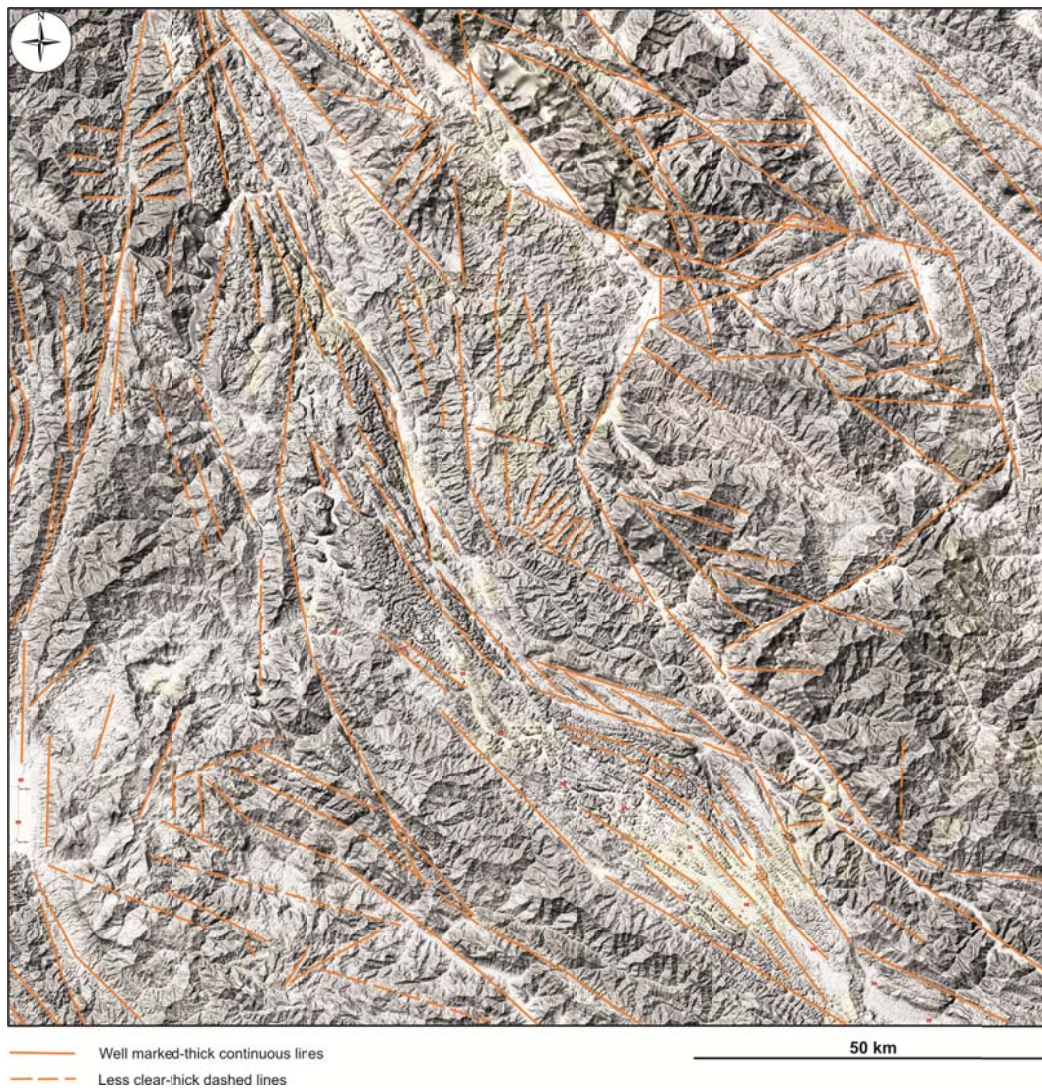


Fig. 5.11. Lineaments extracted from the terrain analysis.

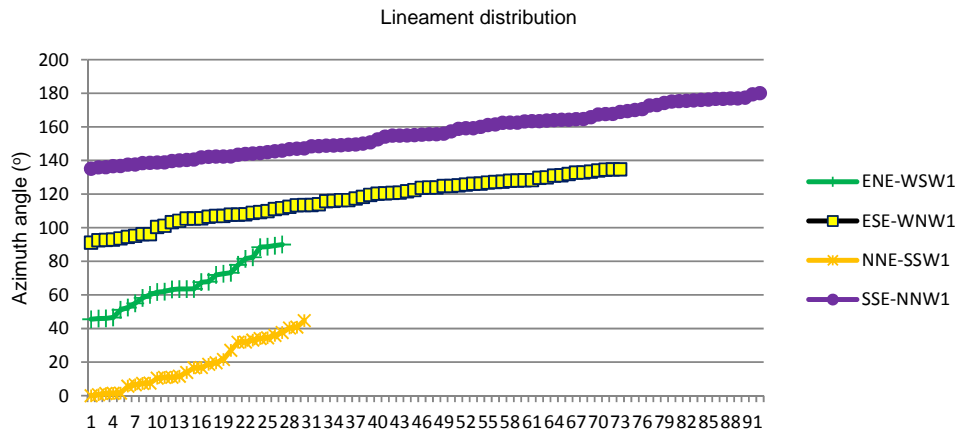


Fig. 5.12. Distribution of lineament groups extracted from the terrain analysis.

**5.2.6. Lineament correlation between the drainage network and terrain analysis**

Lineaments extracted from analysis of the drainage network and terrain illustrates the topographical correspondence with the assigned structures. The obtained results of lineaments analysis from the drainage network are almost identical to distribution of lineaments extracted from the terrain analysis (Fig. 5.13). Distribution of lineament groups from analysis of the drainage network and terrain are quite similar (Figs 5.13 & 5.14). Therefore, the structure of linear system designated by rivers and streams must be regarded as complementary to digital elevation model analysis. A speculative lineament is the Red River line located in Pho Lu segment, other one is along the Chay River line and distributed in northwest slope of the Con Voi mountain range. Illustration showing the lineaments relationship between the drainage network and terrain is given in Figure 5.15. The rose diagram of the lineaments extracted from terrain clearly indicates four dominant directions, which are also observed in the rose diagram for the lineaments extracted from drainage. Visual interpretation of the lineaments over the drainage network suggests that some of the lineaments fit the stream channels indicating that these channels have a structural control. So, the obtained results of different lineament groups imply a strong positive correlation between the drainage networks and terrain.

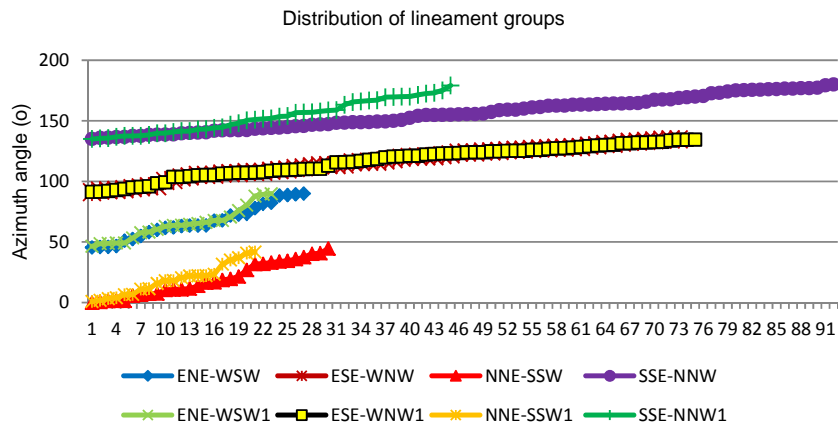


Fig. 5.13. Distribution of lineament groups from the river network and terrain.

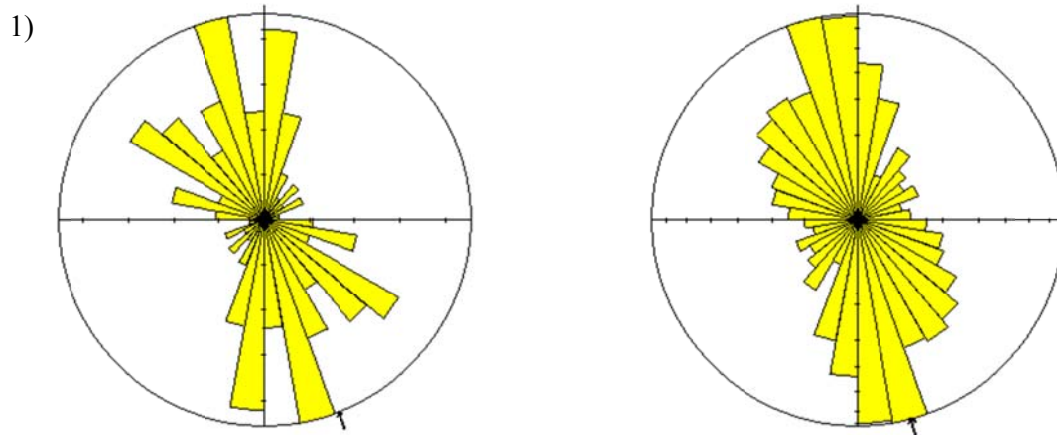


Fig. 5.14. Rose diagrams of directions of: 1 - drainage pattern, 2 - terrain aspect.

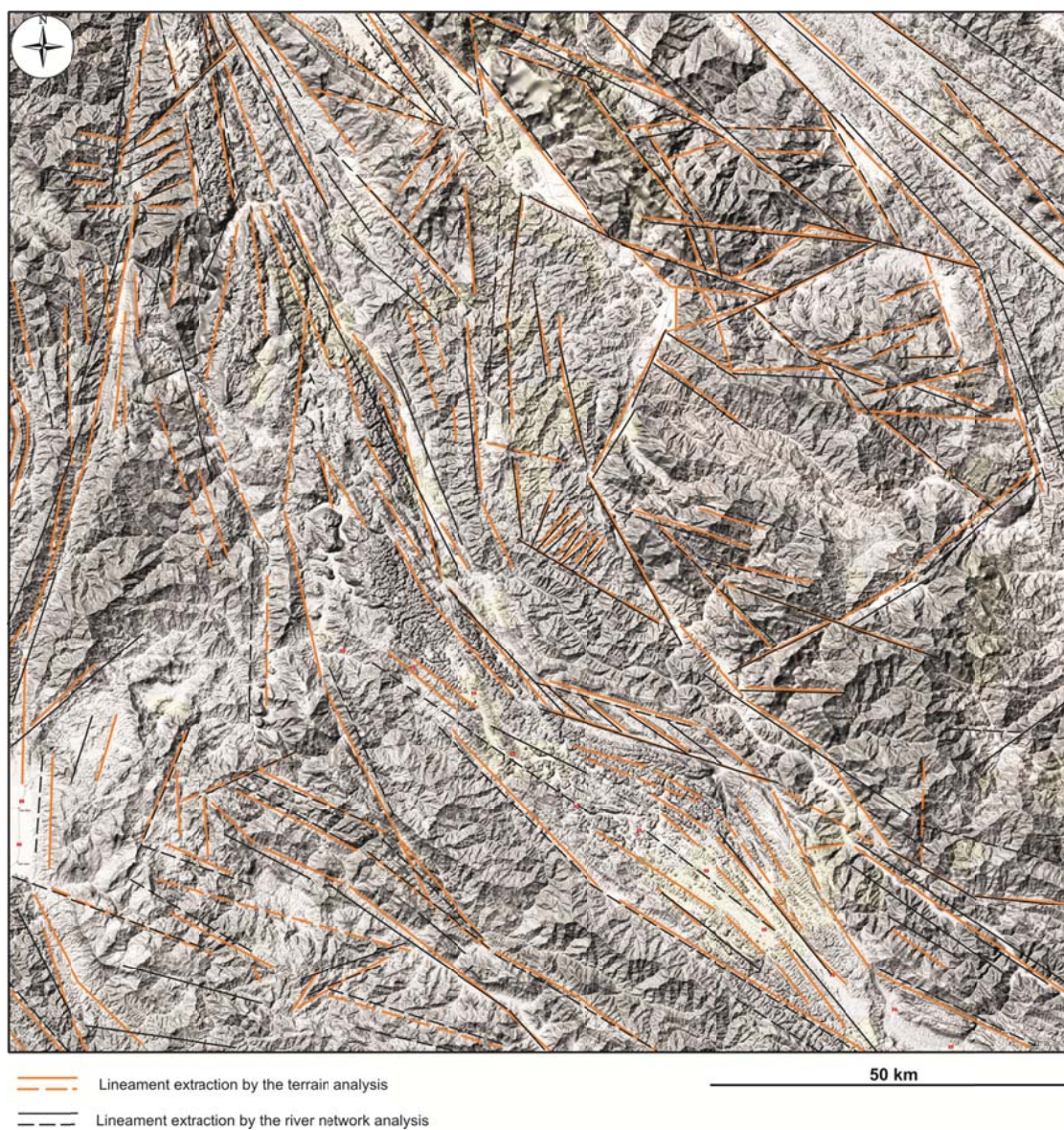


Fig. 5.15. Correlation of the lineament groups resulted from analysis of the drainage network and terrain.

### 5.3. Domain analysis of aligned morphological features and geological field data

Main tectonic lineament structures in the NWVN are the Red River fault zone (RRFZ) and Dien Bien-Lai Chau fault zone (DBFZ). A regional boundary between the Tu Le volcanic and Da River zones is the Van Yen-Nam Xe-Phong Tho fault; it expresses clearly an active normal fault which was suggested by Phan Trong Trinh (2004).

The Red River and Dien Bien-Lai Chau fault zones are considered as conjugate strike-slip faults (Phan Trong Trinh *et al.*, 1999; Zuchiewicz *et al.*, 2004), which in Pliocene-Quaternary times have shown, respectively, right-lateral and left-lateral sense of motion. The RRFZ marks the boundary between the South China and Indochina blocks, main activity occurred in two phases: during sinistral ductile shear active in 27–16 Ma, followed by exhumation and uplift from a depth of 20–25 km, and as dextral, predominantly brittle shear active in Plio-Quaternary times (Leloup *et al.*, 1995), and new structural and geochronological data appear to document the polyphase ductile shear active between Early Cretaceous through Miocene times, which included dextral, sinistral, dextral transpression, and sinistral transtension regimes (Żelaźniewicz *et al.*, 2005). The sinistral displacement was accompanied by rapid uplift and cooling. During the sinistral slip along RRFZ, the stress arrangement was different in particular massifs (Dian Cang Shan, Ailao Shang, Day Nui Con Voi (DNCV)), being all the time transtensive within the DNCV (Anczkiewicz *et al.*, 2007). This change of the sense of motion is related to collision between India and Eurasia.

At a particular scale, some of the tectonic features may appear sharp, well defined although very extensive. On the other hand, other tectonic features may appear as a wide zone, characterized by numerous parallel en-echelons to overlapping lineaments, with a similar sense of displacement, spread over a wide zone, *e.g.* the Red River, and Dien Bien – Lai Chau fault zones (Fig. 5.8).

#### 5.3.1. Red River fault zone (RRFZ)

In Vietnam, the RRFZ comprises four narrow (<20 km wide) high grade metamorphic massifs of the DNCV. All Quaternary valleys are narrows. The size of individual dextral offset of them has been calculated and mentioned by several publications, depending on their size, as: 70 m to 17 km (Nguyen Dang Tuc & Nguyen Trong Yem, 2001), 200-1,200 m (Phan Trong Trinh *et al.*, 1993), 0.3-2 km (Lacassin *et al.*, 1994) or up to 2 km (Nguyen Quoc Cuong & Zuchiewicz, 2001). The corresponding rates of Quaternary dextral slip range, therefore, are between 1 and 9 mm/yr (Allen *et al.*, 1984) or 1 and 4 mm/yr (Weldon *et al.*, 1994).

Particularly, between Cam Duong and Chau Que Thuong, right-lateral offsets are between 941-966m and 1,238-2,866m, where cumulative effect of several deformational episodes resulted in nearly 8.969 km-long dextral offset of a large meander of the Red river.

The amounts of right-lateral offset deduced from deflected drainage pattern, shown in Figures 5.8 and 5.29. Indicators of right-lateral slip include: drainage deflection (from 941m to 2,866m), beheaded streams, shutter ridges, en echelon oriented minor fault and fault-line

scarps, displaced terraces and alluvial fans, rectilinear fault valleys, and long rectilinear fault scarps of relief not exceeding 30-50 m (Nguyen Quoc Cuong & Zuchiewicz, 2001).

At the Bao Ha area, an examples of rectilinear river valleys and drainage offset and deflection are provided by Red River faults, where displacement of alluvial fans and associated terraces is apparent (Fig. 5.16) and near Cam Duong (Figs 5.17 & 5.18 A, B) close to the Chay River fault (Fig. 5.18 D), where well-developed shutter ridges can be found. Beheaded valleys, up to ca. 80-100m long, accompany i.e. one of the Red River fault strands south of Yen Bai (Fig. 5.18 C).

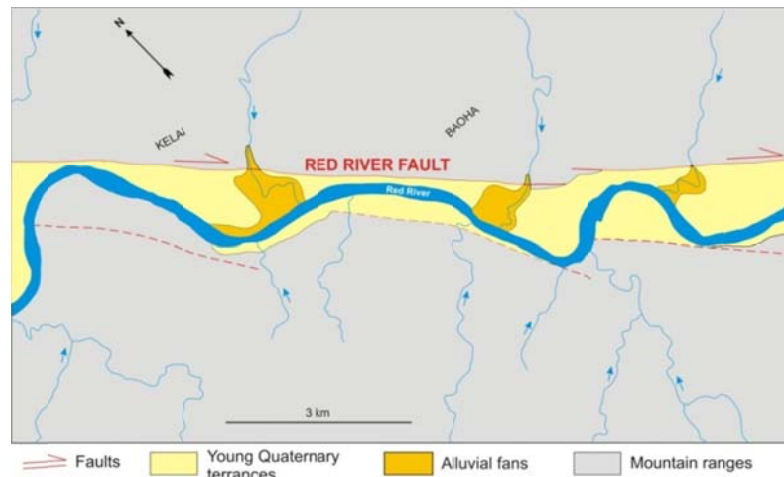


Fig. 5.16. Cartoon showing dextral displacement along a fragment of the RRFZ close to Bao Ha (after Nguyen Quoc Cuong, 2007).

Morphotectonic indicators of normal slip in the SE segments of the Red river include: well-developed triangular facets, ubiquitous occurrence of hanging wine-glass (hour-glass) valleys, and rectilinear fault scarps at the feet of mountain fronts, frequently accompanied by associated half-grabbers and minor horsts or pressure-ridges (Nguyen Quoc Cuong & Zuchiewicz, 2001). Triangular and trapezoidal facets are of relatively small height in the NW portion of the Red River fault, like near Cam Duong (Figs 5.17 a, b & 5.18); while farther SE, close to the Trai Hut (Fig. 5.18 C), they become considerably higher.

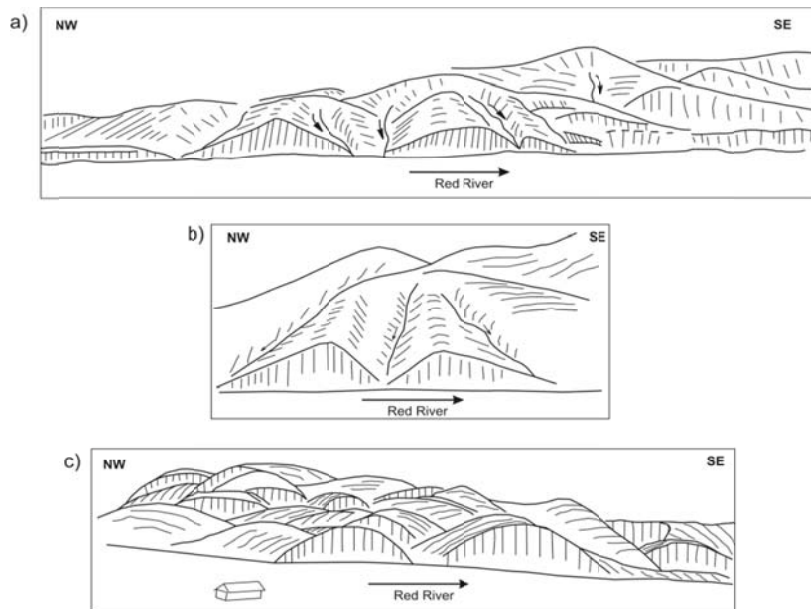


Fig. 5.17. Minor triangular facets accompanying the RRFZ near Cam Duong (a,b) and south of Trai Hut (c) (drawing from photographs of Nguyen Quoc Cuong, 2007).

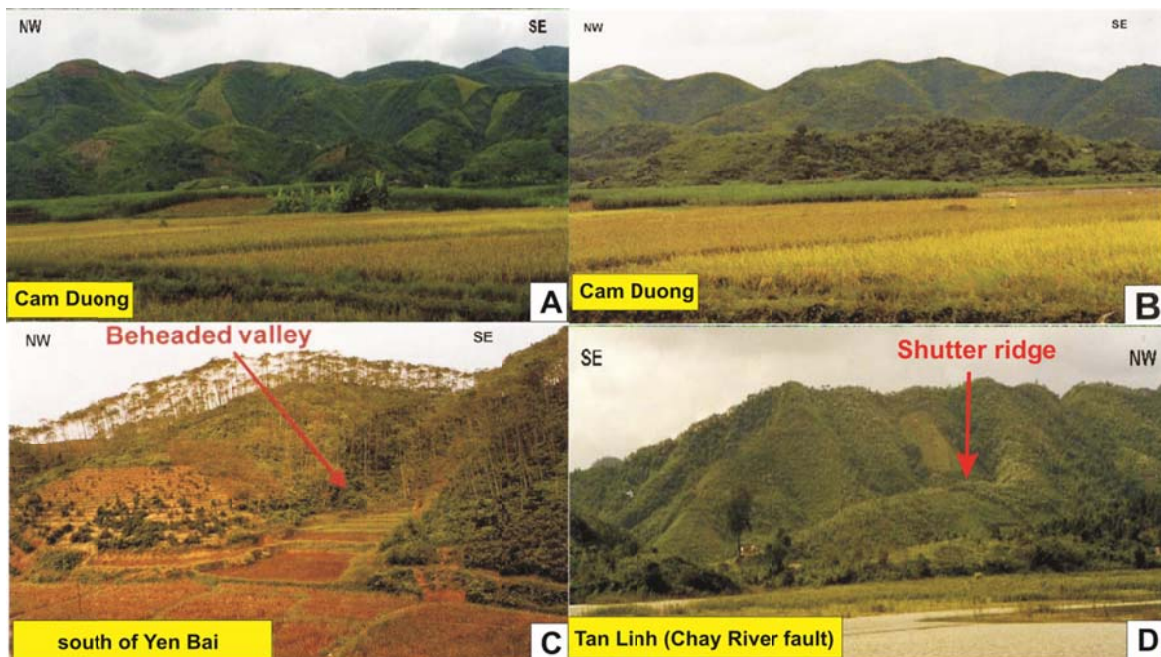


Fig. 5.18. Examples of right-lateral drainage deflection along the Red River (Cam Duong, Yen Bai) and Chay River (Tan Linh) fault zones (Photographs from Nguyen Quoc Cuong, 2007).

Moreover, the evidence of Red River strike-slip fault is also derived from geological features. Based on results of fieldwork investigation many localities are presented along the Red River fault where relatively young gravels can be seen to be cut by the fault. Clasts in Neocene conglomerates are commonly fractured, one of them are situated in the Tertiary strata of Lao Cai basin (Fig. 5.19).

Recent study reveals that the minimum estimate of right-lateral offset of tributary valley along different strands of the RRFZ ranged between some 400 m and 5.3 km, averaging at 1.1-2 km (Nguyen Quoc Cuong, 2007). The cumulative effect of these discrete displacements near Pho Lu amounts to ca. 9 km (Figs 5.8 & 5.29). Trying to calculate rates of slip for the Quaternary time (1.806-2.58 Ma; Gibbard *et al.*, 2004), we obtain values ranging between 0.43-1.1 mm/yr for individual displaced segments to 5.5-7.8 mm/yr for the inferred cumulative displacement.

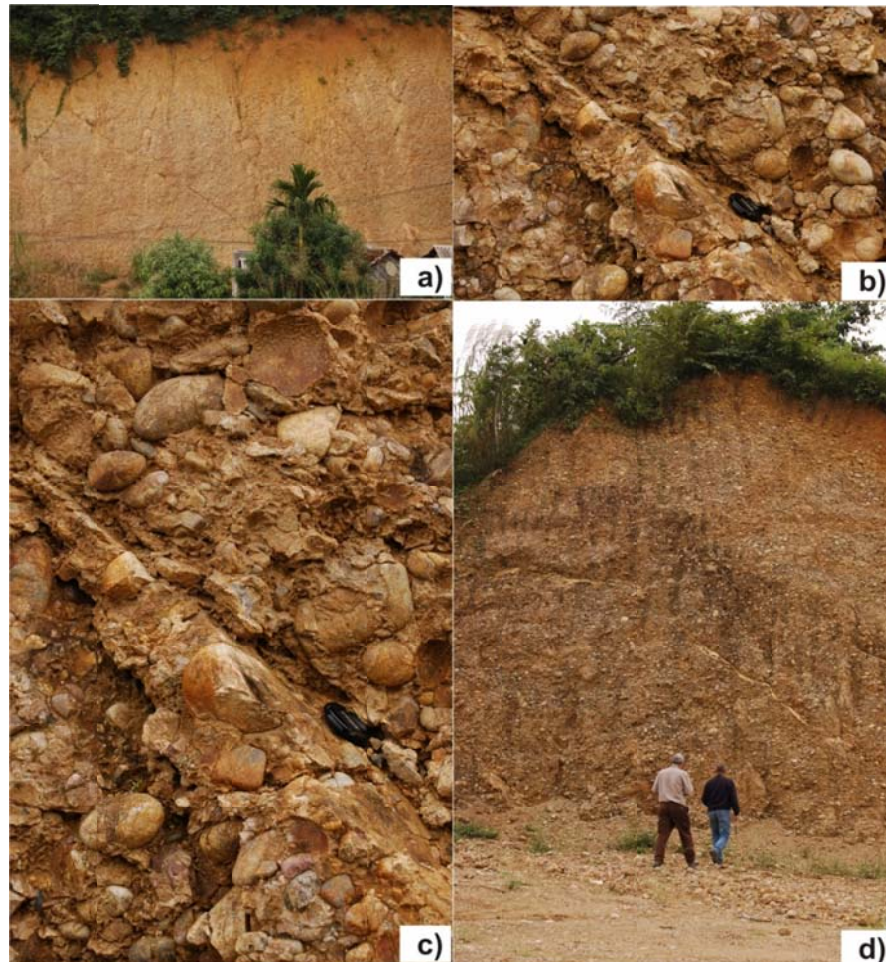


Fig. 5.19. Small-scale tectonic features in the Tertiary strata of the Lao Cai basin; a,b,c,d - Clast-scale joints (arrowed) arranged in linear zone of RRFZ.

### 5.3.2. Dien Bien-Lai Chau fault zone (DBFZ)

The DBFZ is one of the most important structures in the study area. It is clearly indicated by NNE-SSW lineaments (Fig. 5.14), showing good correlation of lineament between the drainage network and terrain analysis. The DBFZ is a strip of valleys lower than 1,000m and belongs to side and bottom of the river-valleys: Nam Ma, Nam Lay, Nam Muc and Nam Rom between Vietnamese-Chinese boundary in the North to the Vietnamese-Laos boundary in the South (Fig. 5.8).

According to the geomorphologic studies, the DBFZ can be divided into three strips. The central strip is situated along lowest part of streams, it includes hills, lower mountains, and

valley flat stands isolated within the valleys (Pa Tan, Chan Nua, Lai Chau, Muong Pon, and Dien Bien – in Fig. 5.20). The eastern strip contains slopes with terraces and abrupt walls tens of meters high and few kilometers long. This strip is separated from the surface of the Ta Phinh plateau and flat peaks of the Huoi Long range by a big wall extending from Pa Tan to Muong Pon. The western strip contains slopes inclining gently towards south with slightly marked terraces.

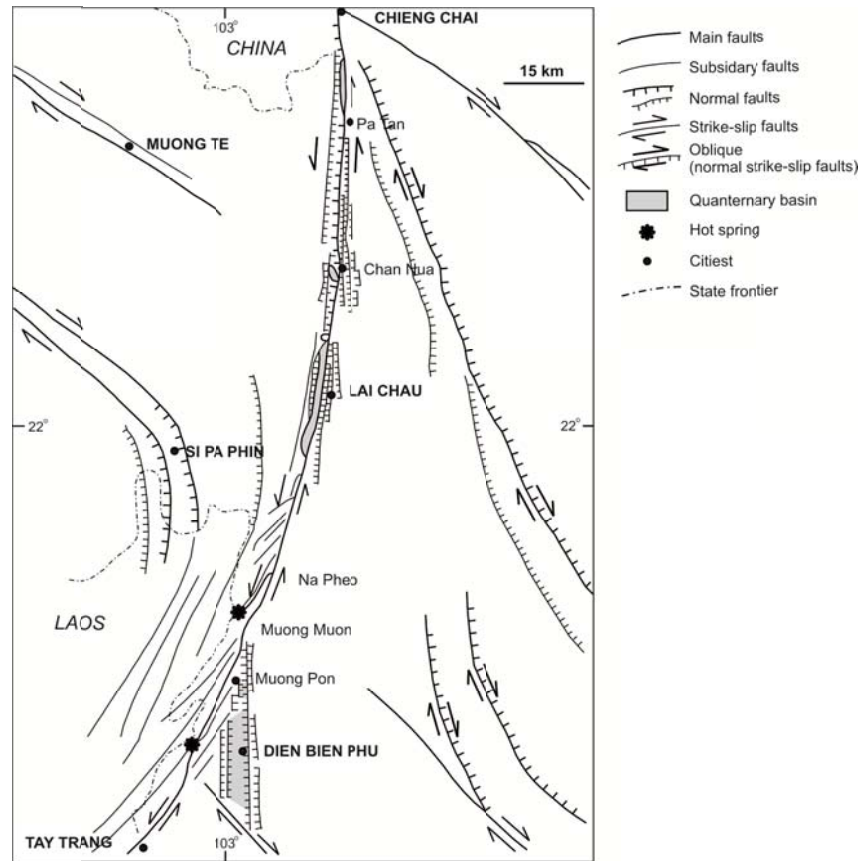


Fig. 5.20. Structural sketch of the Dien Bien Phu fault zone (after Nguyen Van Hung & Hoang Quang Vinh, 2001; see also Zuchiewicz *et al.*, 2004)

Subsidiary faults within the DBFZ created the type of feather structures, especially in southern part of this zone, they formed pull-apart basins filled by Quaternary fluvial sediments (Nguyen Van Hung & Hoang Quang Vinh, 2001; Zuchiewicz *et al.*, 2004). Sizes of these basins increase southwards. The basin's sediments are cut by faults, clasts composing alluvial fans are fractured parallel to the fault traces. These observations contribute to prove strike-slip motion of the DBFZ.

Morphotectonic indicators of sinistral and sinistral-normal faults bounding pull-apart basins in the southern portion of the DBFZ include well-developed triangular facets and shutter ridges (Zuchiewicz *et al.*, 2004). Triangular and shutter ridges are of relatively small height at least in the Dien Bien Phu basin, and NW of Dien Bien city (Figs 5.21 & 5.22).

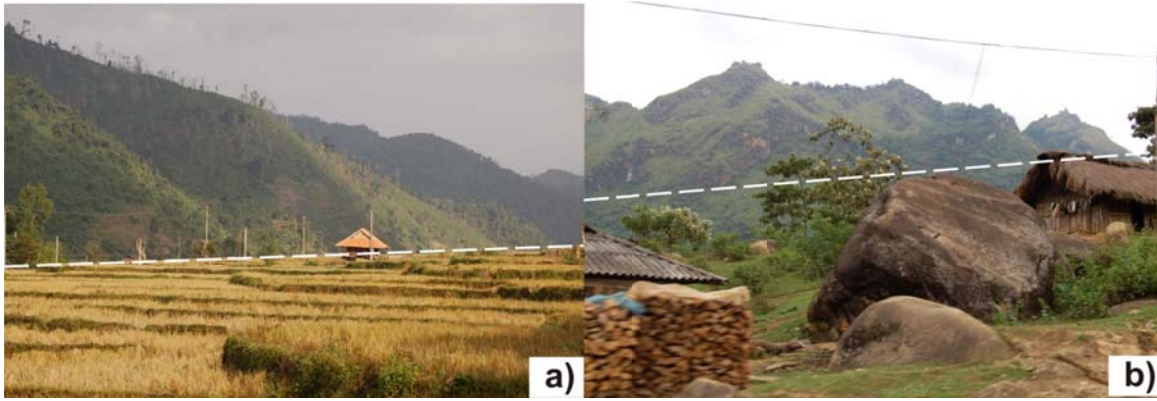


Fig. 5.21. Example of tectonic landform (triangular facets) pointing to differential uplift along Dien Bien – Lai Chau fault zone near Lai Chau province

Furthermore, the evidence of active strike-slip movement is also found on the conjugate Dien Bien-Lai Chau fault by the river features. The measured left lateral offsets of tributaries, river and drainage channels range between 270 and 790 m (Phan Trong Trinh, 2006). In the regional scale, between Lang Sang and Phung Dat, left-lateral offsets are between 458m and 2,244m, where cumulative effect of several deformational episodes resulted in nearly 8.369 km-long left offset of the Nam Ma river (Figs 5.8 & 5.29).

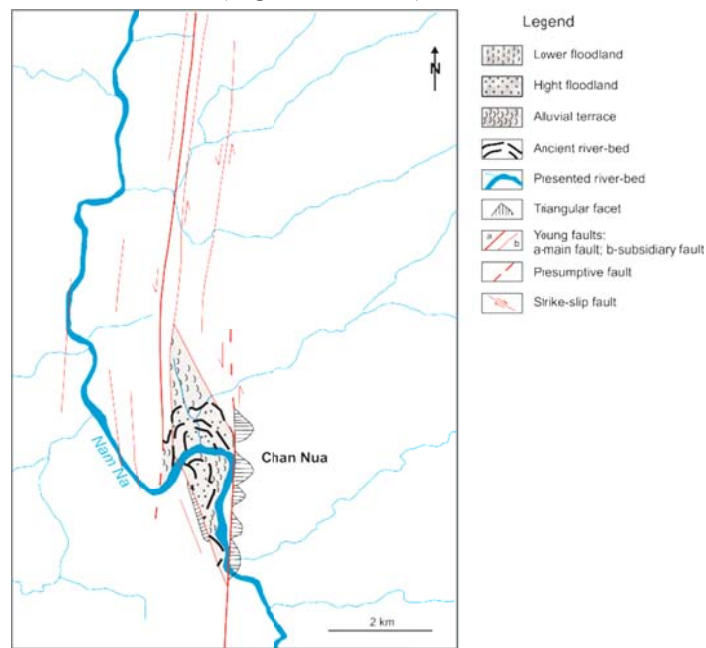


Fig. 5.22. The Chan Nua basin of pull-apart type related to sinistral strike-slip motion of the DBFZ (after Tran Van Thang, 2006)

Studied geomorphic features indicated amplitude of sinistral strike-slip around 500-2,200m in many locations (Figs 5.8 & 5.29). The age of deformation may be Quaternary (1 million year) with rates of sinistral strike-slip ranging from 0.5 to 2.2 mm/yr. The results are similar with obtained by Zuchiewicz (2004), who investigated amplitudes and rates of faults distributed in some valleys along the DBFZ. The displaced Quaternary alluvial sediments in

Dien Bien Phu basin indicate that sinistral strike-slip faults reveal minimum rates ranging from 0.6 to 2 mm/yr in Holocene and 2 to 4 mm/yr in middle-late Pleistocene times (Zuchiewicz *et al.*, 2004).

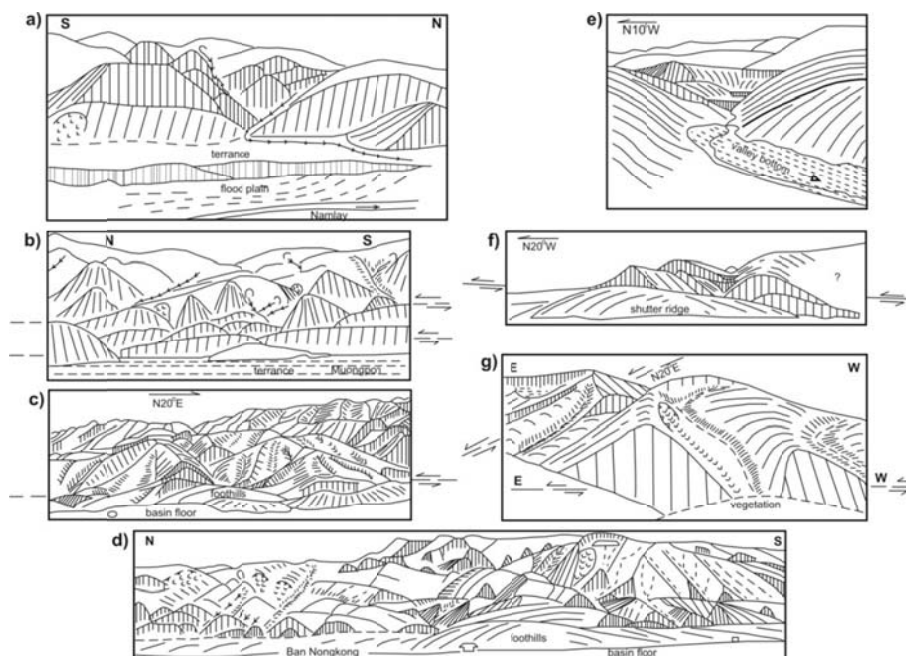


Fig. 5.23. Examples of tectonic landforms preserved in the DBFZ (after Zuchiewicz *et al.*, 2004):

- (a) left-hand side of the Namlay river valley south of Lai Chau;
- (b) left-hand side of the Nampon river at Muongpon, north of Dien Bien Phu;
- (c) western margin of the Dien Bien Phu basin NW of Dien Bien city;
- (d) western margin of the Dien Bien Phu basin, south of Dien Bien city;
- (e) three episodes of young uplift recorded by overhanging valley heads, eastern margin of the Dien Bien Phu basin;
- (f) young sinistral-normal fault on the eastern margin of the Dien Bien Phu basin; note a shutter ridge in the foreground;
- (g) Young strike-slip faults on the eastern margin of the Dien Bien Phu basin.

The zigzag line of Da River when it flows through the DBFZ is caused by sinistral strike-slip motion of the fault zone. The fault's amplitude reaches around 2,240m (within Quaternary basin). Rates of sinistral strike-slip fault zone range from 2.0 to 2.2 mm/yr. Similar values were appropriated for the fault zone in the Chan Nua, Dien Bien Phu basins along Nam Na River.

As was mentioned by Phan Trong Trinh (1999), the actual uplift of Phan Si Pan massif reaching more than 3,000 m may be a result of movement of two great strike-slip fault zones (RRFZ and DBFZ). The rapid uplift of Phan Si Pan massif can be explained by the displacement of some normal fault segments of striking NW-SE and NNW-SSE. Moreover, in the Van Yen, 18 km from the Yen Chau area, there is a leveled Hang Mon surface and the young sediments were discovered there. Vietnamese geologists collected numerous fossil plants and sporoplasms (*Carya*, *Quercus*, *Rhus*, *Pyrhosia*) corresponding to the Upper Miocene Tien

Hung Formation in Ha Noi basin. Thus, this surface probably already exists just before Pliocene.

The Ye Yen Sun granite massif was formed and penetrated the Phu Sa Phin alkaline magma blocks at great depth during Paleocene times. The data gathered in the Song Hong - Phan Si Pan zone indicated that during 33 to 23 Ma the Red River metamorphic rocks were formed under temperature of 650-700°C and pressure of 3 kb indication depth at least 8-12km. During 25 to 15 Ma (time of active sinistral strike slip of the RRFZ) metamorphic rocks were uplifted and changed P-T conditions, particularly the temperature was reduced gradually to 300° C and metamorphic rock (including Ye Yen Sun block) reached depth around 1-4 km. Therefore, Ye Yen Sun massif was uplifted 4-7km reaching present day height of 3km. The average rates of uplift reach around 0.8 to 1.4 mm/yr (Phan Trong Trinh, 1999).

The Van Yen-Nam Xe-Phong Tho fault constitutes regional boundary between Tu Le volcanic and Da River zones. In the central part of the area, this fault has features of normal fault expressed by lineaments. In the segment between Muong La and Bac Yen, the fault changes its direction into NW-SE. The nature of this fault segment indicates into right lateral strike-slip, suggested by river deflection. Between Pa Vang and Ban Mong, right lateral offsets are between 433m and 2,575m. The cumulative effect of several deformational episodes resulted in nearly 17.823 km-long right offset of the Da River (Fig. 5.8).

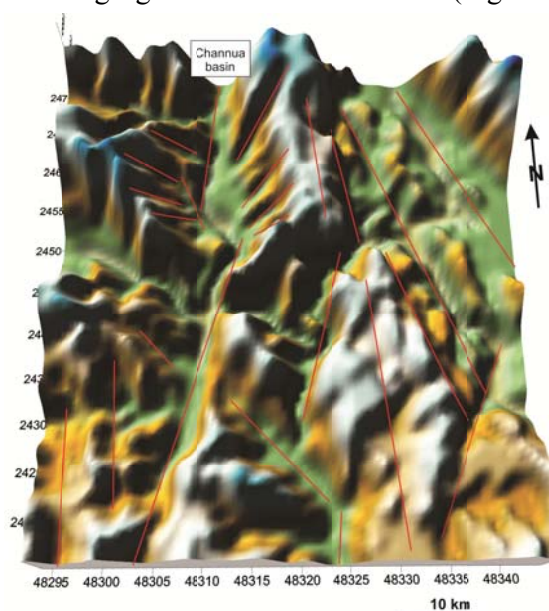


Fig. 5.24. Digital elevation model of the Chan Nua pull-apart basin and showing the DBFZ, the red-lines indicate tectonic lineaments.

At the Pho Lu area, a segment of the RRFZ forms a typical structure of the positive flower type, which reflects transpression regime. Positive flower structure is produced by convergence in strike-slip motion, or a combination of reverse faults (Twiss & Moores, 1992). The development of observed structural type was probably connected with the SE-NW transpression. Tectonic structure of the Con Voi mountain range is parallel to the Phan Si Pan range (Fig. 5.25). A valley is located between two uplifts. The flower structures were also

confirmed by the geological survey and seismic profiles in the Red River basin in South China Sea (Rangin *et al.*, 1995). Subsidence in this basin was caused by transtension regime forming a negative flower structure. Tectonic lineament system in Fig. 5.25 showing valley between uplift correspond to the model in Fig. 5.26.

Subsidiary faults combined with main fault of the DBFZ were observed in the northwestern study area. Most of them belong to the feather structure type and form pull-apart basins (Chan Nua, Lai Chau, Muong Pon, Dien Bien Phu, etc.).

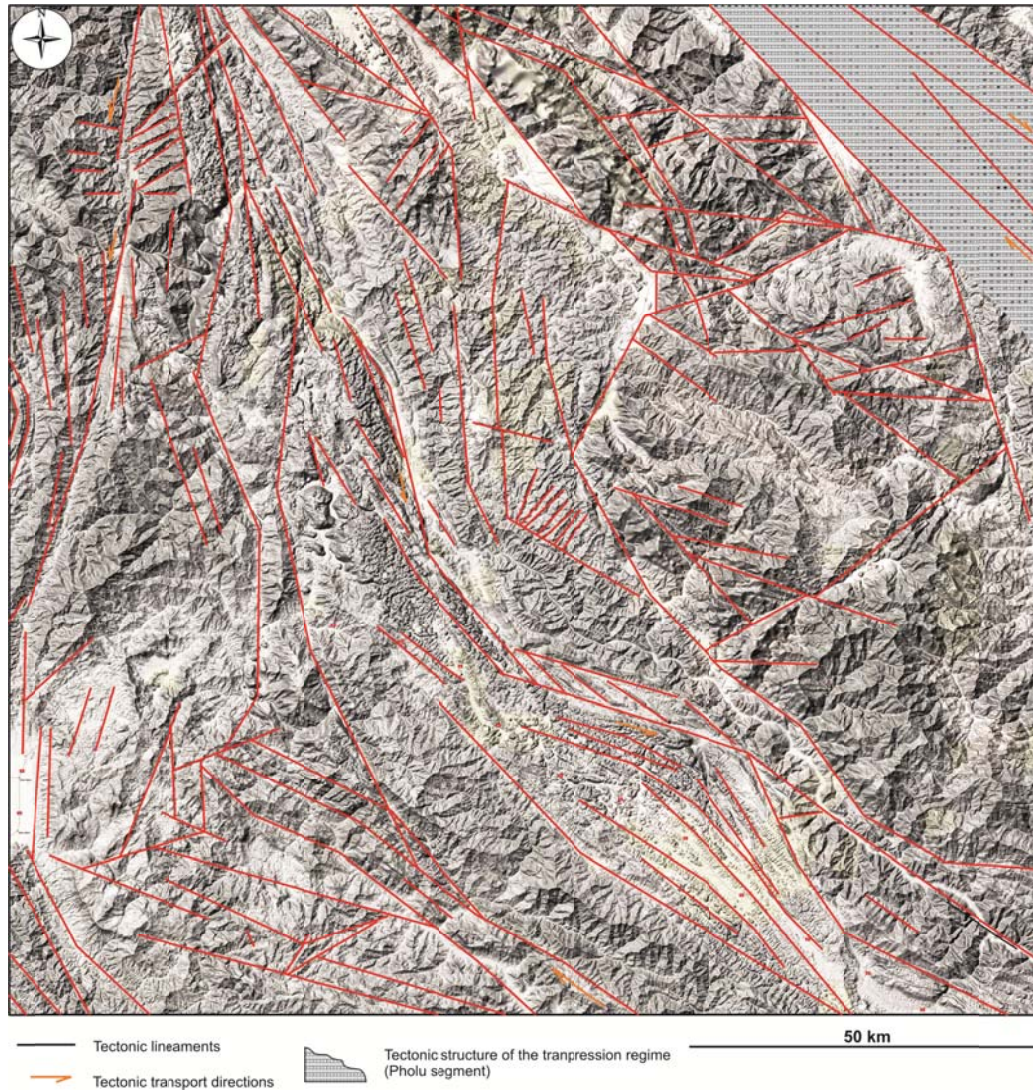


Fig. 5.25. The tectonic structures and tectonic lineaments identified in the NWN area.

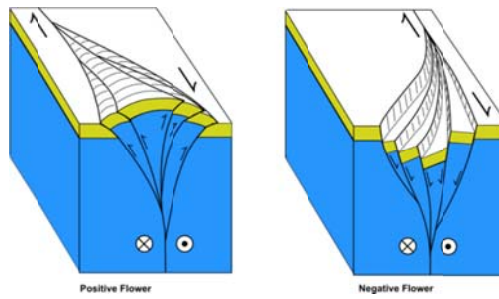


Fig. 5.26. Flower structure models modified from Nilsen & Sylvester (1995) appropriate for the designated structures in the Pho Lu segment of the RRFZ - a positive flower structure reflects the transpression regime in particular.

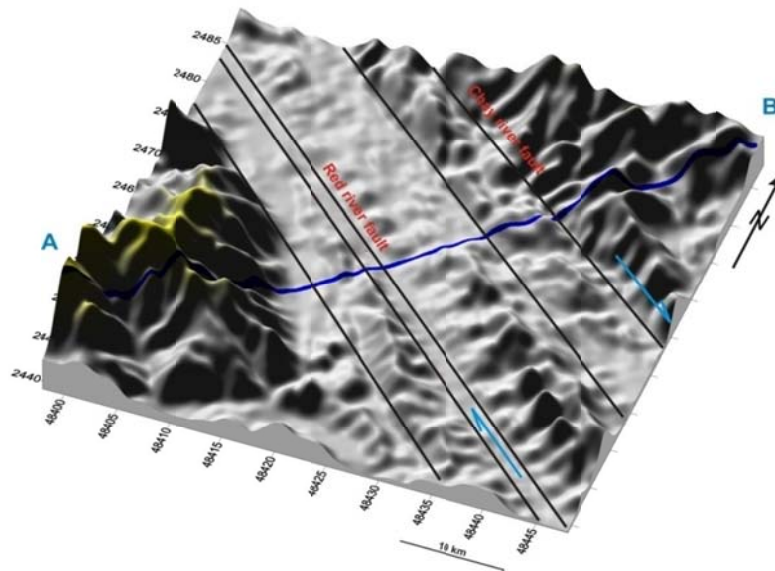


Fig. 5.27. Model landslides of the Red river valley (Pho Lu segment) in the NWVN area.

Selection of the most important lineaments and the imposition of tectonic transport directions inferred from the lineament analysis (Fig. 5.25) indicate existence of the DBFZ and RRFZ, and a valley related to the flower structure within the Pho Lu segment. This work also helps to recognize tectonic lineaments distributed in the central area, they correspond to the Van Yen-Nam Xe-Phong Tho and Da River faults.

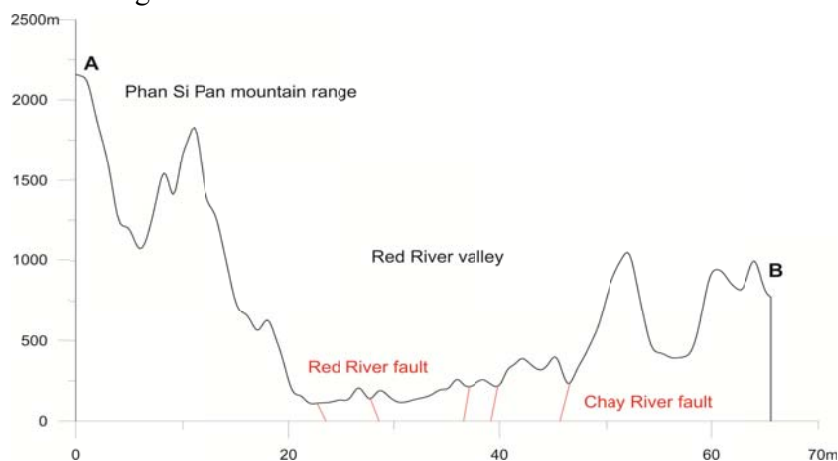


Fig. 5.28. A-B topographic profile (Pho Lu segment)

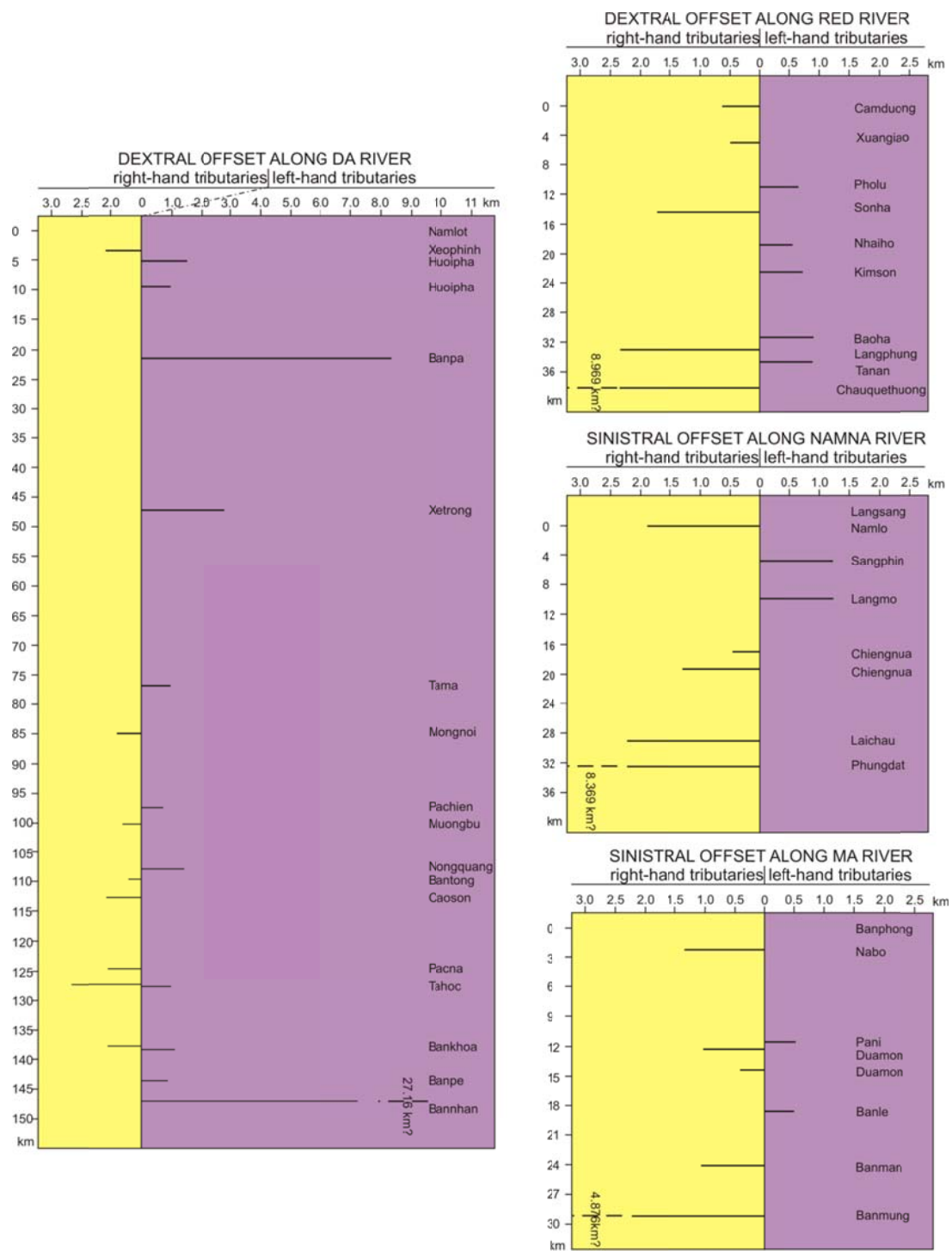


Fig. 5.29. Diagrams portraying incremental displacements of the right- and left-hand tributaries of the Da River, Red River, Nam Na River, and Ma River indicate dextral and sinistral offsets.

#### 5.4. Results and Discussions

Digital elevation model (DEM), the scale of remote sensing images, and the criteria adopted for interpretation of terrain and drainage network are sufficient to designate tectonic

lineaments in the NWVN area. Analysis of shape and extension of the Red River and Chan Nua valleys also helps to recognize the RRFZ and DBFZ.

Drainage network is mostly based on the combinations of two systems; the system with ESE-WNW direction is a more significant one. The valleys primarily based on the NNE-SSW and ENE-WSW directions prevail in the northwestern and northeastern parts of the study area, while the other groups prevail in the remaining area. The typical drainage networks are strongly influenced by tectonics or controlled by abrupt lithological changes. Types of the drainage networks indicate dendritic; rectangular and angular; parallel; and rectilinear geometries. Lineaments analysis allowed recognition of 166 lines. They summarized length is 2,917.1. Most of these lines are oriented ESE-WNW and SSW-NNE quite parallel to the most important regional system that affects the area. It's possible to recognize another organized system, prevalently oriented SSE-NNW. Transect analysis, applied to stream channels developed perpendicularly to lineament systems, shows a right strike-slip kinematics for ESE-WNW lines and a left strike-slip for lines oriented NNE-SSW. Surface roughness, topographic profile, contour maps and hydraulic gradient lets us to discriminate different area affected by tilting in recent period. In particular, at regional scale, the application of this methodologies to hydrographic basins located in the NWVN area (such as the RRFZ and DBFZ), allowed to distinguish four different morphologic regions in the investigation area. The boundary between these regions seems to be due to a lithological change from north to south, whereas in the northeastern region there is a structural boundary corresponding to the Red River dextral strike-slip system, in the northwestern there is also a structural boundary corresponding to the Dien Bien-Lai Chau sinistral strike-slip system. Geomorphic features from the study area vary from north to south and from west to east.

Four groups reflecting the linear structures can be distinguished among the topo-and photo-lineaments. They indicate the ESE-WNW, SSE-NNW, NNE-SSW and ENE-WSW directions. Tectonic lineaments are arranged in extensional (basins), strike-slip, and transpression regimes. The resulted network of tectonic lineaments was compared with the geological map on the scale 1:200,000. In general lineaments, complies with the mapped faults.

The relief and shade of NWVN area emphasize marked tectonic lineaments and the dislocation structures of the area corresponding with these lineaments. In turn, in the northeastern area a valley forms of positive flower structure (the Pho Lu segment). This valley belongs to the RRFZ. In the northwestern area, another dislocation structure of the DBFZ is a dominating feature of the sinistral strike-slip motion forming some pull-apart basins (Chan Nua basin) by combination of the subsidiary faults. Application of this analysis helps finding solutions to the problem of relationship between faults and lineaments partly shown on surface within the mountainous region as well as other small scale lineaments.

As far as we are concerned, the overall picture of the study area from digital elevation model interpretation and field studies revealed that the study area has been seriously affected by tectonics on a large scale and the series of faults detected on the terrain and drainage network are products of geotectonic activities.

## 6. EARTHQUAKES

At the Palaeocene-Eocene boundary, the interactions of two plates (India and Asia or Eurasia) have made an impact on the crust of the NWVN area. This area suffered tectonic stress in many directions, making a complex stress environment. Mantle dynamics and plate interactions in Southeast Asia have been repeatedly examined based on plate tectonic reconstruction, geological and geochemical data (Chung *et al.*, 1997, Metcalfe, 1996a,b, 2000; Golonka *et al.*, 2006a); however, the relatively small number of geophysical surveys and seismic observations means that little is known of the present tectonic stress field and the nature of structures in the deep crust and upper mantle – features that provide a unique constraint on the geodynamic evolution of Southeast Asia. The seismicity of the NWVN area is influenced by India-Asia collision. From the local point of view, seismic activity is classified as high in some regions of Vietnam (Nguyen Dinh Xuyen, 1994). The discussed documentary earthquake material from the investigated area was gathered in catalogues belonging to seismological stations in Vietnam, the National Earthquakes Information Centre (NEIC), the International Seismological Centre (ISC) and the Harvard Centroid-Moment-Tensor (CMT). The papers linked to this subject were also used. Figure 6.1 presents epicentre distribution for earthquakes with a magnitude greater or equal to 4.0. This magnitude was calculated from surface waves recorded in the northern Vietnam during the time period 1975 - September, 2009.

### 6.1. Distribution of earthquake epicentres in the northern Vietnam

Scientists have admitted that the occurrence of earthquakes is related to faults, so the determination of focal mechanism of earthquakes has great scientific and practical significance, which helps to understand the activity of faults in the present time.

In Vietnam, during the XX century, two earthquakes were observed with intensity  $I_0 = 8-9$  (MSK-64) and magnitude  $M = 6.5 - 7$  Richter degrees, fifteen earthquakes with  $I_0 = 7$  and  $M = 5 - 5.9$ , and more than 100 earthquakes with  $I_0 = 6-7$ ;  $M = 4.5-4.9$ . Earthquakes in the northern Vietnam are not scattered but distributed along different fault zones, such as Dien Bien - Lai Chau, Ma River, Da River, Red River, Chay River, Cao Bang – Tien Yen, Dong Trieu, and Ca River - (Figs. 6.1 & 6.3). In recent time eight earthquakes with magnitude of 4.7 to 6.1 have been recorded, and the focal depth of the typical earthquake on 27 February 1969 reached up to 68 km.

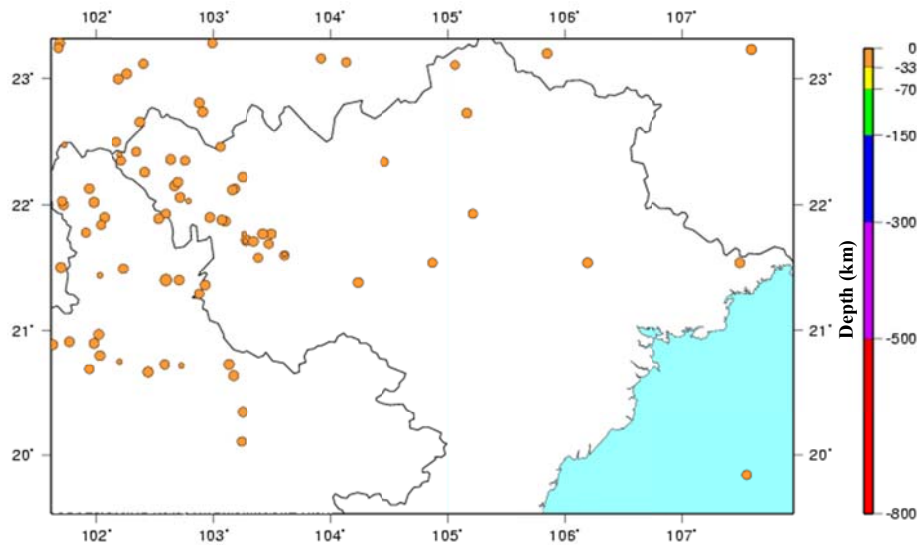


Fig. 6.1. The epicentres of the earthquakes in northern Vietnam and adjacent area for the time 1975-2009,  $M_s \geq 3.6$ ; <http://www.neic.cr.usgs.gov/>

Data for this study are contained in catalogues from: seismological stations in Vietnam (since 1963), the Institute of Geophysics - Vietnam, the National Earthquakes Information Centre (NEIC) [<http://www.neic.cr.usgs.gov/>], the International Seismological Centre (ISC) [<http://www.isc.ac.uk/>], the Global CMT [<http://www.globalcmt.org/>], the China Earthquakes catalogues and relevant Vietnamese literature. In fact, the data from these catalogues differ, especially from earlier times to around the 1990s. The differences are evident mostly in the evaluation of magnitude earthquakes but sometimes also in the time of their occurrence. According to Mortimer (2006) many factors have influenced the evaluation of magnitudes including distance of the registration point from the focus, the directionality of seismic wave radiation and waves' frequency in relation to the registration apparatus. However, a rapid development in seismological technology and an increased distribution of seismological stations, especially after 1975, have resulted in precise location of earthquakes of magnitude as small as 3.5. So as for seismic data to be considered sufficiently precise in Vietnam, a good display of the data has been shown in many investigations (Nguyen Kim Lap, 1989; Cao Dinh Trieu, 1991, 1999; Nguyen Dinh Xuyen, 1994; Nguyen Hong Phuong, 1991; 2001; Phan Thi Kim Van, 2006). The recent seismological stations in northern Vietnam are presented in Fig. 6.2, see also Table 6.1.

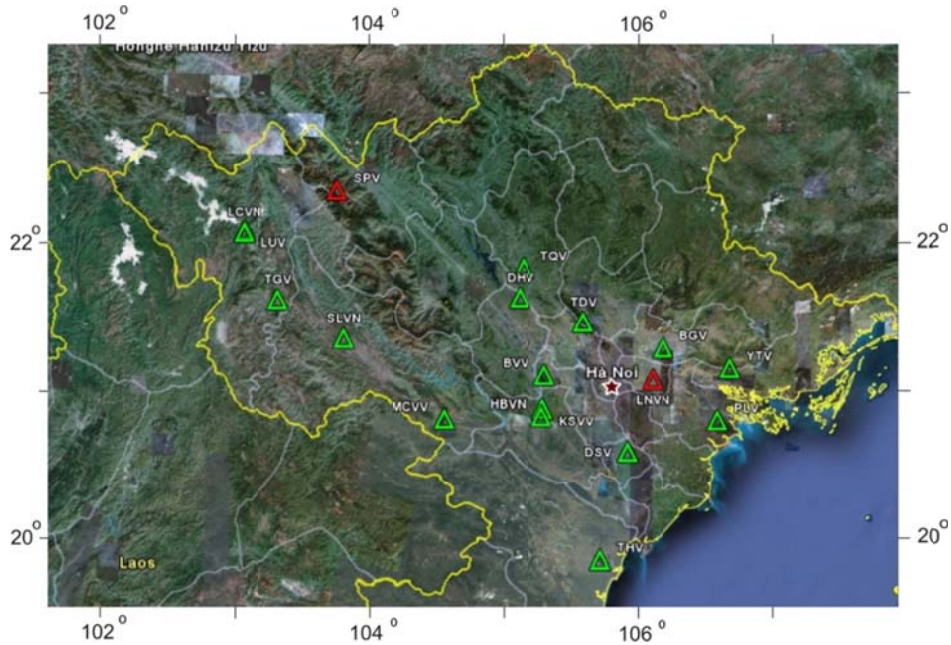


Fig. 6.2. Seismological stations in the northern Vietnam  
<http://iisee.kenken.go.jp/net/hara/Vietnam.htm>

Code	Latitude	Longitude	Elevation	Status	Station name
DBV	21.3900	103.0250	1050.0	Reserved	Dien Bien Phu
DHV	21.6269	105.1838	70.0	Open	Doan Hung
DSV	20.5870	105.9740	70.0	Open	Doi Son
HBVN	20.8259	105.3519	30.0	Open	Hoa Binh
HNV	21.0481	105.7972	6.0	Reserved	Ha Noi
KSVV	20.8550	105.3590	30.0	Open	Ky Son
LCVN	22.0287	103.1543	1100.0	Open	Lai Chau
LNVN	21.0770	106.1540	50.0	Close	Lang Ngam
LUV	22.0519	103.1594	1100.0	Open	Lai Chau
MCVV	20.8000	104.6500	800.0	Open	Moc Chau
PLV	20.8060	106.9260	90.0	Open	Phu Lien
SLVN	21.3338	103.9050	700.0	Open	Son La
SPV	22.3360	103.8311	1570.0	Closed	Sa Pa
TDV	21.4647	105.6457	1200.0	Open	Tam Dao
TGV	21.5898	103.4182	0.0	Open	Tuan Giao
THV	19.8508	105.7820	0.0	Open	Thanh Hoa
YTV	21.1570	106.7170	0.0	Open	Yen Tu

Table 6.1. International registry of seismograph stations  
<http://iisee.kenken.go.jp/net/hara/Vietnam.htm>

Therefore, before 1975 (in particular the period 1903-1975), earthquake magnitudes were partly evaluated from macroseismic data, which were obtained from field investigations of surface deformations and from historical sources. Their parameters were estimated on the basis of paleoseismological and descriptive data. The northern Vietnam region is characterized by linear distribution of the epicentres correlated with the position of the faults (Mortimer, 2006 and references therein).

Earthquakes in Vietnam and NWVN area in particular (Fig. 6.1, Fig. 6.4) have been dated since the year 114. The analysed results by Nguyen Kim Lap (1989) and Cao Dinh Trieu (1999) show the characteristic band distribution of the epicenters consistent with the RRFZ and

the DBFZ systems. Data from the National Earthquakes Information Centre (NEIC-<http://neic.usgs.gov>) also show that the earthquakes are shallow – all occurred at  $h < 35$  km, most at  $10 \leq h < 35$  km (Fig. 6.3).

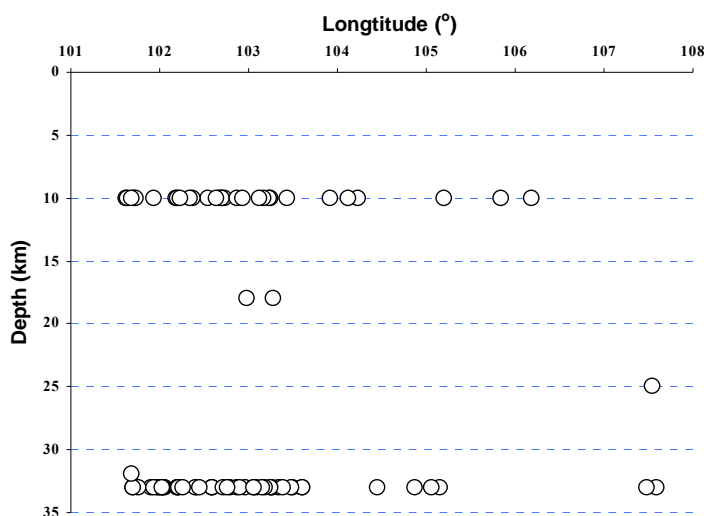


Fig. 6.3. Profile of the depths of earthquake focus in northern Vietnam and adjacent area (from 1975 to 2009; see appendix for detail)

According to Nguyen Kim Lap (1990), the investigation of more than a million earthquakes, which occurred in the north part of Vietnam, indicated that earthquake density is higher in northwestern Vietnam, and almost all hypocenters in this region were in the Earth's crust. The earthquakes are generally related to the tectonic faults and geological structures in the northwest-southeast directions. Some of them were as follows: the Dien Bien earthquake (1935) on the Ma River fault,  $M=6.75$  (the intensity in epicentre  $I_0=9$ ), the Bac Giang earthquake (1961) on the Dong Trieu fault in the Red River delta,  $M=5.9$  ( $I_0=7$ ) and Tuan Giao earthquake (1983) on the Son La fault,  $M=6-7$  ( $I_0=8-9$ ). The intensity “I” is the measurement of the earthquake effects on humans, constructions (damage to buildings) and nature (land). “ $I_0$ ” is the intensity in the epicentre of the earthquake.

Parameters of some earthquake events were determined at the highest reliability as follows (Cao Dinh Trieu, 1999; Le Tu Son & Nguyen Thi Cam, 2002; Nguyen Dinh Xuyen, 1992) - see also Figure 6.4.

1. Earthquake occurrence in the Dien Bien area (1935) -  $M=6.8$  was recorded by 23:22' on 1st Nov. 1935 (Ha Noi time) in the southeast of the Dien Bien City. It caused severe damage to the residential houses in the Dien Bien and Son La provinces.

2. Earthquake in Luc Yen (Yen Bai) in 1953- $M=5.4$ .

3. Earthquake in Luc Yen (Yen Bai) in 1954- $M=5.4$  where the earthquake epicentre was located quite near to that of the earthquake occurred in 1953. These two Luc Yen earthquake events occurred at the same seismic intensity but isoseismic width of the latter incidence (1954) was narrower. This event was also was longer.

4. Tuan Giao earthquake (1983) -  $M=6.7$ . It happened at 14:00 on the 24th Jun., 1983, about 11km northeast from Tuan Giao town, causing heavy losses to the Tuan Giao district and

surrounding areas (Nguyen Dinh Xuyen, Cao Dinh Trieu, 1990). After the event, a series of aftershocks occurred. The greatest aftershock was on the 15<sup>th</sup> of July 1983 in the same place of maximum magnitude  $M = 5.4$ .

5. The Muong Luan earthquake ( $M_s=4.9$ ) occurred on the 23<sup>rd</sup> of Jun., 1996. Its epicentre was  $21^{\circ}26'08$  N,  $103^{\circ}32$  E, the focus depth was about 7 km.

6. The Thin Toc earthquake ( $M_s = 5.3$ ) on the 19<sup>th</sup> of Feb., 2001 had its epicentre of  $21^{\circ}39$  N,  $102^{\circ}83$  E and the focus depth was about 12.3 km.

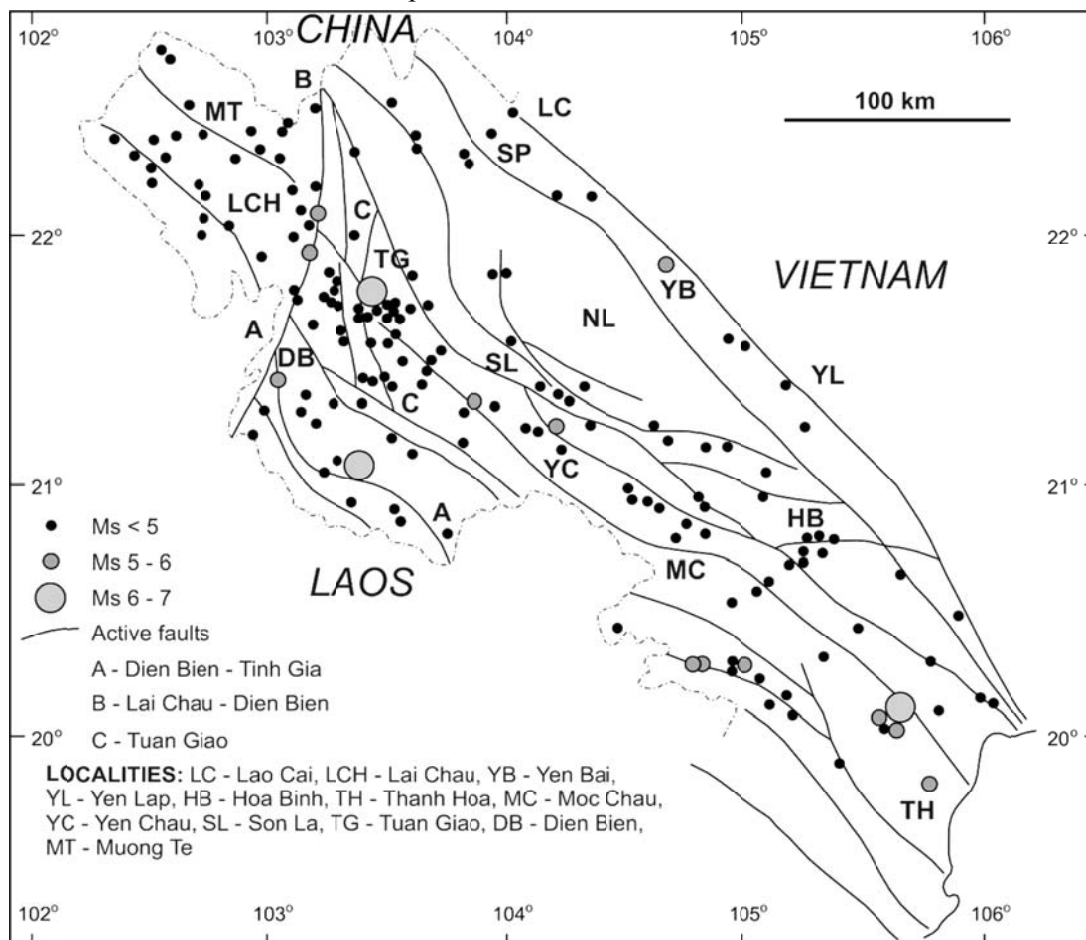


Fig. 6.4. Pattern of seismicity and active faults in NWNVN (based on the work of Cao Dinh Trieu *et al.*, 1999; see also Zuchiewicz *et al.*, 2004).

## 6.2. Focal mechanism of earthquakes in the northwestern Vietnam

In the NWNVN many earthquakes occurred, but only some have had their focal mechanisms determined because of a shortage in seismic observing stations. A number of methods used to determine the focal mechanism of earthquakes were carried out by some Vietnamese workers and other as follows.

1. Calculation of first motion of P wave: this is based on the theory of fault plane by double couple forces (Nguyen Kim Lap, 1989, 2003; Nguyen Ngoc Thuy, 1996; Nguyen Khac Mao, 1973). The method requires a set of sufficient P waves around earthquake. It is applied with satisfactory results in the NWNVN area.

2. The macro seismic field is based on the data obtained from field investigations of surface deformations and from historical sources (Nguyen Van Luong, 1996), with the successful application of the double-couple forces in tectonic interpretation. However, a weak point of this method lies in its being applicable for those earthquakes occurring at ground surface. Gibowicz *et al.* (1987) used this method for analysis of the Tuan Giao earthquake.

3. The moment tensor inversion uses the radiation pattern of body-and/or surface-waves. The complete waveform data is inverted to fit synthetic waveforms calculated for a reference earth model. If the earth's structure is known and waveform data is available, the seismic moment tensor and thus the focal mechanism of an earthquake can be calculated by inversion. From 2000 to present, more than 17-stations (up to 25 stations) for broadband seismic array have been installed in northern Vietnam. The stations are distributed uniformly over the area, and provide a high density of seismic data with a wide dynamic range that enables analysis of the tectonic evolution of the fault zones. The array also provides useful information in determining crustal and mantle structures for the purpose of regional earthquake monitoring and seismic hazard mitigation in this region, for a similar result when the moment tensor inversion method is applied. However, results of the method are not publicly known by many until now. Phan Thi Kim Van (2006) in particular applied this method for the Dien Bien – Lai Chau fault and showed successful results.

Table 6.2. Focal mechanism of earthquakes determined by means of the first motion of long P wave (Nguyen Kim Lap *et al.*, 1989; Le Tu Son, 2000)

No	Event name	Date (d/m/y)	Latitude (N)	Longitude (E)	Depth (km)	Nodal plane (°)			P-axis (°) (compression)		T-axis (°) (dilatation)		Ms
						Strike	Dip	Slip	Azimuth	Dip	Azimuth	Dip	
1	Tuan Giao	24/06/1983	21.71	103.43	11.0	313	60	224	187	35	93	16	6.7
2		15/07/1983	21.41	103.83	7.0	82	72		213	21	123	6	5.4
3		Aftershocks (after Gibowicz <i>et al.</i> , 1987)				7.0	121	50		50	40	268	17
4	Muong Luan	22/06/1996	21.29	103.31	7.0	304	46	67	230	1	137	74	4.9
5	Lai Chau	29/03/1993	21.83	103.15	10.0	155	75	155	-158	6	109	28	4.9
6	Ta Khoa	6/10/1991	21.38	104.17	7.0	135	72	157	-178	2	91	29	4.9

In response to double couple forces, the first motion of P way is symmetrical through the slip surface of the discontinuity of focus and the plane, which is perpendicular to form the change sign of quarterly arcs. Mapping the distribution of first motion of P way by a set of seismic stations by using an appropriate method can determine the parameters of fault plane, the compressive and dilatational stresses in the focus of earthquakes. The focal mechanism of some earthquakes determined by means of the first motion of P wave is listed in Table 6.2.

Table 6.3. The parameters and focal mechanism solutions of three events occurring on the Dien Bien-Lai Chau fault zone from February to April 2001 (Phan Thi Kim Van, 2006)

No	Date (m/d/y)	Time (UTC) (Hr:Mn:Sec)	Latitude (°E)	Long (°N)	Depth (km)	Azimuth (°)	Nodal plane		Slip (°)	Mw	VR (%)	Dist.(km)/sat
							Strike (°)	Dip (°)				
1	2/19/2001	15:51:35.97	21.396	102.715	12	234	299;35	76;68	157;15	5.1	96	485/(CHTO)
						0						413/(KMI)
2	2/19/2001	19:02:52.40	21.292	102.882	12	237	103;37	84;67	-157;-7	4.4	97	494(CHTO)
						358						425(KMI)
3	4/2/2001	20:45:50.92	22.124	103.157	15	231	307;37	89;69	159;1	4.5	96	571(CHTO)
						352						335(KMI)

Table 6.4. The parameters and focal mechanism solutions of events occurring on the Dien Bien-Lai Chau fault zone during the time from 1983 to 1995 (Phan Thi Kim Van, 2006)

No	Date (m/d/y)	Time (UTC) (Hr:Mn:Sec)	Latitude (°E)	Long (°N)	Depth (km)	Nodal plane		Slip (°)	Mw	VR (%)	Catalog
						Strike (°)	Dip (°)				
1	6/24/1983	07:18:22.14	21.721	103.282	12	206;114	72;84	7;161	6.3	94	GS
2	7/15/1983	04:48:54.40	21.93	103.29	15	34;301	78;80	10;168	5.3	53	HRV
3	6/16/1989	20:12:32.80	20.61	102.61	15	25;119	65;82	-9;-154	5.6	81	HRV
4	4/24/1995	16:13:14.20	22.88	103.16	33	102;11	80;83	173;-10	5.2	66	HRV

These results are used through my study for a better understanding and analysis of geodynamic conditions in the NWVN area.

### 6.3. Characteristics of fault based on their focal mechanisms

#### 6.3.1. Son La Fault

The Tuan Giao earthquake (June 24th, 1983 at 07:18:22:26) is registered as No. 062483A event in the Global CMT catalogue (see Appendix) which occurred in Son La fault system (Nguyen Kim Lap, 1989; 2003). The data from this event are also available in some publications (e.g., Gibowicz *et al.*, 1987; Nguyen Kim Lap, 1989). The parameters were: latitude  $j = 21.72^\circ$ , longitude  $l = 103.38^\circ$ , depth 18.0 km, surface-wave magnitude  $M_s = 6.5$ , body-wave magnitude  $M_b = 6.1$ . The focal mechanism, which is seismologist reference to the direction of the slip and the orientation of the fault, is presented as the “beach ball”, which depicts also the stress orientation.

The mechanisms are determined as a right-lateral strike-slip with direction and slip at  $110^\circ$  and  $-156^\circ$  respectively (Fig. 6.5). Another earthquake with  $M_s = 6.9$  occurred on the same day but two hours later. It was accompanied by a series of aftershocks: during next five months 223 shocks with magnitude 2.6 were recorded, half of them on the first four days after the main quake. One may suggest that the quake of June 15th, 1983 ( $l = 103.29^\circ$ ,  $j = 21.93^\circ$ ) with  $M_s = 5.0$  at a depth of 15.0 km (No. 071583B event in the Global CMT catalogue-Fig.6.6) was the precursor of the both strong earthquakes in June 24th or it simply triggered them as a result of stress redistribution.



Fig. 6.5. Focal mechanism of the event – No. 062483A

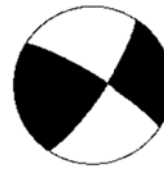


Fig. 6.6. Focal mechanism of the event – No. 071583B

#### 6.3.2. Da River fault

The Ta Khoa earthquake occurred on 6th October 1991 in the Da River fault zone (Le Tu Son, 2000). Major nodal plane of the earthquake had strike of  $135^\circ$  and dip of  $72^\circ$ . The focal

mechanism of this event is determined as a dextral strike-slip with direction and slip at  $135^\circ$  and  $157^\circ$ , respectively (Fig. 6.7, Table 6.2).



Fig. 6.7. Focal mechanism of the Ta Khoa earthquake

### 6.3.3. Dien Bien – Lai Chau Fault

The Thin Toc earthquake (19th Feb., 2001) which is registered as No. 011900C event in the Global CMT catalogue (Appendix ) occurred in the Dien Bien-Lai Chau fault system (Cao Dinh Trieu, 2001). The parameters of the quake were: latitude  $j = 21.33^\circ$ , longitude  $l = 102.84^\circ$ , depth 12.3 km, surface-wave magnitude  $M_s = 5.3$ , and  $I_0 = 7-8$ .

The focal mechanism of this earthquake is determined as a sinistral strike-slip with direction and slips  $64^\circ$  and  $4^\circ$ , respectively (Fig. 6.8).

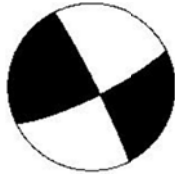


Fig. 6.8. Focal mechanism of the Thin Toc earthquake – No. 011900C (<http://www.globalcmt.org>)

Moreover, during the period from 1983 to 1995, there were four moderate earthquakes with magnitude ranging from  $M_{5.2}$  to  $M_{6.3}$  occurring in the Dien Bien-Lai Chau fault zone (Phan Thi Kim Van, 2006). The results of focal mechanism solutions of these events show that they are strike-slip along left-lateral planes with dips ranging from  $65^\circ$  to  $80^\circ$  and strikes ranging from  $11^\circ$  to  $34^\circ$  (Fig. 6.9; Table 6.3).

In recent time, based on the data collected by the National Earthquake Information Centre (Fig. 6.9 and Table 6.4), there were three earthquakes with magnitude ranging from  $M_{4.4}$  to  $M_{5.1}$  occurring in the Dien Bien-Lai Chau fault zone, one of them should be correlated with the Thin Toc event, which gives us the opportunity to evaluate and interpret their focal mechanisms. The results show that the mechanisms are pure strike-slip along left-lateral faults with dips ranging from  $67$  to  $69^\circ$  and strikes ranging from  $35$  to  $37^\circ$ .

In general, most results of investigation showed the sinistral strike-slip character of DBFZ, which corresponds to geomorphic features. A dextral strike-slip movement occurred, however, in this fault during the Lai Chau earthquake (Le Tu Son, 2000; see also Table 6.2).

### 6.3.4. Chieng Khuong Fault

The Muong Luan earthquake on the 22nd June 1996 occurred along the Chieng Khuong fault in Song Ma fault zone (Cao Dinh Trieu & Le Tu Son, 1997; Le Tu Son, 2000). The parameters of the earthquake were: latitude  $j = 21.29^\circ$ , longitude  $l = 103.31^\circ$ , depth 7.0 km, surface-wave magnitude  $M_s = 4.9$ .

The focal mechanism of this earthquake determined a thrust or oblique reverse character of this fault with direction and slips at  $304^\circ$  and  $67^\circ$  respectively (Fig. 6.10; see also Table 6.2).



Fig. 6.10. Focal mechanism of the Muong Luan earthquake

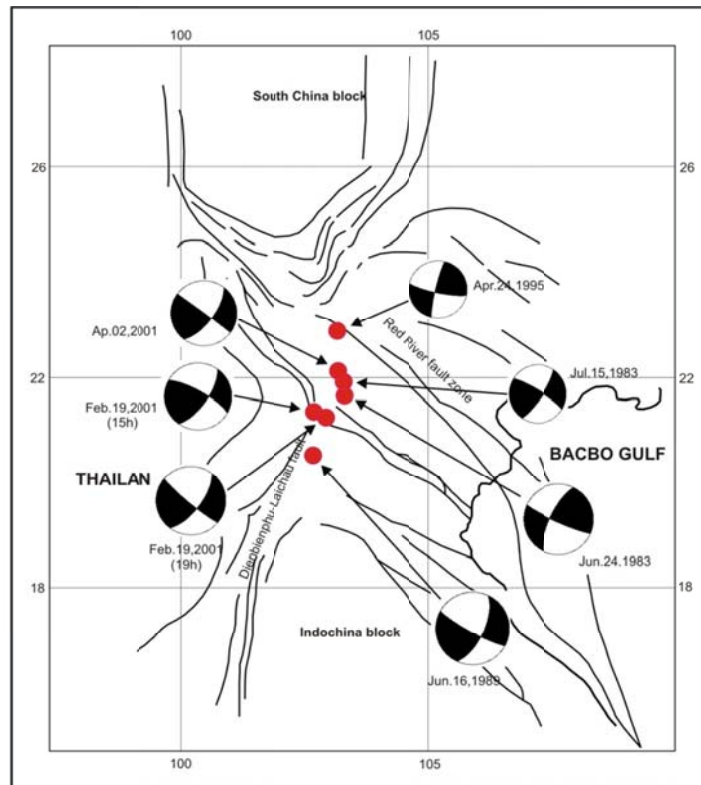


Fig. 6.9. Location and focal mechanisms of earthquakes with magnitude ranging from 4.0 to 6.3 occurring on the Dien Bien-Lai Chau fault zone during the time from 1983 to 2001 (modified from Phan Thi Kim Van, 2006).

### 6.3.5. Red River fault zone (RRFZ)

Along the Ailao Shan-Red River fault zone, distributed in the China and Northern Vietnam segments, earthquakes of  $M > 7.0$  have been recorded (Allen *et al.*, 1984; Nguyen Kim Lap, 1989, 1991). It is indicated by the maps of epicenters (Figs 6.1 & 6.4) that the RRFZ has an apparent sparse seismic activity. At present time may be a long recurrence interval of strong earthquakes (around 1.8 Ma) in this zone (Allen *et al.*, 1984) and locking time for the fault at a depth of 5-20 km (Duong Chi Cong & Feigl K. L., 1999). In the northern Vietnam segment the focal mechanism of earthquake was determined very rarely, therefore, earthquake parameter data from Global CMT and China Earthquakes catalogues were used.

The earthquake coded as event No.042495B in the Global CMT catalogue (Appendix) occurred on the 24th April 1995 in the RRFZ in Yunnan province, near Chinese-Vietnamese boundary. It is also listed in other publications (see Zhu *et al.*, 2004). The parameters of the earthquake were: latitude  $j = 22.88^\circ$ , longitude  $l = 103.16^\circ$ , depth 33.0 km, body-wave magnitude  $M_b = 4.9$ . The source was connected with the south part of Ailao Shan-Red River fault zone (Zhu *et al.*, 2004) with the epicenter near Vietnam segment.

The focal mechanism of this event determined right-lateral strike-slip with direction and slip at  $102^\circ$  and  $-173^\circ$  respectively (Fig. 6.11): A strike-slip mechanism with a NW-SE striking nodal plane (A) dipping  $80^\circ$  towards SSW (azimuth  $192^\circ$ ) with oblique sinistral lateral slip (strike slip:  $-173^\circ$ ) and NE-SW striking plane (B) dipping  $83^\circ$  towards NW (azimuth  $281^\circ$ ) with oblique dextral lateral slip (strike slip:  $-10^\circ$ ). The compression axis (T) dips  $2^\circ$  towards EN (azimuth:  $57^\circ$ ). The dilatation axis (P) dips  $12^\circ$  towards NW (azimuth:  $326^\circ$ ).



Fig. 6.11. Focal mechanism of the event – No. 042495B (see also Zhu *et al.*, 2004).

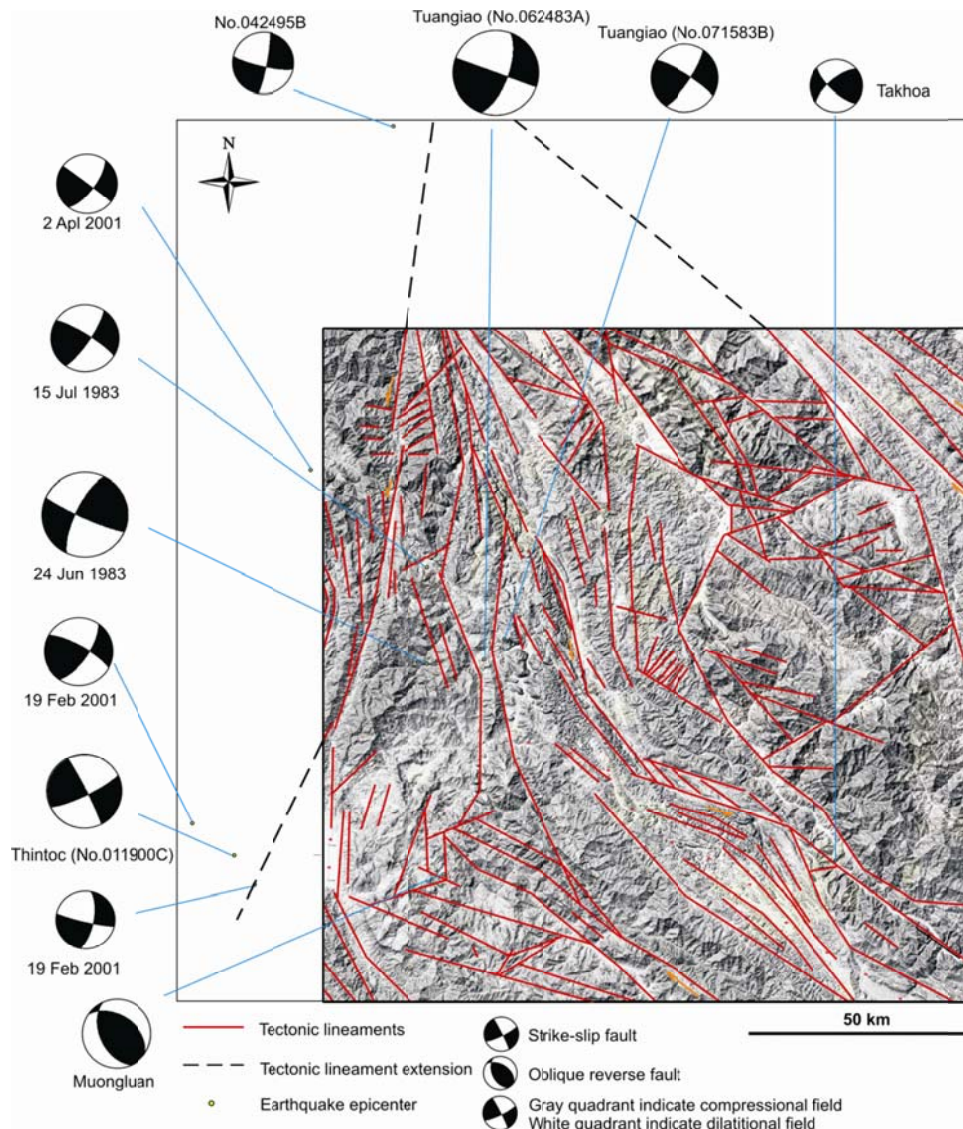


Fig. 6.12. Analysis and results of fault kinematics are represented by the focal mechanism solution of earthquake “beach balls” for the NWN area.

#### 6.4. Discussion

Active faulting in NWVN is a direct indicator of active crustal extrusion of Indochina due to the convergence between India and Asia (Tapponnier *et al.*, 1982; Golonka *et al.*, 2006a and references therein). Since in many cases movements along active faults of north Vietnam have been associated with earthquakes, the study of active faults can be based on strong scrutiny of available earthquake data. Geomorphological and geomorphotectonic characteristics, mechanisms and the trend of active fault zones in the area have been discussed while considering their tectonic differences. The focal mechanism solutions of the earthquakes within the investigated area point to the presence of both thrust and strike-slip faulting in the basement, whereas in the rest of the country most active fault reaches the surface. The earthquake mechanism solution along active fault systems imply dominance of strike-slip faulting in a transpression regime in western and central NWVN, while oblique reverse faults in convergent regime prevail in southwestern part of NWVN area.

The study of earthquake focal mechanisms allows us to view the geometry and orientation of the faults at the time of movement. By combining the focal mechanism data with the longer-term geological record, it is possible to reconstruct the tectonic process of a region through time. In this study, although the observed mechanisms of the minor earthquakes are rather diverse, and over time, the focal mechanism distribution may vary, we do see some intriguing patterns already. Among the 11 events shown in the Fig. 6.13, reverse faulting was observed only in the southwestern part of NWVN, with P-axes trending NE-SW. Strike-slip faulting dominated in the remaining NWVN area with P axes trending NNW-SSE or NW-SE and T axes trending ENE-WSW or NE-SW. Thus, a certain degree of regionalization of focal mechanisms can be seen in the NWVN area.

The Himalayan event is frequently mentioned as a typical example of the extrusion, having extensive effect on NWVN area (Tapponnier *et al.*, 1982; Leloup *et al.*, 1995). In the model, the deformation and metamorphics of this belt is dominated by strike-slip faults and combination with some pull-apart basins. In this study, only 3 out of the 11 earthquake events in the area are shallower than 15 km, while the other 8 are located in the mid- and lower-crustal levels. Most of these events have nodal planes dipping at high angles ( $> 30^\circ$ ). These mostly steeply dipping nodal planes and the depths of these reverse faulting earthquakes show that reverse faulting in the NWVN is not confined above the assumed shallow detachment surface but occurs in the crystalline basement at high angles.

In an extruding motion, strike-slip faulting is generally the dominant mode of deformation, but the completely opposite mechanism is also commonly recognized within the NWVN (Leloup *et al.*, 1995; Nguyen Van Hung & Hoang Quang Vinh, 2001; Zuchiewicz & Cuong, 2004). As mentioned above, active strike-slip faulting is taking place in the southwestern portion of the area at both the shallow ( $\leq 15$  km) and deep (15-33 km) levels. The shallow faulting may be related to the extensive effect caused by the Himalayan event in the NWVN to the outer portion of the core. On the other hand, the finding of deep faulting under the northeastern and northwestern area is certainly not new, and the cause of the deep strike-slip faulting is rather intriguing, for example the Red River and Dien Bien-Lai Chau fault zones. As

the focal mechanism solutions accumulate over time, they can be used to examine whether the NWVN basement height indeed acts as an indenter. Nevertheless, the best-fitting stress models in these areas are in agreement with the results of Nguyen Van Hung (2002) and are consistent with the plate motion vectors in the vicinity of NWVN (Lacassin *et al.*, 1994; Findlay & Phan Trong Trinh., 1997; Becker, 2000; Phan Trong Trinh *et al.*, 2004; and references therein).

## **7. MINERALIZATION**

These igneous and eruptive activities have formed many mineralizations in whole area of the NWVN. Totally around 100 ore deposits and occurrences have been discovered from the area (Fig. 7.1). These deposits comprise iron, chromium, copper, lead-zinc, molybdenum, gold, and the non-metal ores including barite and fluorite, pyrite, graphite, potassium-sodium, rare earth and radioactive ores. Based on geochronological and geochemical data of the igneous and eruptive rocks that constitute main lithologies in the NWVN, it is possible to estimate the timing of each mineralization related to the host rocks and to discuss their implication to tectonic setting and metallogeny in the northwestern Vietnam. Detailed geological, geochemical and mineralogical data were given by the Department of Geology and Minerals of Vietnam (2000). This interpretation is supported by field relationships, magmatic petrographic and isotopic data, and theoretical considerations. The distribution of mineralization in NWVN reflects several events of magmatism, tectonism, and metamorphism.

### **7.1. Mineral deposits**

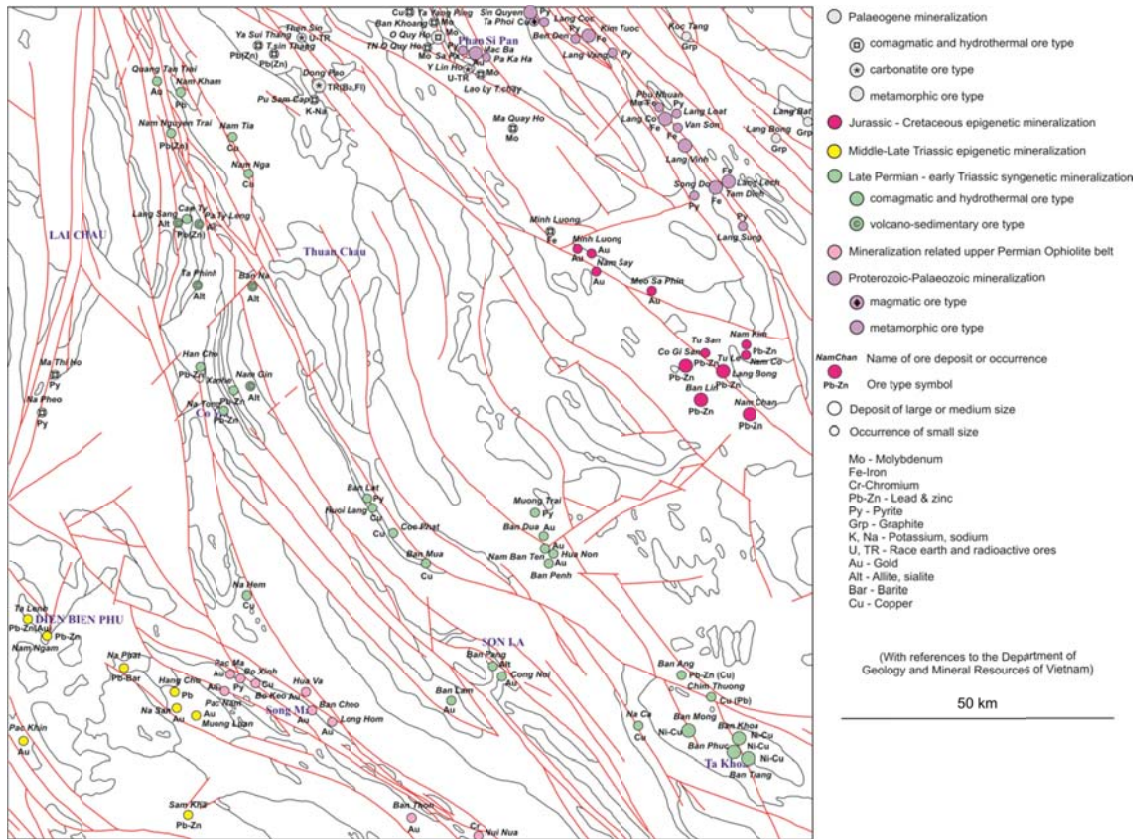


Fig. 7.1. Mineral deposits distribution map of the NWN

The main types of deposits the author wish to draw attention to, are as follows.

### 7.1.1. Iron

Seven iron ore deposits and occurrences have been registered, namely Kim Tuoc, Phu Nhuan, Lang Co, Van Son, Tam Dinh, Lang Lech and Minh Luong. They occur mainly in the Sinh Quyen metamorphic rocks and west Ye Yen Sun granite rocks, respectively.

Most of the iron ore mineralization is metamorphic type deposit except for the Minh Luong occurrence. They are formed in the contact zones between Proterozoic metamorphic sedimentary rocks of the Sinh Quyen Formation and Proterozoic diabase-gabbroic intrusion of the Bao Ha complex. These ores have seam shape with various sizes, from some meters to thousands meters in length, less than 1 to 14-15m in thick. The mineral assemblage comprises magnetite, minor hematite, pyrite and pyrrhotite; non-ore mineral is quartz. Iron contents varies from over 20 to 50% (Tran Van Tri, 2000).

The Minh Luong iron ore occurrence is situated in the Phan Si Pan-Song Hong structural zone and hosted by Palaeogene granites. Ore minerals consist mainly of hematite and pyrite. The thickness of the ore bodies reaches 1.5m, stretching discontinuously on 4-5 km. The Fe content reaches over 60%; the ore occurrence is associated with the west Ye Yen Sun granite massif. One suggest that may be it formed in relation to immediate sources of igneous accumulations, they can be arranged in comagmatic genesis of syngenetic type.

### **7.1.2. Chromium**

There are two chromium occurrences in the Thanh Hoa province, both located in the Song Ma zone (one of them is not shown in Figure 7.1 because it's situated outside the investigated area), namely Nui Nua and Lang Mun. They occur in the Nui Nua ultramafic rocks. The chromium mineralization is categorized into a podiform type hosted by serpentinized peridotite (Nguyen Van Chien, 1963). The ore occurs as chromian spinel concentrations (chromitite) in forms of lenses 3-4.5m wide and 10-15 m long. The ores have been exploited on small scale. Ore grades vary from 29.83 to 33.98 Cr<sub>2</sub>O<sub>3</sub>, 9.06 to 9.89 Fe<sub>2</sub>O<sub>3</sub>, 0.01 to 0.03 Ni, 0.017 to 0.05 Cr in wt % and Cr<sub>2</sub>O<sub>3</sub>/FeO ratio larger than 2.5. The classification for formation of mineral deposits (Economou & Naldrett, 1984; Naldrett, 2004; Misra, 1999) suggest that the Nui Nua chromium hosted by Nui Nua serpentine body formed as concentration of ore minerals as direct consequence of magmatic crystallization (orthomagmatic origin). However, the podiform chromites could be formed by the interaction between mantle harzburgite and an exotic magma (Arai, 1997). The Nui Nua ultramafic complex allows unraveling history of the emplacement and cooling of hosted pluton. It contains sulfide liquid which was extracted from a sulfur-saturated mafic magma at late stage of its crystallization.

### **7.1.3. Copper**

Eighteen copper mineralization sites have been discovered. The host rocks are Proterozoic metamorphic rocks of the Sinh Quyen, Carboniferous-Permian carbonate of the Ban Pap, Permian basalt of Vien Nam formations, and Ban Xang ultramafic complex, and sometimes Devonian limestone of the Da Dinh, Cha Pa formations.

Based on the chemical and mineral composition of copper mineralization, four types of mineralization have been recognized, forming major ore deposits: (1) nickel-copper (Ni-Cu-PGE); (2) copper sulfide; (3) native copper; and (4) copper, copper-gold related to metamorphic rocks.

*First and second ore types* are distributed in the Song Da zone and hosted by Permian Ban Xang ultramafic rocks and Vien Nam mafic effusives. Four small deposits of first ore type have been registered, namely Ban Phuc, Ban Khoa, Ban Trang, Ban Mong. Most of the copper deposits occur in the confines of the Ta Khoa anticline, closely related to Permian ultramafic intrusions of Ban Xang complex. The mineral composition of this ore type is relatively complex. The ore contain mainly pyrrhotine, magnetite, pentlandite, chalcopyrite, and pyrite and in minor quantities sphalerite, galenite, nickeline, skutterudite, mawsonite, rammelsbergite, kremnerite, violarite, cubanite, ilmenite, etc. Mineralized zones depend on the size of intrusive bodies. These zones form bodies of compact or disseminated ores at the bottom or in fixed position within intrusive bodies. In the hardening process, the ores could penetrate the surrounding rocks or the intrusive massif itself forming vein-shaped bodies.

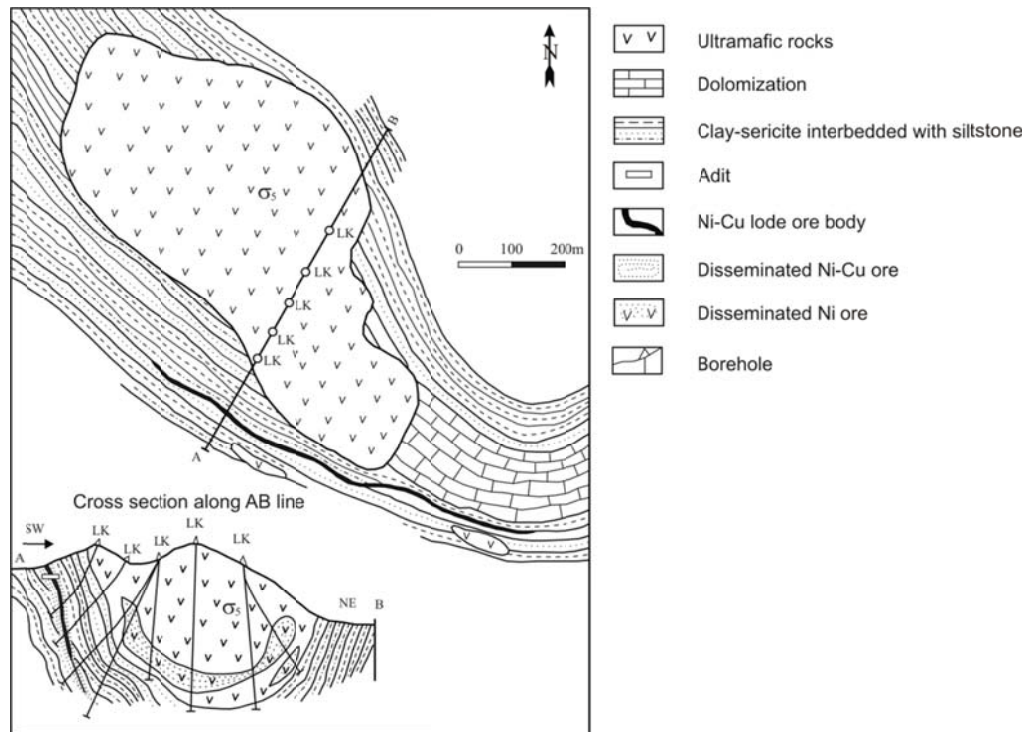


Fig. 7.2. Geological plan, Ban Phuc Ni-Cu ore mine (after Ha Phat Vinh & Du Khai Co, 1961)

Nature and distribution of two deposit ore types at Ban Phuc district can be explained as follows: The first one is disseminated sulfide deposit; nickel-copper mineralization associated with the Ta Khoa ultramafic intrusion. These deposits resemble the ores known from the Thompson Nickel Belt in Manitoba, Canada (Leighton, 2003). Mineralized layers concentrated near the base and walls of the ultramafic intrusions are of primary origin, due to separation of an immiscible sulfide melt at the base of the intrusion due to its high density.

Second Ban Phuc ore type is massive sulfide vein deposit. Massive Ni-Cu sulfide veins and their envelopes of disseminated mineralization are located in a shear zone developed in metasedimentary rocks in the foot wall of Ban Phuc ultramafic intrusion. The massive sulfide ores have been derived from a pool of immiscible sulfide melt expelled from the ultramafic intrusion into the shear zone (Glotov & Polyakov, 2001; Ban Phuc Company, 2007).

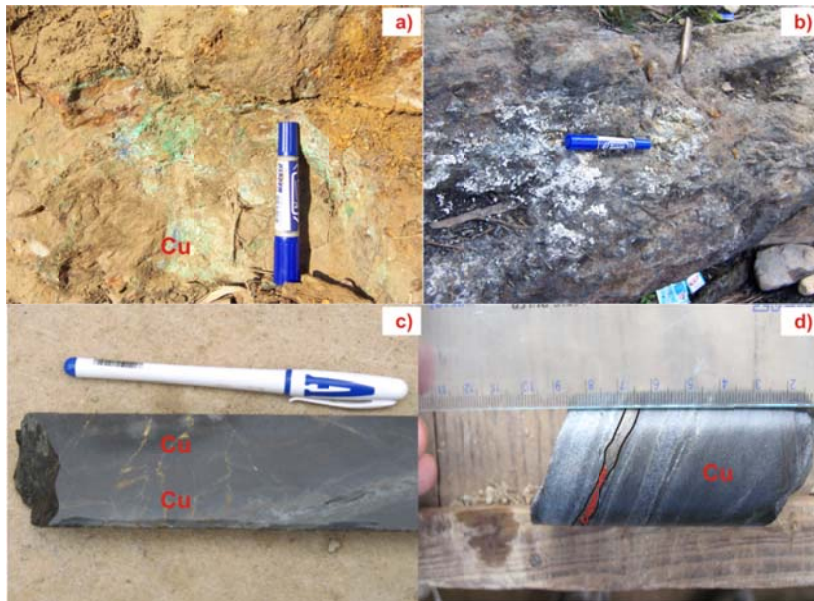


Fig. 7.3. a) Copper manifestation in the Ban Phuc area; b) Zone of sulfur released from sulfur bearing ultramafic rocks; c) Copper veins in core sample of ultramafic rocks; d) Copper ore veins in accordance with host rock indicated its syngenetic the Ban Xang ultramafic rocks.

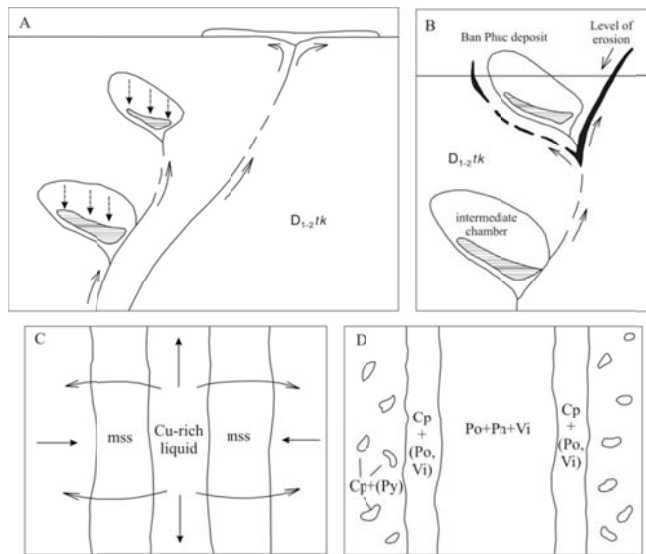


Fig. 7.4. A schematic diagram illustrating a succession of processes of ore formation for the Ban Phuc deposits (Glotov & Polyakov, 2001).

Note:

A - Intrusion of Ban Xang ultramafic melt toward the surface with the formation of subvolcanic chambers and concentration of sulfide liquid near the bottom (shaded).

B - Formation of veined orebodies, with a sulfide melt supplied from an intermediate chamber.

C - Fractional crystallization of the sulfide liquid with an Mss (monosulfide solid solution) cumulates formed along the walls of the vein and concentration of a residual sulfide melt in its central part.

D - Distribution of ore types in the veined orebody after solidification.

*Another copper sulfide ore type* occurs in Permian Vien Nam mafic effusives. Ore mineralization developed as veins or vein zones, the vein zones usually coincide with crushed and compressed zones of strongly altered effusives (propylitization). These ores have lenses shape with small size; coincide with the plane of host rocks. Ore minerals consist of chalcopyrite and pyrite; in minor chalcosine, covellite, malachite, azurite, bornite, etc. The copper content in the ores varies from 0.2 - 0.3 to around 10%, in average 1-2%. Beside, copper

is main useful component, there still is lead-zinc with sometimes high content, and the ores have been considered as polymetals.

Existing forming conditions of Cu-Pb-Zn mineralization analysis (Nguyen Van Nhan, 2005) of fluid inclusion and homogenization temperature in the Hoa Binh and adjacent areas (Song Da zone), support the concept of a magmatic component in the hydrothermal fluids of the deposit type.

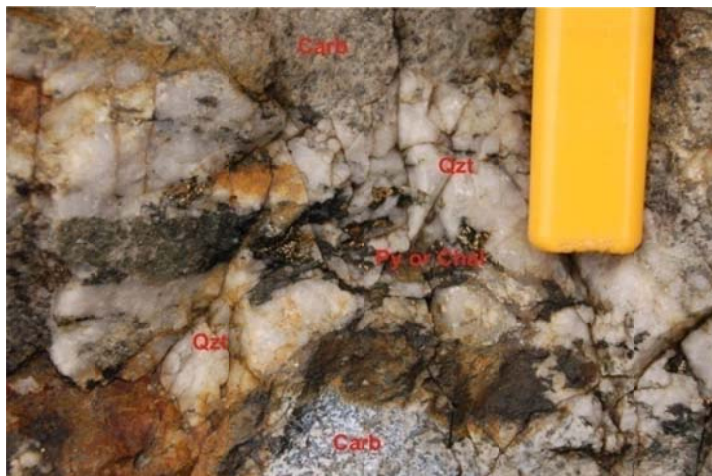


Fig. 7.5. Pyrite or Chalcopyrite mineralization bearing quartz vein and located in the Song Da zone, near Son La province

*Third ore type* is represented by two native copper ore occurrences, namely Na Ca and Bo Keo located in the Song Da and Song Ma zones. They occur in Permian mafic effusives of the Vien Nam and Huoi Hao formations, respectively. Mineralization is concentrated in the crushed, compressed and altered zones of basalts, and form ore bodies of 10-15 m in width with unclear boundaries. Ore mineral consists of native copper in the form of plates with the thickness of less than 1 mm to some centimeters; they are developed in the plane of compression or within fissures of the host rocks. Beside these mineralized zones, copper bearing quartz-sulfide veins also have been met. Ore content varies in different occurrences and different places of the orebody. Certain characteristics common to the area suggest a close genetic relationship between native copper and mafic effusive.

Moreover, the ideas on the native copper origin of Cornwall (1956) suggest that the Na Ca and Bo Keo native copper formed as reduction of primary copper sulfides by later hydrothermal solutions and belong to epigenetic concentrations of native copper that are in lava sequence adjacent to permeable zone.

*Finally, the fourth ore type is related to Proterozoic metamorphic rocks:* Four occurrences and a deposit are discovered, namely the Lang Nhon, Lang Phat, An Luong, Ta Yang Ping and Sin Quyen. The most promising seems to be the Lao Cai area, where the Sin Quyen deposit, found in the 1960s is located. Its mineralization is represented by lenses, several meters thick and a few hundred meters long, of magnetite, chalcopyrite, pyrrhotite, pyrite and orthite in the hornblendite dikes. Ore grades vary from 0.5 to 2.5% Cu, about 2 g/t Au and some nickel. The area potential is estimated at 200,000 t of copper.

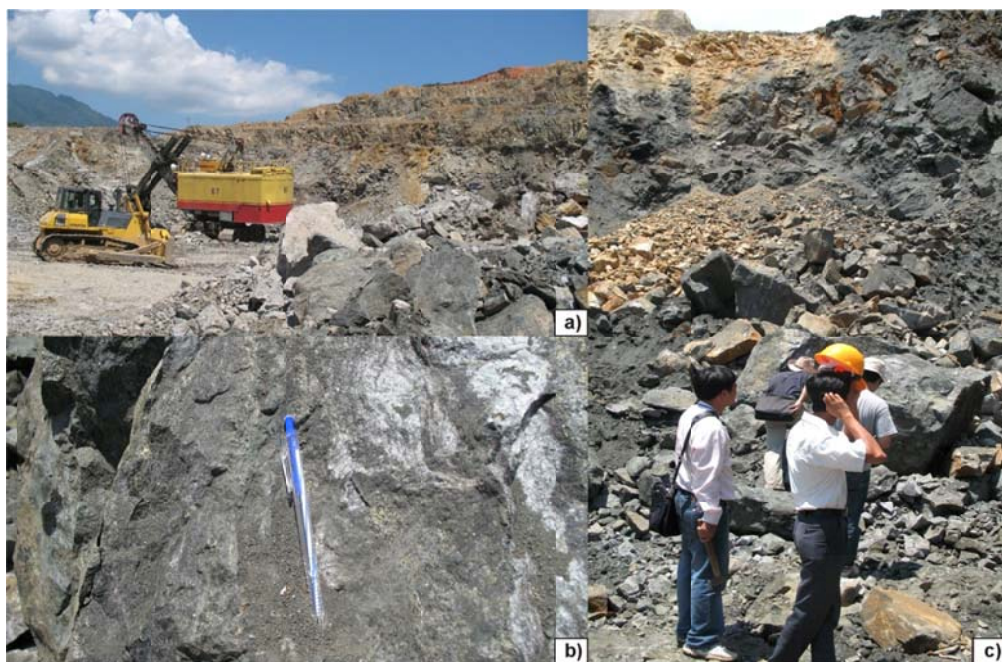


Fig. 7.6. The Sin Quyen copper mine - Bat Xat Lao Cai: (a) - Quarry copper; (b, c) - Copper ore disseminated in metamorphic rocks of the Sinh Quyen Formation

Generally, the structure of mining area is trending in NW-SE direction and is controlled by the Red River fault zone in the North. Irregularly metamorphic zone is made up of two-mica schist, biotite plagiogneiss, biotite and biotite-garnet schist, amphibolite and quartzite lenses, biotite-garnet bearing quartz-graphite schist, graphite quartzite, biotite plagiogneiss, garnet bearing quartz - two mica schist. The orebodies occur in beds of host rocks and their boundaries are usually unclear. Near the Sin Quyen area, the Po Sen granite massifs are discovered and intruded Proterozoic metamorphic rocks. The relations suggest that copper mineralization was support by products of metamorphic process and is closely related to tonalite-plagiogranite association.

Recently, an investigation of Cui *et al.*, (2005) showed that the Sin Quyen or Shengquan (Chinese name) mine is a large copper deposit characterized by an association of Cu-Co-Ni-REE that occurs in the same mineral belt as Longbohe in Yunnan province, China. It is therefore concluded that there is good potential for discovery of a large, Sin Quyen-style copper deposit in western Longbohe. It opens the opportunity for prospecting of copper mineralization along the Ailao Shan-Red River fault zone.

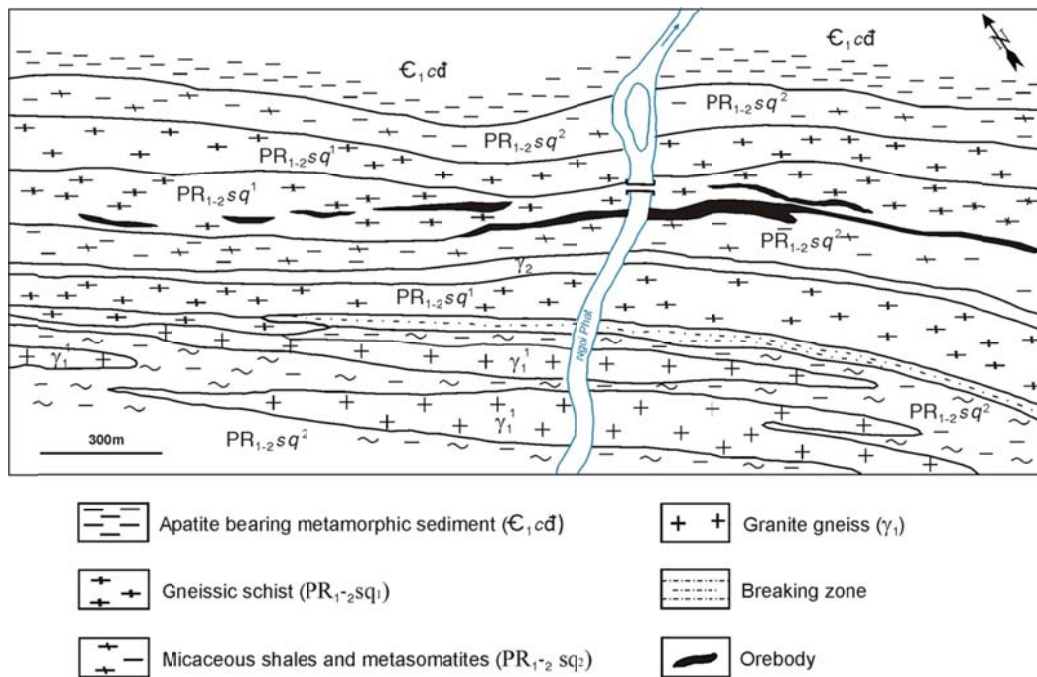


Fig. 7.7. Geological plan, Sin Quyen copper mine, Lao Cai province (after Ta Viet Dung, 1968)

Another copper occurrence is also located in the Phan Si Pan zone, namely Ta Phoi. Copper mineralization is hosted mainly by Lower Proterozoic Po Sen granites and forms stocked, lensed, disseminated ore type; sometimes occur as dispersed veinlet. The age of Ta Phoi copper occurrence in the Phan Si Pan can be dated as Early Palaeozoic based on the age of Po Sen granites. Ore minerals content is simple, ore consists mainly of chalcopyrite, cubanite, pyrite and a little molybdene, magnetite. Ore contents include Cu: 0.01 - 9.18%; in average: 1.50% (in the trenches). Beside copper as main useful component, there still is Mo, Au and Ag.

Dinh Van Dien (2005) pointed out that ore-forming processes were divided into three hydrothermal stages as follows: quartz magnetite, quartz-pyrite-molybdene, and quartz-chalcopyrite - cubanite and fluid inclusion data gave the value of 150 - 399°C. According to the research on the Ta Phoi occurrence, copper orebodies in the Phan Si Pan zone are associated with the Po Sen porphyritic intrusive rocks and with the fluids that accompany them during the transition and cooling from magma to rock. Therefore, Ta Phoi copper occurrence can be classified as the copper porphyry type. This problem is worthy to pay attention in further research.

#### 7.1.4. Lead-zinc

A variety of not very rich in either metal lead-zinc ore sites (twenty one) were found in four areas in the NWN. Most of them are located in the Sam Nua, Song Da and Tu Le zones and are hosted by the late Devonian carbonate rocks of the Ban Pap, Carboniferous-Permian Bac Son formations, and Triassic granitoids of the Phia Bioc, Song Ma complexes as well as Triassic sediments of the Tan Lac, Dong Giao and Suoi Bang formations.

*In the Sam Nua zone*, five Pb-Zn ore occurrences occur in Triassic granite intrusions of the Phia Bioc, Song Ma complexes, namely Ta Lenh, Nam Ngam, Na Phat, Hang Cho, and Sam Kha. The ore veins formed and developed in the cataclastic and alteration zones of some meters in width and over 2000 m in length. They are trending in the NE-SW direction, their thickness is below 50 cm. Ore minerals consist of sphalerite, galenite, minor chalcopryrite, pyrite and pyrrhotine. Ore grades vary from 0.02 to 12% Pb, 0.01 to 14.71% Zn, and 0.001 to 0.03% Cu. In the Sam Kha, a lead-zinc ore occurs, bearing quartz vein penetrating Triassic sandstone and calcareous siltstone of the Suoi Bang Formation. It is important to note that in the Pac Khin area, there is an ore vein of 1 m thick, of N-S direction and dipping southwestward in coincidence with the fault in the Song Ma granites, surrounding by coal-bearing beds of the Suoi Bang Formation. Stratigraphical relationship suggests that the ore occurrence was epigenetic; it perhaps was produced by hydrothermal fluids from late magmatic activity of the Song Ma granite intrusions.

*In the Song Ma zone*, there are known six lead-zinc occurrences, namely Nam Kham, Nam Nguyen Trai, Can Ty, Han Cho, Na Tong and Xa Nhe. Lead-zinc ores occur in Devonian carbonates or terrigenous sediments interbedded with carbonates of the Ban Pap Formation. Host rocks are usually altered to dolomite, and crushed. Mineralization is dominantly within the disseminated and replacement ore, or fills up fissures in the host rocks. Ore minerals compose of galenite, sphalerite, pyrite, chalcopryrite, pyrrhotine, tetrahadrite and native gold. Ore grades vary from 0.1 to 12% Pb and 0.3 to 5.6% Zn; accompanied by Cu and Cd (low content). It is possible that the full range of ores, from exhalative sedimentary to Mississippi valley type occurs. Permian Cam Thuy and Vien Nam mafic effusives are located near the ore occurrences, it suggests an origin of the hydrothermal ore fluids.

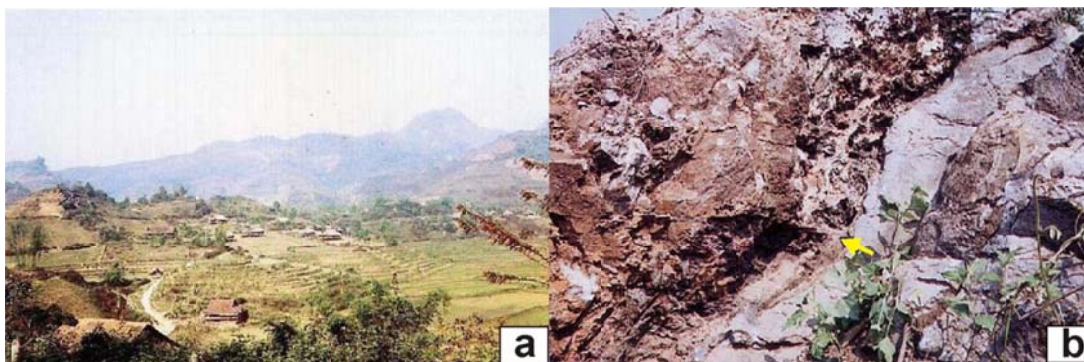


Fig. 7.8. a) View of Na Tong - Han Cho lead-zinc ore occurrence; b) Outcrop of Lead-zinc ore in Na Tong-Han Cho ore occurrence

*In the Song Da zone*, three occurrences have been registered, namely Ya Sui Thang, T.sin Thang, and Ban Ang. They occur in Triassic terrigenous sediments of the Tan Lac Formation, except for the Ban Ang occurrence, which occurs in Permian mafic effusive of the Vien Nam Formation. The Tan Lac Formation is intruded by leucocratic syenite and granosyenite of the Pu Sam Cap complex, which cause hydrothermal alteration of the host rocks. Feldspathization, quartzification, sericitization, chloritization occur there. Mineralization usually forms ore veins of small thickness, penetrating rocks of different composition. Ore mineral composition

consists of galenite, sphalerite, pyrite and chalcopryrite. The lead-zinc content in ore varies from few percents to nearly 40%.

Based on the mineral association, host rocks, shape of orebody and hydrothermal alteration, Tran Xuan Duc (1963) and Nguyen Ngoc Lien (1990) considered that most of the lead-zinc mineralizations in the Song Da and Song Ma zones represent mesothermal and epithermal genesis. The formation of mineralization is associated with granite intrusion of the Pu Sam Cap complex, and basalt rocks of the Vien Nam Formation.

*In the Tu Le zone*, the lead-zinc deposits and occurrences form 3 large bands of NW-SE direction; each band has a length of 10-20 km, a width of 2-6 km. These ores are often located in hydrothermal quartz veins, penetrating Cretaceous felsic effusives of the Tu Le-Ngoi Thia complex and volcano-terrigenous sediments of the Tram Tau Formation. Main mineral compositions consist of galenite, sphalerite, a little pyrite, chalcopryrite; non-ore minerals are quartz, dolomite, calcite, etc. Veins, 0.5-1m in thickness, up to 600 m in length (Co Gi San deposit), consist principally of the silver-bearing galena (4-5 kg/t Ag). They are hosted in the slightly metamorphosed, volcano-sedimentary rocks of Triassic and Lower Jurassic. Ore grades vary from 4 to 6% Pb and 1 to 2.5% Zn. Most of the lead-zinc mineralizations belong to the hydrothermal type, formed chiefly in Late Mesozoic (Do Hai Dung, 1990).

Thus, syngenetic and epigenetic mineralizations were distinguished within NWN lead-zinc ores. First one perhaps was formed in epithermal to mesothermal process in an exhalative environment of Phia Bioc, Song Ma granitoids, or was associated with Pu Sam Cap and Tu Le-Ngoi Thia subvolcanic rocks. The second one perhaps was formed in basinal brines dominated carbonate rocks, probably it was related to submarine volcanic process within Cam Thuy Formation during Late Permian - Early Triassic times. Perhaps faults also played a key role in providing conduit for the hydrothermal fluids to site of mineralization (Misra, 1999).

#### **7.1.5. Gold**

Gold has been mined in Vietnam since ancient times. At present, its production is probably about 1 ton/year, part of which is produced by the local population. Nineteen gold mineralization sites are known, they are located mainly along the Sam Nua, Song Ma, Song Da and Tu Le structural zones with primary genetic types. The gold ore occurrences are distributed in various rocks and quite prospective.

*In the Song Ma zone*, gold mineralizations can be divided into 2 groups. First group is located in terrigeno-metamorphic rocks; there are 4 occurrences, namely Pac Ma, Ban Cheo, Lom Hom, and Ban Lam. Gold ore occur in quartz-sulfide veins and forms crushed and crumpled zone, or in the bedding surface of Upper Permian quartz-sericite schist of the Nam Ty and early Devonian Nam Pia formations, sometime in Cambrian clay shale of the Song Ma Formation. The common ore bodies are lenses including nest or string types and veins. Mineralized zones and ore bodies are generally composed of many quartz veins ranging from few mm to tens cm in thickness. Main sulfide minerals consist of pyrite, arsenopyrite, galenite, chalcopryrite, etc. Gold content reaches from 0.3 to 2.83 g/ton, sometimes reaches 4 g/ton.

Second group occurs in basalt and diabase; there are 3 occurrences, namely Hua Va, Cong Noi and Ban Thon. Gold mineralization has generally large distributive area with high Au content, and forms mineralized zones or independent ore bodies. Gold ores are associated with Permian Cam Thuy basalt, and Huoi Hao metabasalt. Mineralized zones or ore veins stretch generally on some tens to 1000 m with a thickness of 0.2 - 6 m, they are also composed of many micro-veins of quartz-sulfide-gold or of lenses, nests and so on. Alterations of vein side consist of quartzification, sericitization, chloritization and epidotization. Sulfide minerals are pyrite, pyrrhotine, chalcopyrite, arsenopyrite and chalcocite. Gold content reaches from 0.3 to 2 g/ton. This group bears characters of volcanic massive sulfide deposit type (VMS).

Generally, gold mineralization in the Song Ma zone is associated with late Palaeozoic shales and Permian basalts; the host rocks for the gold deposits are Lower Proterozoic metamorphic rocks intruded by late Palaeozoic granitoids. Gold mineralization is distributed in quartz brecciated zone situated in the destruction zone of sericite schist of the Song Ma Formation. Sometimes, it is distributed in coincidence with large fault. For this reason, gold ore types are related to basalt rocks of the Huoi Hao, Cam Thuy formations, and were formed after the last effusive phase of the Huoi Hao, Cam Thuy formations.

*In the Sam Nua zone*, gold mineralization occurs in felsic intrusives, there are 4 occurrences, namely Pac Khin, Pac Nam, Muong Luan and Na San. Gold mineralization is distributed along crushed zones in Permian - Triassic granitoids of the Song Ma and Dien Bien Phu complexes. Gold ores commonly forms ore bodies 100-300 m long, 2-5 m up to 70-80 m wide. Ore minerals are pyrite, arsenopyrite, chalcopyrite, galenite, sphalerite and antimonite, sometimes cinnabar, hematite (Pac Khin). Gold content reaches from 0.2 to 6 g/ton (Muong Luan); locally reach from 0.5 to 2 g/ton (Pac Nam). Most of the ores are associated with Permo-Triassic of the Song Ma, Dien Bien Phu granite rocks and Permian Cam Thuy volcanic rocks and treated as a byproduct of exploitation of Cu-Pb-Zn ore types.

*In the Tu Le zone*, there have been known three occurrences, namely Minh Luong, Nam Say, and Meo Sa Phin; they are situated in the middle of the Tu Le volcanic zone near the Phan Si Pan range. Gold mineralization occurs in Cretaceous porphyritic rhyolite rocks of the Phu Sa Phin complex. Gold ore bearing quartz-sulfide veins intruded Cretaceous effusive, such as orthophyre, quartz orthophyre of the Tu Le - Ngoi Thia complex and volcano-sedimentary beds of the Tram Tau Formation. Hydrothermal alterations *of the surrounding rocks* are commonly chloritization, sericitization or pyritization. Gold content commonly reaches from 0.7 to 11.2 g/ton, somewhere gold is accompanied by Pb, Zn and Cu. Both gold ore veins and rhyolite rocks of the Phu Sa Phin complex intruded volcanic rocks of the Tu Le subcomplex. Therefore, gold ores are associated with rhyolite rocks of Phu Sa Phin complex. The stratigraphical relations indicate that gold ores may be supplied by hydrothermal fluids from granitoids of Phu Sa Phin complex.



Fig. 7.9. a) Gold bearing quartz vein in Minh Luong area;  
b) Come back from Saphin gold deposit.

*In the Song Da zone*, four gold ore occurrences were discovered, and developed mainly around the Pi Toong - Muong Trai area, namely Ban Dua, South Ban Ten, Hua Non, Ban Penh. Structure of the area is dominated by NW-SE and sublongitudinal trending faults. Gold mineralization was introduced through numerous extension fractures, and located in the cataclastic and crushed zones, or schistose zone of terrigeno-carbonate beds of the Muong Trai Formation, as well as in Permian mafic effusive of the Vien Nam Formation trending parallel to the fault trends. Mineralized zone varies from 10 to 30 m in thickness, and some hundreds meters in length, somewhere reaches from 70 to 100 m in thickness and over 1000 m in length (Ban Penh). Hydrothermal alterations consist mainly of quartzification, sericitization, chloritization, carbonatization, kaolinitization and adularization. Ore minerals are pyrite, chalcopyrite, native gold, minor bornite, hematite; rarely met galenite, sphalerite, arsenopyrite, malachite, pyrrhotine and chalcocite. Gold content varies from 0.4 to 3.4 g/ton (Ban Penh, south Ban Ten); and from 1 to 57 g/ton (Hua Non, Ban Dua). Beside gold mineralization, some elements as Pb, Zn, As, and Cu are usually accompany ores.

Nguyen Dac Lu (2005) by using experimental research argued that the gold mineralization in the Song Da zone (Doi Bu, Suoi Chat) have been formed at intermediate depths (120°-370°C, high pressure 1.1-2.5 kbar), the salinity of the fluids (total dissolved solid constituents in wt %) varies from 4.7 to 13.8%. These parameters allow us to arrange the ore type in mesothermal genesis (Misra, 1999).

Gold ore mineralizations in the NWVN are hosted by sediments of the Song Ma, Nam Pia formations, associated with mafic effusive of the Huoi Hao, Cam Thuy, Vien Nam, Nam Ty formations and granitoids of the Song Ma, Chieng Khuong, Dien Bien Phu, Tu Le, Pu Sam Cap complexes. Moreover, gold mineralization is often located in the cataclastic zone which pointed out that the ore-forming process is closely related to developed faults. Gold is also treated as a byproduct of exploitation of Cu-Pb-Zn ore deposit type.

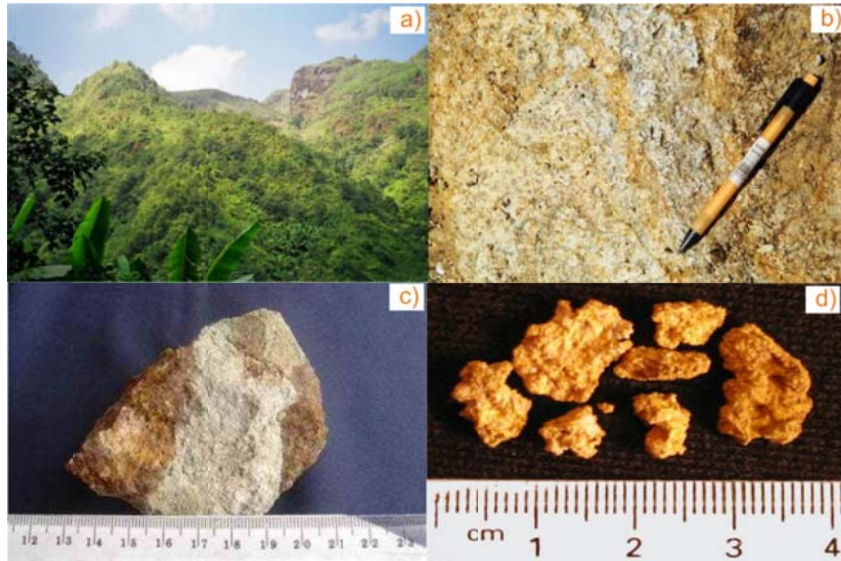


Fig. 7.10. Gold mineralization in the Pu Sam Cap area, (a) Pu Sam Cap mountain, (b) Altered volcanic breccia-agglomerate, (c) Finely disseminated pyrite in zone of silicic-argillic alteration, (d) Gold recovered from Crater mountain (Photographs from Howell *et al.*, 2007)



Fig. 7.11. a) Upper Nam Dich drill core, alteration and mineralization in syenite; b, c) Mineralized breccia, Can Ho mine (Photographs from Howell *et al.*, 2007)

### 7.1.6. Allite - siallite

Formerly, the described allite-siallite occurrences were attributed by different geologists to bauxite; however the analytic results have been shown that the silica modulus of the ores is low, the  $Al_2O_3$  content is low, at the same time that of  $SiO_2$  and  $Fe_2O_3$  is high, so the ore do not answer the standard of bauxite ore, but they have been considered as high-aluminum raw material for fireproof material industry.

Six allite-siallite ore occurrences have been registered, namely Ta Phinh, Bac Na, Nam Gin, Ban Pang, Lang Sang and Pa Ty Leng. Allite-siallite mineralization is concentrated in margin of the synclines formed by Permian mafic effusive, lying unconformably upon

Carboniferous to Lower - Middle Permian sediments. Ore bearing Permian mafic beds of the Cam Thuy Formation forms ore seams 1-5m thick (in average 3 m), extending discontinuously on 1-10 km. The ore seams contain usually interbeds of non-ore rocks. Main ore mineral is hydrargillite, in minor quantity occur diasporite, gibbsite, boehmite; in addition, leucosilite and some other minerals. Ore grades vary from 19.95 to 35.36%  $Al_2O_3$ , 5.1 to 48.26%  $SiO_2$ , and 9.13 to 40.89%  $Fe_2O_3$ , 0.74 to 5.25%  $TiO_2$ , and 0.06 to 0.18%  $P_2O_5$ .

Allite-sialite ore mineralizations occur in Permian basalt of the Cam Thuy, and limestone of Yen Duyet formations with seam shapes. They are composed mainly of hematite, goethite, gibbsite, boehmite and diasporite. One suggests that the ore type is associated with volcano-sedimentary origin of the Cam Thuy Formation; and belong to the allite-sialite types, but locally reaching characteristics of the bauxite.

### **7.1.7. Molybdenum**

There are five registered molybdenum occurrences and deposit, namely O Quy Ho (deposit), Ban Khoang, TN O Quy Ho, Ma Quay Ho, La Ly Tchay. Most of molybdene deposits and occurrences are distributed in developmental field of Proterozoic metamorphic rocks of the Sinh Quyen and Suoi Chieng formations, and along their contact with the Ye Yen Sun subalkaline intrusive. They are situated in the eastern slope of the Ye Yen Sun range, stretching on about 40 km in NW-SE direction from Muong Hum through Sa Pa to Lao Cai.

Molybdenum mineralization is of large scale, with the worth attention content. Molybdene ores occur in quartz small veins or vein nets, or are disseminated in the contact zone between the Ye Yen Sun subalkaline intrusive and metamorphic rocks of the Sinh Quyen Formation. The penetration of Ye Yen Sun alkaline granites form ore bodies with the thickness varying from 0.45 to 4.42 m, the length from 150 to 1408 m. Ore minerals are molybdene, chalcopyrite, magnetite and hematite. The Mo content varies from 0.09 to 0.4%, locally; it reaches up to 53.48% (O Quy Ho). Molybdenum mineralization belongs to quartz-pyrite-molybdene and copper-molybdene ore types (Nguyen Van Nhan, 1988; 2008). From recent studies, granite rocks of the Ye Yen Sun complex can be separated into two different magmatic massifs (Tran Tuan Anh, 2002): The west of O Quy Ho granite massif (35Ma) and the east of O Quy Ho granite massif (72-41 Ma). In the east granite there have been met the veins of leucocratic aplitic granite or quartz veins containing molybdenum mineralization which may be the last products of the west granite. This one proves that the west granite was formed later than the east one. The fieldwork results indicated that molybdene quartz veins, molybdenum sulfide quartz veins and fluorite molybdene sulfide quartz veins in O Quy Ho and Ban Khoang deposits are likely related to small porphyritic plutons, granite aplite and granite pegmatite. They intrude gneissic granite of east O Quy Ho granite massif (Fig. 5.12). A reasonable interpretation of molybdenum mineralization is that it is genetically related to west O Quy Ho granite massif.

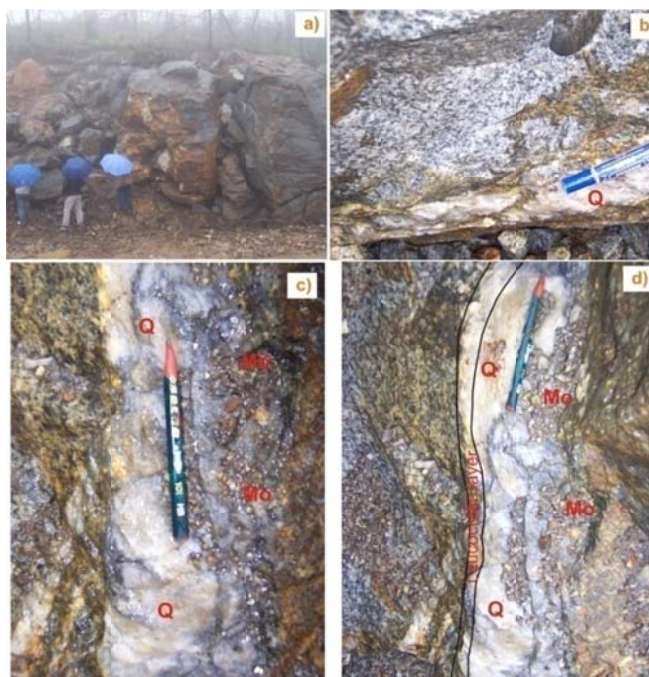


Fig. 7.12. The outcrop, 50m to Bac waterfall; a) Granite Ye Yen Sun block; b) Molybdenum mineralization disseminated in and quartz vein penetrated the granite block; c, d) Molybdene-bearing quartz vein in granite block

The problem solving Rb-Sr dating of the single grain pyrite from molybdene mineral association is carried out in the Isotope Geochemistry Laboratory - Institute of Geology and Geophysics Chinese Academy of Sciences. The resulted dating of single grain pyrite give value of 38Ma, it is also considered as time of forming molybdenum mineralization. Therefore, the result indicates a strong correlation to the west of O Quy Ho granite massif. Moreover, the  $(^{87}\text{Sr}/^{86}\text{Sr})_i$  ratio reaches around 0.70960 showing difference in comparison with surrounding rocks (Nguyen Trung Chi, 1999) (see appendix for detail). It indicates that a part of ore-forming fluids may be supplied from surrounding rocks, meteoric water and sources of material is relatively complex. The generation of the Mo-Cu deposits may be related to alkaline or subalkaline along the Ailao Shan-Red River shear zone, with the age of 34-36Ma. We can consider the O Quy Ho-Ban Khoang Mo-Cu deposit as a part of the metallogenic belt, and the ore type can be arranged in hydrothermal genesis of epigenetic type.

#### 7.1.8. Pyrite

Thirteen pyrite occurrences have been discovered; they are distributed mainly along the Song Ma, Song Da and Song Hong structural zones.

*In the Song Ma zone*, there are three pyrite ore occurrences, namely Ma Thi Ho, Na Pheo, and Bo Xinh. Most of pyrite mineralization is situated along the Dien Bien-Lai Chau fault zone, and occur in the crushed and tectonic contact zone between Proterozoic quartz-sericite schist, greenschist of the Nam Co Formation and Triassic sandstone, siltstone of the Lai Chau Formation, except for the Bo Xinh occurrence occur in Permian metabasalt of the Huoi Hao

Formation. Mineralization is developed as ore veins and lenses of some cm to 50-60 cm thick. Ore minerals are composed mainly of quartz and pyrite with the content of (%): S= 37.56-39.53, SiO<sub>2</sub>=4.68-13.86, As=0.09-0.3, P=0.003-0.018. Near the ore occurrence location, two gabbroid bodies were found and dated as 5Ma (Koszowska E., *et al.*, 2004). Possibly, the pyrite ore mineralization is formed as Ni-rich pyrite and chalcopyrite hydrothermal genesis that produces by gabbroic intrusions.

Located in the Bo Xinh area, pyrite ore is in the form of nests and lenses, hosted by greenschist and quartz-sericite schist of the Nam Ty Formation and associated with metabasalt of the Huoi Hao Formation. Pyrite mineralization is mainly developed in cataclazite zone of NW-SE direction and played a role cementing tectonic breccias, in some places; ore filled cracks and formed ore veins few meters thick.

Nguyen Ngoc Lien (1990) point out that pyrite mineralization cemented breccias of quartz and volcanic tuff; hydrothermal alterations are chloritization, sericitization, quantization, epidotization. It indicates a hydrothermal genesis of the epigenetic ore type.

*In the Song Da zone*, there are two pyrite occurrences, namely Muong Trai and Ban Lai. They are situated in both sides of the Song Da zone, respectively. Pyrite mineralization bearing brecciated quartz veins form a zone 50-60 m wide, over 1 km long and located in a fault of NW-SE trend. They occur in Triassic sandstone, siltstone of the lower Muong Trai Formation (Muong Trai) and in Permian mafic effusive of the Vien Nam Formation (Ban Lai). Small-grain pyrite is concentrated in compact veins or disseminated in the rock. Main ore minerals are quartz, pyrite; in minor quantity is goethite, malachite and azurite. Ore grades vary from 12.78 to 13.6% S, 0.03 to 0.62% Cu, 0.001 to 0.007% Pb-Zn, and 0.4 g/ton Au (atom absorption spectrometry analysis).

Together with copper, gold and lead-zinc mineralizations, pyrite ore in the Song Da zone is also formed by epithermal process during Permian-Triassic times. It also suggests that ore-forming processes of sulfides mineralization are at or immediately beneath sea floor and related to volcanic activities, precipitation and concentration of ascending hydrothermal ore forming fluids in the sea water. Both syngenetic and epigenetic ore types are present. The Ban Lai ore occurrence bears characteristics of volcanic massive sulfide deposits (VMS).

*In Song Hong zone*, eight pyrite ore occurrences have been found and investigated, namely Lang Coc, Ben Den, Lang Vang, Lang Loat, Van Son, Song Do, Lang Sung and Sa Pa. They form mainly accumulations of erratic boulders of ore, located usually along the fault lying between the Da Dinh, Sinh Quyen, and Cam Duong formations. In the area where primary ore has been found, it is in the form of veinlets and lenses, or disseminated in limestone or schists of cataclastic zone. Ore mineral composition is pyrite, chalcopyrite, galenite, pyrrhotite. Sulfur content varies from 6 to 20%, locally up to 36% (Lang Coc), 40% (Then Thau).

Generally, the pyrite ore types in Song Hong zone originated during metamorphose of the Sinh Quyen, Cam Duong sedimentary rocks (Tran Van Tri ed., 2000).

### 7.1.9. Potassium-sodium

Ore occurrence has been found recently in the Pu Sam Cap Mountain. Main mineral components are KOH and NaOH, they belongs to alkaline effusives of the Pu Tra Formation, which are composed mainly of trachyte and minette veins; besides, there is a little shonkinite within the Pu Sam Cap complex. Rhyolitic rocks of the Pu Tra Formation were derived from felsic volcanic magma containing relatively high quantities of sodium, potassium and are composed of more than 65% silica. They are distributed in long bands of NW-SE trend. Ore content reach 9% KOH, 7% NaOH (in average). Following that potassium-sodium mineralization is considered as syngenetic and related to alkaline rhyolite of the Pu Tra Formation.

### 7.1.10. Graphite

There are three graphite occurrences, namely Koc Tang, Lang Bat, Lang Bong, they are situated in the Song Hong zone, near Lao Cai area. The ores are found along shear zones within Precambrian metamorphic rocks that were intruded by granites and pegmatites of Palaeogene age. Graphite ore was developed as lenses, layer shapes of few meters to 6.5 m thick and some tens to 100m long, sometime disseminated in pegmatite massifs, which intruded biotite gneiss, and graphite-silimanite-felspate schist of the Ngoi Chi Formation. These pegmatite massifs are considered as Pu Sam Cap alkaline granite. One suggest that the organic matter within the Ngoi Chi Formation changed to graphite by thermal effect of metamorphic and pressure process related to intrusion of the Pu Sam Cap granite massif during Palaeogene. Carbon content in the lens shape ore is 12.45 wt % (in average), 17.43% A<sup>k</sup> (ash), and 5.5% V (volatile).

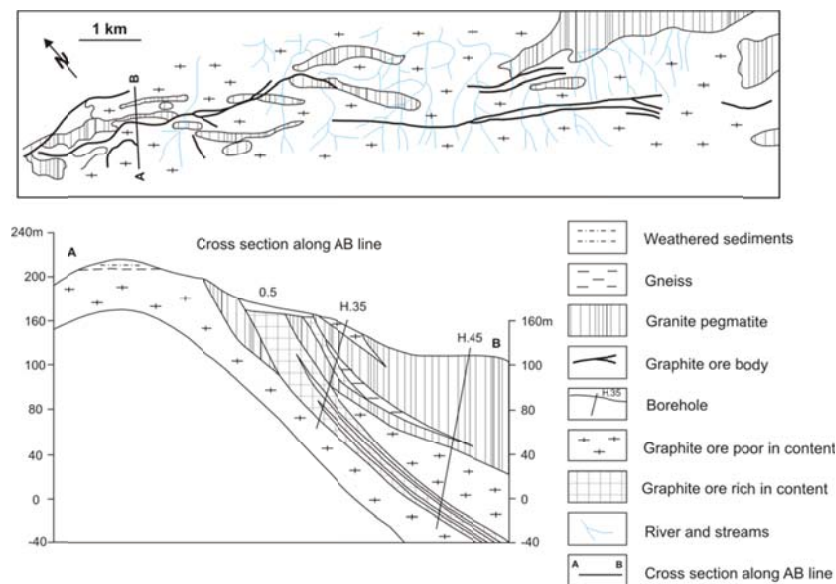


Fig. 7.13. Geological plan, Koc Tang graphite mine - Nam Thi area, Lao Cai province (after Le Thac Xinh, 1990)

### **7.1.11. Rare earth and radioactive ores**

There are many occurrences of rare earth and radioactive ores. They were discovered in the process of geological mapping and mineral prospecting at 1:200,000 scales, among them two deposits and one occurrence have been recognized, namely Then Sin, Dong Pao and Y Lin Ho, they are distributed in the western slope of Phan Si Pan zone.

Mineralization anomalies are situated in the two sides of Phong Tho fault separating the Phan Si Pan and Song Da zones. Strongly developed Palaeogene alkaline intrusions of the west Ye Yen Sun and Nam Xe - Tam Duong complexes are located east of the fault. West of the fault, there are small intrusions of the Nam Xe - Tam Duong and Pu Sam Cap complexes. The ores are hosted in a zone of crushed Carboniferous-Permian limestones and volcanics that were affected by metasomatism at the margin of Palaeogene alkaline volcanics and syenite. The ores consist of bastnaesite, parisite, barite and fluorite (Dinh Van Dien, 1990). The weathered zone, to a depth of 20 m, contains 4-5% of RE oxides and the primary ore is averaging 1.4% REO (mainly Ce, La, Nd, Pr, Y, but also Gd and Eu - 4% of REO), 1.1% Nb, 200-300 ppm U and 30% Ba. The reserves are huge: 7.8 Mt of REO, from which 1.7 Mt are proved at Nam Xe North alone (Le Thac Xinh, ed., 1990). Dong Pao deposit, situated 40 km S has about 7 Mt REO of a similar quality. It is hosted in a Palaeogene syenitic intrusion of the Pu Sam Cap complex (53 Ma).

The genesis of rare earth and radioactive ores, until now it is still hot topic of debate. Vlackov (ed., 1960) investigated the North of Nam Xe mine and explained mineralization as carbonatitic products, based on the stratigraphical relation. Dinh Van Dien (1976) also considered hydrothermal metasomatism genesis of this ores. Extensive collection of carbonatitic samples from the Nam Xe area allowed arranging them in the Pu Sam Cap complex (Nguyen Thi Ngoc Huong, 1994). Moreover, Bui Minh Tam (1995) affirmed presence of carbonatite of alkaline magmatic genesis in the Nam Xe-Phong Tho area. Tran Trong Hoa (1995, 1996) discovered some inclusions in pyroxene of dyke rocks; their compositions are in similarity with carbonatite solutions of the Dong Pao area. In addition, To Van Thu (1996) described carbonatitic dykes penetrating Upper Permian limestone at the Then Thau, Ban Mao areas; they have similar origin with minetic dykes, sonkinitite, etc. In summary, as was mentioned above we can consider carbonatite genesis the ores supplied by magmatic, and hydrothermal metasomatic sources (Manthilake *et al.*, 2008).

So far as we are concerned, the genetic model of the rare earth deposits can be understood as follows. The Triassic system in this region were subjected to the Indosinian orogenic movement and broken into a number of blocks by major faults and fracture systems trending mostly in the NW-SE direction. In the early Palaeogene, intrusions of alkaline magmas were initiated along the NW-SE trending fault systems at depth in the Lai Chau area and then formed syenite bodies. Magmatic melt at the bottom was enriched in volatile matters and then in rare earth elements as the vapor pressure increased. The high-pressure and high-temperature vapor enriched in volatile matters migrated through cooling-joints, formed in the peripheries of syenite bodies or through fractures formed in surrounding limestone. The vapor, as ascending through joints and fractures, was mixed with groundwater and cooled down to precipitate rare

earth minerals, barite and fluorite under certain pressure and temperature conditions, which resulted in formation of ore deposits in this area. The syenite body has been exposed on the surface as the limestone on the top was removed by erosion.

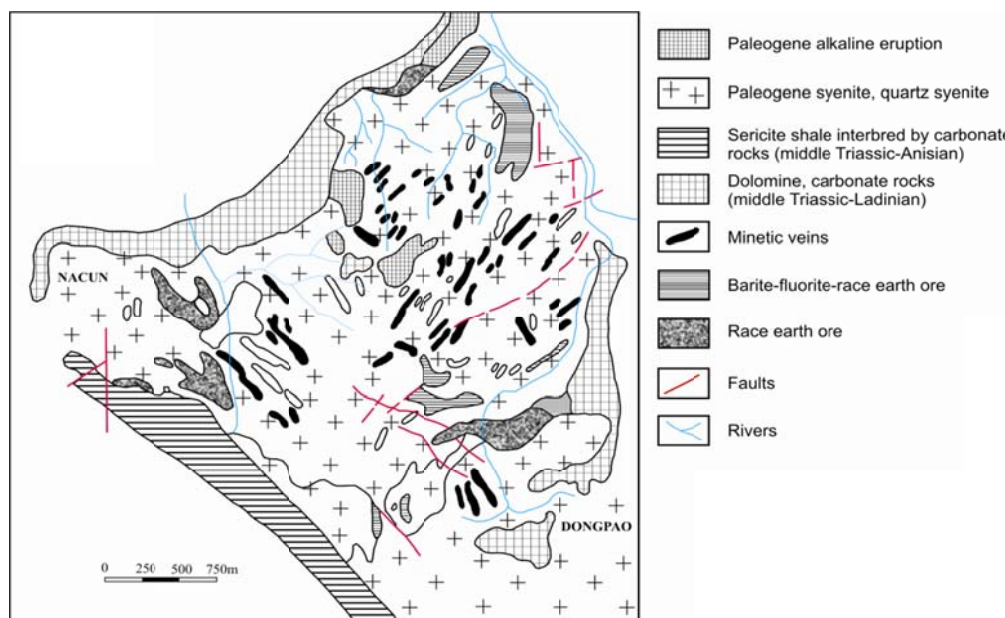


Fig. 7.14. Geological plan, Dong Pao Barite-Fluorite-Race earth mine, Lai Chau province (after Le Thac Xinh, eds., 1990; Nguyen Van Hoai, 1995)

## 7.2. Discussion

### 7.2.1. Mineralization related to geological setting

The interpretation of geological setting and its relation to mineralization obviously requires detailed study of the ore occurrence and its host rock in term of petrology, geochemistry, distribution, structural elements, forming temperatures, and the timing of mineralization. It is also important to realize that an ore occurrence is merely manifestation of special conditions that existed in the course of the overall geological evolution of the area. Obtaining an indication of ore potential of rocks formed in various settings and of the preferred location within the setting for mineralization provides the main aims of relating ore and mineralization to geological setting

#### 1. Mineralization related to lithologies

In NWNV area, the ore forming control, genesis and relationship between ore and stratigraphy is indicated through specific case studies of iron, copper, copper sulfide, lead-zinc, gold, allite-sialite, pyrite, and potassium-sodium mineralizations. Limestone of the Ban Phap, Bac Son formations, metamorphic rocks of the Sinh Quyen and Cam Duong formations as well as basalt effusions of the Huoi Hao, Cam Thuy and Vien Nam formations play key role as ore sources, enabling also studies of environment for syngenetic and epigenetic mineralization.

Representative of close relationship between ore and magmatic intrusion are specific cases of chromium, copper-nickel disseminated in ultramafic rock, iron, lead-zinc, gold, molybdenum, pyrite, rare earth and radioactive ore mineralization. Generally, the referred ores formed in relationship to magmatism activity. Chromium ore represent syngenetic segregation of fractional crystallization of peridotites from the Nui Nua ultramafic complex. Copper mineralization hosted by ultramafic rocks was formed in magmatic crystallization process of the Ban Xang ultramafic complex. Molybdenum and iron were formed in relation to the West Ye Yen Sun alkaline granite. Lead-zinc and gold are associated with the Dien Bien Phu, Song Ma granites. Other group of lead-zinc and gold mineralizations is hosted by the Tu Le-Ngoi Thia, Phu Sa Phin volcano-plutonic rocks. Pyrite is associated with Palaeogene gabbroids. Graphite, rare earth and radioactive ores are hosted by the Nam Xe-Tam Duong alkaline granite and Pu Sam Cap syenite.

Permian (260 Ma) Cu-Ni-(PGE) mineralization was revealed in ultramafic intrusions of the Song Da zone (Ban Phuc massif) (Tran Trong Hoa, 2005). The gold-sulfide ore mineralization includes Au-sulfide (gold-arsenopyrite), Au-Sb, Au-Sb-Hg mineralization, widespread in the Song Da zone (there are known as the Ban Dua, South Ban Ten, Hua Non, and Ban Penh ore occurrences). The Ar-Ar age of these ore associations reaches 252-228 Ma (Tran Trong Hoa, 2008), which is consistent with the Rb-Sr dating age reaching 257 Ma (Tran Trong Hoa, 1998) of the volcanic rocks in relation to the ore deposits. Thus, these ores are spatially associated with Late Permian volcanic rocks of the Cam Thuy and Vien Nam formations.

Palaeogene (38 Ma) molybdene mineralization was revealed in alkaline granite of the Phan Si Pan zone (the west of O Quy Ho massif). Ore deposits of the metamorphic types include iron, pyrite, graphite, copper and copper-gold. They are related to Proterozoic and Cambrian metamorphic rocks of the Ngoi Chi, Sinh Quyen, and Song Chay formations. These ores are located mainly in the Song Hong (Red River) zone.

Published data on SHRIMP U-Pb zircon of Tran Ngoc Nam (1998, 2006) and TIMS U-Pb zircon of Lan (2001) showed at least two metamorphic events that affected the Phan Si Pan-Song Hong zone (gneiss rocks of the Con Voi mountain range in particular). The first event took place in Neoproterozoic ( $838 \pm 45$ Ma) produce mineralization group consisting of pyrite, copper and copper-gold associated with granitoids of the Xom Giau, and Po Sen complexes as well as Bao Ha gabbros. The second event, in Cenozoic ( $30 \pm 11$ Ma), produced graphite mineralization.

## *2. Mineralization related to geological structures*

Geological structures including faults, photolineaments, and fractures can control circulation of mineralizing fluids and hence ore and mineralization. Structures (faults, photolineaments, and fractures) are considered as type of geological setting often formed prior to a mineralizing event. Therefore, they control on formation of rocks other than hydrothermal ores is indirect. These structures are also related to erosion and sedimentation in the adjacent area. Structures formed after a mineralizing event, may be responsible for offset or removal of

mineralized zones. These structures are referred to as “post-mineral”. In some cases the formation of structures and mineralization appear to be nearly synchronous. In these situations, shearing was probably ongoing during the mineralization event. This is evidenced by ore minerals localized along deformed fault planes.

In the study area, the relationship between ore and faults is expressed by most of the ore occurrences. In the Song Ma zone, the intrusions of Nui Nua ultramafic, Song Ma and Chieng Khuong granites, gabbroids of the Bo Xinh complexes and Huoi Hao metabasalt are controlled and distributed along Song Ma marginal deep-seated fault and Na Hiem-Phieng Na fault. Chromium in ultramafic rock, gold, pyrite ore and their geochemical anomalies always have genesis and spatial relation to the Nui Nua intrusions and Huoi Hao eruptions. Thus, only in the southwestern Song Ma zone, in strip between Song Ma fault and Na Hiem – Phieng Na fault is responsible for origin of ore deposits of chromium, gold, and pyrite in mafic and ultramafic rocks. Southwestward within the study area, Sam Nua zone is formed by volcano-sedimentary and carbonate beds of the Dong Trau and Hoang Mai formations, coal-bearing beds of the Suoi Bang Formation and granitoids of the Song Ma complex. Coals and quartz veins bearing lead-zinc and barite are located in the crushed zones of the Suoi Bang Formation. Occurrences of gold are located in altered or crushed zones in granitoids of the Song Ma and Dien Bien Phu complexes. Perhaps hydrothermal fluids were supplied from plutonic rocks and formed mineralization.

The Cam Thuy and Vien Nam mafic effusive are abundant in the Song Da zone, they are controlled and distributed along the Song Da, Son La and Van Yen-Nam Xe-Phong Tho fault zones. Copper sulfide, native copper, gold, lead-zinc, pyrite ore and their geochemical anomalies always have genesis and spatial relation to the Cam Thuy, Vien Nam effusions. The intrusion of Ban Xang ultramafic rock is controlled and distributed along the Ta Khoa anticline. Copper-nickel (Ni-Cu-PGE) mineralization and its anomaly also have genesis and spatial relation with the Ban Xang intrusion. The copper-nickel ore in ultramafic rock occurs in the Ta Khoa anticline. Northwestward within the Song Da zone, the Pu Sam Cap and Pu Tra magmatic rocks are distributed along southwestern side of the Phan Si Pan range. They display a strong spatial relationship with the barite-fluorite, rare earth and radioactive ore, and potassium-sodium mineralizations.

In the Tu Le volcanic depression, the intrusions of Nam Chien, Tu Le, Ngoi Thia, Phu Sa Phin, Nam Xe-Tam Duong complexes and Suoi Be volcanic rocks are controlled and distributed along the Van Yen-Nam Xe-Phong Tho and Phong Tho faults. Lead-zinc, gold mineralizations are displaying a spatial relationship with Tu Le, Ngoi Thia subvolcanic granites. Especially the Tu Le ladle contains the lead-zinc, gold ore deposits. Beside the Tu Le zone, the Ye Yen Sun (west and east of O Quy Ho massifs), Po Sen and Song Chay granites developed along right side of the Phong Tho fault, and are located in the Phan Si Pan-Red river zone. Mineralizations in this area consist of lead-zinc, iron, copper, and molybdenum; they display a very strong spatial relationship with granite intrusions of West Ye Yen Sun, and Po Sen complexes.

The strike-slip fault zones display a strong spatial relationship with minerals in the study area. Particularly, graphite and pyrite ore types are distributed in the Song Hong, Dien Bien-Lai Chau fault zones, respectively. They are related to metamorphic events, geomorphologic features, and geodynamics during Palaeogene times.

The Quang Tan Trai ore strip consists of gold, copper, lead-zinc, and allite-sialite and so on. It extends from the Quang Tan Trai to Son La areas and occurs along cataclastic zone of the Son La fault zone. Mafic-effusive rocks are located along this fault. This relationship suggests that the mineralization is controlled by the fault zone.

Transpressive synsedimentary tectonics is associated with basin opening. When faults undergo displacement (*e.g.* strike-slip motion), they change their fluid transmissibility properties by juxtaposing varying lithologies (and lithological properties) across the fault. During this process, some pull-apart basins were formed along the fault zone by combination of the subsidiary faults. Sedimentary materials were deposited within these basins. These fault types are referred to as “synsedimentary faults”. Most of the NW-SE intrazonal faults in Song Da zone belong to the synsedimentary fault type. A synsedimentary fault system was active at the time of mineralization (Goodfellow *et al.*, 1993). Therefore, most of ore mineralizations in Song Da zone including copper, lead-zinc, gold, pyrite and their geochemical anomalies are displaying spatial relationship associated with those synsedimentary fault type (Nguyen Ngoc Lien, 1990).

Some high-angle deep-seated faults define the southwestern margin of the Song Ma zone, southwestern and northeastern Song Da zone are the Song Ma, Song Da, and Van Yen-Nam Xe-Phong Tho faults, respectively. They are the primary conduit for vertical flow of the hydrothermal fluids forming mineralization. Based on the anomalously high density of Cr-Ni, Cu, and Ba distributions dominating these faults, the present author suggests that the faults must have high permeability. Deep permeability along the faults is consistent with observations of a high incidence of deep (~10-15 km) seismicity following the earthquake that ruptured a large segment of the NWVN area (see chapter 6). In the study area, the Song Ma, Song Da, Van Yen-Nam Xe-Phong Tho fault zones play the role of boundaries between IDB and SCB; between the Song Ma and Song Da zones; between the Song Da and Tu Le zones, respectively. Chromite ores are distributed along the southwestern Song Ma fault zone, copper ores are in the southwestern Song Da fault, lead-zinc and gold ores are on the right side of Van Yen-Nam Xe-Phong Tho fault.

The gold mineralization accompanied by cinnabar strong anomalous zone is underlain by the Cam Thuy, Vien Nam basalt rocks. Their genesis is known as initially syngenetic and genetically related to eruption of adjacent submarine volcano. Cinnabar geochemical anomalies zone distribution display close spatial relationship between those zones and NE-SW tectonic lineament (Nguyen Ngoc Lien, 1990). It is possible that Hg has been supplied from underneath sources along NE-SW tectonic lineament in the Song Da zone.

Open fractures provide ready pathways for fluids and space for vein-forming minerals. In the brittle upper crust, fractures tend to open in directions perpendicular to the least principal stress, especially if they are newly formed, rather than inherited. There is good evidence that

most epithermal veins form in this way, as do magmatic dykes and sills. In the NWWN, most veins and dykes that were formed by hydraulic fracturing are almost vertical and horizontal, indicating that the least principal stress was NW-SE and NE-SW. In local scale, along the Dien Bien-Lai Chau and Red River fault zones, most veins strike NNE-SSW and WNW-ENE and they are compatible with regional extension marked by pull-apart basins mentioned in the chapter 5.

### 7.2.2. Geochemical anomaly related mineralization

Based on results of investigation of Nguyen Ngoc Lien (1990) some anomalous zones for each element were recognized in the whole Song Ma and Song Da areas (Fig. 7.15 and Table 7.1). Fig. 7.15 mapped some anomalous zones of elements. Areas with concentration of anomalous elements were distinguished. These anomalous zones are considered as indicating features for ore mineralization.

No	Element	Anomalous elements contents (n.10 <sup>-3</sup> %)		
		Background	Min	Max
1	Cu	1.2	3	
2	Pb	1.5	3	
3	Ag	0.3	1	
4	Zn	5	10	
5	As	5	10	
6	Sb	5	10	
7	Cr	6.8	10	
8	Co	1	3	
9	Ni	4.9	10	
10	Sn	1	3	
11	Mo	0.3	1	
12	Be	0.2	1	
13	Nb	5	10	
14	La	5	10	
15	Th	5	10	
16	Au	over some tens of grains/m <sup>3</sup>		

Table 5.1. Anomalous elements contents



The Cr-Ni and copper anomalies indicate relatively dense Cr-Ni and Cu distribution. Anomalous zones of Cr and Ni overlap one over another in the Song Ma zone, along Song Ma fault. These elements are believed to have been supplied from the Nui Nua ultramafic serpentine intrusions, and were verified by chromium ore occurrence in Song Ma area.

Copper shows strong positive correlation with Cr-Ni. The copper mineral anomaly is found in some parts of the Ban Xang area especial those surrounding the Ban Xang and Ban Phuc massifs. Thus, Cu anomalies suggest that the existence of copper mineralization accompanies the Ban Xang dunite-peridotite.

The Pb-Zn anomalies are distributed within large area on the known lead-zinc mineralization occurrences, and have relationship with the Cam Thuy, Vien Nam effusive rocks and Song Ma granitoid intrusions. Thus, there is possibility that anomaly indicate lead-zinc ore. Pb-Zn anomalies are limited in Song Da zone. They are distributed along the Van Yen-Nam Xe-Phong Tho deep fault zone and indicate the relationship between fault and mineralization.

### ***7.2.3. Hydrothermal alteration related to mineralization***

Mineral deposits formed from hydrothermal fluids are often accompanied by alteration of the surrounding rocks by the same fluids. In essence, the process of hydrothermal alteration is the response of a rock to new conditions of temperature, pressure, and composition imposed by the introduced fluid; the result is an altered rock with changed mineralogy and texture that may provide an interpretable signature of the characteristics of hydrothermal fluid. Thus, each ore style contains individual characteristic hydrothermal alteration. In the study area, the data from Vietnamese literature (Nguyen Ngoc Lien ed. 1999; Tran Van Tri *et al.*, 2000; and references therein) indicate the following relationship:

Dolomitization, quartzitization, ankeritization, and sideritization are main hydrothermal alterations in lead-zinc bearing carbonate rocks.

Gold-sulfur-quartz mineralization is distributed along the Song Da zone; mineralization is closely related to basalt rocks, where widespread hydrothermal alteration of propylitization, chloritization, and silicification occurs.

Copper, copper-nickel mineralization is distributed along the Song Ma and Song Da zones, hydrothermal alterations include common chloritization and epidotization.

## **8. SUMMARY AND CONCLUSIONS**

### **8.1. Geological evolution and tectonics in northwestern Vietnam**

The suggested model for the tectonic evolution of the NWVN is depicted in Fig. 8.1. The core of South China block was formed during the Proterozoic times (Khuong The Hung, 2010). The NWVN mafic and acid rocks of the Bao Ha, Xom Giau and Po Sen correspond to the major episodes of crustal formation of this block (Li *et al.*, 1999). The gabbros of the Bao Ha complex represent a spreading process of continental margin and they also indicate the existence of Palaeo-South China Sea between the Yangtze and Cathaysia plates during

Proterozoic times. The metamorphic rocks of Suoi Chieng and Sinh Quyen formations dominate along the Phan Si Pan-Red River zone (Tran Ngoc Nam, 1998; 2006). They belong to Early Proterozoic petrotectonic assemble of the basement and existed before the amalgamation of Yangtze and Cathaysia.

The Jinning episode may represent the Late Proterozoic collision between Yangtze and Cathaysia plates (Tran Ngoc Nam, 2003). The other events may be related to the early effects of the mantle plume that initiated the breakup of Rodinia (Li *et al.*, 1999), or to earliest collisions leading to formation of Gondwana (Metcalf, 2006), resulted in a united Palaeo-South China plate. This collision produced the Late Proterozoic granitoids of the Xom Giau and Po Sen complexes. The granitoids of Xom Giau complex were formed in relation to subduction zone, while the granitoids of the Po Sen complex in syn- collisional tectonic setting. The micro-continental plates, perhaps derived from Gondwanaland existed during Palaeozoic times (Metcalf, 1996, 2000; Golonka *et al.*, 2006a,b,c).

Based on the global plate tectonics and palaeogeographic studies of Southeast Asia, Krobicki and Golonka (2006) showed that South China (SCB) and Indochina (ICB) were separated by deep-water basin with thinned continental or may be oceanic crust in Ordovician times (Fig. 8.1). The presences of Ordovician-Silurian sediments and the uplift and volcanic rocks support this possibility (Khuong The Hung, 2010). According to Shouxin & Yongyi (1991), the southern part of the SCB is covered by deep water synorogenic clastic deposits – more than 4000m of weakly metamorphosed flysch, sandstones and graptolitic shales. Similar rocks formed on the margins of Indochina block. They are known as Pa Ham Formation in the Northern Vietnam. The deep water Ordovician and Silurian synorogenic deposits were replaced by continental Early Devonian red beds (Tran Van Tri, ed., 1979). The Lower Paleozoic greenschists of deep sea origin are also unconformably covered in many localities by Devonian redbeds. This redbeds were followed, particularly in Song Ma zone, by Lower Devonian Nam Pia Formation composed mainly of terrigenous sediments and Lower-Middle Devonian Huoi Nhi Formation composed of marl, medium-bedded to massive fine-grained limestone (Khuong The Hung, 2010). These formations represent shallow water sediments (Phan Son, ed. *et al.*, 1978). Perhaps the Late Silurian-Early Devonian was time of the first accretion of ICB to SCB in the collisional process. The granitoids of Song Chay complex are linked to this event. Plate tectonic reconstructions (Metcalf *et al.*, 1996) indicate the possibility of connection between the Early Devonian deformation and uplift and the rifting of the South China block from Gondwanaland. This event is perhaps also related to the global Caledonian orogenic process. The Devonian shallow-water sedimentary rocks were followed by Carboniferous-Permian sequences, represented the limestone of Carboniferous-Permian Bac Son, clay shale of Lower-Middle Permian Si Phay, and the limestone of Middle Permian Na Vang formations (Phan Son, ed. *et al.*, 1978). The new oceanic basin opened between ICB and SCP plates during Late Permian times, recorded by ophiolite belt, which consists of the Nui Nua, Bo Xinh, Chieng Khuong complexes, Huoi Hao Formation and perhaps ultramafic Ban Xang complex. Its origin is related to the closure of the Palaeotethys Ocean between Sibumasu and ICB by subduction below Indochina (Fig. 8.1) (Golonka *et al.*, 2006a, Khuong The Hung, 2010).

The discovery of the Hon Vang serpentinite body within the ICB and SCB (located outside the investigated area) provided additional information about ophiolite belt in this area (Nguyen Minh Trung *et al.*, 2006, 2007). The ages of these ophiolites, are still somewhat uncertain. Probably, they crystallization and accretion process was completed by Late Permian times (Khuong The Hung, 2010).

The widespread volcanic eruption took place in the Song Da zone during Permian times. This event is related to the origin of the Cam Thuy and Vien Nam formations. The cause of this event is still subject of hot debate. Some geologists argued that Cam Thuy and Vien Nam formations were perhaps related to the plate reorganization and mantle plume activity, known in China and Indochina as Emeishan plumes and related to Siberian basaltic traps (Hanski *et al.*, 2004; Tran Trong Hoa *et al.*, 2008b; Krobicki & Golonka, 2008 and references therein). They were formed in within-plate (intraplate) setting, related to back-arcs spreading (Lepvrier *et al.*, 1997, 2004; Golonka *et al.*, 2006a,c) or Song Da rift of Tran Van Tri (ed., 1979). The preferred geodynamic reconstruction assumes that this magmatism was formed during the convergence of the Sibumasu and the newly formed Indochina-South China block. The oceanic crust was subducted southward under ICB (Tran Trong Hoa *et al.*, 2008a). This subduction led to the origin of Late Permian – Triassic magmatic events and Song Da volcanism (Khuong The Hung, 2010).

Remnants of oceanic lithosphere were accreted into the northern edge of the IDB and appeared in Song Ma fault zone and Sam Nua zone (Golonka *et al.*, 2006a; Nguyen Minh Trung *et al.*, 2007 and references therein). The Indosinian orogeny of Fromaget (1937, 1941) represents the final stage of this closure. The orogeny was recorded by magmatic, metamorphic and deformation events in Truong Son, Sam Nua, Nam Co, and Song Ma structural zones (Hutchison, 1989; Tran Ngoc Nam, 1998; Lepvrier *et al.*, 1997, 2004, 2008; Lan *et al.*, 2000). The folded Triassic and older rocks were unconformably covered by Upper Triassic coal bearing molasse beds of the Suoi Bang Formation. The granitoids of the Dien Bien Phu, Song Ma and Phia Bioc complexes, are related to Indosinian orogeny. The granitoids of Dien Bien Phu complex were formed in syn-collisional, while the granitoids of the Song Ma and Phia Bioc complexes in post-collisional tectonic setting (Khuong The Hung, 2010).

During the Jurassic times, the strong volcano-plutonic activities, known as an Yanshanian tectonic cycle, related to the collision between the Izanagi Plate (proto-Pacific Ocean) and South China blocks, appeared in the southeastern China (Metcalf, 1996a,b; Golonka, 2007). This event was not restricted to the southeastern China but was also recorded in many areas of Vietnam including the NWVN. The Jurassic - Cretaceous intraplate magmatism, which includes basalt of the Suoi Be Formation, gabbro from Nam Chien, rhyolitic Tu Le, Ngoi Thia subcomplexes and granosyenite and granite of the Muong Hum, Phu Sa Phin, East Ye Yen Sun complexes provides the evidence of the Yanshanian tectonic cycle activity in the NWVN. However, based on the similarity of lack of depletion in the high field strength elements (Nb, Ta and Ti), it is possible to speculate that late Permian-early Triassic Song Da basalts may serve as the source material for Jurassic to Cretaceous A-type granitic rocks of the Phu Sa Phin complex as well as rhyolites of Tu Le and Ngoi Thia subcomplexes (Khuong The Hung, 2010).

During Palaeogene times, the extrusion, transpression, transtension and extension related processes, which resulted from the India-Asia collision (Himalayan tectonic cycle), produced high-potassic rocks in the northwestern Yunnan and northern Vietnam (Laplou, 1995; Lan *et al.*, 1999, 2001; Golonka *et al.*, 2006a). The related tectonic activities formed the leucocratic granite, rhyolite and calc-alkaline intraplate rocks of the West Ye Yen Sun complex, Pu Tra Formation, Nam Xe-Tam Duong, Pu Sam Cap, and Coc Pia complexes. Following the Himalayan cycle activities, the transtension tectonics accompanying the mantle plumes have moved from the South China Sea southwestward to ICB continent (Nguyen Hoang & Martin, 1996). This movement led to the formation of intraplate volcanism of "pull-apart" type with the assemblage of basaltic effusives in Vietnam's territory including the Late Neogene basalt in Dien Bien Phu basin of the NWVN (Koszowska *et al.*, 2004, Khuong The Hung, 2010). Besides, several faulted segments accompanied by this event dominate in this area with strike-slip characters along Red River, Dien Bien-Lai Chau, Ma River, Da River, and Son La fault zones. Most of them are also recorded on the topographic surface by geomorphological features, and by focal mechanisms of earthquakes.

Results of DEM analysis also help to recognize the Dien Bien-Lai Chau, and Red River fault zones which formed the tectonic lineaments and distributed in the northeastern and northwestern parts of the area, respectively. Along the RRFZ, a typical structure was determined as the positive flower structure of Pho Lu segment, suggesting a transpressive tectonic regime. Also, in the DBFZ some small pull-apart basins are dominated as the Chan Nua basin.

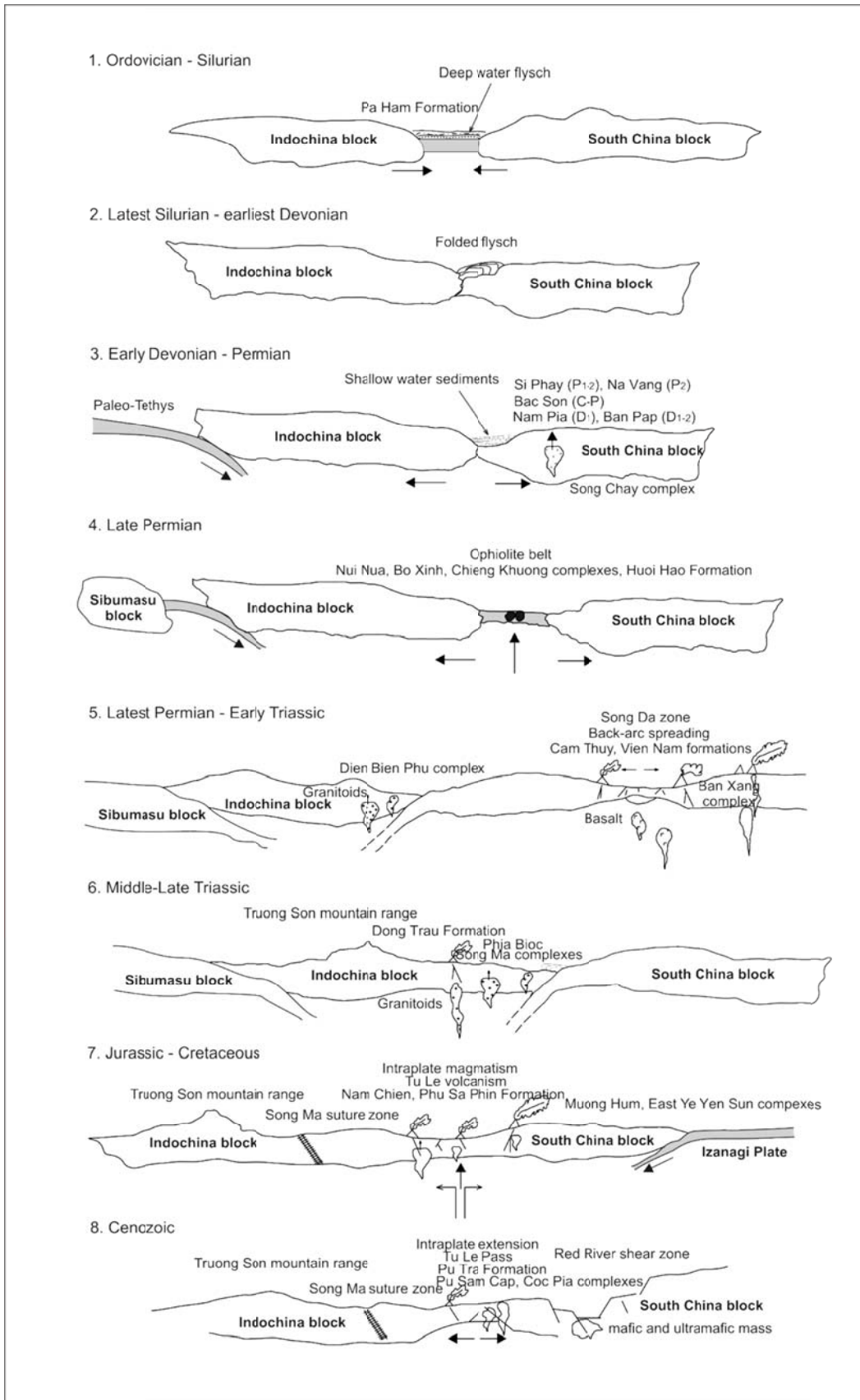


Fig.8.1. Geological evolution and tectonics in the NWVN area

## **8.2. Metallogeny**

The localization of the mineral deposits is controlled by tectonic setting, which in turn is also controlled by others factors favorable for the formation of mineral deposits. These factors include genesis, forming age, distribution, textural form, and composition of the associated igneous bodies, the formation of sedimentary basins and the characteristic of sediments that fill up the basins, the development of fault that provides conduits for mineralizing fluids or distributes mineralization in shear zones (Snelgrove, 1971; Staude & Barton, 2001; Bierlein *et al.*, 2002; Pirajno, 2004; Groves *et al.*, 2005). Therefore, many authors have interpreted the metallogeny of specific mineral deposit areas on the basis of some factors including their genesis, forming age, and spatial distribution of mineral deposits and their relation to the tectonic setting of that area (Misra, 1999). The metallogeny of mineral deposits in NWVN was discussed following that idea.

Several tectonic settings have been identified for the igneous and eruptive rocks in the NWVN. On the basis of the ore forming ages, deposit types, and the relationship between ore deposits and their host igneous rocks as well as and tectonic settings, reconstruction is possible for five distinguished metallogenic types in the NWVN.

### ***8.2.1. Metallogenic type related to metamorphic rocks during Proterozoic***

Iron, pyrite, copper and copper-gold mineralization are distributed in metasomatic rocks of Proterozoic basement and genetically connected with metamorphic process and magmatic events. In turn, iron, copper ore mineralizations of metamorphic type are produced by the Bao Ha gabbros and Sinh Quyen metamorphic rocks. Particularly, the Sinh Quyen sedimentary rocks were metamorphosed to epidote-amphibolite facies during Late Proterozoic (Tran Ngoc Nam, 2006). Copper and gold mineralization of gabbros of the Dong An massif of Bao Ha complex is related to hydrothermal alteration. Other copper, copper-gold ore mineralizations of the metasomatic type were produced by the Po Sen granitoids and Sinh Quyen metamorphic rocks. Copper porphyry is related to the Proterozoic Po Sen granitoids. Pyrite metamorphic ore type was produced by the metamorphic process of Sinh Quyen Formation. The Proterozoic metallogenic types are related to the Jinning event, caused by the collision between Yangtze and Cathaysia plates (Tran Ngoc Nam, 2003), or to earliest collisions leading to formation of Gondwana (Metcalf, 2006). They are closely related to the Phan Si Pan – Red River zone.

### ***8.2.2. Metallogeny in Early Palaeozoic –Devonian- Carboniferous***

The main tectonic activities during so-called Caledonian event took place in South China plate. They do not have a significant effect on mineralization in the study area. Particularly, in the Phan Si Phan – Song Hong zone, we found only early Devonian granite rocks of the Song Chay complex which was generated in post orogenic setting, and is considered a product of the first accretion of IDB to SCB. Mineralizations consist of iron, pyrite, and graphite, copper and

copper-gold are distributed around the complex. However, it looks like the hydrothermal and thermal processes, which supplied most of the ore-forming metals, are related to the Proterozoic Po Sen granite complex which was intruded later by the Song Chay granite complex. Therefore, the “Caledonian” metallogeny is not very well recognized in the study area and requires further research.

### ***8.2.3. Metallogenic type related to Upper Permian Ophiolite belt***

This metallogenic type includes mineralization that is related to the igneous rocks of upper Permian ophiolite belt. It consists of chromium of orthomagmatic origin hosted by the Nui Nua ultramafic, and epithermal pyrite, gold, copper and pyrite are related to the Bo Xinh gabbros and Huoi Hao metabasalt Formation of the Song Ma structural zone.

### ***8.2.4. Metallogeny in Late Permian-Triassic Indosinian***

#### *1. Metallogenic type related to Indosinian*

Generally in the whole Vietnam's territory and particularly the NWVN, it has been considered that the Permo-Triassic metallogenic type coincides with Indosinian tectonic cycle. This metallogenic type is related to the Permo-Triassic magmatism in the Song Ma and Sam Nua zones, i.e. mineralizations related igneous rocks that were formed in collision magmatic setting. They consist of hydrothermal gold, lead-zinc of the Dien Bien Phu, Song Ma and Phia Bioc granitoids. In general, syngenetic mineralization types are formed by epithermal and mesothermal processes. They are closely related to the sedimentary rocks of the Suoi Bang Formation and plutonic rocks of the Dien Bien Phu, Song Ma and Phia Bioc complexes, which have been formed in a continental collision setting (Tran Trong Hoa, 2008).

#### *2. Metallogenic type related to Permian intraplate extension*

Progressive convergence between South China and Indochina plates, the Nam Co block could break apart from the southwest margin of South China plate, the volcanic eruption was took place as widespread as over Song Da zone. This event led to formation of the Cam Thuy, Vien Nam Formations and Ban Xang ultramafic complex accompanied by mineralization as well. The metallogenic type is related to the Permian basalt volcanism and ultramafic intrusion that were formed in intraplate extension setting, related to back-arc spreading. They consist of magmatic segregation and hydrothermal nickel - copper (Ni-Cu-PGE) of Ban Xang ultramafic rocks, and copper sulfide, native copper, lead-zinc, gold, pyrite, allite-siallite hosted by the basalt and carbonate rocks. In general, syngenetic mineralization types are formed by epithermal and mesothermal processes. They are closely related to Devonian, Carboniferous - Permian carbonate rocks of the Ban Pap, Bac Son formations and late Permian volcanic rocks.

### **8.2.5. Metallogeny in Yanshanian (Jurassic-Cretaceous)**

Presently, this metallogenic type in the NWVN is known by several types of small syngenetic mineralization such as ore deposit type of gold and lead-zinc occurrences. They were formed by epithermal process, and were originated from Jurassic-Cretaceous within plate calc-alkaline magma. It includes volcanic rocks of the Tu Le, Ngoi Thia complexes, Suoi Be, Tram Tau formations and its comagmatic intrusions of the Nam Chien, Muong Hum complexes.

### **8.2.6. Metallogeny in Himalayan (Palaeogene)**

The ore deposits specified to Himalayan metallogenic period in the NWVN are syngenetic, epigenetic mineralization, which were formed by magmatic and hydrothermal processes of carbonatite mineralization of rare earth and radioactive ores; and hydrothermal mineralization of molybdene, iron, and potassium-sodium of volcanic origin. Their genesis is related to Palaeogene within plate alkaline magma of the west Ye Yen Sun, Nam Xe-Tam Duong and Pu Sam Cap syenite; which might has been produced by upwelling of mantle asthenosphere during Palaeogene caused by the activation of Red River shear zone (Tran Trong Hoa *et al.*, 2004).

## **8.3. Conclusion, tectonic processes conducive to the formation of the mineral deposits**

The NWVN area is rich in mineral resources and has a wide diversity of deposit types. The region has undergone multiple tectonic and magmatic events and related metallogenic processes throughout the earth history. Many tectonic settings create conditions conducive to the generation of water-rich magma, hydrothermal fluid flows, they also influence on formation of mineralization. Crustal influence is evident in the strong structural controls on the location and morphology of many ore deposits in NWVN. Fault and fracture systems, many involving strike-slip elements, have provided the fabric for major plumbing systems. These tectonic and metallogenic processes were responsible for the formation of the diverse styles of mineral deposits in NWVN making it one of the resource-rich regions in Vietnam country.

The crust of South China block corresponds to the convergence between the Yangtze and Cathaysia blocks or the breakup of Rodinia during the Proterozoic. Although old, the Phan Si Pan-Song Hong zone suffered only low-grade metamorphism and its rocks and ore deposits are remarkably well preserved (Tran Ngoc Nam, *et al.*, 1998, 2006). The metallogenic type of endogenic ore related to metamorphic rocks of the Phan Si Pan-Song Hong zone are characterized by iron, pyrite, copper and copper-gold, copper porphyry mineralization.

During continued evolution of the NWVN the new oceanic basin opened between ICB and SCB in Late Permian. A remnant of Upper Permian Ophiolite belt is characterized by chromium podiform- of orthomagmatic origin. It was formed by concentration of ore minerals as a direct consequence of magmatic crystallization of ultramafic tectonites as component of remnant ophiolite. It consists of epithermal pyrite, gold related to the Bo Xinh gabbros and Huoi Hao metabasalt Formation. The chromium ores are hosted by Nui Nua ultramafic, pyrite,

gold hosted by Bo Xinh gabbros and Huoi Hao metabasalt; they are closely related to the Song Ma fault zone.

During the Late Permian- Early Triassic, the subduction of the oceanic crust under the continental crust of Indochina led to the formation of the Triassic continental volcanic arc in Song Ca of Truong Son mountain range (Tran Van Tri ed., 1979; Tran Trong Hoa, 2007) or in Sam Nua zone. Following a period of compressional tectonics, crustal-scale thrusting thickened the continental crust of the Song Ma zone. Compression is related to formation of the Dien Bien Phu syncollisional magmatism and of a network of faults trending mostly in the NW-SE direction as Song Ma, Song Da, and Son La fault zones and so on. A significant shift in the compressional tectonics was accompanied by granulite-facies metamorphism from the Song Ma suture zone (Nakano, N. *et al.*, 2006, Nakano, N. *et al.*, 2008). In the Laos country, near Truong Son fold belt, the geologists have discovered the Carboniferous copper-gold porphyry mineralization (Manaka, *et al.*, 2008), Middle Triassic (230 Ma) gold-copper-molybdene mineralization (Newsletter, 2003). Early Triassic copper-molybdene porphyry was discovered in the Sa Thay area and central Vietnam (Tran Trong Hoa *et al.*, 2006). These deposits originated also in collisional plate tectonic setting.

The evolution of collision between ICB and SCB blocks in the NWVN during Permo-Triassic time is recognized by the existence of Dien Bien Phu, Song Ma and Phia Bioc granitoids. The Permo-Triassic metallogenic type related to continental collision is the most important in the ore-forming processes in NWVN's. These processes are clearly associated with the origin of the Dien Bien Phu, Song Ma and Phia Bioc granitoid intrusions and sedimentation. The ore deposits of the gold, lead-zinc types are epigenetic mineralizations which were formed by hydrothermal solutions via magmatic resource in a collisional environment related to continental collision. Generally, these ores and mineralization are located near the Song Ma faults.

Meanwhile, the Nam Co block could break apart from the southwest margin of South China plate. This break, related to the back-arc spreading, formed Song Da Ocean along the Song Da and Son La fault zones, where large scale of magmatic segregation and hydrothermal nickel - copper (Ni-Cu-PGE) of Ban Xang ultramafic rocks, and copper sulfur, native copper, lead-zinc, gold, pyrite, allite - siallite are associated with oceanic volcanism and hosted by carbonate rocks. Most of the ore deposits of copper-nickel, copper, lead-zinc, gold, pyrite, and allite - siallite types represent syngenetic mineralizations, which were formed by epithermal and mesothermal processes via precipitation and concentration in an exhalative environment related to submarine volcanic processing. They are closely related to the Song Da and Son La fault zones.

The broad-scale calc-alkaline magmatism of the Tu Le volcanic depression appears to have been controlled by Yanshanian tectonic processes. These processes provided the source for hydrothermal fluids that gave rise to gold and lead-zinc mineralizations. Ore formations are associated with volcanic rocks. Generally, Yanshanian metallogeny period is characterized by Jurassic - Cretaceous intraplate metallogeny in southeastern China, and particularly Jurassic-Cretaceous in the NWVN. However, this metallogeny period is not as typical as that in

southeastern China, where it is called Yanshanian metallogenic explosion with very rich and mineral resources of gold, tin and especially wolframite (Hua, R. *et al.*, 2003; 2005; Zaw, K. *et al.*, 2006). In the study area, Yanshanian metallogeny period is known by several small syngenetic mineralization types such as gold and lead-zinc ores. They were formed by epithermal process, and originated from Jurassic-Cretaceous intraplate calc-alkaline magma, which produced volcanic rocks of the Tu Le, Ngoi Thia complexes, Suoi Be, Tram Tau formations.

Finally, the ore deposits related to Himalayan tectonic cycle in the NWVN belong to Himalayan metallogeny period within Palaeogene exhibiting intraplate metallogeny characteristics. This metallogeny period consists of syngenetic mineralizations of barite-fluorite, rare earth and radioactive ores; and hydrothermal mineralization of gold (skarn or porphyry), molybdene, iron, and potassium-sodium; metamorphic mineralization of pyrite and graphite. Their origin is related to Palaeogene intraplate potassic magma of the Pu Sam Cap, west Ye Yen Sun, and Nam Xe-Tam Duong. In the NWVN, they represent leucocratic granite, rhyolite and calc-alkaline granite, which appear in a close relation to the upwelling mantle asthenosphere during Palaeogene times. Large pull-apart basins formed along main tectonic lines of strike-slip character, such as Song Hong (Red River) and Dien Bien-Lai Chau fault zones. These were compartmentalized into smaller linked subbasins with half-graben and positive flower structure geometries, filled with sedimentary, metamorphic and volcanic rocks. The most likely source of hydrothermal fluids and metals in the NWVN is in middle crust, associated with the magmatic intrusions, and that small extensional zones in a transpressional setting provided pathways for the rise of fluids to higher crustal levels where a range of mineral deposits was formed.

## ACKNOWLEDGEMENTS

I am deeply indebted to my advisor, Dr hab. inż Jan Golonka Professor AGH for being an outstanding advisor and excellent professor. His constant support, encouragement, and invaluable suggestions made this work successful. He has been everything that one could want in an advisor. Without his help, this work would not be possible.

I am grateful to the members and colleagues at the AGH - University of Science and Technology; Faculty of Geology, Geophysics and Environmental Protection; Department of General Geology and Environment Protection, Cracow - Poland for their support, profitable discussions and comradeships; especially to Prof. dr hab. inż. Antoni Tajduś (provided scholarship), Prof. dr hab. inż. Tadeusz Słomka (provided accomodation and work space), Prof. dr hab. inż. Jacek Matyszkiewicz (provided grant), Prof. dr hab. Witold A. Zuchiewicz, and Dr inż. Michał Krobicki.

I would like to express my heartily thanks to my university (Ha Noi University of Mining and Geology), and my Department (Department of Prospecting and Exploration) for allowing me to study abroad.

Many thanks should go to all Polish friends in my office and PhD group, Mr. Piotr Dymytrowski, Mr. Jakub Pająk, Mr. Tomasz Śliwa, Mr. Grzegorz Madeja, Ms. Magdalena Górna, Ms. Paulina Mrowczyk, and others, who gave me help on studying and made me feel friendly to be here.

To all my friends who are working in Vietnam and are studying in Poland, I would like to say thanks for their support and help. Thank you!

Very special thanks go particularly to my family. I am much indebted and extremely grateful to my parents, my wife and my son for their continuous and unflinching encouragement and support in various ways. Therefore, I would like to dedicate my thesis to them.

## REFERENCES

- Allen, C. R., Gillepsie, A. R., Han, Y., Sieh, K. E., Zhang, B. & Zhu, C., 1984. Red River and associated faults, Yunnan province, China: Quaternary geology, slip rates, and seismic hazard. *Geological Society of America Bulletin*, 95: 686-700.
- Anczkiewicz, R., Viola, G., Muntener, O., Thirlwall, M. F., Villa, I. M., & Nguyen Quoc Cuong, 2007. Structure and shearing conditions in the Day Nui Con Voi massif: Implications for the evolution of the Red River Shear Zone in northern Vietnam. *Tectonics*, 26, article number: TC2002.
- Anthony, E. Y., 2005. Source regions of granites and their links to tectonic environment: examples from the western United States. *Lithos*, 80: 61– 74.
- Arai, S., 1997. Origin of podiform chromitites. *Journal of Asian Earth Sciences*, 15(2-3): 303-310.
- Arndt, N. T., Leshner, C. M. & Czamanske, G. K., 2005. Mantle-Derived Magmas and Magmatic Ni-Cu-(PGE) Deposits. *Society of Economic Geologists, Inc. Economic Geology 100th Anniversary*: 5–23.
- Balykin, P. A., Poliakov, G. V., Petrova, T. E., Hoang Huu Thanh, Tran Trong Hoa, Ngo Thi Phuong & Tran Quoc Hung, 1996. Petrology and evolution of the formation of Permian-Triassic mafic-ultramafic associations in North Vietnam. *Journal of Geology (Ha Noi), Series B*, No 7-8: 59-64.
- Barton, M. D., 1996. Granitic magmatism and metallogeny of southwestern North America. *Earth Sciences*, 87: 261-280.
- Batchelor, R. A. & Bowden, P., 1985. Petrogenetic interpretation of granitoid rock series using multicationic parameters. *Chemical Geology*, 48: 43–55.
- Becker, M., Reinhart, E., Nordin, S. B., Angermann, D., Michel, G. & Reigbe, C., 2000. Improving the velocity field in South and South-East Asia: The third round of geodysea. *Earth Planets Space*, 52: 721–726.
- Bierlein, F. P., Gray, D. R. & Foster, D. A., 2002. Metallogenic relationships to tectonic evolution - the Lachlan Orogen, Australia. *Earth and Planetary Science Letters*, 202: 1 - 13.

- Bourret, R., 1922. Études géologiques sur le Nor-Est du Tonkin (feuilles de Bao Lac, Cao Bang, Ha Lang, Bac Kan, That Khe, Long Te Heou). *Bulletin du service géologique de l'Indochine*, XI/1, 174 : 227-229
- Bourret, R., 1925. La chaîne annamitique et les plateaux du Bas Laos, à l'Ouest de Hué. *Bulletin du service géologique de l'Indochine*, XIV/3, 181: 724-726
- Bui Cong Hoa (ed.), 2004. *Report on geology and mineral resources of the Quynh Nhai sheet group at 1:50,000 scale*. Unpublished report, Ha Noi.
- Bui Minh Tam, Pham Dinh Long, To Van Thu, Trinh Xuan Hoa, 1995. New data on volcanites and vein rocks in Phong Tho-Lai Chau area. *Geology and Petroleum mineralization in Vietnam*, 1: 98-96.
- Bui Phu My (ed.), Nguyen Van Hoanh, Phan Viet Ky & Tran Dang Tuyet, 1977. *Geological map of Vietnam at 1:200,000 scale. Lao Cai-Kim Binh sheet, with the explanatory note "Geology of the Lao Cai-Kim Binh sheet"*. Published by Department of Geology and Minerals of Vietnam, Ha Noi, 118 pp.
- Burbank, D. W. & Anderson, R. S., 2001. *Tectonic Geomorphology*. Blackwell Sciences, Inc., Malden, 274 pp.
- Cao Dinh Trieu, 1991. *Deep structures and characteristics of seismic activities on the Territory of Vietnam*. Ha Noi, 140 pp.
- Cao Dinh Trieu, 1999. Probable approach for long-term earthquakes prediction in Vietnam based on regulation of epicentral distribution. *Journal of Geology (Ha Noi), Series A*, No 251: 14-21.
- Carter, A., Roques, D. & Bristow, C., 2001. Understanding Mesozoic accretion in Southeast Asia: Significance of Triassic thermotectonism (Indosinian orogeny) in Vietnam. *Geology*, 29: 311-314.
- Chappell, B. M., White, A. J. R. & Wyborn, D., 1987. The importance of residual source material (restite) in granite petrogenesis. *Journal of Petrology*, 28: 1111-1138.
- Chung, S. L., Lee, T. Y., Lo, C. H., Wang, P. L., Chen, C. Y., Nguyen Trong Yem, Tran Trong Hoa & Genyao, W., 1997. Intraplate extension prior to continental extrusion along the Ailao Shan-Red River shear zone. *Geology*, 25: 311-314.
- Condie, K. C., 1997. *Plate tectonics and Crustal evolution*. 4<sup>th</sup> edition. Butterworth-Heinemann Linacre House, Oxford, UK, Woburn, MA, USA, 280 pp.
- Cornwall, H. R., 1956. A summary of ideas on the origin of native copper deposits. *Economic Geology*, 51: 615-631.
- Cox, K. G., Bell, J. D. & Pankhurst, R. J., 1979. *The interpretation of igneous rocks*. London George Allenn & Unwin Boston, Sydney, 450 pp.
- Cui, Y., Qin, D., Chen, Y., 2005. Copper mineralization in the western Longbohe area, SE Yunnan, China – a comparison with the Shengquan copper deposit, Vietnam. In: *Meeting the Global Challenge, Proceedings of the Eighth Biennial SGA Meeting Beijing, China 4-13 (Publisher: Springer Berlin Heidelberg)*. 369-374pp.
- Dao Dinh Thuc, 1976. On granitoid formations in the riverhead of Ma River. (In Vietnamese). *Journal of Geology (Ha Noi), Series A*, No 126: 9-14.

- Dao Dinh Thuc, Huynh Trung (eds), Pham Duc Luong, Bui Minh Tam & Phan Thien, 1995. *Geological map of Vietnam – Vol. 2. Magmatic formations*. (In Vietnamese). Geological Department of Vietnam, Ha Noi, 359 pp.
- Dinh Minh Mong (ed.), 1977. *Geological map of Vietnam at 1:200,000 scale, Van Yen sheet, with the explanatory note “Geology of the Van Yen sheet”*. Geological Department of Vietnam, Ha Noi, 145 pp.
- Dinh Van Dien (ed.), 1976. *Distributed features of Rare earth and radioactive ore material composition in Nam Xe-Hoang Lien Son mine*. (Unpublished report). Vietnam Institute of Geosciences and Mineral resources.
- Dinh Van Dien, Bui Xuan Anh & Dinh Thanh Binh, 2005. The features of porphyry copper at Ta Phoi, Lao Cai area. *60<sup>th</sup> anniversary of Vietnam Geology, Ha Noi*, 610-621.
- Dmitriev, L.V., Ukhanov, A. V. & Sharaskin, A. Ya., 1972. On the question about the composition of the upper mantle matter. *Geokhimiya*, 10: 1155-1167.
- Dovjikov, A. E. (ed.), Bui Phu My, Vasilevskaia, E. D., Jamoida, A. I., Ivanov, G. V., Izokh, E. P., Le Dinh Huu, Mareitchev, A. I., Nguyen Van Chien, Nguyen Tuong Tri, Tran Duc Luong, Pham Van Quang & Pham Dinh Long, 1965. *Geology of North Vietnam. Explanatory note of the Geological Map of North Vietnam at 1:500,000 scale*. Geological Department of Vietnam, Ha Noi, 584 pp.
- Do Hai Dung, 1990. Gold deposits. In: Le Thac Xinh, Tran Van Tri, Do Hai Dung (eds.). *Geology and Mineral resources of Vietnam*. Mineral Development Co, Ha Noi, Vietnam, 108-127.
- Dussault, L., 1920. Exploration géologique de la province de Sam Nua (Laos). Bulletin du service géologique de l'Indochine, X/2, Ha Noi, 60pp. In: Fromaget, J., 1928. *Carte géologique de L'Indochine au 500,000e. Feuille de Vinh avec notice explicative*. Service Géologique de l' Indochine, Ha Noi.
- Duong Chi Cong & Feigl, K. L., 1999. Geodetic measurement of horizontal strain across the Red River fault bears Thac Ba, Vietnam, 1963-1994. *Journal of Geodesy*, 73: 298-310.
- Economou, M. I., & Naldrett, A. J., 1984. Sulfides Associated with Podiform Bodies of Chromite at Tsangli, Eretria, Greece. *Mineral Deposita*, 19: 289 - 297.
- Fan, P. F., 2000. Accreted terranes and mineral deposits of Indochina. *Journal of Asian Earth Sciences*, 18: 343-350.
- Ferrari, O. M., Hochard, C., Stampfli, G. M., 2008. An alternative plate tectonic model for the Palaeozoic–Early Mesozoic Palaeotethyan evolution of Southeast Asia (Northern Thailand–Burma). *Tectonophysics*, 451: 346–365.
- Findlay, R., 1997. The Song Ma Anticlinorium, northern Vietnam: The structure of an allochthonous terrane containing early Palaeozoic island arc sequence. *Journal of Asian Earth Sciences*, 15: 453-464.
- Findlay, R. & Phan Trong Trinh, 1997. The structural setting of Song Ma region, Vietnam and the Indochina - South China plate boundary problem. *Gondwana Research*, 1: 11-33.
- Fromaget, J., 1937. *Études géologiques sur le Nord-Ouest du Tonkin et le Nord du Haut-Laos*. Chef du Service Géologique de l' Indochine, 153 pp.

- Fromaget, J., 1941. L'Indochine Francaise, sa structure geologique, ses roches, ses mines et leur relation possible avec la tectonique. *Bulletin du service géologique de l'Indochine*, 26 (2): 1-140.
- Ganas, A., Pavlides, S. & Karastathis, V., 2005. DEM-based morphometry of range-front escarpments in Attica, central Greece, and its relation to fault slip rates. *Geomorphology*, 65(3-4): 301-319.
- Gatinxki, Iu. G., Tran Van Tri, Isaev, E., Le Van Cu, Kamenetski, A., Kujenur, N., Raskazov, Yu., Sukhov, V., 1970. Discussions on tectonic division of the northern Vietnam. *Geology, No 89-90*. Ha Noi, 1-41.
- Gibbard, P. L., Boreham, S., Kohen, K. M. & Moscarriello, A., 2004. Global chronostratigraphical correction table for the last 2.7 million years. *Quaternary Palaeoenvironments Group, Inst. Quatern. Res., Dept. Geogr., Univ. Cambridge, UK*.
- Gibowicz, S. J., Niewiadomski, J., Pham Van Thuc, 1987. Source study of the Tuan Giao earthquake on 24 June 1983. *Journal of Geology (Ha Noi), Series B*, No 9: 33-42.
- Glotov, A. I. & Polyakov, G. V., Tran Trong Hoa, Balykin, P. A., Akimtsev, V. A., Krivenko, A. P., Tolstykh, N. D., Ngo Thi Phuong, Hoang Huu Thanh, Tran Quoc Hung & Petrova, T. E., 2001. The Ban Phuc Ni-Cu-PGE deposit related to the Phanerozoic komatiite-basalt association in the Song Da rift, northwestern Vietnam. *The Canadian Mineralogist* 39: 573-589.
- Golonka, J., 2007. Late Triassic and Early Jurassic palaeogeography of the world. *Palaeogeography, Palaeoclimatology, Palaeoecology*, 244: 297-307.
- Golonka, J., Krobicki, M., Pająk, J, Nguyen Van Giang & Zuchiewicz, W., 2006a. *Global plate tectonics and paleogeography of Southeast Asia*. Faculty of Geology, Geophysics and Environmental Protection, AGH-University of Science and Technology; Arkadia, Kraków, 128 pp.
- Golonka, J., Krobicki, M., Paul, Z. & Khudoley, A., 2006b. Central Asia-Southeast Asia connection during Palaeozoic orogenies: Problems and questions. *Geolines*, 20: 21-23.
- Golonka, J., Krobicki, M., Pająk, J. & Nguyen Van Giang, 2006c. Paleogeographic maps of Southeast Asia. *Geolines*, 20: 71-74.
- Goodfellow, W. D., Lydon, J. W., & Turner, R. J. W., 1993. Geology and genesis of stratiform sedimenthosted (SEDEX) zinc-lead-silver sulfide deposits. *Geological Association of Canada Special*. 40: 201-252.
- Graciano, P. Y. J., Zhou, M. F., Wang, C. Y., Zhao, T. P. & Dimalant, C. B., 2008. Geology and geochemistry of the Shuanggou ophiolite (Ailao Shan ophiolitic belt), Yunnan Province, SW China: Evidence for a slow-spreading oceanic basin origin. *Journal of Asian Earth Sciences* 32: 385-395.
- Green, J. & Poldervaart, A., 1958. Petrochemical fields and trends. *Geochimica et Cosmochimica Acta*, 13: 87-122.
- Groves, D. I., Vielreicher, R. M., Goldfarb, R. J., Hronsky, J. M. A. & Condie, K.C., 2005. Tectonic and lithospheric controls on the heterogeneous temporal distribution of mineral deposits. In: *Mineral Deposit Research: Meeting the Global Challenge, Proceedings of*

- the Eighth Biennial SGA Meeting Beijing, China 4-13 (Publisher: Springer Berlin Heidelberg): 11-14.*
- Gupta, R. P., 2002. *Remote sensing in geology. Second Edition*, Springer, 655 pp.
- Hanski, E., Richard, J. W., Hannu, H., Polyakov, G. V., Pavel, A. B., Tran Trong Hoa & Ngo Thi Phuong, 2004. Origin of the Permian-Triassic komatiites, northwestern Vietnam. *Contributions to Mineralogy and Petrology*, 147: 453–469.
- Ha Phat Vinh & Du Khai Co, 1961. Geological characteristics and prospecting signs of copper - nickel ores in the Ban Sang deposit. (In Vietnamese). *Journal of Geology (Ha Noi), Series A*, No 3: 20-27.
- Hoang Quang Vinh, Phan Trong Trinh, Nguyen Van Huong, Ngo Van Liem & Le Minh Tung, 2006. Remote sensing and GIS for seismic risk assessment in Hoa Binh hydropower dam. *In: International Symposium on Geoinformatics for Spatial Infrastructure Development in Earth and Allied Sciences 2006*. 1-6
- Howell, B., Nguyen Thi Thuc Anh, Farmer, M. & Bui Xuan Vinh, 2007. Some preliminary results on the gold exploration program of Pu Sam Cap project of triple plate junction Ltd, Vietnam. *Journal of Geology (Ha Noi), Series B*, No 30: 57-69.
- Hua, R., Chen, P., Zhang, W. & Lu, J., 2005. Three large-scale metallogenic events related to the Yanshanian period in Southern China. In: *Mineral Deposit Research: Meeting the Global Challenge, Proceedings of the Eighth Biennial SGA Meeting Beijing, China 4-13 (Publisher: Springer Berlin Heidelberg): 401-404.*
- Hua, R., Chen, P., Zhang, W., Liu, X., Lu, J., Lin, J., Yao, J., Qi, H., Zhang, Z., & Gu, S., 2003. Metallogenic systems related to Mesozoic and Cenozoic granitoids in South China. *Science in China*, 46: 816-829.
- Huang, T. K., 1977. An outline of the tectonic characteristics of China. *Acta Geological Sinica*, 57(2): 117-135.
- Hutchison, C. S., 1975. Ophiolite in Southeast Asia. *Geological Society of America Bulletin*, 86: 797-806.
- Hutchison, C. S. & Taylor, D., 1978. Metallogenesis in SE Asia. *Geological Society of London*, 135: 407-428.
- Hutchison, C. S., 1989. *Geological Evolution of Southeast Asia*. Oxford Monographs on Geology and Geophysics, Oxford, UK, Clarendon Press, 376 pp.
- Irvine, T. N. & Baragar, W. R. A., 1971. A guide to the chemical classification of the common volcanic rocks. *Canadian Journal of Earth Sciences*, 8: 523-545.
- Jacob, C., 1921. *Etudes géologiques dans le Nord Annam et le Tonkin*. Bulletin du service géologique de l'Indochine, X/1, Ha Noi, 204pp.
- Jamieson, S. S. R., Sinclair, H. D., Kirstein, L. A. & Purves, R. S., 2004. Tectonic forcing of longitudinal valleys in the Himalaya: morphological analysis of the Ladakh Batholith, North India. *Geomorphology*, 58: 49-65.
- Jensen & Rickwood, P. C., 1989. Boundary lines within petrologic diagrams which use oxides of major and minor elements. *Lithos*, 22: 247-263.

- Jordan, G., 2003. Application of digital terrain modelling and GIS methods for the morphotectonic investigation of the Kali Basin, Hungary. *Zeitschrift für Geomorphologie*, 47: 145-169.
- Jordan, G., Meijninger, B. M. L., Hinsbergen, D. J. J. V., Meulenkamp, J. E. & Dijk, P. M. V., 2005. Extraction of morphotectonic features from DEMs: Development and applications for study areas in Hungary and NW Greece. *International Journal of Applied Earth Observation and Geoinformation*, 7: 163-182.
- Kamykov, A. F., 1957. *These reports on geological exploration in Cam Duong, Lang Coc areas*. Department of Geology and Mineral resource of Vietnam, Ha Noi.
- Keckler, D., 1994. *Surfer for Windows User's Guide*. Golden Software, Inc. USA.
- Keller, E.A. & Pinter, N., 1996. *Active Tectonics: Earthquakes, Uplift and Landforms*. Prentice Hall, New Jersey.
- Khuong The Hung & Golonka, J., 2008. Major plates and events shaping the complex tectonic of Northwest Vietnam. In: Németh, Z. & Plašienka, D. (eds), *SlovTec 08, 6<sup>th</sup> Meeting of the Central European Tectonic studies Group (CETeG) & 13 Meeting of the Czech Tectonic Studies Group (ČTS), 23-26 April 2008, Upohlav, Pieniny Klippen Belt, Slovakia. Proceedings and Excursion Guide*. Dionyz Štúr Institute, Bratislava: 60-61.
- Khuong The Hung, 2009. Tectonics and magmatism in northwest Vietnam. *Geologia 2009-Tom 35-Zeszyt 2/1*: 345-351.
- Khuong The Hung, 2010. Overview of magmatism in Northwestern Vietnam. *Annales Societatis Geologorum Poloniae*, 80: 185-226.
- Koszowska, E; Wolska, A; Zuchiewicz, W., Nguyen Quoc Cuong & Pécskay, Z., 2004. Crustal contamination of Late Neogene basalts in the Dien Bien Phu Basin, NW Vietnam: Some insights from petrological and geochronological studies. *Journal of Asian Earth Sciences*, 29: 1-17.
- Krobicki, M. & Golonka, J., 2006. Caledonian orogeny in Southeast Asia: questions and problems. *Geolines*, 20: 75-78.
- Krobicki, M., & Golonka, J., 2008. Emeishan volcanism of northwestern Vietnam and their connection with SE Asia palaeogeography and Permian/Triassic mass extinction event. *Gondwana 13, Dali, China*: 96-97 (in abstract).
- Lacroix, A., 1933. Contribution à la connaissance de la composition chimique et mineralogique des roches eruptive de l'Indochine. *Bulletin du service géologique de l'Indochine*, 20: 770-776.
- Lacassin, R., Tapponnier, P., Leloup, H., Phan Trong Trinh & Nguyen Trong Yem, 1994. Morphotectonic evidence for active movements along the Red River fault zone. In: *Actes du Colloque Int. sur la sismotectonique et la risque en Asie du Sud Est, 27 Janv.-41994*, Ha Noi, 66-71.
- Lacassin, R., Leloup, H., Phan Trong Trinh & Tapponnier, P., 1998. Unconformity of red sandstones in North Vietnam: field evidence for Indosinian orogeny in northern Indochina. *Terra Nova*, 10:106-111.

- Lan, C. Y., Chung, S. L., Shen, J. J. S., Lo, C. H., Wang, P. L., Tran Trong Hoa, Hoang Huu Thanh & Stanley, A. M., 2000. Geochemical and Sr±Nd isotopic characteristics of granitic rocks from northern Vietnam. *Journal of Asian Earth Sciences*, 18: 267-280.
- Lan, C. Y., Chung, S. L., Lo, C. H., Lee, T. Y., Wang, P. L., Tianjin, H. L. & Dinh Van Toan, 2001. First evidence for Archean continental crust in northern Vietnam and its implications for crustal and tectonic evolution in Southeast Asia. *Geology*, 29: 219–222.
- Leighton, D. G., 2003. *Geological Report on the AMR Nickel-Copper Prospects*, Vietnam. Technical Report.
- Leloup, P. H., Tapponnier, P., Lacassin, R., Searle, M. P., Dailai, Z., Xiaoshan, L., Langshang, Z., Shaocheng, J. & Phan Trong Trinh, 1995. The Ailao Shan-Red River shear zone (Yunnan, China). Tertiary transform boundary of Indochina. *Tectonophysics*, 251: 3-84.
- Leloup, P. H., Amaud, N., Lacassin, R., Kienast, J. R., Harrison, T. M., Phan Trong Trinh, Replumaz, A. & Tapponnier, P., 2001. New constraints on the structure, thermochronology, and timing of the Ailao Shan-Red River shear zone, SE Asia. *Journal of Geophysical Research*, 106 (B4): 6683-6732.
- Leloup, P. H., Tapponnier, P., Lacassin, R. & Searle, M. P., 2006. Discussion on the role of the Red River shear zone, Yunnan and Vietnam, in the continental extrusion of SE Asia. *Journal of the Geological Society*, 163: 1025-1036.
- Le Maitre, R. W., 1989. *A classification of igneous rocks and glossary of Terms: Recommendations of the international Union of Geological Sciences. Subcommission on the systematics of igneous rocks*. Blackwell, Oxford, 193 pp.
- Le Nhu Lai, 1980. Some outlines on tectonics of the Vietnam and studied on the continental shelf geology. *Proceeding and Scientific Reports of the University of Mining and Geology*, Ha Noi, 48-58.
- Le Nhu Lai, 1983. *Studied methods on the neotectonics and their application to analyze tectonics in the western edge and southwestern Pacific Ocean*. Ph.D. Thesis, Freiberg, 120pp.
- Lepvrier, C., Nguyen Van Vuong, Maluski, H., Phan Truong Thi & Vu Van Tich, 2008. Indosinian tectonics in Vietnam. *Comptes Rendus Geosciences*, 340: 94–111.
- Lepvrier, C., Maluski, H., Nguyen Van Vuong, Roques, D., Axente, V. & Rangin, C., 1997. Indosinian NW-trending shear zones within the Truong Son belt (Vietnam): <sup>40</sup>Ar–<sup>39</sup>Ar Triassic ages and Cretaceous to Cenozoic overprints. *Tectonophysics*, 283: 105–127.
- Lepvrier, C., Maluski H., Vu Van Tich, Layreloup, A., Phan Truong Thi & Nguyen Van Vuong, 2004. The Early Triassic Indosinian orogeny in Vietnam (Truong Son Belt and Kontum Massif): implications for the geodynamic evolution of Indochina. *Tectonophysics*, 393: 87-118.
- Le Thac Xinh & Ta Hoang Tinh, 1975. Try to analyse the structure and metallogenic epoches in the southeast Asia by using the global plate tectonics. (In Vietnamese). *Geology (Ha Noi)*, No 118.
- Le Thac Xinh & Nguyen Dang Dat, 1984. The metallogenic zone of Hoang Lien Son block. (In Vietnamese). *Journal of Geology (Ha Noi)*, No 4.

- Le Thac Xinh (ed.) *et al.*, 1990. *Geology and Mineral resources of Vietnam*. (Unpublished report). Department of Geology and Mineral resources Vietnam.
- Le Tu Son, 2000. Focal mechanism of the Ta Khoa, Lai Chau and Muong Luan earthquakes in Northwest of Vietnam. (In Vietnamese). *Journal of Geology (Ha Noi), Series A*, No 22: 355-360.
- Le Tu Son, Nguyen Thi Cam, 2002. Re-evaluation of the depth and the magnitude of earthquakes detected by macroseismic investigations (1903-1962). (In Vietnamese). *Journal of Science and Earth*, 24/3: 227-232.
- Li, Z. X., Li, X. H., Kinny, P. D. & Wang, J., 1999. The breakup of Rodinia: Did it start with a mantle plume beneath South China? *Earth and Planetary Science Letters*, 173: 171–181.
- Li, Z., Zhu, Q. & Gold, C., 2005. *Digital terrain modeling - Principles and Methodology*. CRC Press, 2000 N.W. Corporate Blvd., Boca Raton, Florida 33431, 324pp.
- Manaka, T., Zaw, K. & Meffre, S., 2008. Geological and tectonic setting of Cu-Au deposits in Northern Lao PDR. *Proceeding of the International Symposia on Geoscience Resources and Environments of Asian Terranes*, 254-257.
- Maniar, P. D. & Piccoli, P. M., 1989. Tectonic discriminations of granitoids. *Geological Society of America Bulletin*, 101: 635–643.
- Manthilake, M. A. G. M., Sawada, Y. & Sakai, S., 2008. Genesis and evolution of Eppawala carbonatites, Sri Lanka. *Journal of Asian earth sciences*, 32 (1): 66-75.
- Mark, D. L., 2003. *Dictionary of geology and mineralogy* - 2nd. Ed McGraw-Hill, Professional Publishing, Two Penn Plaza, New York, NY10121-2298.
- Meschede, M. 1986. A method of discriminating between two different types of Mid-oceanic Basalts and Continental Tholeiites with the Nb-Zr-Y Diagram. *Chemical Geology*, 56: 207-218.
- Metcalf, I., 1996a. Gondwanaland dispersion, Asian accretion and evolution of Eastern Tethys. *Australian Journal of Earth Sciences*, 43: 605-623.
- Metcalf, I., 1996b. Pre-Cretaceous evolution of SE Asia. Tectonic Evolution of Southeast Asia. *Geological Society Special Publication, London*, 106: 97-122.
- Metcalf, I., 1998. Palaeozoic and Mesozoic geological evolution of the SE Asian region, multidisciplinary constraints and implications for biogeography. In: Hall, R. & Holloway, J. D. (eds), *Biogeography and Geological Evolution of SE Asia*. Backhuys Publishers, Amsterdam, 25-41.
- Metcalf, I., 2002. Permian tectonic framework and paleogeography of SE Asia. *Journal of Asian Earth Sciences*, 20: 551-566.
- Metcalf, I., 2006. Palaeozoic and Mesozoic tectonic evolution and palaeogeography of East Asian crustal fragments: The Korean Peninsula in context. *Gondwana Research*, 9: 24-46.
- Misra, K. C., 1999. *Understanding mineral deposits*. Kluwer Academic Publishers (Dordrecht, Boston, Mass): 845 pp.
- Mortimer, Z., 2006. The seismicity of Vietnam. *Geoturystyka*, 1: 71-80.
- Nakano, N., Osanai, Y., Nguyen Thi Minh, Miyamoto, T., Hayasaka, Y., Owada, M. & Tran Ngoc Nam, 2006. Discovery of eclogites and related high-pressure rocks

- from the Song Ma Suture zone in North Vietnam. (In Vietnamese). *Journal of Geology (Ha Noi)*, Series A, No296: 16-27.
- Nakano, N., Osanai, Y., Nguyen Thi Minh, Miyamoto, T., Hayasaka, Y. & Owada, M., 2008. Discovery of high-pressure granulite-facies metamorphism in northern Vietnam: constraints on the Permo-Triassic Indochinese continental collision tectonics. *Comptes Rendus Geoscience*, 340: 127-138.
- Nakano, N., Osanai, Y., Miyamoto, T., Hayasaka, Y. & Owada, M., 2008. Crustal Melting During the Indochinese Continental Collision: Evidences from High-pressure Granulite in the Song Ma Suture zone, Vietnam. *Proceedings of the International Symposia on Geoscience Resources and Environments of Asian Terranes (GREAT 2008)*, 4th IGCP 516, and 5th APSEG; November 24-26, 2008, Bangkok, Thailand, 109-111.
- Naldrett, A. J., 2004. *Magmatic sulfide deposits - Geochemistry, geology and exploration*. ISBN 3-540-22317-7 Springer Berlin Heidelberg New York, 727 pp.
- Ngo Thuong San, 1965. Some problems of the tectonics in the northern Vietnam. *Geology* 50: 5-19; 51: 15-25. Ha Noi.
- Ngo Van Liem, Phan Trong Trinh & Hoang Quang Vinh, 2006. The active faults and the maximum earthquakes of the Red River fault zone in Lao Cai-Yen Bai area. *Journal of Earth Science*, 28: 110-120.
- Nguyen Dac Lu, Prokofiev, V. I. & Rokov, A. N., 2005. The resulted researches of gas-fluid inclusions of some copper, gold ore positions in Vien Nam area, Song Da depression. (in Vietnamese). *Journal of Geology (Ha Noi)*, Series A, No 289: 35-41.
- Nguyen Dang Tuc & Nguyen Trong Yem, 2001. Amplitude and rate of slip of the Red River Zone in late Cenozoic. (In Vietnamese, English abstract). *Journal of Earth Science*. 23: 344-353.
- Nguyen Dinh Xuyen, 1994. Status of Seismic Hazard Assessment in Vietnam, in "Global Seismic Hazard Assessment Program (GSHAP), *Proceedings of Workshop on Implementation of Global Seismic Hazard Assessment Program in Central and Southern Asia*, 17-21 October, 1994, Neijing, China, 74-89.
- Nguyen Hoang & Martin, F., 1996. Petrogenesis of Cenozoic Basalts from Vietnam: Implication for Origins of a 'Diffuse Igneous Province'. *Journal of Petrology*, 39: 369-395.
- Nguyen Hoang, Nguyen Dac Lu & Nguyen Van Can, 2004. Effusive rock of Palaeozoic Song Da: Origin and geodynamic Manti. (In Vietnamese). *Journal of Geology (Ha Noi)*, Series A, No 283: 10-20.
- Nguyen Hong Phuong, 1991. Probabilistic assessment of earthquake hazard in Vietnam based on seismotectonic regionalization. *Tectonophysics*, 198: 81-93.
- Nguyen Hong Phuong, 2001. Probabilistic Seismic Hazard Assessment along the Southeastern Coast of Vietnam. *Natural Hazards*, 24: 53-74.
- Nguyen Khac Mao, 1973. Focal mechanism of the Bac Quang earthquake in 1961. *Journal of Organic - Earth sciences (Ha Noi)*, 1-2.
- Nguyen Kim Lap, 1987. Earthquake activity in the northern part of Vietnam, *Progress in Scientific Research* 2, Ha Noi, 13-15.

- Nguyen Kim Lap, 1989. Characteristics of the focus of the Tuan Giao earthquake. *Journal of Geology (Ha Noi), Series A*, No 11: 1-5.
- Nguyen Kim Lap, 1989. The seismographic network in Vietnam. *Acta Geophysica Polonica*, 36: 243-246.
- Nguyen Kim Lap, 1990. Seismicity of the territory of Vietnam. *Acta Geophysica Polonica*, 37: 247-262.
- Nguyen Minh Trung, Tsujimori, T. & Itaya, T., 2006. Hon Vang serpentinite body of the Song Ma fault zone, Northern Vietnam: A remnant of oceanic lithosphere within the Indochina–South China suture, *Gondwana Research*, 9: 225-230.
- Nguyen Minh Trung, Nguyen Dieu Nuong & Itaya, T., 2007. Rb-Sr Isochron and K-Ar ages of igneous rocks from the Sam Nua Depression Zone in Northern Vietnam. *Journal of Mineralogical and Petrological Sciences*, 102: 86-92.
- Nguyen Ngoc Lien (chief author) *et al.*, 1990. *Report on metallogenic investigation and mineral prospecting in the Song Ma and Song Da zones at mean scale and for detail some areas - Two volumes.*(In Vietnamese). Institute of Geology and Mineral resources of Vietnam, Ha Noi, 290 pp.
- Nguyen Nghiem Minh, 1978. *The characteristics of geological structure and its development related to metallogeny in the Northern Vietnam.* Doctor of Science's Thesis, Geology, 143.
- Nguyen Nghiem Minh & Vu Ngoc Hai, 1991. Metallogenic map of Vietnam. (In Vietnamese). Research Institute of Geology and Mineral Resources, Ha Noi.
- Nguyen Thi Ngoc Huong (ed.) *et al.*, 1994. Normal collective samples of Petrology and ore in Vietnam. (Unpublished report). Research Institute of Geology and Mineral Resources, Ha Noi.
- Nguyen Trong Yem, Tokarski, A. K., Tran Trong Hoa, Zuchiewicz, W. A., Tran Tuan Anh, Świerczewska, A., Nguyen Quoc Cuong (eds.), 2009. *The Cenozoic geodynamics of northern Vietnam. Monograph. Special issue dedicated to the 10th anniversary of scientific research cooperation on geology between Vietnam and Poland: 1999–2009.* Publishing House of Natural Science and Technology, Ha Noi, 294 pp.
- Nguyen Trung Chi, 1999. *The petrologic alkaline granitoids in Northwestern Vietnam.* (In Vietnamese). Unpublished Ph.D. Thesis, 155 pp.
- Nguyen Van Chien, 1963. The mafic – ultramafic intrusions and they related to mineral deposits in the Northern Vietnam. (In Vietnamese). *Science news and activity*, No10, Ha Noi.
- Nguyen Van Chien, 1964. The Nui Nua ultramafic block. (In Vietnamese). *Journal of Geology (Ha Noi), Series A*, No 31: 3-5.
- Nguyen Van Hoai (ed.) *et al.*, 1995. Potential assessment of geological economics of uranium mineralization in the Vietnam territory. KT01 program. (Unpublished report). Research Institute of Geology and Mineral Resources, Ha Noi.
- Nguyen Van Hung & Hoang Quang Vinh, 2001. Moving characteristics of the Lai Chau - Dien Bien fault zone during Cenozoic. *Journal of Geology (Ha Noi)*, No 17-18: 1-16.

- Nguyen Van Luong, 1996. Results of the determination of focal mechanism of earthquakes based on the model of the seismic field in Vietnam. (In Vietnamese). *Journal of Geology (Ha Noi)*, No 18 (3): 145-152.
- Nguyen Van Nhan, 1988. Formations of endogenous ore deposits and mineralization in Vietnam. Scientific bulletins of StanislawstaszicAcademy of Mining and Metallurgy, Krakow, Poland, *Geology bulletin*, 38, 134.
- Nguyen Van Nhan & Nguyen Thi Hoang Ha, 2005. Mineral features and formed conditions of Cu-Pb-Zn ore mineralizations in Hoa Binh and adjacent areas. (In Vietnamese). *Journal of Geology (Ha Noi), Series A*, No 291: 38-43.
- Nguyen Van Nhan, 2006. The characteristics of molybdenum types in Vietnam. (In Vietnamese). *Journal of Geology (Ha Noi), Series A*, No 305: 51-62.
- Nguyen Van The (ed.), 1999. *Report on geology and mineral resources of the Luc Yen-Yen Chau sheet group at 1:50,000 scale*. Unpublished report, Ha Noi, 50 pp.
- Nguyen Van Thuat (ed.), 1999. *Report on geology and mineral resources of the Dien Bien sheet group at 1:50,000 scale*. Unpublished report, Ha Noi, 60 pp.
- Nguyen Vinh (ed.), Gulaiev, I. S., Doan Ky Thuy, Nguyen Cong Luong & Phan Truong Thi, 1977. *Geological map of Vietnam at 1:200,000 scale. Yen Bai sheet, with the explanatory note "Geology of the Yen Bai sheet"*. Geological Department of Vietnam, Ha Noi, 129 pp.
- Nguyen Quoc Cuong & Zuchiewicz, W., 2001. Morphotectonic properties of the Lo River fault near Tam Dao in North Vietnam. *Natural Hazards and Earth System Sciences*, 1: 15-22.
- Nguyen Quoc Cuong, 2007. *Late Tertiary to recent tectonics of the Red River fault zone (Vietnam part) based on studies of sedimentary rocks and geomorphic data*. Ph.D. Thesis. Institute of geological sciences, Kraków Research Centre, PolishAcademy of Sciences, 140 pp.
- Nguyen Xuan Bao, 1970. New data on the geological structure of the Van Yen area. (In Vietnamese). *Journal of Geology, Ha Noi, Series A*, No 91-92: 63-67.
- Nguyen Xuan Tung, 1982. Geodynamic evolution of the Vietnam and adjacent area. *Geology and Mineral deposits*, first volume. (In Vietnamese). Vietnam Institute of Geosciences and Mineral resources, 38pp.
- Nguyen Xuan Tung & Tran Van Tri, 1992. *The geologic formations and dynamics of Vietnam*. (In Vietnamese). Institute of Geology and Mineral resources of Vietnam, Ha Noi, 269 pp.
- Nielsen, T. N. & Sylvester, A. G., 1995. Strike-slip basins. In: (Busby, C. J. & Ingersoll, R. V., eds) *Tectonics of sedimentary basins*. Backwell Science, 425-457.
- Pająk, J., Golonka, J., Krobicki, M., Nguyen Van Giang, Zuchiewicz, W., 2006. Exploring the northwestern mountain area of Vietnam. Ancient and modern orogens, geoturistic objects and geological processes. *Geoturystyka*, 1: 27-49.
- Panizza, M., Castaldini, D., Bollettinari, G., Carton, A. & Mantovani, F., 1987. Neotectonic research in applied geomorphological studies. *Zeitschrift für Geomorphologie*, 63: 173-211.
- Pearce, J. A. & Norry, M. J. 1979. Petrogenetic Implications of Ti, Zr, Y, and Nb Variations in Volcanic Rocks. *Contributions to Mineralogy and Petrology*, 69: 33- 47.

- Pearce, J. A., Harris, N. B. & Tindle, A. G., 1984. Trace element discrimination diagrams for the tectonic interpretation of granitic rocks. *Journal of Petrology*, 25: 956-983.
- Pearce, T. H., Gorman, B. E. & Birkett, T. C., 1977. The relationship between major element chemistry and tectonic environment of basic and intermediate volcanic rocks. *Earth and Planetary Science Letters*, 36:121-132.
- Pham Dinh Tuong (ed.), 1999. *Report on geology and mineral resources of the Son La sheet group at 1:50,000 scale*. Unpublished report, Ha Noi.
- Pham Trung Hieu, Chen, F. K., Wang, W., Bui Minh Tam, Tran Binh Nguyen, Tran Xuan Hoa & Li, X. H., 2008. Formation age of granites and metabasalts in the Song Ma Belt of northwestern Vietnam and their tectonic implications. *Gondwana 13*, Dali, China (abstract),p.163.
- Pham Trung Hieu, Chen, F. K., Zhu, X. Y., Wang, W., Nguyen Thi Bich Thuy, Bui Minh Tam & Nguyen Quang Luat, 2009. Zircon U-Pb ages and Hf isotopic composition of the Po Sen granite in northwestern Vietnam. (In Chinese, English abstract). *Acta Petrologica Sinica*, 25(12): 3141-3152.
- Phan Cu Tien (ed.), Tran Quoc Hai, Le Dinh Huu, Phan Viet Ky, Bui Phu My & Nguyen Vinh, 1977. *Legend of the Northwest Vietnam geological map sheet series*. Publishing House of Science and Technology, Ha Noi: 9-61.
- Phan Cu Tien (ed.), 1989. *Geology of Kampuchea, Laos and Vietnam. (Explanatory note to the geological map of Kampuchea, Laos and Vietnam at 1/1000000 scale)*, Institute for Information and Documentation of Mines and Geology, Ha Noi, 149 pp.
- Phan Son (ed.), Dao Dinh Thuc, Nguyen Duc Thang & Tran Van Ty, 1974 (compiled), 1978 (revised). *Geological map of Vietnam at 1:200,000 scale. Son La sheet, with the explanatory note "Geology of the Son La sheet"*. Geological Department of Vietnam, Ha Noi, 118 pp.
- Phan Trong Trinh, Lacassin, R., Tapponnier, P., Leloup, P. H. & Nguyen Trong Yem, 1993. Evidence for active strike-slip movements in Northwestern Vietnam. *Terra Abstracts, Abstract Suppl. No. 1 to Terra Nova*, 5: 265.
- Phan Trong Trinh, Tran Van Tri, Nguyen Can, Dang Van Bat, Pham Huy Tien, Van Duc Chuong, Hoang Quang Vinh, Le Thi Lai, Doan Van Tuyen, Tran Trong Hue, Nguyen Van Hung, Nguyen Dich Dy, Tran Dinh To, Nguyen Tran Hung, Doan Kim Thuyen, Huynh Tuoc, 1999. Active tectonics and seismic hazards in Son La hydropower dam (North Vietnam), *Journal of Geology, Series B*, No 13-14: 19-32.
- Phan Trong Trinh & Hoang Quang Vinh, 2004. Remote sensing in the study of active tectonics and seismic hazards in Son La hydropower dam. International Symposium on Geoinformatics for Spatial Infrastructure Development in Earth and Allied Sciences. *Public Knowledge Project 2002*, 7pp.
- Phan Trong Trinh, Hoang Quang Vinh, Leloup H., Giuliani G., Garnier V., Tapponnier P., 2004. *Cenozoic deformation, thermodynamic evolution, slips mechanism of Red River Shear Zone and ruby formation*. (In Vietnamese). Basic research program 2001-2003, Ha Noi: 5-74.

- Phan Thi Kim Van, 2006. The Lai Chau-Dien Bien neotectonic fault zone and its acting manifestation by moderate local earthquakes. *Journal of Geology (Ha Noi), Series B*, No 27: 30-39.
- Pirajno, F., 2004. Hotspots and mantle plumes: global intraplate tectonics, magmatism and ore deposits. *Mineralogy and Petrology*, 82: 183–216.
- Ramsay, J. & Huber, M., 1987. The techniques of modern structural geology. *Volume 2: folds and fractures*. Academic Press Limited, London.
- Rangin, C., Klein, M., Roque, D., Le Pichon, X. & Le Van Trong, 1995. The Red River fault system in the Tonkin Gulf, Vietnam. *Tectonophysics*, 243: 209-222.
- Schoenbohm, L. M., Burchfiel, B. C., Chen, L. & Yin, J., 2006. Miocene to present activity along the Red River fault, China, in the context of continental extrusion, upper-crustal rotation, and lower-crustal flow. *Geological Society of America Bulletin*, 118: 672-688.
- Serdusenko, D., 1969. Original series of phosphoric and apatite deposits. (In Vietnamese). *Journal of Geology (Ha Noi), Series A*, No PT: 46-49.
- Shouxin, Z. & Yongyi, Z., 1991. The geology of China. In: Moullade, M. & Nairn, A. E. M. (eds), *The Palaeozoic. A The Phanerozoic Geology of the World I*. Elsevier, Amsterdam: 219-274.
- Smith, M. J. & Clark, C. D., 2005. Methods for the visualization of digital elevation models for landform mapping. *Earth Surface Processes and Landforms*, 30(7): 885-900.
- Snelgrove, A. K., 1971. Metallogeny and the new global tectonics. *Seismological Soc. Amer. Bull.*, 61(2): 132-149.
- Staude, J. M. G. & Barton, M. D., 2001. Jurassic to Holocene tectonics, magmatism, and metallogeny of northwestern Mexico. *Geological Society of America Bulletin*, 113 (10): 1357-1374.
- Struska, M., 2008. *Neogeńsko-Czwartorzędowy rozwój strukturalny kotliny orawskiej w świetle badań geologicznych, geomorfologicznych oraz teledetekcyjnych*. Ph.D. thesis. AGH University of Science and Technology, 150 pp.
- Sun, S. & McDonough, W. F., 1989. Chemical and isotopic systematics of ocean basalts: implications for mantle composition and processes. In: Saunders, A. D. & Norry, M.J. (eds.) *Magmatism in the Ocean Basin*. *Geological Society of London Special Publication*, 42: 313-345.
- Tapponnier, P., Peltzer, G., Le Dain, A. Y., Armijo, R. & Cobbold, P., 1982. Propagating extrusion tectonics in Asia: New insights from simple experiments with plasticine. *Geology*, 10: 611-616.
- Ta Viet Dung (ed.) et al., 1968. *Detailed exploration of Sin Quyen copper mineralization in Lao Cai area*. (Unpublished report). Research Institute of Geology and Mineral Resources, Ha Noi.
- To Van Thu (ed.), 1996. *Report on geology and mineral resources of the Phong Tho sheet group at 1:50,000 scale*. Unpublished report, Ha Noi.

- Tokarski, A. K. & Świerczewska, A., 2005. Neofractures versus inherited fractures in structural analysis: A case study from Quaternary fluvial gravels (Outer Carpathians, Poland). *Annales Societatis Geologorum Poloniae*, 47: 147-161.
- Tokarski, A. K. & Zuchiewicz, W., 1998. Fractured clasts in the Domański Wierch series: Contribution to structural evolution of the Orava Basin (Carpathians, Poland) during Neogene through Quaternary times. (In Polish, English summary). *Przegląd Geologiczny*, 46: 62–66.
- Tran Duc Luong, 1970. Indosinian structure of the northern Vietnam and its tectonic history evolution. *Geology, No 91-92*: 46-57; 42-59. Ha Noi.
- Tran Duc Luong & Nguyen Xuan Bao, 1988. *Geological map of Vietnam at 1:500,000 with a summary explanatory note*. Geological Department of Vietnam, Ha Noi, 52 pp.
- Tran Duc Luong & Nguyen Xuan Bao (eds), 1995. *Geology of Vietnam - two volumes*. (In Vietnamese). Geological Department of Vietnam, Ha Noi. 737 pp.
- Tran Ngoc Nam, 1998. Thermotectonic events from Early Proterozoic to Miocene in the Indochina craton: implication of K±Ar ages in Vietnam. *Journal of Asian Earth Sciences*, 16: 475-484.
- Tran Ngoc Nam, Hyodo, H., Itaya, T., Matsuda, T., 2002.  $^{40}\text{Ar}/^{39}\text{Ar}$  single grain dating and mineral chemistry of hornblendes South of the Red River Shear Zone (Vietnam): New Evidence for Early Proterozoic Tectonothermal Event. *Gondwana Research*, 5(4): 801 - 811.
- Tran Ngoc Nam, Sano, Y. & Chung, S. L., 2003. New evidences of 2840 Ma from Shrimp U-Pb zircon dating for Archean age of the Ca Vinh complex and tectonothermal implication. (In Vietnamese, English summary). *Journal of Geology (Ha Noi), Series A*, No 273: 21-24.
- Tran Ngoc Nam, 2006. U-Pb zircon age of the gneiss rocks from Con Voi mountain range: the Cenozoic metamorphism-deformation overprinted in Neoproterozoic rocks. (In Vietnamese). *Journal of Geology (Ha Noi), Series A*, No 296: 1-6.
- Tran Quoc Hai, 1967. Some options about the origin of Po Sen complex. (In Vietnamese). *Journal of Geology (Ha Noi), Series A*, No 75: 8-16, & No 76: 4-9.
- Tran Trong Hoa, Nguyen Trong Yem, Ngo Thi Phuong, Vu Van Van, Hoang Huu Thanh, Tran Quoc Hung, Bui An Nien, Hoang Viet Hang, Poliakov, G. V., Balykin, P. A., Panina, L. I. & Tran Tuan Anh, 1995. Magnesian-ultrapotassic magmatic rocks and lamproite problem in the Northwest Vietnam. *Journal of Geology (Ha Noi), Series B*, No 5-6: 412-419.
- Tran Trong Hoa, 1996. Magmatic activities of Northwestern Truong Son belt in Mesozoic-Cenozoic. Material substances, forming conditions and mineral resource potential. *Journal of Science of the Earth (Vietnam)*, 18 (3): 218-227.
- Tran Trong Hoa, Hoang Huu Thanh, Tran Tuan Anh, Ngo Thi Phuong & Hoang Viet Hang, 1998. Permian-Triassic titanium-high basaltoid associations of the Song Da rift- material composition and geodynamic forming conditions. (In Vietnamese, English summary). *Journal of Geology (Ha Noi), Series A*, No 244: 7-15.

- Tran Trong Hoa, Hoang Huu Thanh, Ngo Thi Phuong, Tran Tuan Anh, Hoang Viet Hang, 1999. Potassic alkaline magmatic rocks in Northwest Vietnam: manifestation of late Palaeogene intraplate extension. (In Vietnamese, English summary). *Journal of Geology (Ha Noi), Series A*, No 250:7-14.
- Tran Trong Hoa, Tran Tuan Anh, Ngo Thi Phuong, Phan Luu Anh & Hoang Huu Thanh, 2000. Origin of ultramafic rocks in the Red River zone on the basis of new results of mineralogical, geochemical and isotopic analyses. *Journal of Geology (Ha Noi), Series B*, No 15-16: 62-75.
- Tran Trong Hoa, Tran Tuan Anh, Ngo Thi Phuong, Pham Thi Dung, Tran Viet Anh, Izokh, A. E., 2004. *Mezozoic-Cenozoic magmatism of the Phan Si Pan-Song Hong uplifted block in Northwest Vietnam*. (In Vietnamese). Basic research program 2001-2003, Ha Noi, 297-371.
- Tran Trong Hoa, Tran Tuan Anh, Ngo Thi Phuong, Pham Thi Dung, Tran Viet Anh, 2005. Permian-Triassic magmatism of Vietnam and their potential of associated precious metals (Pt, Au). Proceedings of the scientific conference: 60<sup>th</sup> anniversary of Vietnam Geology 10, 63-79.
- Tran Trong Hoa, Borisenko A. S., Tran Tuan Anh, Izokh A. E., Ngo Thi Phuong, 2006. Cu-Mo-Au porphyry type in Sa Thay area in the west of Kon Tum block. *Journal of Geology (Ha Noi), Series B*, No 28: 71-83.
- Tran Trong Hoa, Tran Tuan Anh, Ngo Thi Phuong, Pham Thi Dung, Tran Van Anh, Andrey E. I., Alexander S. B., Lan C. Y., Chung S. L., Lo C. H., 2008a. Permo-Triassic intermediate-felsic magmatism of the Truong Son belt, eastern margin of Indochina, *Comptes Rendus Geoscience* 340: 112–126.
- Tran Trong Hoa, Izokh, A. E., Polyakov, G. V., Borisenko, A. S., Tran Tuan Anh, Balykin, P. A., Ngo Thi Phuong, Rudnev, S. N., Vu Van Van & Bui An Nien, 2008b. Permo-Triassic magmatism and metallogeny of Northern Vietnam in relation to the Emeishan plume. *Russian Geology and Geophysics*, 49: 480–491.
- Tran Tuan Anh, Tran Trong Hoa & Pham Thi Dung, 2002. Granites of the Ye Yen Sun complex and their significance in tectonic interpretation of the early Cenozoic stage in West Bacbo. *Journal of Geology (Ha Noi), Series B*, No19-20:43-53.
- Tran Tuan Anh, Tran Trong Hoa, Lan, C. Y., Chung, S. L., Lo, C. H., Wang, P. L., Lee, T. Y. & Mertzman S. A., 2003. Geochemical and Nd-Sr isotopic constraints on the genesis of Mesozoic alkaline magmatism in the Tu le basin, northern Vietnam. *European Geophysical Society, Geophysical Research Abstracts* 5: 02096.
- Tran Tuan Anh, Tran Trong Hoa, Lan, C. Y., Chung, S. L., Lo, C. H., Wang, P. L. & Mertzman, S. A., 2004. Mesozoic bimodal alkaline magmatism in the Tu le basin, north Vietnam: Constraints from geochemical and isotopic significances. *Journal of Geology (Ha Noi), Series B*, No24: 29-39.
- Tran Van Thang & Van Duc Tung, 2006. Characteristics of the Pliocene-Quaternary tectonics in northwest Vietnam region. *VNU. Journal of Science, National Sciences & Technology, T.XXII, No 2A*, 86-99.

- Tran Van Tri (ed.), 1979 (1977 in Vietnamese). *Geology of Vietnam, (the North part)*. Explanatory note to the geological map on 1:1,000,000 scales. Ha Noi, Science and Technology Publishing House, 354 pp. (In Vietnamese), 78 pp. (In English).
- Tran Van Tri, 1994. Geotectonic framework of Vietnam and adjacent area. *Proceedings 29th CCOP Annual session*, Ha Noi, Vietnam. CCOP, Bangkok, 2: 183-189.
- Tran Van Tri (Editor in chief) *et al.*, 2000. *Mineral resources of Vietnam*. Ha Noi, Department of Geology and Minerals of Vietnam. Publish House, 354 pp.
- Tran Xuan Duc, 1963. Summary of Lead-Zinc deposits Origin in North Vietnam.(In Vietnamese). *Journal of Geology (Ha Noi), Series A*, No 17: 4-5.
- Tran Xuyen, Phan Xuan Anh & Phan Viet Soai, 1983. Introduction to the geological mapping and prospection for mineral resources at 1:50,000 scale in the Hoa Binh-Tan Lac map sheets. (In Vietnamese). *Journal of Geology (Ha Noi), Series A*, No166: 20-22.
- Twiss, R. J. & Moores, E. M., 1992. *Structural geology*. W. H. Freeman and Company, New York, 532 pp.
- Vu Khuc & Bui Phu My (eds), 1989. *Geology of Vietnam. Volume 1 – Stratigraphy*. Geological Department of Vietnam, Ha Noi, 378 pp.
- Wang, C. Y., Zhou, M. F. & Qi, L., 2007. Permian flood basalts and mafic intrusions in the Jinping (SW China)-Song Da (northern Vietnam) district: Mantle sources, crustal contamination and sulfide segregation. *Chemical Geology*, 243: 317-343.
- Wang, J., Yin, A., Harrison, T. M., Grove, M., Zhou, J., Zhang, Y., & Xie, G., 2003. Thermochronological constraints on two pulses of Cenozoic high-K magmatism in eastern Tibet. *Science in China, Series D*, 46(7): 719-729.
- Wang, P. L., Lo, C. H., Chung, S. L., Lan, C. Y., Lee, T. Y. & Lee H., 1999. Early Tertiary uplifting of the Tibet plateau: Evidence from  $^{40}\text{Ar}/^{39}\text{Ar}$  thermochronological data for granitoid in northern Vietnam. *Eos*, 80:1043-1044.
- Weldon, R., Sieh, K., Zhu, Ch. N., Han, Y., Yand, J. W. & Robinson, S., 1994. Slip rate and recurrence interval of earthquakes on the Hong He (Red River) fault, Yunnan. *PRC. Proc. IWSSH-SEA, 27 Jan.-4. Feb. 1994*, Ha Noi, 244-248.
- Winter, T., & Costaz, J., 1993. *Hoa Binh area. Geological mapping*. UNDP Program VIE/92/035. Coyne et Bellier, Paris, 51 ms. Pp. (unpublished report).
- Ollier, C. D., 1981. *Tectonics and landforms. Geomorphology texts*, 6. Longman Group Limited, New York, 324 pp.
- Onorati, G., Ventura, R., Poscolieri, M., Chiarini, V. & Crucilla, U., 1992. The Digital Elevation Model of Italy for geomorphology and structural geology. *Catena*, 19(2): 147-178.
- Zaw, K., Peters, S. G., Cromie, P., Burrett, C. & Hou, Z., 2007. Nature, diversity of deposit types and metallogenic relations of South China. *Ore Geology Reviews*, 31: 3–47.
- Zhang, L. S. & Schärer, U., 1999. Age and origin of magmatism along the Cenozoic Red River shear belt, China. *Contributions to Mineralogy and Petrology*, 134: 67-85.

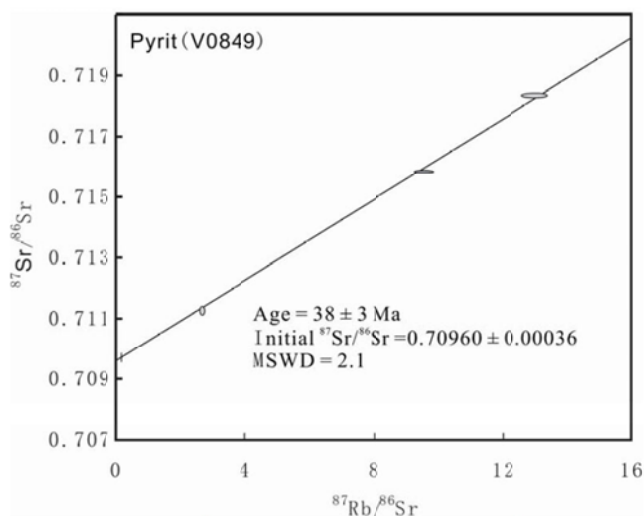
- Zhang, Q., Zhou, D. J., Zhao, D. S., Huang, Z. X., Han, S., Jia, A. Q. & Dong, J. Q., 1994. Ophiolites of the Hengduan Mountains, China: Characteristics and tectonic settings. *Journal of Southeast Asian Earth Sciences*, 9: 335–344.
- Zhu, J., Zhan, W., Qiu, X., Xu, H. & Tang, C., 2004. Earthquake focal mechanism and its tectonic significance along the two sides of the Red River fault zone. *Geotectonica et Metallogenia*, 28(1): 79-92.
- Zuchiewicz, W., Nguyen Quoc Cuong, Bluszcz, A., Michalik, M., 2004. Quaternary sediments in the Dien Bien Phu fault zone, NW Vietnam: a record of young tectonic processes in the light of OSL-SAR dating results. *Geomorphology*, 60: 269–302.
- Żelaźniewicz, A., Tran Trong Hoa & Fanning, M., 2005. Continental extrusion along the Red River Shear Zone, NW Vietnam: New structural and geochronological data. *Geolines*, 19: 121-122.
- <http://earth.google.com>  
<http://www.neic.cr.usgs.gov/>  
<http://www.isc.ac.uk>  
<http://www.globalcmt.org/>  
<http://iisee.kenken.go.jp/net/hara/Vietnam.htm>  
<http://demonstrations.wolfram.com/earthquakefocalmechanism>

## APPENDIX

### Appendix 1: Geochronological data and chemical compositions of ore deposits, size and content of orebodies, and their statistical distribution, list of ore deposits and occurrences in relation to host rocks of the NWVN.

Table 1. Rb-Sr isochronal age of pyrite mineral for the V0849 sample; in which MSWD is an average value of weight, the O Quy Ho deposit of Northwestern Vietnam

No	Mineral	Point in analysis	Rb [µg/g]	Sr [µg/g]	<sup>87</sup> Rb/ <sup>86</sup> Sr	<sup>87</sup> Sr/ <sup>86</sup> Sr	Error (2σ)
V0849	Pyrite	1	0,037	0,041	2,58	0,71127	0,00011
	Pyrite	2	0,040	1,266	0,09	0,70972	0,00012
	Pyrite	3	1,437	0,437	9,52	0,71583	0,00004
	Pyrite	4	1,652	0,369	12,98	0,71835	0,00006



The process sample, chemical analysis, and isotope dating are carried out at the Isotope Geochemistry Laboratory - Institute of Geology and Geophysics Chinese Academy of Sciences.

Table 2. Size and content of orebodies of the Sin Quyen copper mine

No	Orebodies	Length (m)	Depth (m)	Thick (m)	Cu (%)
1	1	2.875	395	7.79	1.16
2	1a	2.185	408	6.29	1.23
3	2	2.223	278	4.39	1.19
4	3	2.129	568	13.94	1.03
5	4	1.480	314	6.43	0.88
6	5	1.070	319	3.74	0.68
7	6	508	344	3.40	0.62
8	7	1.005	471	9.63	0.71
9	10	445	555	3.52	0.78
10	12	330	279	3.67	1.31
11	8	1.580	385	2.11	0.43
12	9	1.070	345	4.19	0.40
13	11	820	497	2.30	0.50
14	13	242	200	8.01	0.28

Table 3. Size of the main ore bodies of the Dong Pao mine

No	Ore body	Sizes (m)		
		Length	Width	Depth
1	F7	900-1000	200	300-400
2	F3	700	300	200
3	F14	800	600	200
4	F6	120	24	30
5	F8	160	24	40
6	F9	560	300	140
7	F10	680	200	170
8	F25	550	100	140
9	F16	540	190	135
10	F17	460	200	115
11	F18	220	55	55
12	F23	500	55	125

Table 4. Ore chemical compositions of the Dong Pao mine

No	Oxides	Content of ore type (%)		
		Race earth-barite-fluorite	Race earth-barite	Race earth-fluorite
1	SiO <sub>2</sub>	9.0300	10.9300	10.7400
2	TiO <sub>2</sub>	0.1590	0.2140	0.1220
3	Fe <sub>2</sub> O <sub>3</sub>	1.5300	2.6700	2.3800
4	Al <sub>2</sub> O <sub>3</sub>	0.5400	2.0500	1.7800
5	MnO	0.9430	1.3670	0.4910
6	CaO	24.7200	4.1100	35.7300
7	MgO	0.2800	0.300	0.2800
8	BaO	24.4800	35.6200	18.4500
9	Nb <sub>2</sub> O <sub>3</sub>	0.0250	0.0400	0.0210
10	TR <sub>2</sub> O <sub>3</sub>	10.8400	15.5900	3.7000
11	ThO <sub>2</sub>	0.0160	0.0180	0.0160
12	U <sub>3</sub> O <sub>8</sub>	0.0065	0.0043	0.0077
13	BeO	0.0025	0.0018	0.0044
14	ZnO	0.0002	0.0040	-
15	SrO	0.8400	0.6200	0.5200
16	PbO	0.3500	0.4600	0.3800
17	CuO	0.0110	0.0250	0.0140
18	Na <sub>2</sub> O	0.0600	0.0500	0.0080
19	K <sub>2</sub> O	0.500	0.1200	0.4100
20	P <sub>2</sub> O <sub>5</sub>	0.2970	0.5190	0.5410
21	SO <sub>3</sub>	12.8700	19.5100	9.6300
22	CO <sub>2</sub>	3.2200	302800	0.4100
23	F	15.9400	2.8800	23.8600
24	H <sub>2</sub> O	0.3300	0.7000	0.3600
25	H <sub>2</sub> O <sup>+</sup>	0.3100	1.0800	0.4300

Table 5. Distribution Rare earth elements of Rare earth oxides of Dong Pao mine

Ore type	Oxide contents (%)															Y <sub>2</sub> O <sub>3</sub> /TR <sub>2</sub> O <sub>3</sub>
	La <sub>2</sub> O <sub>3</sub>	CeO <sub>2</sub>	Pr <sub>6</sub> O <sub>11</sub>	Nd <sub>2</sub> O <sub>3</sub>	Sm <sub>2</sub> O <sub>3</sub>	Eu <sub>2</sub> O <sub>3</sub>	Gd <sub>2</sub> O <sub>3</sub>	Tb <sub>2</sub> O <sub>3</sub>	Dy <sub>2</sub> O <sub>3</sub>	Ho <sub>2</sub> O <sub>3</sub>	Er <sub>2</sub> O <sub>3</sub>	Tm <sub>2</sub> O <sub>3</sub>	Yb <sub>2</sub> O <sub>3</sub>	Lu <sub>2</sub> O <sub>3</sub>	Y <sub>2</sub> O <sub>3</sub>	
Race earth - fluorite	40.91	6.38	0.503	1.220	0.0923	0.0195	0.0333	0.0028	0.0143	0.0020	0.0050	0.0006	0.0030	0.0004	0.1030	1.11
	5.32	7.69	0.593	1.470	0.1240	0.289	0.0486	0.0043	0.0218	0.0029	0.0062	0.0007	0.0031	0.0004	0.0102	1.34
Race earth-fluorite-barite	4.85	5.81	0.420	0.890	0.0400	0.0074	0.0103	0.0007	0.0031	0.0004	0.0008	0.0001	0.0005	0.0001	0.0185	0.50
	2.46	2.76	0.185	0.408	0.244	0.0049	0.0075	0.0006	0.0035	0.0006	0.0065	0.0002	0.0013	0.0002	0.00243	0.60
	4.54	5.28	0.557	1.640	0.1480	0.0327	0.0568	0.0044	0.0211	0.0030	0.0058	0.0007	0.0031	0.0005	0.0900	0.94
	7.01	9.25	0.835	2.240	0.1820	0.0391	0.696	0.0056	0.0265	0.0004	0.0079	0.0010	0.0043	0.0006	0.1420	1.49
Race earth-barite	11.89	17.50	1.400	3.730	0.3160	0.0818	0.691	0.0069	0.0324	0.0052	0.0103	0.0012	0.0046	0.0007	0.2130	1.36
	2.40	16.40	1.390	3.780	0.2910	0.0579	0.0990	0.0071	0.0340	0.0044	0.0101	0.0012	0.0056	0.0008	0.1920	1.31
	12.25	14.30	1.120	3.020	0.2520	0.0452	0.0723	0.0051	0.0249	0.0031	0.0068	0.0008	0.0001	0.0005	0.1000	0.13
	12.95	15.10	1.310	3.630	0.2820	0.0538	0.0838	0.055	0.0251	0.0031	0.0060	0.0007	0.0026	0.0004	0.1170	1.26
	8.73	13.35	1.020	2.570	0.2200	0.0425	0.0634	0.0044	0.0189	0.0024	0.0040	0.0005	0.0017	0.0002	0.0763	1.26
	12.10	18.15	1.320	3.450	0.2770	0.0504	0.0703	0.0046	0.0202	0.0026	0.0048	0.0006	0.0023	0.0003	0.1090	1.13

Table 6. Statistical content characteristics of main compositions of ore types in Dong Pao mine

Ore type	Parameter study	Average content (%)	Variance ( $\sigma^2$ )	Coefficient of variation V (%)	Distributed model
Race earth-fluorite	TR <sub>2</sub> O <sub>3</sub>	2.87	3.05	60.88	Gamma
	BaSO <sub>4</sub>	6.63	6.05	38.70	
	CaF <sub>2</sub>	45.32	15.37	8.86	
	Y <sub>2</sub> O <sub>3</sub>	0.09	0.0019	49.41	
Race earth-fluorite-barite	TR <sub>2</sub> O <sub>3</sub>	4.14	5.18	58.10	
	BaSO <sub>4</sub>	21.45	173.19	61.34	
	CaF <sub>2</sub>	20.06	129.28	56.67	
	Y <sub>2</sub> O <sub>3</sub>	0.22	0.04	85.61	
Race earth-barite	TR <sub>2</sub> O <sub>3</sub>	5.37	13.62	68.65	
	BaSO <sub>4</sub>	28.28	499.08	77.51	
	CaF <sub>2</sub>	8.36	51.55	85.84	
	Y <sub>2</sub> O <sub>3</sub>	0.28	0.03	56.00	

Table 7. List of ore deposits and occurrences, their relationship to host rocks in NWNV

N°	Name of deposits, occurrences	Main (associated) minerals	Size	Host and country rocks		Genesis	Metallogenic zone
				Formation	Complexes		
1	KipTuoc	Fe	Sma.	Sinh Quyen		Mesomatics	Red river
2	Ben Den	Py	Occ.	Sinh Quyen		Mesomatics	Red river
3	Koc Tang	Gra	Occ.	Ngoichi		Mesomatics	Red river
4	Lang Vang	Py	Occ.	Sinh Quyen		Mesomatics	Red river
5	Lang Loat	Py	Occ.	Sinh Quyen		Mesomatics	Red river
6	Van Son	Py	Occ.	Cam Duong		Mesomatics	Red river
7	Lang Bat	Gra	Occ.	Ngoichi		Mesomatics	Red river
8	Lang Bong	Gra	Occ.	Ngoichi		Mesomatics	Red river
9	Song Do	Py	Occ.	Cam Duong		Mesomatics	Red river
10	Lang Lech	Fe	Sma.	Sinh Quyen		Mesomatics	Red river
11	Tam Dinh	Fe	Occ.	Sinh Quyen		Mesomatics	Red river
12	Ta Phoi	Cu	Occ.		Po Sen	Hydrothermal or Porphyr?	Red river
13	Lang Coc	Py	Occ.	Da Dinh		Hydrothermal	Red river
14	Sa Pa	Py	Occ.	Da Dinh		Hydrothermal	Red river
15	Dong Pao	TR (Bar,Fl)	Lar.	Dong Giao	Pu Sam Cap	Hydrothermal	Red river
16	Pu Sam Cap	K,Na	Occ.		Pu Sam Cap	Magma	Red river
17	LaoTyT.Chay	Mo	Occ.		West Ye Yen Sun	Hydrothermal	Red river
18	Y Lin Ho	U,TR	Occ.	Ban Nguon	Sinh Quyen	Hydrothermal	Red river
19	Ma Quay Ho	Mo	Occ.		West Ye Yen Sun	Hydrothermal	Red river
20	Tay Ang Ping	Cu	Occ.		West Ye Yen Sun	Hydrothermal	Red river
21	Ban Khoang	Mo	Occ.		West Ye Yen Sun	Hydrothermal	Red river
22	O Quy Ho	Mo	Lar.		West Ye Yen Sun	Hydrothermal	Red river
23	TNO Quy Ho	Mo	Occ.		West Ye Yen Sun	Hydrothermal	Red river
24	Minh Luong	Fe	Occ.		West Ye Yen Sun	Hydrothermal	Red river
25	Lang Sung	Py	Occ.		East Ye	Hydrothermal	Red river

N°	Name of deposits, occurrences	Main (associated) minerals	Size	Host and country rocks		Genesis	Metallogenic zone
				Formation	Complexes		
					Yen Sun		
26	Ma Thi Ho	Py	Occ.	Song Ma		Epithermal	Ma river
27	NaPeo	Py	Occ.	Song Ma		Epithermal	Ma river
28	Han Cho	Pb-Zn	Occ.	Banphiet		Hydrothermal	Ma river
29	Nam Gin	Atl	Occ.	Yen Duyet		Volcanic sediments	Ma river
30	Xa Nhe	Pb-Zn	Occ.	Banphiet		Hydrothermal	Ma river
31	Na Tong	Pb-Zn	Occ.	Banphiet		Hydrothermal	Ma river
32	Hua Va	Au	Occ.	Nam Pia		Hydrothermal	Ma river
33	Ban Cheo	Au	Occ.	Huoi Hao		Hydrothermal	Ma river
34	LongHom	Au	Occ.	Nam Pia		Hydrothermal	Ma river
35	Cong Noi	Au	Occ.	Cam Thuy		Hydrothermal	Ma river
36	BoCam	Au	Occ.	Cam Thuy		Hydrothermal	Ma river
37	Ban Lam	Au	Occ.	Song Ma		Hydrothermal	Ma river
38	NaHem	Cu	Occ.	Banphiet		Hydrothermal	Ma river
39	Pac Ma	Au	Occ.	Huoi Hao		Hydrothermal	Ma river
40	Bo Xinh	Py	Occ.	Huoi Hao		Hydrothermal	Ma river
41	Bo Keo	Cu	Occ.	Huoi Hao		Hydrothermal	Ma river
42	Pac Nam	Au	Occ.	Huoi Hao	Chieng khuong	Hydrothermal	Ma river
43	Ban Thon	Au	Occ.	Huoi Hao		Hydrothermal	Ma river
44	Ta Lenh	Pb-Zn (Au)	Occ.		Phia Bioc	Hydrothermal	Sam Nua
45	Nam Ngam	Pb-Zn	Occ.		Phia Bioc	Hydrothermal	Sam Nua
46	Na Phat	Pb, Bar	Occ.		Dien Bien	Hydrothermal	Sam Nua
47	Pac Khin	Au	Occ.		Song Ma	Hydrothermal	Sam Nua
48	Na San	Au	Occ.		Dien Bien	Hydrothermal	Sam Nua
49	Muong Luan	Au	Occ.		Dien Bien	Hydrothermal	Sam Nua
50	Sam Kha	Pb-Zn	Occ.	Suoi Bang		Hydrothermal	Sam Nua
51	Ban Lai	Py	Occ.	Vien Nam		Hydrothermal	Da river
52	HuoiLang	Cu	Occ.	Vien Nam		Hydrothermal	Da river
53	CocPhat	Cu	Occ.	Vien Nam		Hydrothermal	Da river
54	Muong Trai	Py	Occ.	Muong Te		Hydrothermal	Da river
55	Ban Dua	Au	Occ.	Muong Te		Hydrothermal	Da river
56	Nam BanTen	Au	Occ.	Vien Nam		Hydrothermal	Da river
57	Hua Non	Au	Occ.	Vien Nam		Hydrothermal	Da river
58	Ban Penh	Au	Occ.	Vien Nam		Hydrothermal	Da river
59	Ta Phinh	Alt	Occ.	Cam Thuy		Volcanic sediments	Da river
60	Bac Na	Alt	Occ.	Cam Thuy		Volcanic sediments	Da river
61	BanMua	Cu	Occ.	Vien Nam		Hydrothermal	Da river
62	Ban Pang	Alt	Occ.	Dong Giao		Volcanic sediments	Da river
63	Ya Sui Thang	Pb (Zn)	Occ.	Dong Giao		Hydrothermal	Da river
64	T. Sin Thang	Pb (Zn)	Occ.	Dong Giao		Hydrothermal	Da river
65	Then Sin	U,TR	Occ.	Pu Tra		Hydrothermal	Da river
66	QuangTanTrai	Cu	Occ.	Bac Son		Hydrothermal	Da river
67	Nam Kham	Pb	Occ.	Tan Lac		Hydrothermal	Da river
68	Nam Nguyen Trai	Pb (Zn)	Occ.	Bac Son		Hydrothermal	Da river
69	NamTia	Cu	Occ.	Vien Nam		Hydrothermal	Da river
70	NamNga	Cu	Occ.	Vien Nam		Hydrothermal	Da river
71	Can Ty	Pb (Zn)	Occ.	Cam Thuy		Hydrothermal	Da river
72	Lang Sang	Alt	Occ.	Yen Duyet		Volcanic sediments	Da river
73	Pa Ty Leng	Alt	Occ.	Cam Thuy		Volcanic sediments	Da river

N°	Name of deposits, occurrences	Main (associated) minerals	Size	Host and country rocks		Genesis	Metallogenic zone
				Formation	Complexes		
74	Na Ca	Cu	Occ.	Conoi		Epithermal	Da river
75	Ban Mong	Ni,Cu(Co)	Sma.	Ban Cai	Ban Xang	Comagma and hydrothermal	Da river
76	ChimThuong	Cu(Pb)	Occ.	Vien Nam	Ban Xang	Hydrothermal	Da river
77	Ban Khoa	Ni,Cu(Co)	Sma.		Ban Xang	Comagma and hydrothermal	Da river
78	Ban Phuc	Ni,Cu(Co)	Lar.	Ban Cai	Ban Xang	Comagma and hydrothermal	Da river
79	Ban Trang	Ni,Cu(Co)	Sma.	Ban Cai	Ban Xang	Comagma and hydrothermal	Da river
80	NaLui	Cu	Occ.	Conoi		Epithermal	Da river
81	Nam Say	Au	Occ.		Tu Le	Hydrothermal	Tu Le
82	Meo Sa Phin	Au	Occ.	Tram Tau		Hydrothermal	Tu Le
83	Nam Kim	Pb-Zn	Occ.		Ngoi Thia	Hydrothermal	Tu Le
84	TuSan	Pb-Zn	Occ.		Ngoi Thia	Hydrothermal	Tu Le
85	Nam Co	Pb-Zn	Occ.		Tu Le	Hydrothermal	Tu Le
86	CoGiSan	Pb-Zn	Sma.	Tram Tau		Hydrothermal	Tu Le
87	HuoiPao	Pb-Zn	Sma.	Tram Tau		Hydrothermal	Tu Le
88	BanLin	Pb-Zn	Sma.	Tram Tau		Hydrothermal	Tu Le
89	NamChan	Pb-Zn	Sma.	Tram Tau		Hydrothermal	Tu Le
90	Ban Ang	Pb,Zn,Cu	Occ.	Vien Nam		Hydrothermal	Tu Le

**Note:**

Au – Gold  
 Alt- Allite, sialite  
 Ap- Apatite  
 Bar – Barite  
 Cu – Copper  
 Zn – Zinc

Mo – Molybdene  
 Pb-Zn - Lead & zinc  
 Py – Pyrite  
 Grp – Graphite  
 K, Na – Potassium, sodium  
 U, TR- Radioactive ores

**Appendix 2 - NEIC: Earthquake Search Results (<http://www.neic.cr.usgs.gov>)**

U.S. GEOLOGICAL SURVEY - EARTH QUAKE DATA BASE

FILE CREATED: Sun Nov 22 14:18:55 2009  
 Geographic Grid Search Earthquakes = 82  
 Latitude: 23.316N - 19.533N  
 Longitude: 107.953E - 101.617E  
 Catalog Used: PDE  
 Data Selection: Historical & Preliminary Data

No	Year	Month	Date	Origin time	Latitude	Longitude	Depth	Magnitude	IEM NFO TF	DTS VNWG	Distance (km)
1	1975	8	18	152038.6	22.73	105.16	33	4.9	mbGS	...	-
2	1975	10	27	231853.6	21.5	101.7	33	5.1	mbGS	...	-
3	1977	10	19	24448.4	23.23	107.59	33	5.1	MsGS	...	-
4	1978	9	28	102230.1	21.78	101.91	33	4.3	mbGS	...	-
5	1979	1	9	232844.3	20.91	101.77	33	4.8	mbGS	...	-
6	1979	1	9	233344.6	20.97	102.02	33	4.9	mbGS	...	-
7	1979	3	18	64122.7	20.9	101.98	33	4.6	mbGS	...	-
8	1982	2	20	92517.01	22.26	102.42	33	4.6	mbGS	...	-
9	1982	6	1	61216.39	22.02	101.98	33	5.2	MsGS	...	-
10	1982	6	7	21206.46	21.9	102.07	33	4.4	mbGS	...	-
11	1982	6	12	20549.4	21.84	102.04	33	4	mbGS	...	-
12	1982	10	17	85203.81	20.8	102.03	33	4.7	mbGS	...	-

No	Year	Month	Date	Origin time	Latitude	Longitude	Depth	Magnitude	IEM NFO TF	DTS VNWG	Distance (km)
13	1983	6	24	71822.14	21.72	103.28	18	6.6	MsGS	6FM	-
14	1983	6	24	84342.73	21.77	103.5	33	4.6	mbGS	...	-
15	1983	6	24	90714.3	21.4	102.6	33	6.9	MsGS	...	-
16	1983	6	24	142516.08	21.71	103.35	33	4.5	mbGS	...	-
17	1983	6	24	154505.54	21.6	103.61	33	4.1	mbGS	...	-
18	1983	6	25	35202.53	21.71	103.27	33			...	-
19	1983	6	25	131624.43	21.61	103.61	33			...	-
20	1983	6	25	174034.24	21.69	103.48	33	4.2	mbGS	...	-
21	1983	7	15	44852.65	21.77	103.43	10	5.1	mbGS	...	-
22	1983	9	4	163940.1	21.77	103.26	33			...	-
23	1984	11	11	1639.49	23.12	102.41	33	4	mbGS	...	-
24	1985	3	20	135449.21	20.89	101.63	10	4.8	mbGS	...	-
25	1985	6	9	52240.45	21.93	102.6	33	4.3	mbGS	...	-
26	1985	8	19	134118.81	22.15	102.67	10	4.8	mbGS	...	-
27	1985	8	19	163147.99	22.18	102.7	10	4.9	mbGS	...	-
28	1985	11	13	161502.68	22.03	102.79	33			...	-
29	1986	3	5	235210.74	21.9	102.97	33	4.4	mbGS	...	-
30	1987	1	6	104554.13	21.54	106.19	10	4.9	MLBJI	...	-
31	1987	11	13	164802.13	21.58	103.39	33	4.3	mbGS	...	-
32	1988	1	30	44842.56	22.81	102.88	33	4.4	MLBJI	...	-
33	1988	8	8	143153.86	20.72	102.73	10			...	-
34	1988	10	22	1111.02	20.73	102.59	33	4	mbGS	...	-
35	1989	5	22	230543.21	22.34	104.46	33	4.1	mbGS	...	-
36	1989	6	16	201231.26	20.67	102.45	33	5.5	MsGS	..M	-
37	1989	10	15	143603.66	22	101.72	10	4.5	MLBJI	...	-
38	1991	3	5	91801.71	23	102.2	33	5	MLBJI	...	-
39	1991	7	12	192623.32	20.75	102.21	33			...	-
40	1991	10	6	105044.46	21.38	104.23	10	4.5	mbGS	.F.	-
41	1991	10	11	22629	21.93	105.21	10	4.1	MLBJI	...	-
42	1992	8	7	84322.59	23.16	103.92	10	4.3	MLBJI	...	-
43	1993	3	29	11729.17	21.87	103.1	33	4.6	mbGS	...	-
44	1993	3	30	135709.19	21.88	103.07	33	4.4	mbGS	...	-
45	1993	9	19	201414.94	22.13	101.94	33	4.8	MLBJI	...	-
46	1993	10	23	35838.23	21.54	104.87	33	4.2	MLBJI	...	-
47	1993	12	21	100405.48	22.22	103.25	10	4.5	MLBJI	...	-
48	1994	9	23	40250.63	21.54	107.49	33	4.6	mbGS	...	-
49	1995	4	24	161311.48	22.74	102.91	33	5.2	MwHRV	..M	-
50	1995	6	21	31557.56	20.11	103.24	10	4.2	mbGS	...	-
51	1995	6	21	90701.66	20.35	103.25	33	4.4	mbGS	...	-
52	1995	7	25	154124.5	23.2	105.85	10	4.7	MLBJI	...	-
53	1995	11	9	205517.68	22.06	102.72	33	4.7	MLBJI	...	-
54	1996	2	2	225958.74	22.13	103.18	33	4.3	MLBJI	...	-
55	1996	4	27	95219.7	22.35	102.22	33	3.7	mbGS	...	-
56	1996	11	13	185150.45	22.35	102.76	33	4.3	mbGS	...	-
57	1997	4	22	114355.37	23.11	105.06	33	3.6	mbGS	...	-
58	1997	10	24	93042.54	22.48	101.73	10			...	-
59	1997	11	19	65158.06	22.03	101.71	33	3.8	MLBJI	...	-
60	1999	3	31	31916.06	19.53	101.64	10	4.5	mbGS	...	-
61	2000	12	13	234624.42	21.44	102.03	33			...	-
62	2001	2	19	155135.97	21.4	102.71	10	4.9	MsGS	.C.	-
63	2001	2	19	190252.4	21.29	102.88	10	4	mbGS	...	-
64	2001	3	4	201851.2	21.36	102.93	10	4.7	MLBJI	...	-
65	2001	4	2	204550.92	22.12	103.16	33	4.4	mbGS	...	-
66	2001	4	30	224933.83	23.04	102.27	33	4.6	MLBJI	...	-
67	2001	6	4	210216.44	21.89	102.54	10	4.6	MLBJI	...	-
68	2001	11	28	44221.77	22.46	103.06	33	4	MLBJI	...	-
69	2002	4	12	50448.81	22.36	102.64	10	4.5	mbGS	...	-
70	2003	4	3	234824.64	20.64	103.17	10	4.7	mbGS	.F.	-

No	Year	Month	Date	Origin time	Latitude	Longitude	Depth	Magnitude	IEM NFO TF	DTS VNWG	Distance (km)
71	2004	1	1	111413.1	23.28	102.99	18	4.2	mbGS	...	-
72	2005	9	26	134836.82	22.5	102.18	10	4	mbGS	...	-
73	2006	1	12	10533.24	23.28	101.69	32	4.6	mbGS	.F.	-
74	2006	4	3	170655.81	19.84	107.55	25	4	mbGS	...	-
75	2006	11	23	163002.13	22.66	102.38	10	4.5	mbGS	...	-
76	2007	5	2	20213.91	20.73	103.13	10	4.5	mbGS	...	-
77	2008	3	2	182644.94	22.42	102.35	10	4	mbGS	...	-
78	2008	10	17	213746.33	23.13	104.13	10	3.8	mbGS	.F.	-
79	2008	12	29	194952.92	22.4	102.21	10			...	-
80	2009	4	4	220352.57	23.24	101.68	10	4.3	mbGS	...	-
81	2009	5	22	185024.23	21.49	102.24	10	4.4	mbGS	...	-
82	2009	10	14	15837.73	20.69	101.94	10	4.3	mbGS	...	-

### Appendix 3: Global CMT Catalog

#### 1. Event name: 062483A (Tuan Giao)

Region name: SOUTHEAST ASIA

Date (y/m/d): 1983/6/24

#### Information on data used in inversion

Wave	nsta	nrec	cutoff
Body	23	57	45
Mantle	0	0	0
Surface	0	0	0

#### Timing and location information

	hr	min	sec	lat	lon	depth	mb	Ms
PDE	7	18	21.90	21.72	103.38	18.0	6.1	6.5
CMT	7	18	27.30	21.85	103.67	10.0		
Error			.20	.02	.03	.0		

Assumed half duration: 4.0

#### Mechanism information

Exponent for moment tensor: 25 units: dyne-cm

	Mrr	Mtt	Mpp	Mrt	Mrp	Mtp
CMT	-0.208	-1.566	1.77	-1.028	0.531	-1.993
Error	0.060	0.056	0.079	0.218	0.201	0.052

Mw = 6.2 Scalar Moment = 2.84e+25

Fault plane: strike=20 dip=66 slip=0

Fault plane: strike=110 dip=90 slip=-156

Eigenvector: eigenvalue: 2.98 plunge: 16 azimuth: 243

Eigenvector: eigenvalue: -0.27 plunge: 66 azimuth: 111

Eigenvector: eigenvalue: -2.71 plunge: 17 azimuth: 338



#### 2. Event name: 071583B (Tuan Giao)

Region name: SOUTHEAST ASIA

Date (y/m/d): 1983/7/15

#### Information on data used in inversion

Wave	nsta	nrec	cutoff
Body	11	26	45

Mantle	0	0	0
Surface	0	0	0

#### Timing and location information

	hr	min	sec	lat	lon	depth	mb	Ms
MLI	4	48	52.60	21.77	103.44	10.0	5.1	5.0
CMT	4	48	54.40	21.93	103.29	15.0		
Error			0.50	0.07	0.09	0.0		

Assumed half duration: 1.8

#### Mechanism information

Exponent for moment tensor: 23 units: dyne-cm

	Mrr	Mtt	Mpp	Mrt	Mrp	Mtp
CMT	-1.698	-7.718	9.416	-0.963	3.570	-4.044
Error	0.562	0.479	0.748	1.691	1.292	0.537

Mw = 5.3 Scalar Moment = 1e+24

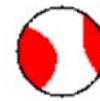
Fault plane: strike=34 dip=78 slip=10

Fault plane: strike=301 dip=80 slip=168

Eigenvector: eigenvalue: 11.37 plunge: 16 azimuth: 257

Eigenvector: eigenvalue: -2.74 plunge: 74 azimuth: 83

Eigenvector: eigenvalue: -8.63 plunge: 1 azimuth: 348



#### 3. Event name: 061689C (Dien Bien)

Region name: SOUTHEAST ASIA

Date (y/m/d): 1989/6/16

#### Information on data used in inversion

Wave	nsta	nrec	cutoff
Body	13	25	45
Mantle	0	0	0
Surface	0	0	0

#### Timing and location information

	hr	min	sec	lat	lon	depth	mb	Ms
MLI	20	12	31.30	20.62	102.43	33.0	5.1	5.5
CMT	20	12	32.80	20.61	102.61	15.0		
Error			0.30	0.04	0.06	0.0		

Assumed half duration: 2.5

#### Mechanism information

Exponent for moment tensor: 24 units: dyne-cm

	Mrr	Mtt	Mpp	Mrt	Mrp	Mtp
CMT	-0.535	-1.788	2.323	-1.090	0.383	-1.551
Error	0.097	0.084	0.123	0.305	0.207	0.094

Mw = 5.6 Scalar Moment = 2.85e+24

Fault plane: strike=25 dip=65 slip=-9

Fault plane: strike=119 dip=82 slip=-154

Eigenvector: eigenvalue: 2.99 plunge: 12 azimuth: 249

Eigenvector: eigenvalue: -0.28 plunge: 63 azimuth: 135

Eigenvector: eigenvalue: -2.71 plunge: 24 azimuth: 345



#### 4. Event name: 011900C (Dien Bien)

Region name: SOUTHEAST ASIA

Date (y/m/d): 2000/1/19

**Information on data used in inversion**

Wave	nsta	nrec	cutoff
Body	40	73	45
Mantle	0	0	0
Surface	0	0	0

**Timing and location information**

	hr	min	sec	lat	lon	depth	mb	Ms
PDE	20	59	28.20	19.83	101.29	33.0	5.1	5.1
CMT	20	59	26.20	19.92	101.33	15.0		
Error			0.30	0.04	0.03	0.0		

Assumed half duration: 1.2

**Mechanism information**

Exponent for moment tensor: 24 units: dyne-cm

	Mrr	Mtt	Mpp	Mrt	Mrp	Mtp
CMT	-0.087	-1.203	1.290	0.001	0.324	0.920
Error	0.038	0.048	0.058	0.144	0.175	0.041

Mw = 5.4 Scalar Moment = 1.58e+24

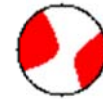
Fault plane: strike=64 dip=80 slip=4

Fault plane: strike=333 dip=86 slip=170

Eigenvector: eigenvalue: 1.65 plunge: 10 azimuth: 288

Eigenvector: eigenvalue: -0.13 plunge: 79 azimuth: 131

Eigenvector: eigenvalue: -1.51 plunge: 4 azimuth: 19

**5. Event name: 042495B**

Region name: YUNNAN PROVINCE, CHINA

Date (y/m/d): 1995/4/24

**Information on data used in inversion**

Wave	nsta	nrec	cutoff
Body	21	37	45
Mantle	0	0	0
Surface	0	0	0

**Timing and location information**

	hr	min	sec	lat	lon	depth	mb	Ms
PDE	16	13	11.60	22.70	102.85	33.0	4.6	4.9
CMT	16	13	14.20	22.88	103.16	33.0		
Error			0.60	0.07	0.06	0.0		

Assumed half duration: 1.0

**Mechanism information**

Exponent for moment tensor: 23 units: dyne-cm

	Mrr	Mtt	Mpp	Mrt	Mrp	Mtp
CMT	-1.707	-2.195	3.902	-0.737	-0.940	-7.101
Error	0.339	0.396	0.434	0.871	0.752	0.367

Mw = 5.2 Scalar Moment = 7.85e+23

Fault plane: strike=102 dip=80 slip=-173

Fault plane: strike=11 dip=83 slip=-10

Eigenvector: eigenvalue: 8.60 plunge: 2 azimuth: 57

Eigenvector: eigenvalue: -1.48 plunge: 78 azimuth: 157

Eigenvector: eigenvalue: -7.11 plunge: 12 azimuth: 327

